SEDIMENTOLOGY AND GEOMORPHOLOGY

OF THE

GLACIAL LAKE HIND AREA,

SOUTHWESTERN MANITOBA, CANADA

BY

CHUANYU (STEPHEN) SUN

A THESIS

SUBMITTED TO THE FACULTY OF GRADUATE STUDIES
UNIVERSITY OF MANITOBA
IN PARTIAL FULFILMENT OF THE REQUIREMENTS
FOR THE DEGREE OF DOCTOR OF PHILOSOPHY
IN GEOLOGY

THE DEPARTMENT OF GEOLOGICAL SCIENCES
UNIVERSITY OF MANITOBA
WINNIPEG, MANITOBA CANADA

SEPTEMBER 1996

ISBN 0-612-16319-9

THE UNIVERSITY OF MANITOBA

FACULTY OF GRADUATE STUDIES

COPYRIGHT PERMISSION

SEDIMENTOLOGY AND GEOMORPHOLOGY OF THE GLACIAL LAKE HIND AREA, SOUTHWESTERN MANITOBA, CANADA

BY

CHUANYU (STEPHEN) SUN

A Thesis/Practicum submitted to the Faculty of Graduate Studies of the University of Manitoba in partial fulfillment of the requirements for the degree of

DOCTOR OF PHILOSOPHY

Table of Content

List of Figures

LIST OF TABLES

ABSTRACT

Glacial Lake Hind was a 4000 km^2 ice-marginal lake which formed in southwestern Manitoba during the last deglaciation. It received meltwater from western Manitoba, Saskatchewan, and North Dakota via at least 10 channels, and discharged into glacial Lake Agassiz through the Pembina Spillway.

Surface sediment outside of the area covered by glacial Lake Hind is dominantly till. There are two types of tills based on their carbonate content and calcite/dolomite ratios: one that has high carbonate content and a low calcium/dolomite ratio (Dh), which occurs east of glacial Lake Hind, and another that has low carbonate content and a high calcite/dolomite ratio (Dl), which occurs north, west, and south of glacial Lake Hind, and may underlie Lake Hind sediments. Four till units have been identified based on carbonate content, texture, and color. They are the Wawanesa till, Souris till, Fairfax till, and Carroll till.

Sediments in the Lake Hind basin consist of up to 30 m of silt and clay, 25 m of sand and deltaic gravels. Much of the uppermost lacustrine sand in the central part of the basin has been reworked into aeolian dunes. No beaches have been recognized in the basin. Around the margins, clayey silt occurs up to an elevation of 457 m, and deltaic gravels occur at 434 - 462 m. In addition, there are a total of 12 deltas around the lake basin, and these can be divided into 3 groups based on the elevation of their surfaces: 1) above 457 m along the eastern edge of the basin and in the narrow southern end; 2) between 450 and 442 m at the western edge of the basin; and 3) below 442 m.

The earliest stage of glacial Lake Hind began shortly after 12 ka, as a small lake formed

between the eastern edge of the Souris Lobe and the western edge of the Red River Lobe in southwestern Manitoba. Two deltas at an elevation of above 457 m were formed in this lake. At the same time, the western edge of the Souris Lobe retreated far enough to allow glacial Lake Souris to expand northward along the western side of the basin from North Dakota; three deltas were built at an elevation of between 457 and 466 m in the Canadian part of this proglacial lake. Continued retreat of the Souris Lobe allowed the merger of glacial Lake Souris with the interlobate glacial Lake Hind. Subsequent erosion of the outlet into the Pembina valley allowed waters in the glacial Lake Hind basin to become isolated from glacial Lake Souris, and four deltas formed between 442 and 450 m by meltwater from the west. Next, a catastrophic flood from the Moose Mountain uplands in southeastern Saskatchewan flowed through the Souris River valley to glacial Lake Souris, in turn, spilling into Lake Hind and depositing another delta at an elevation of about 442 m. This resulted in further incision of the outlet into the deep and wide Pembina spillway, and a new level of glacial Lake Hind was established at 434 m. A second flood through the Souris River valley, this time from glacial Lake Regina, further eroded the outlet; most of glacial Lake Hind was drained as a result of this flood except for the deeper northern part. Coarse gravel was deposited by this flood, which differs from previous flood gravel because it is massive and contains less shale.

Acknowledgments

Data for this thesis were collected as part of the Geological Survey of Canada Prairie NATMAP Project, co-ordinated by Dr. R.J. Fulton. Dr. Fulton also provided essential guidance and help in the field and in compiling surficial geology maps; special thanks to him for exchanges of ideas and for providing financial supported for lab analyses. Support also came from a Natural Sciences and Engineering Research Council of Canada Research Grant to James T. Teller. Thanks to Professor Teller for very thoughtful reviews of this thesis and for discussions during my Ph.D. research. Atomic absorption analyses were done by the Saskatchewan Research Council; Chittick apparatus analyses were carried out by the Geological Survey of Canada. Field assistance was provided by Jason Bjornson, Brad Spence, Stephen Whetherup, and Tim Hodge.

CHAPTER 1

INTRODUCTION

1.1 Location of the Study area

Lake Hind was named by Elson (1956) after Henry Youle Hind, who had explored the Canadian Prairies in the 1860's. The basin is located in southwestern Manitoba between the towns of Brandon to the east and Virden to the west, and between the International Border to the south and the town of Virden on the north (Fig. 1-1). Topographically the basin is a lower region between the lower slopes of Turtle Mountain to the south, Riding Mountain to the north, Moose Mountain to the west, and Tiger Hills to the east. The total study area covers about 9000 km^2 and is bounded by latitudes 49°00' N and 50°15'N, and longitudes 100°00' and 101°20'. Glacial Lake Hind covered a total of about 4000 km^2. The area is included in the Virden 62F, 1:250,000 topographic map sheet, and the research has been concentrated in nine 1:50,000 topographic map sheets (62F/2, 3, 7, 8, 9, 10, 14, 15, and 16). In addition, the Assiniboine River valley to the north was studied from Virden to its junction with Qu'Appelle River valley; the Souris valley was examined from glacial Lake Hind to glacial Lake Regina in the headwaters; the Souris-Moose Mountain valley was investigated from its junction with the Souris River valley north to glacial Lake Arcola and Lake Indian Head; and the Pipestone valley was explored from Lake Hind to Lake Indian Head (Fig.1-1).

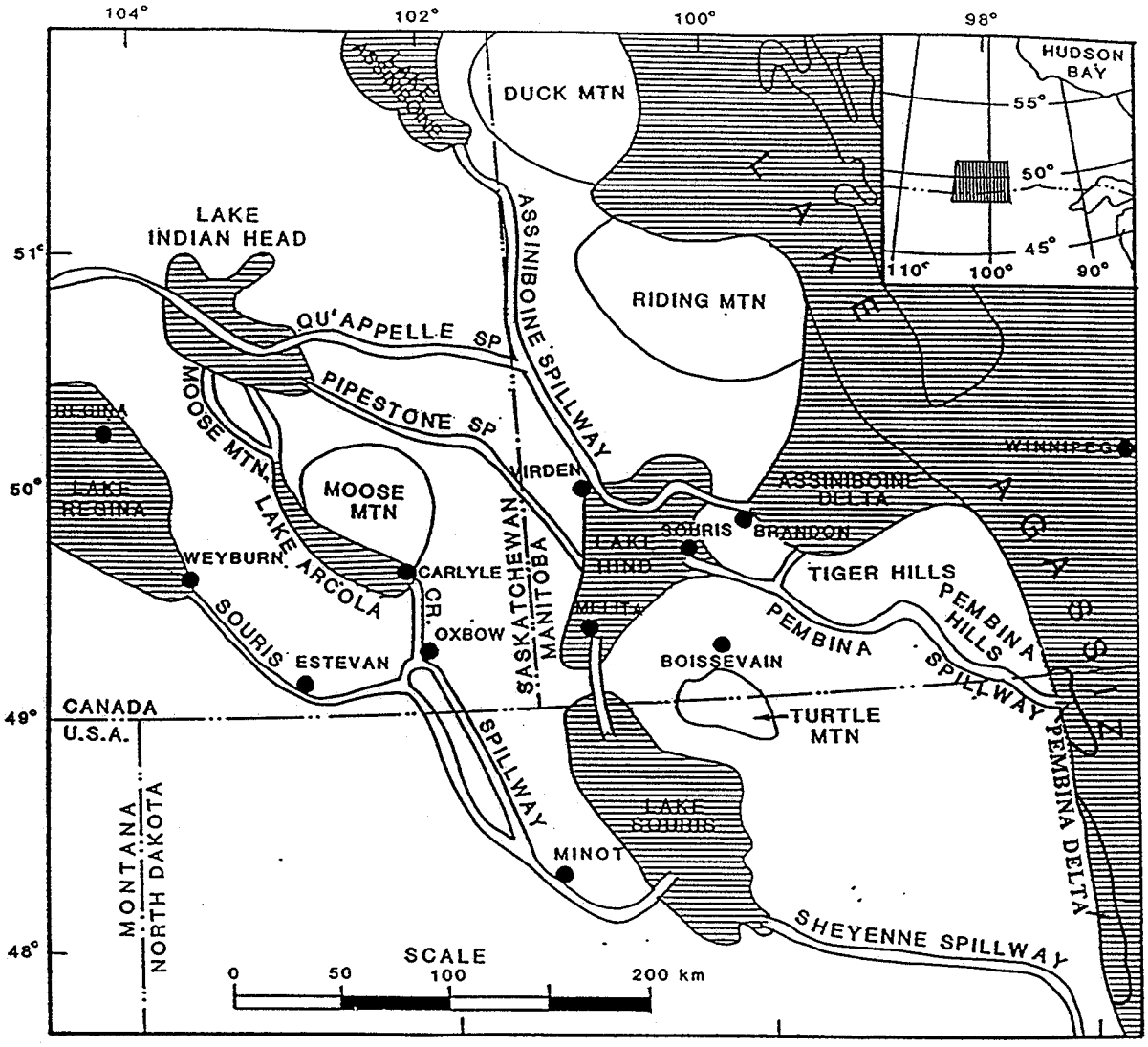

Fig. 1-1 Location map and physiographic division of southwestern Manitoba, southeastern Saskatchewan, and northern North Dakota, showing glacial lakes, meltwater spillways, and uplands (after Kehew & Teller, 1994).

1.2 Elaboration of objectives of this research

During late Wisconsinan time, Lake Hind received meltwater flows from southern Saskatchewan, northern North Dakota, southwestern Manitoba, and southern Alberta, and overflowed to Lake Agassiz. Therefore, the deglaciation chronology of Lake Hind area is critical to the understanding of the deglaciation history of middle North America.

The general purpose of this research was to establish the late Pleistocene stratigraphy and map the distribution of surficial sediments in the Lake Hind basin. From this, I have reconstructed the history of deglaciation and history of meltwater flows in the Lake Hind region, and linked Lake Hind with Lake Agassiz to the east and the Saskatchewan region to the west. In addition, I had several other specific goals.

Goal 1 was to determine the late glacial areal extent of the Assiniboine Ice Lobe, which flowed from the northwest, and the Red River Ice Lobe (Sub-Assiniboine Lobe, Klassen, 1983a), which flowed from northeast. These were the last glacial advances into the region. These ice lobe positions, which were related to the direction of local ice advances and retreats, controlled the position of ice marginal lakes and many routes of meltwater flow.

This goal was achieved by studying and comparing till textures, till fabric, carbonate content, mineral composition, pebble lithology, and striations on boulder pavements under the surface till, as well as the location of end moraines and interlobate moraines. Previous studies in the Riding Mountain area (Klassen, 1979), Saskatchewan (Christiansen, 1990), and Tiger Hills area (Conley, 1986) suggest that till of the

Assiniboine Lobe has lower carbonate content than that of the Red River lobe, which lies to the east.

Goal 2 was to evaluate the effect of a late glacial floods from Lake Souris to Lake Hind. According to Kehew and Lord (1986), Kehew and Clayton (1983), and others, this flood was catastrophic, starting from the southern end of glacial Lake Regina near Weyburn, Saskatchewan, and cutting the Souris River valley from Lake Regina to Lake Souris. In a domino fashion, it caused Lake Souris water to burst northward into the Lake Hind basin, which in turn, overflowed into Lake Agassiz, and deepened the Pembina Spillway. Both the magnitude of the flood and Lake Hind water level during the flood are important in order to estimate the effect the flood had on Lake Hind. To study this flood, sedimentary textures and structures of fluvial sediments in the Souris River valley in glacial Lake Hind were examined to estimate the nature and magnitude of the flood. The surface elevation of sediments, erosional marks, and their relationship to lacustrine sediments were examined to estimate the lake level during flood.

Goal 3 was to study the origin of the Pipestone River valley, which is one of a dozen creeks west of Lake Hind. Did it start as a subglacial channel? or ice marginal channel? This is important in helping to determine the direction of the last ice retreat (northwest vs northeast) across the region west of Lake Hind. If it was an ice marginal channel, major meltwater deposits may occur on the southern side of the river and undulating to hummocky till will occur along the northern side where it was occupied by ice. If it was formed as a subglacial tunnel, the channel should be narrow, deep, and straight, possibly with discontinuous gravel deposits in places.

Goal 4 was to determine the main suppliers of coarse sediment (sand and gravel) to Lake Hind, and their age relative to the age of Lake Hind. This was done by mapping the mean size of surface sediments that are at least 1 km away from sand dunes, and by stratigraphic correlation between coarser delta sediments and finer lacustrine sediments. In addition, lithological analysis of the 4 to 16 mm gravel size was done to distinguish different sources.

Goal 5 was to study the lower parallel ridges, kames, and a huge esker north of the Assiniboine River, named by Elson (1956) as the Arrow Hill Esker. These low linear ridges, which are surrounded with a horse-shoe-kind of depression, are similar to Shaw's (1991) drumlins of subglacial meltwater floods. If they were formed by a subglacial meltwater flood, where did the meltwater come from, and where did the flood water go? Was the esker formed by the same event(s)? This is important to the deglaciation history in that area.

1.3 Previous work in Lake Hind area

The bedrock of the study area was mapped by Wickenden (1945) on the scale of 1 inch to 8 miles (1:506,880). Bedrock topography and buried valleys in this area were studied and mapped by Klassen et al. (1970), Betcher (1983), and Teller et al. (1976). Quaternary deposits (glacial, glaciofluvial, glaciolacustrine, and eolian) were mapped and studied by Elson (1956, 1967), Klassen (1975), Klassen et al. (1970), Betcher (1983), and Manitoba Mineral Resources Division (1980). Alluvial sediments in the Assiniboine River Valley were examined by Klassen (1975, 1983a), while the origin of the Souris

channel was studied by Kehew (1982), Kehew and Clayton (1983), and Kehew and Lord (1986), and Kehew and Teller (1994a). Aggregate resources in Lake Hind area have been mapped and compiled by Groom (1988) and Manitoba Energy and Mines (1988). Soils in the Virden area were studied by Ehrlich et al. (1956), Podolsky (1985), and Eilers (1978). Groundwater availability studies in the Virden map-sheet area have been done by Halstead (1959), Mayboom et al., (1966), and Betcher (1983), the Water Resources Branch of Manitoba Natural Resources (1976). Many wells have been drilled for stratigraphic information by the Geological Survey of Canada, the Manitoba Mines Branch, and the Manitoba Water Resources Branch, and these, plus normal water well log descriptions, are available in computer data base by Water Resources Branch of Manitoba, as well as in published format for the years 1955-1976.

1.4 Previous work in the adjacent areas

1.4.1 Introduction

Lake Hind was a proglacial lake during late Wisconsinan time, impounded by ice lobes to the east and north, and by topographic highs to the west and south. Lake Hind received meltwater flows from Saskatchewan, northern North Dakota, and western Manitoba through the Qu'Appelle-Assiniboine River valley system, Souris River valley, Pipestone River valley, and a half dozen small rivers, and drained east to Lake Agassiz through the Pembina Spillway and/or the Assiniboine valley. Because of the tight linkage among Lake Hind, Lake Agassiz, and meltwater channels from Saskatchewan, the deglaciation history of the Lake Hind area had to be reconstructed within the framework

of the deglaciation chronology in the Lake Agassiz basin (Kehew and Teller, 1994a; Teller, 1985, 1987; Fenton et al., 1983; Clayton and Moran, 1982), and in the Saskatchewan area (Christiansen, 1979; Klassen, 1975, 1983a, 1989).

1.4.2 Disagreement on chronology of events in the eastern Prairies

There are two schools of deglaciation chronology in the region. An old chronology proposed by Christiansen (1979) and Klassen (1975, 1983a, 1989), and a younger chronology proposed by Clayton and Moran (1982), Fenton and others (1983), Teller (1985, 1987, 1989), and Teller et al.(1980).

Based on a dozen radiocarbon dates on carbonate silt, peat, and organic detritus, and two radiocarbon dates on wood, Christiansen (1979) suggested the following old chronology of deglaciation in Saskatchewan, including the western glacial Lake Agassiz basin area (Fig. 1-2):

1) Deglaciation in southern Saskatchewan started at about 17,000 BP.

2) Meltwater from glacial Lake Regina discharged into Lake Agassiz through the Souris River valley and Pembina Spillway at about 15,500 BP, which implies that the Lake Agassiz basin in southern Manitoba was ice free before 15,500 BP (Ice margin number 3, Fig. 1-2).

3) Qu'Appelle River valley and Assiniboine River valley areas became ice free, and meltwater from the two valleys started to build the Assiniboine delta into Lake Agassiz at about 14,000 BP. Support for this age was given by Klassen (1983a) as the dated wood from a depth of 50 m in Qu'Appelle alluvium of

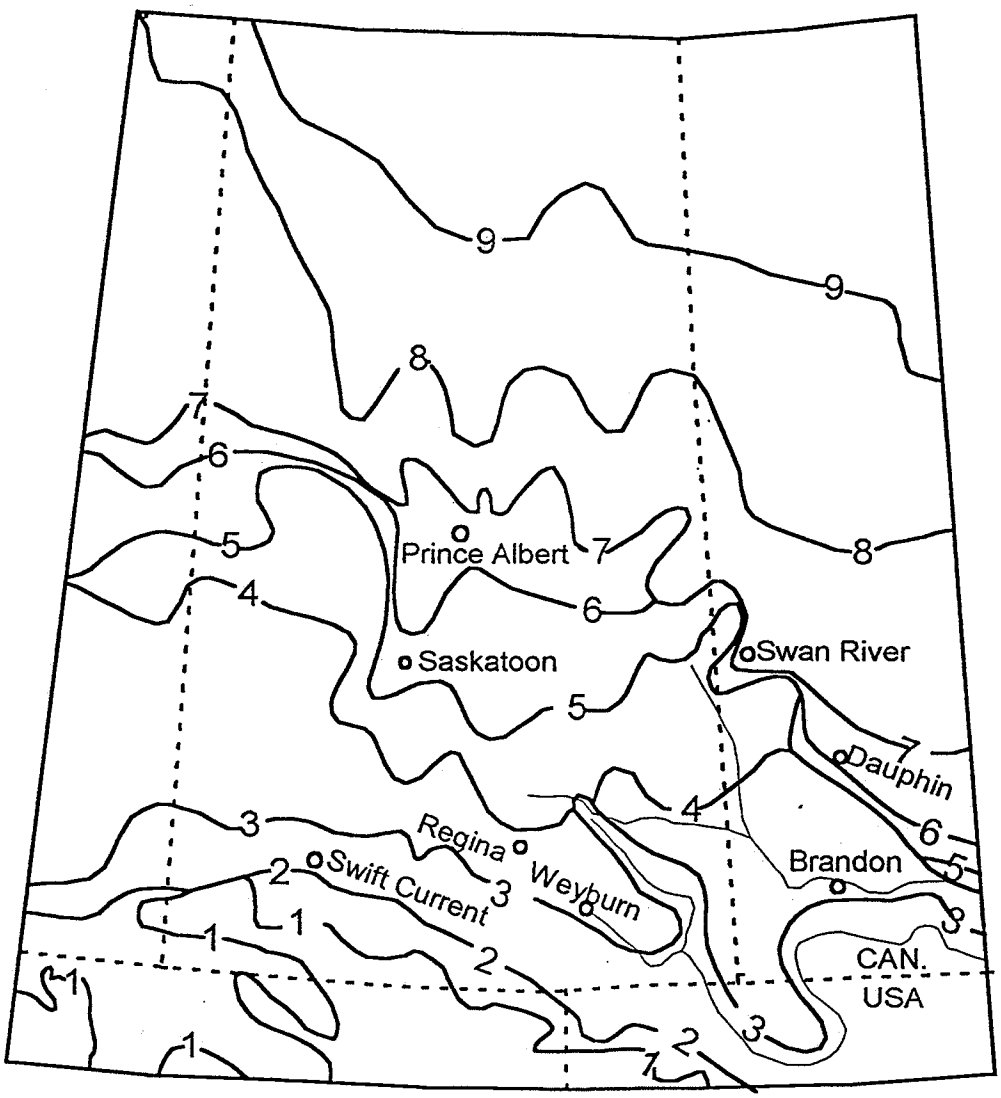

Fig. 1-2 Sequence of ice marginal positions in Saskatchewan and adjacent areas during the last deglaciation (after Christiansen, 1979).

12,025± 205 BP (S-553), and wood from the Assiniboine alluvium near Virden dated at 11,600 ± 430 BP (GSC-1081) (Ice margin number 4, 5, 6, and 7 in Fig. 1-2).

4) Deposition of the Saskatchewan River Delta into Lake Agassiz north of the Duck Mountain started at about 11,000 BP (Ice margin number 8 in Fig. 1-2).

This chronology is in conflict with the younger deglaciation chronology. Based on 6 radiocarbon dates on wood beneath and within Wisconsinan till in South Dakota (Table 1-1), and on the concern that the old chronology was largely based on organic material that may have contain old reworked organic detritus, Teller et al. (1980), Clayton and Moran (1982), Fenton et al. (1983), Teller (1989), and others pointed out that the ice margin was in southern South Dakota at about 12,300 BP, which indicates that the Lake Agassiz basin was occupied by ice until after 12,300 BP. Therefore, the Pembina Spillway and the Assiniboine River Valley were not eroded before 12,300 BP, as advocated by Klassen (1983a) and Christiansen (1979), and probably were not ice free until after 11,500 BP and 11,400 BP respectively (Teller, 1989).

1.4.3 Summary of deglaciation history of the Lake Agassiz Basin

Introduction

Lake Agassiz was connected to Lake Hind by two major channels: the Pembina River valley and the Assiniboine River valley. Meltwater from the Pembina River valley deposited the Pembina delta of Lake Agassiz in North Dakota, while meltwater from the Assiniboine River valley deposited the Assiniboine fan delta into Lake Agassiz (Fig. 1-1).

Table 1-1 Radiocarbon dates on wood from till in southern South Dakota (after Clayton and Moran, 1982)

AGE	SAMPLE NO.	COMMENTS
12,350±350 BP	W-987	12m below soil, beneath top till.
12,200±400 BP	W-1372	12m below soil, beneath top till.
12,050±300 BP	W-1189	58 m below soil, beneath top till.
12,340±300 BP	W-1756	Base of top till.
12,200±400 BP	W-801	Within top till.
12,300±180 BP	Y-452	Base of top till.
12,520±100 BP	Y-925	Base of top till.
12,180±760 BP	GX-5611	Forest root in lake clay beneath top till.
12,680±700 BP	W-1757	3m in fluvial sediments.

The history of deglaciation in the region and of Lake Agassiz has been proposed by many workers (Clayton and Moran, 1982; Fenton et al., 1983; Elson, 1956, 1967; Klassen, 1975, 1989; Teller, 1985, 1987, 1989; Teller and Thorleifson, 1983). Fenton et al. (1983) and Teller (1985) proposed 5 phases for Lake Agassiz: Case-Lockhart Phase (a high lake stage at 11,700-10.800), Moorhead Phase (a low lake stage at 10,800-9900), Emerson Phase (a high lake stage at 9900-9500), Nipigon Phase (a declining stage routed through the Great Lakes at 9500-8500), and Ojibway Phase (a declining lake routed through glacial Lake Ojibway at 8500-7500) (Fig. 1-3). This represents the most widely accepted view of Lake Agassiz history, and is based on radiocarbon ages on wood only (Fenton et al., 1983), as compared to that of Christiansen (1979) and Klassen (1975, 1983a, 1989), who used all dated organic remains, which Nambudiri et al. (1980), Teller et al. (1980), Clayton and Moran (1982), Teller (1989), and others have shown to be in error because of contamination by old carbon.

Case-Lockhart Phase

During the late Wisconsinan, ice from the Labradorean centre advanced southwestward to about the western edge of the Lake Agassiz basin, covering the Manitoba Lowland. Ice from the second centre, the Keewatin centre west of Hudson Bay, flowed southward slightly later and was deflected westward around the Labradorean ice, flowing over shale terrain (Fenton et al., 1983). As the Labradorean ice began to waste, the Keewatin ice centre expanded east to the area formerly occupied by the Labradorean ice. By about 20,000 BP the Keewatin ice reached Iowa (Fenton et al., 1983). This was

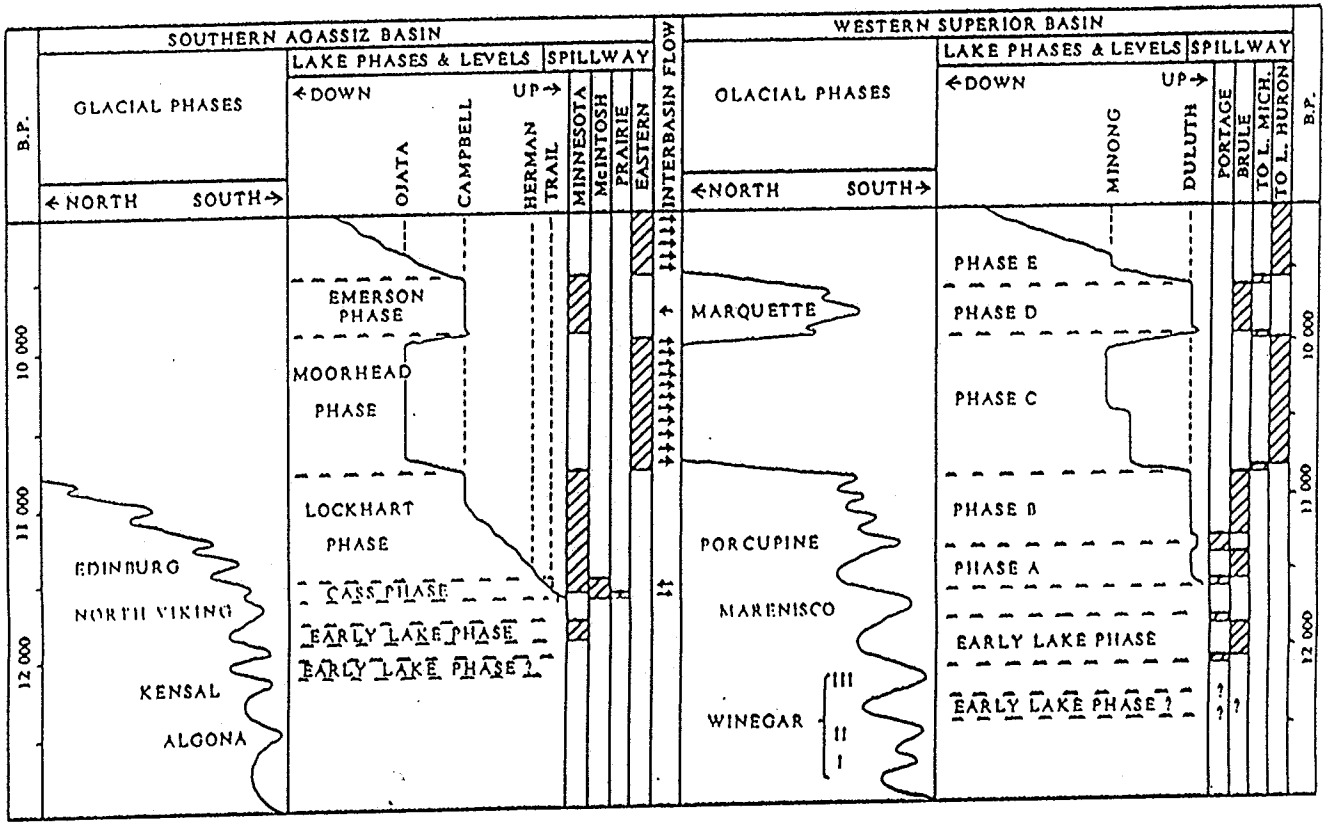

Fig. 1-3 Chronology of Lake Agassiz and its drainage to the eastern and southern outlets (after Clayton, 1983, p.259).

followed by a major withdrawal of ice.

The retreat of ice from 20,000 BP to 12,300 BP was interrupted by several readvances. One major readvance (of the Des Moines Lobe) that pushed the ice margin into central Iowa and deposited the Cary Drift in northern Iowa occurred between 13,500 and 14,000 BP (Ruhe, 1969). This is supported by 16 radiocarbon dates on wood: 4 within the Cary till, one from the base of the top till (Cary Drift), and the other 11 from Tazewell loess that underlies the Cary drift (Ruhe, 1969) (Table 1-2). After a period of retreat, another major readvance sent the ice to the southern border of South Dakota at about 12,300 BP, as suggested by eight radiocarbon ages on wood beneath and within the till deposited by the ice in southeastern South Dakota (Fenton et al., 1983; Clayton and Moran, 1982) (Table 1-1). These radiocarbon dates suggest that the Lake Agassiz basin was covered by ice until after 12,300 BP.

There are no radiocarbon dates to indicate exactly when Lake Agassiz first came to exist (Clayton and Moran, 1982). It is suggested that the Red River Lobe retreated into the Red River Valley at about 11,700 BP, which gave birth to infant Lake Agassiz (Fenton et al., 1983; Clayton, 1983; Clayton and Moran, 1982; Teller, 1987) (Fig.1-3). As the ice retreated farther, Lake Agassiz expanded northward. By 11,500 to 11,300 BP, Lake Agassiz had expanded at least to the International Boundary. By 11,000 BP, Lake Agassiz expanded northward into central Manitoba (Teller, 1987).

Moorhead Phase

The Moorhead low water phase started shortly after 11,000 BP due to the opening

TABLE 1-2, RADIOCARBON DATES OF WOOD FROM WISCONSIN TILLS AND LOESS IN IOWA (FROM RUHE, 1969)

SAMPLE	DATE (yrs BP)	WOOD	STRATIGRAPHIC LOCATION
C-596	11,952±500	Hemlock	Within Cary till
C-912	12,120±530	Hemlock	Gravel bed within Cary till
C-563	12,200±500	Hemlock	Within Cary till
C-913	13,300±900	Hemlock	Gravel bed within Cary till
I-1268	13,900±400	Spruce	Base of Cary till
W-513	13,820±400	Spruce	Tazewell loess beneath Cary till
W-517	13,910±400	Spruce	Tazewell loess beneath Cary till
I-1402	14,200±500	Spruce	Tazewell loess beneath Cary till
W-512	14,470±400	Hemlock	Tazewell loess beneath Cary till
W-153	14,700±400	Hemlock	Tazewell loess beneath Cary till
I-1270	16,100±1000	Spruce	Tazewell loess beneath Cary till
I-1024	16,100±500	Spruce	Tazewell loess beneath Cary till
C-528	16,367±1000	Hemlock	Tazewell loess beneath Cary till
W-126	16,720±500	Hemlock	Tazewell loess beneath Cary till
C-481	>17,000	Hemlock	Tazewell loess beneath Cary till
I-1023	21,360±850	Spruce	Tazewell loess beneath Cary till

of lower elevation eastern outlets to the Superior basin (Teller, 1985, p.4). As one after another lower eastern outlets opened (Fig.1-3), the Lake Agassiz water level rapidly declined in steps, exposing large parts of the lake floor in the southern basin. Warman (1991) indicated that the varved sequence in northwestern Ontario did not indicate that level fell as low as Gimli beach level, which others had predicted.

Emerson phase

A readvance of ice across the Lake Superior basin (the Marquette advance) at about 10,000 BP dammed the eastern Lake Agassiz outlets. This caused Lake Agassiz water to rise at least to the Campbell beach level (Teller and Thorleifson, 1983) and again begin to overflow through the southern outlet (Fig. 1-3). Klassen's (1975, Table 3) study along the Assiniboine valley shows that the highest terraces were graded to the Tintah level (350 m) during the Emerson phase, suggesting that the lake level was higher than the Campbell beach level in early Emerson phase. Thorleifson (1983) also suggested that the lake rose above the Campbell level at this time, based on the gradient differences (truncational relationship) between the Herman beaches and the Norcross beaches, which are the highest two beaches of Lake Agassiz, and on the distribution of red clay in northwestern Ontario..

Nipigon phase

The Emerson phase came to an end by about 9500 BP (Teller and Thorleifson, 1983; Teller, 1987). The level of Lake Agassiz fell rapidly from the Campbell level to

Gimli level. The decline in lake level was due to the undamming of the lower eastern outlets of Lake Agassiz to Lake Nipigon. This phase is equivalent to Klassen's (1983b) phases 1, 2, and 3 of history in northern Manitoba.

Ojibway phase

The Nipigon phase came to an end because ice retreated north of the Nipigon basin and Lake Agassiz overflow was then directed toward the east into proglacial Lake Ojibway at about 8500 BP (Teller and Thorleifson, 1983). By about 8000 BP, Lake Agassiz had drained into the Tyrrell Sea (Vincent, 1989); Klassen (1983b) suggests that it drained at about 7500 BP.

1.4.4 A problem remains with the younger chronology

There still remains a problem with the younger chronology of Lake Agassiz. A piece of wood from the Assiniboine clayey alluvium near Virden gives a radiocarbon date of 11,600 $\pm$430 BP (Klassen, 1975, 1983a). If this is not a reworked piece of wood, it suggests that the Assiniboine Valley was excavated before 11,600 BP, and that the Assiniboine fan delta area of western Lake Agassiz was partially ice free before 11,600 BP. If Lake Agassiz first began to develop in the south at about 11,700 BP, as suggested in the younger chronology, in order to accommodate the date of 11,600 BP, the ice margin would have to have retreated at least 750 km in 100 years from the southern end of Lake Agassiz basin to the Assiniboine Delta area and the Assiniboine River valley would have to have been eroded and the alluvium would have to have been deposited .

This is unlikely, if not impossible.

There are two possible solutions for this problem. 1) the piece of wood from the Assiniboine alluvium is reworked older material from deglaciated Saskatchewan or Alberta. Therefore, it does not indicate an early deglaciation in the Assiniboine and Qu'Appelle River areas; 2) Lake Agassiz started at about 12,000 BP rather than 11,700 BP, and the ice margin was at the Assiniboine delta area by 11,600 BP.

The beginning of Cass phase of Lake Agassiz is not well dated (Clayton and Moran, 1982). A radiocarbon date of 11,740 $\pm$ 200 BP (I-1327, Wright, 1972) on organic sediments from the base of an ice block depression on the Herman beach level was used by Clayton and Moran (1982) as the age of Lake Agassiz. But Wright (1972), who reported the radiocarbon date first, suggested that this data represents the withdraw of glacial Lake Agassiz from the Herman beach level. In other words, the age of Lake Agassiz could be 12,000 BP if we add the time period when Lake Agassiz was at the Herman beach to the date of 11,700 BP. Besides, Clayton and Moran (1982) correlated their phase L with Christiansen's phase 3, a radiocarbon date of 12,025 $\pm$ 205 BP on wood (S-553, Christiansen, 1979) from the Qu'Appelle alluvium beyond the phase 3 ice margin was mentioned as the maximum date of phase L, or age of Lake Agassiz. Therefore, it is possible that Lake Agassiz started at about 12,000 BP. One, somewhat troubling aspect of this is that the Des Moine Lobe must waste back more than 500 km by 12,000 BP from its well dated position at 12,300 BP in South Dakota, and than waste back 750 km to the Assiniboine fan delta from the southern end of Lake Agassiz by 11,600 BP.

1.5 Methodology

To accomplish these objectives and goals, I collected surficial sediment and morphological data from the field, did lithological analyses on tills and fluvial gravels (4 to 16 mm clasts), made carbonate and mineral composition analyses on till samples, and sieved lacustrine sand samples.

1.5.1 Field Data Collection

Surficial sediment data

Field mapping began in 1992, as part of the Prairie NATMAP project of the Geological Survey of Canada. The prime objective of the NATMAP Project was to develop a prototype GIS geology database of unconsolidated sediments, which would help hydrogeologists, engineers, land managers, planners, etc. in solving developmental and environmental problems in the region (Sun and Fulton, 1993). In comparison, the prime objective of my thesis was to construct the areal distribution and morphology of lacustrine sediments, fluvial sediments, and tills, to interpret and model the deposition mechanisms for these sediments, and to reconstruct the history of deglaciation and meltwater flows in this region.

The surficial materials were divided into six major genetic groups, including morainal deposits (T), glaciofluvial deposits (G), glacial lacustrine deposits (L/M), lacustrine deposits (L), alluvial deposits (A), and colluvial deposits (C). Each genetic grouping includes a specific type of material (Table 1-3) (Fulton, 1994).

Observation sites were placed mostly where section roads cross, or where exposures were available, and were usually spaced at one to two miles. When a fresh exposure was not available, materials from the upper 1 m were extracted by a hand auger. In till areas, an effort was made to examine till at one mile or shorter intervals, and double till samples were taken at about every two to three mile interval for mineral analysis (X-ray diffraction) and for pebble counting. In sand areas, sand samples immediately below the soil zone are taken at 2- to 5-mile intervals for grain size analysis (Appendix I). In places where a gravel exposure is available, about 2 kg of gravel was taken from each stratigraphic units for pebble counting.

Geomorphological data

Mapping and studying of landforms may provided important information about the past. For example, modern landforms may have been inherited from the underlying bedrock or till, such as lacustrine silt deposits draping over hummocky till deposits. Alteratively they may reflect their depositional setting, such as hummocky topography resulting from stagnant ice and flat morainal plain resulting from steady retreating of ice.

Landforms in the study area were examined and mapped using air photos before going into the field, and re-examined in the field. The terminology used for landforms was simple, eg. level, plain (gently undulating), undulating, rolling, and hummocky, each term was used to characterize the landform in each genetic group. If the original landform had been modified by subsequent processes, a process modifier was added, eg. T-w indicates wave washing or fluvial erosion on till. These landforms are used to define

TABLE 1-3 SUMMARY OF MAPPING UNITS IN THE LAKE HIND AREA
(FULTON, PERSONAL COMMU. 1994)

MATERIAL TYPE / (GENETIC)	LANDFORMS	MODIFYING TERMS
Morainal deposits (T) - material deposited directly by glacial. Glaciofluvial deposits (G) - materials deposited by flowing glacial meltwater. Glacial lacustrine deposits (L/M) - glacial lake derived material. Lacustrine deposits (L) - lake derived material. Alluvial deposits (A) - stream and river derived material. Colluvial deposits (C) - slope and slump material.	Fan (f) - single or coalescing fans; relief 2-5m. Terrace (t) - narrow bench or series of stack benches extending along a valley wall; relief within a single terrace <2m. Level Plain (i) - very low mounds and shallow swales, relief <2m. Gently Undulating Plain (p) - low mounds and short ridges with swales or shallow channels; relief <5m. Undulating Plain (u) - low broad ridges, hummocks, and mounds with shallow close depressions; relief 3-10 m. Ridged Plain (r) - broad to sharp crested ridges; relief 2-20m. Hummocky plain (h) - mound and hummocks generally marked by steep but short slopes and often accompanied by closed depressions; relief 3-20 m. Complex (x) a mixture of landforms which can not be separated at the scale mapping.	Rim ridges (+c) -Partial or complete rim ridges occur adjacent to shallow depresions. Scattered ridges (+r) - 2 to 5 m relief. Isolated mounds (+m) - 5 to 15 m relief. Washed (-w) - wave washed or eroded by streams.

subunits under each genetic material grouping (Table 1-3) (Sun and Fulton, 1993).

1.5.2 Sieving analysis

Prior to sieving, sand samples of about 200 grams were dried in an oven at a temperature of 90°C. These samples were then weighed and sieved in sieves ranging from -2ϕ to 4ϕ, with a half Phi increment in sieve size. The sieved samples in each size range were weighed, and a mean grain size was calculated based on Folk and Ward equation (1957) (Appendix I).

1.5.3 Pebble lithology

Pebble lithology counting was done on all till samples (Appendix II). Till samples were first soaked in 5% Calgon solution for 6 hours before being washed. 100 to 300 pebbles ranging from 4 to 16 mm in diameter were extracted from each sample by using a 4 mm sieve and a 16mm sieve. In most cases 11 lithic types of pebbles were identified and counted, including 1) carbonate (in most cases carbonate was subdivided into tan carbonates and grey carbonate to separate eastern from western sources), 2) shale, 3) ironstone, 4) chert, 5) poorly-cemented Tertiary sandstone, 6) coarse-grained quartzite (strongly cemented Cordilleran or Athabasca type), 7) fine grained quartzite (strongly-cemented older) , 8) basalt and other dark colored fine-grained Precambrian lithologies, 9) metamorphic (gneiss and schist), 10) granitic, and 11) unidentified.

1.5.4 Till fabric analyses

Till fabric analyses have been done on sites that have fresh exposures and a steep slope. At each exposure, 27 to 51 pebble-sized clasts were randomly selected for till fabric analyses. Matrix surrounding each pebbles was gently removed until the orientation of the long axis of the pebble could be determined. The orientation and dip of the pebble was then measured with a Compass. In some cases, the pebble was removed and replaced by a ruler which was aligned with the pebble socket. The orientation and dip of the ruler was measured using a Compass and a clinometer.

1.5.5 Carbonate content analyses : Chittick, AA, and XRD

Chittick apparatus

Carbonate content of till by Gasometer (Chittick apparatus) method (Dreimanis, 1962) was done in the Geological Survey of Canada laboratory in Ottawa Appendices IV and V). The analyses were based on the fact that all very fine grained calcite and about 4% dolomite dissolved in 20% hydrochloric acid during the first 5 to 25 seconds, whereas, all dolomite dissolved in 6 to 24 hours. Before the analyses, the less-than-2 mm fraction of each sample was ground to less than 0.0625 mm to allow for active contact with acid when it was soaked in 20% hydrochloric acid. During the analyses two readings were taken: the first reading of total CO_2 volume was taken at 20 to 30 seconds after the mixing of acid with samples, 96% CO_2 of the first reading comes from calcite and 4% from dolomite (Dreimanis, 1962); the second reading of total volume of CO_2 was taken after a complete reaction of dolomite with acid, about 24 hours later. Because

of the inclusion of about 4% CO_2 from dolomite in the first reading, the CO_2 value for calcite was corrected by deducting 4% from the first reading, and the CO_2 value for dolomite was obtained by subtracting 96% of the first reading from the second reading, i.e.

$$\textit{Weight \% of } CO_2 \textit{ of calcite} = (1-4\%) * \textit{first reading}$$

$$\textit{Weight \% of } CO_2 \textit{ of dolomite} = \textit{second reading} - \textit{first reading} * (1-4\%)$$

The weight percentages of calcite and dolomite in a sample can be calculated by the following two equations:

$$\textit{Weight \% of calcite} = \textit{weight \% of } CO_2^C * \frac{100.09(\textit{molecular weight of } CaCO_2)}{44.01(\textit{molecular weight of } CO_2)}$$

$$\textit{Weight \% of dolomite} = \textit{weight \% of } CO_2^D * \frac{96.705\ (\textit{molecular weight of } \frac{1}{2} CaM}{44.01\ (\textit{molecular weight of } C}$$

Atomic absorption analyses (AA)

Carbonate content analyses of till samples by atomic absorption methods were done at the Saskatchewan Research Council (Appendices IV and VI,). <2mm portion of till samples were soaked in 50% hydrochloric acid for 20 hours to get calcium and magnesium in solution (Ross, 1986). The percentage weight of calcium and magnesium

in the solution were determined by the atomic absorption method. From that the dolomite and calcite contents in each sample were calculated. By assuming ideal dolomite ($Ca_{0.5}Mg_{0.5}CO_3$) and assuming that there were no Ca^{++} or Mg^{++} ions derived from any other mineral, the dolomite content of a sample was calculated by dividing the percentage weight of magnesium with magnesium atomic weight (24.312), multiplying by 2, and then multiplying by the formula weight of dolomite (92.20535), that is:

$$\frac{\%weight\text{-}of\text{-}Mg}{24.312} * 2 * 92.20535$$

The percentage of calcite in a sample was calculated by dividing the percentage weight of calcium by the calcium atomic weight (40.08), minus the % weight of magnesium divided by the magnesium atomic weight (the amount of calcium borrowed in the dolomite calculation), and then multiplying by the calcite formula weight (100.09), that is:

$$\left(\frac{Ca\%weight}{40.08} - \frac{Mg\%weight}{24.312}\right) * 100.09$$

There are some problems with the atomic absorption analyses. The biggest problem may be the assumption that there was no Ca^{+} or Mg^{+} derived from other minerals. This problem will be discussed in the next section by comparison of XRD, Chittick, and AA analyses on the carbonate content of till.

XRD analysis-mineral content

Conventional X-ray diffraction (XRD) analysis was used to determine basic mineral types and abundances in till samples (Appendix VII). The purpose of this analyses was to evaluate the atomic absorption results, and to find possible sources of additional magnesium and calcium supply if there were any disagreements between the AA and Chittick analyses.

During the analyses, a tiny amount of till sample was ground to less than 0.0625 mm. A small amount of this powder was spread over a slide. The slide was then mounted in an X-ray diffractometer and was bombarded by X-rays. The intensity of the reflected X-rays was measured by XRD detectors; and signals from the detector were recorded digitally on a disc and, at the same time, printed out (Potts, 1987).

In the mineral searching stage, a PDF Search/Match Program was used to match a sample XRD pattern with standard mineral XRD pattern, which consists of a series of peaks of varying heights (intensity) and spaces ('d' space) defined by the Bragg Law ($n\lambda=2d*\text{Sin}\theta$; Potts, 1987; Jenkins, 1989). As a result, the computer will list all of the minerals that match at least a portion of the peak on the X-ray pattern, in the order of best matching to least matching. Next, the sample XRD pattern was compared manually with the standard XRD patterns of minerals on the short list of PDF search. The intensity and phi-values of these confirmed minerals were stored in Excel files.

The percentage content of a given mineral was calculated by multiplying the intensity of its strongest peak by an empirical factor (Table. 1-4), which was determined by Last (personnel communication, 1996) according to the procedure described by

Table 1-4 Factors used for quantitative interpretation of bulk mineralogy in tills of southwestern Manitoba (Last, Personal communication, 1996).

Mineral	Identification Peak (s) (2° θ)	Intensity Factor
Quartz	26.7	3.33×10^{-5}
Plagioclase	27.8-27.9	1.67×10^{-4}
K-feldspar	27.4-27.5	1.43×10^{-4}
Calcite	29.4-29.8	9.17×10^{-5}
Dolomite	30.9	1.28×10^{-4}
Total clay minaral	19.9-20.1	1.82×10^{-3}
Gypsum	11.5-11.6	5.36×10^{-4}
Hydro-magnesite	37.3-37.5	1.2×10^{-4}

Schultz (1964). This empirical intensity factor was derived from duplicate diffractometer traces of slides of the pure minerals from local or regional bedrock sources. Table 1-4 lists all the factors used in this study.

1.5.6 Comparison of XRD, AA, and Chittick methods

There were problems in carbonate content analysis using the atomic absorption method. One of the problems is negative calcite content for some samples (Appendices IV, VI), suggesting additional magnesium suppliers other than dolomite. Another problem was that, for samples from the same geographic area, the AA analysis results gave values of calcite and dolomite that were about 60 to 100% higher than determined by the Chittick method (Appendix IV). It is likely that this is due to the presence of gypsum and other calcium-bearing HCl-soluble minerals and, in fact, about 35% of the samples contain 10 to 35 % gypsum (Appendix VII). XRD analyses on selected samples suggest that about 65% of the analyzed samples contain 3 to 5% magnesium hydroxide ($Mg(OH)_2$). There is no question that gypsum can be dissolved in water to release Ca-ions. A simple test showed that gypsum crystals with a surface area from 0.5-1 cm^2 will lose about 20 (15-24) percent of their original weight in 10% HCl solution within 12 hours. Gypsum crystals are small and very abundant in till samples from the Virden area, and probably in many tills in the Prairies. High AA reading may also relate to the way the Ca^{++} and Mg^{++} concentration were calculated. This can be explained by comparing with XRD data. The total carbonate concentrations (Appendix IV, column 9) by XRD method are in the same range as the Chittick results when calcite and dolomite peaks are

weighted against all identified minerals. However, when the calcite and dolomite peaks are weighted against only selected minerals excluding clay minerals and gypsum, the derived carbonate concentrations (Appendix IV, column 11) are similar to the AA results.

Despite the problems mentioned above, Schreiner (1990) and Ross (1986) found a general linear correlation of carbonate content by Chittick method and atomic absorption method. Correlation on the total carbonate content and calcite/dolomite ratio in this study found a correlation coefficient (r) about 0.51 (Fig.1-4).

There are some problems with the XRD analysis results as well. Correlation analyses on the total carbonate and calcite/dolomite ratio between XRD and AA results, and between XRD and Chittick results does not show any linear relationships (Fig.1-4). This may be due to the fact that the XRD intensity of the first order peak, used as a measure of the percentage of calcite and dolomite, is affected by the roughness of a sample surface and the level of background (Potts, 1987; Nill Ball, 1995, personnel communication). Despite all these problems, XRD powder analysis is a good tool for qualitative and semi-quantitative analysis.

Based on the above discussion, I feel that Chittick results are the most reliable, followed by the AA analyses. In this thesis, all carbonate contents and calcite/dolomite ratios mentioned will be from Chittick analysis results, unless specified otherwise.

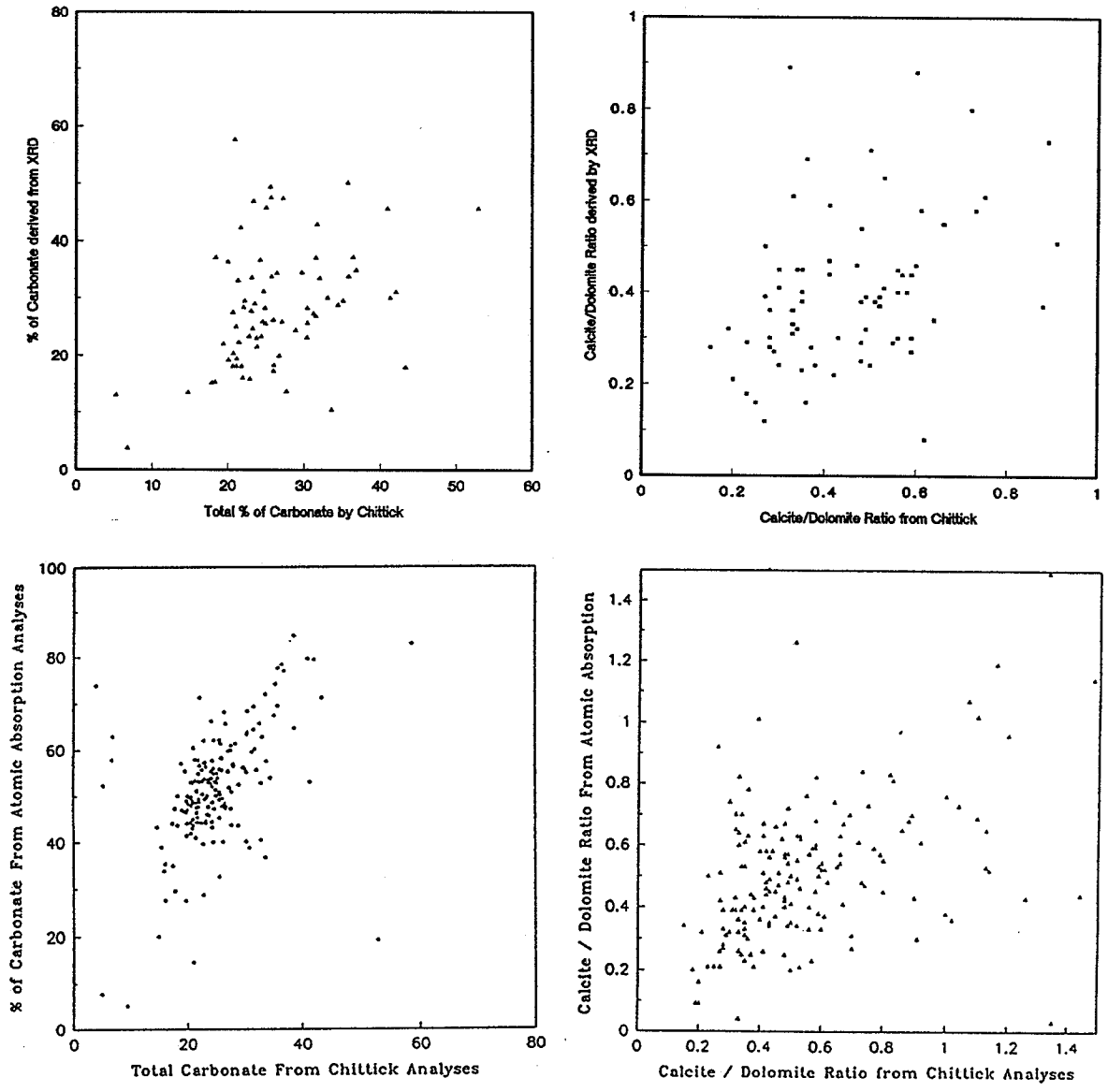

Fig. 1-4 Plot of total percentage of carbonate content and calcium/dolomite ratio from Chittick analyses against those from atomic absorption and XRD analyses. See text for details.

CHAPTER 2

GEOLOGICAL SETTING

2.1 Physiographic Divisions

The Virden map-sheet area is located entirely within the Saskatchewan Plain, which has been subdivided into the Turtle Mountain Upland, Boissevain Plain, Lake Hind Basin, Souris River Plain, and Assiniboine River Plain. Physiographic provinces that are outside of the Virden map sheet, but which are important to the study, include the Tiger Hills Upland, Assiniboine Delta, Riding Mountain Upland, Moose Mountain Upland, Lake Regina Basin, Lake Arcola Basin, Lake Souris Basin, Lake Indian Head Basin, and Lake Assiniboine Basin.

2.2 Bedrock geology

Bedrock topography is an important factor that contributes to the thickness and surficial morphology of till, glaciofluvial deposits, and lacustrine deposits. The nature of the bedrock has an important effect on the composition and texture of till and outwash.

Bedrock in Manitoba consists of three major groups: 1) Precambrian rocks, which occupy a wide zone from northwestern to southeastern Manitoba, 2) Palaeozoic rocks, which are exposed in a NW-SE belt through the Lake Winnipeg and Lake Manitoba basins, and 3) Mesozoic rocks, which outcrop west of Lake Manitoba westward into Saskatchewan (Fig.2-1). In subsurface Mesozoic and Palaeozoic rock unit dip gently to the southwest and wedge out to the northeast (Teller and Bluemle, 1983) (Fig. 2-1).

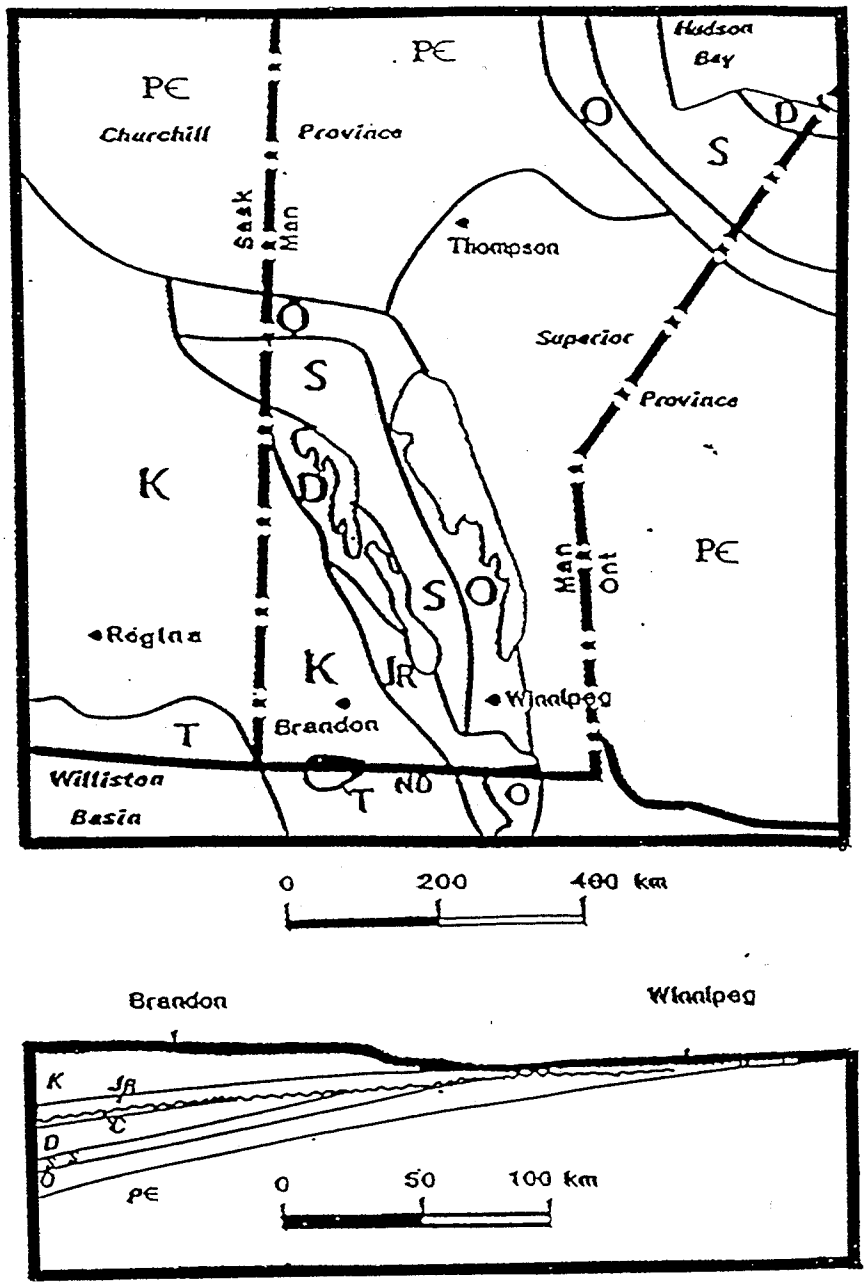

Fig. 2-1 Bedrock geology of Manitoba with W-E cross section through Brandon and Winnipeg. Pε=Precambrian, O=Ordovician, S=Silurian, D=Devonian, M=Mississippian, J_R=Jurassic, K=Cretaceous, and T=Tertiary (after Teller and Bluemle, 1983).

Precambrian bedrock:

Precambrian rocks in Manitoba have been subdivided into two geological Provinces: the Churchill Province of northwestern Manitoba and the Superior Province of eastern Manitoba (Fig. 2-1). The Archaean rocks of the Superior Province are composed of granite, greenstone, schist, and gneiss rocks. The Churchill Province includes two types of rocks: the older Archaean and Proterozoic metavolcanic granulites and granitoids and the younger Proterozoic metasedimentary supracrustal rocks (Manitoba Mineral Resources Division, 1979).

Palaeozoic bedrock:

Palaeozoic rocks in Manitoba consist of carbonate, (mainly dolostone, dolomitic limestone intercalated with some shale), and in places sandstone, conglomerate, and anhydrite (McCabe, 1971). Cambrian rock is confined to the southwestern corner of Manitoba and is not exposed. Ordovician rocks unconformably overlie Precambrian rocks in the outcrop belts. The lithology of the lower Ordovician is mainly sandstone, while the upper Ordovician and lower Devonian are dominated by dolostone (Teller and Bluemle, 1983; McCabe, 1971). The Silurian, upper Devonian, and Mississippian rocks are marked by the co-existence of anhydrite and limestone-dolostone.

Mesozoic bedrock

Mesozoic rocks are composed of mainly shales with some sandstone and thin limestones, and are overlain directly by Quaternary sediments in most parts of

southwestern Manitoba and southeastern Saskatchewan. In several small locations in the Lake Hind area, Mesozoic bedrock lies at the surface.

The oldest Mesozoic rocks in southwestern Manitoba are Jurassic in age, and consist of red shale, sandstone, and gypsum (Halstead, 1959). Cretaceous bedrock in southern Manitoba consists of six formations, and is dominated by shale, calcareous shale, and sandstone. Three of the seven formations, the Vermilion River Formation, Pierre Shale, and Boissevain Formation (McNeil and Caldwell, 1981), are exposed at the surface in the Lake Hind area. The Vermilion Formation, which consists of black and soft shale, is exposed along the Assiniboine River west of Brandon. Three members of the Pierre Shale, the Millwood Member, Odanah Member, and the Coulter Member, occur in the Lake Hind region. The Millwood Member is dominated by soft greenish brown bentonitic silty shale; the Odanah Member is dominated by hard grey siliceous shale, and is the most important bedrock in the Lake Hind area. The youngest member of the Pierre Shale, the Coulter Member, is dominated by light grey to buff clayey siltstone and shale, and occurs in the northern flank of the Turtle Mountain only. The Boissevain Formation, which is the youngest Cretaceous bedrock formation, consists of grey, brown, green sandstone and minor siltstone (Wickenden, 1945; Bamburak, 1978; Betcher, 1983).

Tertiary bedrock

The Turtle Mountain Formation is the only Tertiary bedrock and occurs in the Turtle Mountain area. It consists of grey, brown and yellow shale, sandstone, silt, and lignite that are largely unconsolidated. This formation is confined to the area underlying

Turtle Mountain (Betcher, 1983). and outcrops locally (Sun and Fulton, 1995).

2.3 Bedrock topography in the study area

The bedrock topography in southern Manitoba has been mapped by Klassen (1970), Teller et al. (1976), and Betcher (1983). In general, the elevation of the bedrock surface is shown to be lower in the Lake Hind basin, with a deep valley entrenched across its northern end (Fig.2-2). The entrenched valley extends roughly parallel to the modern Assiniboine River valley, but is not everywhere coincident with it. Branching south from this bedrock valley and extending across the Lake Hind basin into the U.S. is another narrow bedrock valley, with its own branch westward into Saskatchewan (Fig.2-2).

2.4 Quaternary deposits

Quaternary deposits blanket the bedrock, and form the local landforms. Most of the Quaternary deposits in southwestern Manitoba, including till, glacial lacustrine deposits, and glacial fluvial deposits, were deposited during Pleistocene glaciations. Only a small portion of the Quaternary deposits, which include eolian dunes, alluvium, and peat, were deposited during the Holocene or other interglacials.

Till of glacial deposits

Till is a term "applied to a sediment that has been transported by glacier ice and subsequently deposited by or from it with little or no sorting by water" (Dreimanis and

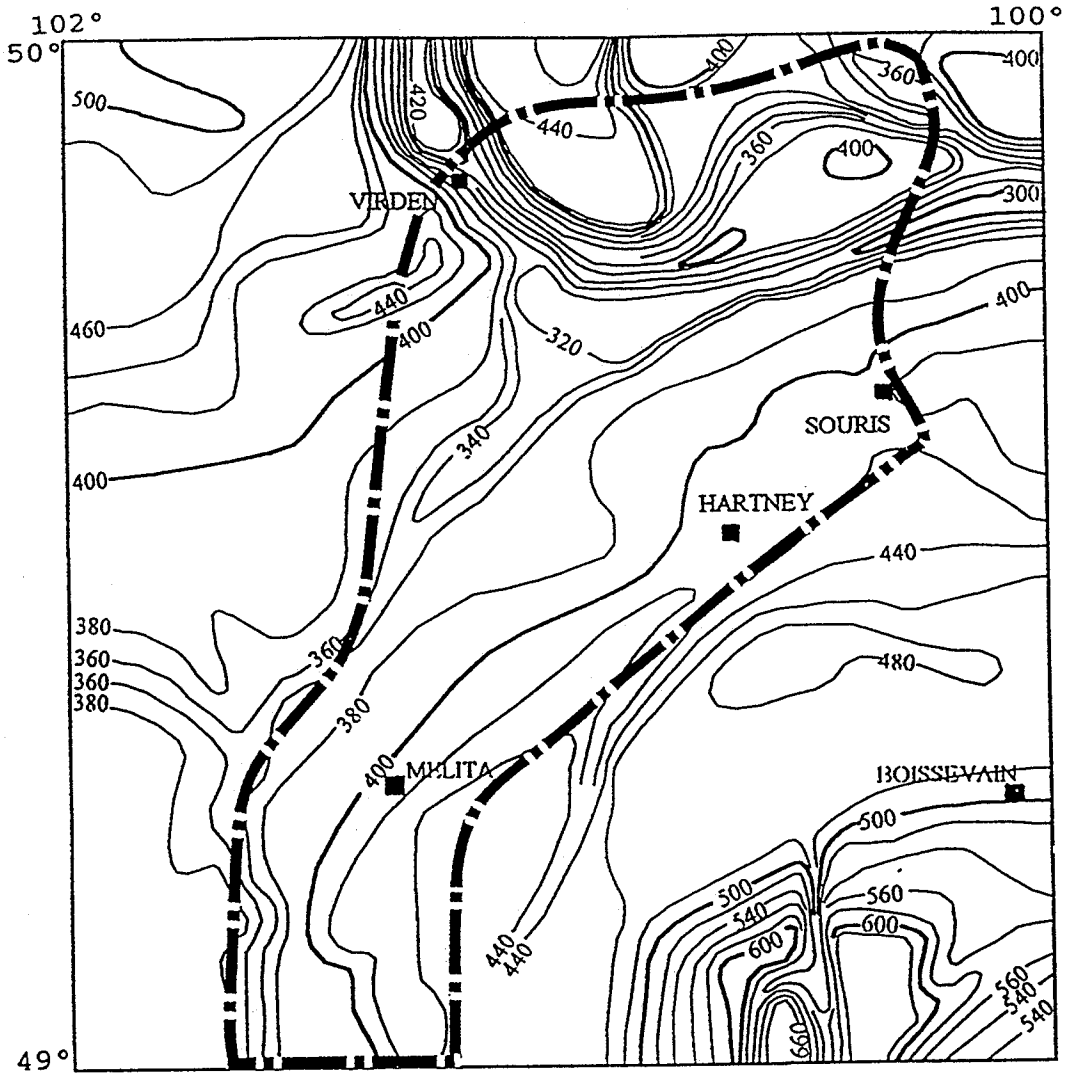

Fig. 2-2 Elevation (meters above M.S.L) of bedrock subsurface in the Lake Hind area, southwestern Manitoba (After Betcher, 1983). Dashed line shows the outline of glacial Lake Hind.

Lundqvist, 1984; Klassen, 1989). In southwestern Manitoba and southeastern Saskatchewan, till is from 10 to 120 m thick (Klassen, 1989, Figure 2-17). It is thin in the Boissevain Plain and Assiniboine River Plain and becomes thicker in the southern Souris River Plain, Tiger Hills Upland, Moose Mountain Upland, and the Riding Mountain Upland. Till is exposed at the surface in most of the area except in the Lake Hind basin and the southern Assiniboine River plain where it is either overlain by glacio-lacustrine and glacio-fluvial sediments or is absent (Fig. 2-3).

Glaciolacustrine deposits

Lacustrine deposits occur in former glacial lake basins such as Lake Hind in the Virden map-area, and in the Lake Agassiz immediately to the east which was connected to Lake Hind through the Pembina Spillway and Assiniboine River Valley (Fig. 1-1). Sediments in these lake basins consist of clay and silt, as well as sand and some gravel. Glaciolacustrine sediments in the Lake Hind area are a few meters to 60 meters thick, and consist of 2 to 25 m of sand overlying 5 to 30 m of silt and clay. In Lake Agassiz, glaciolacustrine sediments may be more than 30 meters thick (Teller et al., 1976), and consist dominantly of clay and silt except along the western side where sand is dominant.

Glaciofluvial deposits

Glaciofluvial deposits consist of sand and gravel that are mostly stratified. They occur as eskers, deltas, fans, and channel fill. Landforms of glaciofluvial deposits in the Lake Hind area include the Arrow Hill Esker, a major inter-channel bar in the

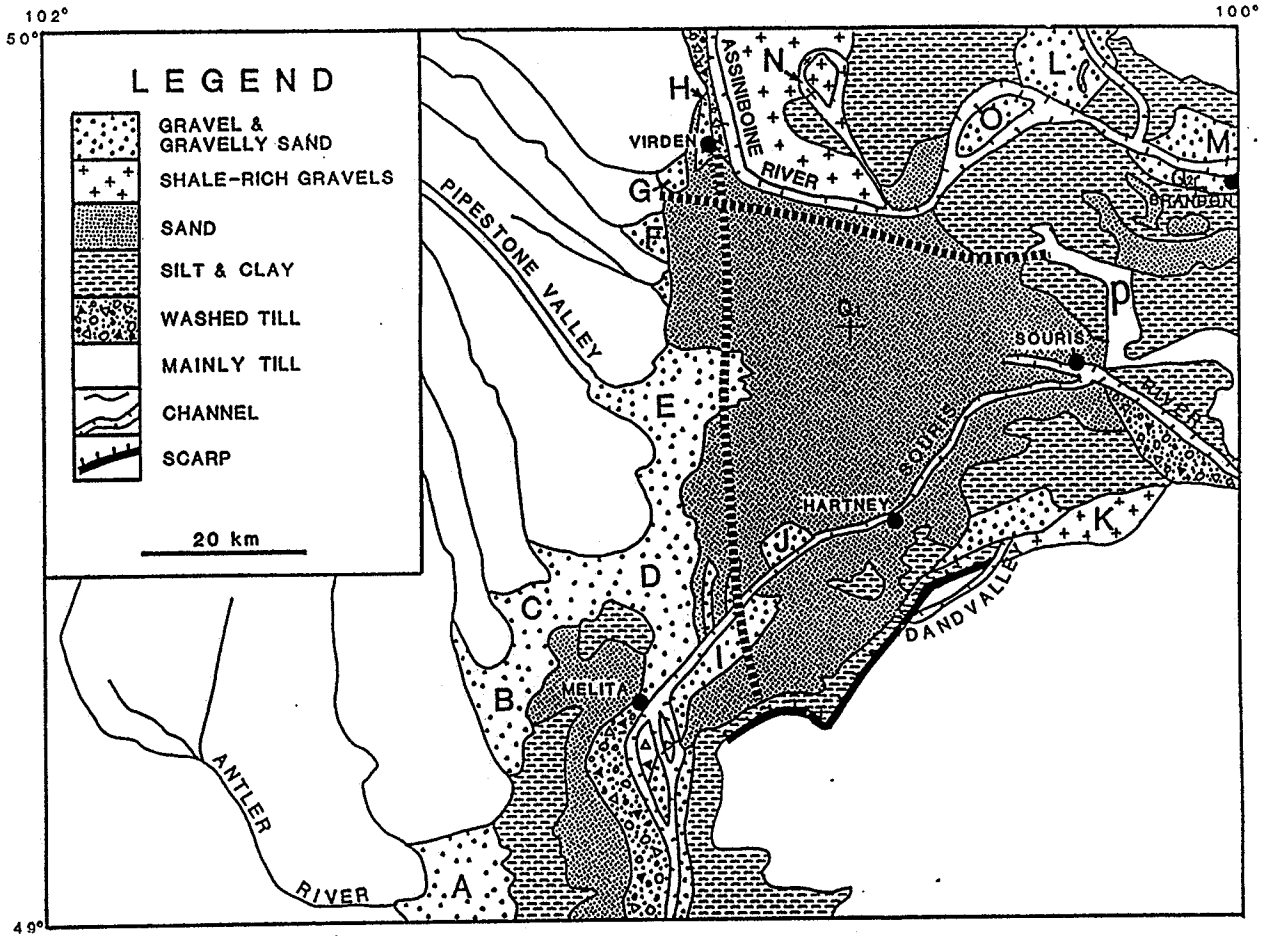

Fig. 2-3 Surficial geology and topography of the glacial Lake Hind basin (After Sun & Fulton, 1995a, 1995b). The dashed lines shows the location of the two cross sections in Figure 3-13. Letters identify location of the Antler delta (A), Graham delta (B), Jackson delta (C), Stony delta (D) Pipestone delta (E), Gopher delta (F), Bosshill delta (G), Virden delta (H), Melita delta (I), Lauder delta (J), Dand Delta (K), Little Saskatchewan delta (L), Brandon sandur (M), Arrow Hill esker (N), Assiniboine Flats (O), Alexander moraine (P), boreholes in Fig.3-9 (Q_1) and Fig.3-18(Q_2), and Darlingford moraine (R).

Assiniboine valley at Assiniboine Flat, and a number of deltas, such as the Pipestone Creek Delta (deposited by meltwater from the Pipestone Creek), Souris River Delta (deposited by meltwater from the Souris River Channel), and Little Saskatchewan River Delta (Fig.2-3) (deposited by meltwater from the Little Saskatchewan River near the town of Rivers). Major glaciofluvial landforms in the western Lake Agassiz basin include the Assiniboine Delta that was deposited by meltwater from the Assiniboine River, and the Pembina Delta that was deposited by meltwater from the Pembina Spillway (Fig.1-1).

2.5 Drainage Systems

The modern drainage system (Fig. 2-3) in the Lake Hind area can be divided into 4 areas: (1) Souris River Basin that drains south from Weyburn, Saskatchewan, to Minot, North Dakota, where it turns north toward Melita. The river flows across the Lake Hind basin in a relatively shallow and narrow channel from Melita to the head of the Pembina Spillway near Souris. The Pembina Spillway is a large deep channel that starts at the Lake Hind basin and ends at the Pembina Delta in the western Lake Agassiz basin (Fig. 1-1).

(2) West of the Lake Hind basin, a dozen roughly parallel rivers and creeks, including Pipestone River, Bosshill Creek, Stony Creek, Jackson Creek, Graham Creek, and Gainsborough Creek, start from the Moose Mountain Upland, flow southeastward to the western Lake Hind basin. Most of these turn and flow east or northeast after entering the Lake Hind basin (Fig.2-3).

(3) The Assiniboine River is the major river system in the study area. It starts

from glacial Lake Assiniboine (Fig.1-1) near Kamsack, Saskatchewan, and is joined by the Qu'Appelle Valley and the Shell Valley on the way south to Virden, where it turns east toward the Assiniboine delta in the western Lake Agassiz basin.

(4) The Little Saskatchewan River enters the Lake Hind basin from the northeast, and joins the Assiniboine River west of Brandon (Fig. 2-3).

CHAPTER 3

LITHOFACIES AND STRATIGRAPHY

3.1 Introduction

Sediments in the glacial Lake Hind area can be divided into 5 lithofacies and 9 sub-lithofacies (Table 3-1), based on their textural composition, lithology of rock fragments, sorting, and sedimentary structures. They are diamicton lithofacies, gravel lithofacies, sand lithofacies, sand-mud couplets, and mud lithofacies. In the following sections, each lithofacies is introduced with a general description, followed by detailed sub-divisions. I also will discuss lithofacies that occur in the Souris River valley, Moose Mountain valley, Pipestone valley, and Assiniboine River valley because they are important in reconstructing the history of meltwater flows from glacial lakes Regina, Indian Head, and Arcola to glacial Lake Hind. Following the description of lithofacies and sub-lithofacies are the discussions of general surface landform and geographic distribution of each lithofacies and sub-lithofacies, surface elevation and late glacial elevation of deltas, and description of stratigraphy. The purpose of these discussions is to pave the way for investigating the depositional environments and hydrodynamics of lithofacies and for reconstructing the history of deglaciation and meltwater discharges in the glacial Lake Hind region.

TABLE 3-1 FACIES CLASSIFICATION

LITHOFACIES	SUBLITHOFACIES		DESCRIPTION
DIAMICTON (D)	LOW $CaCO_3$ (Dl)		Carbonate content: 17-28% calcite/dolomite ratio: 0.2-1 carbonate/Shield rock ratio: <2
	HIGH $CaCO_3$ (Dh)		Carbonate content: 24-45% calcite/dolomite ratio: 0.2-0.7 carbonate/Shield rock ratio: >2
GRAVEL (G)	Massive (Gm)	Matrix supported (Gm)	Poorly sorted, non-stratified 50-70% sand and mud 30-50% gravel
		Clast supported (Gc)	Massive to stratified sand and mud: <50% gravel: >50%
		Pebbly sand (Gms)	Massive, non-stratified non-graded, lack silt and clay 5-20% pebbles
	Cross bedded (Gx)		Cross bedded Graded
SAND (S)			Massive to stratified well sorted to poorly sorted gravels: <5%
SAND-MUD COUPLET (Sl)			Interbeddings of sand and mud sand beds: 0.1-1.8m-thick clay&silt beds: 0.3-1.6 m-thick
MUD (M)	Massive (Fm)		Massive, non-stratified some dropstones
	Laminated (Fl)		Couplet beds of silt and clay silt beds: 20-100 cm-thick clay beds: 1-5 cm-thick

3.2 Description of Lithofacies

3.2.1 Diamicton Lithofacies (D)

Although lenses of well sorted gravel and sand are common in some places, the majority of the diamicton lithofacies consists of unsorted, matrix-supported, non-graded, and slightly stony mixture of sand, silt, and clay (Fig. 3-1). The average textural composition of 222 samples is 7% gravels, 38% sand, 34.5% silt, and 20.5% clay (see Appendix III for percentage of sand, silt, and clay). Many lithologies are present in the gravel-sized fraction; most of these are carbonate (15 to 55%), Shield rocks (granite, basalt, and metamorphic rocks) (10-40%), and shale (10-50%) (Appendix II). There are also some sandstone, quartzite, chert, ironstones, lignite particles, and poorly lithified reddish silt clasts. The sand-sized particles are dominantly quartz, feldspar, and shale fragments, with some lignite fragments and reddish silt clasts. In some areas where the diamicton unit overlies bedrock directly, the shale content can reach as high as 90%.

The diamicton lithofacies can be divided further based on 1) total carbonate contents and calcite/dolomite ratios (Fig. 3-2), and 2) carbonate/Shield rock ratios (Fig. 3-3). Carbonate content has been used alone by Klassen (1979) to define seven till units in the Riding Mountain, Duck Mountain, and Assiniboine River Plain, and by Christiansen (1979) to identify till stratigraphy in the central Saskatchewan area. In the glacial Lake Hind area, a plot of total carbonate content against calcite/dolomite ratio successfully distinguishes two surface till units (Fig. 3-2). The low-carbonate diamicton sub-lithofacies has low-carbonate content and high calcite/dolomite ratio, based on Chittick analysis results, while the high carbonate sub-lithofacies has a high carbonate

Fig. 3-1 A photograph of diamicton lithofacies (Dh) from a river-cut near the town of Wawanesa at Sec.23 Tp7 R17W (see also Fig. 3-18). The pick is placed over a pinkish olive till bed that is sandwiched by olive grey till beds above and below the pick. The pick handle is about 0.55 m long.

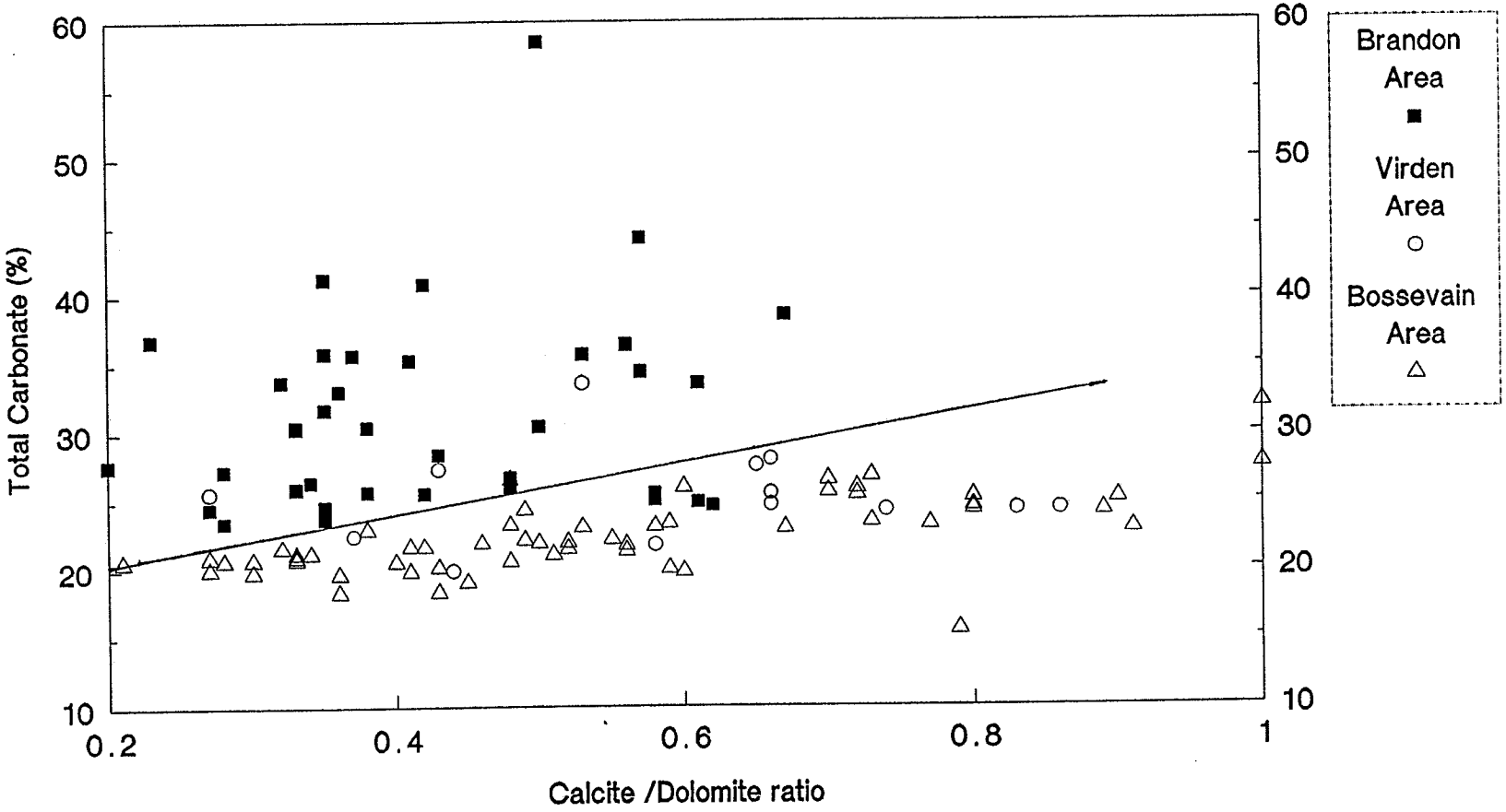

Fig. 3-2 Plot of total carbonate content against calcite / dolomite ratio of Chittick analysis results on surface till samples from the Virden, Brandon, and Turtle Mountain areas.

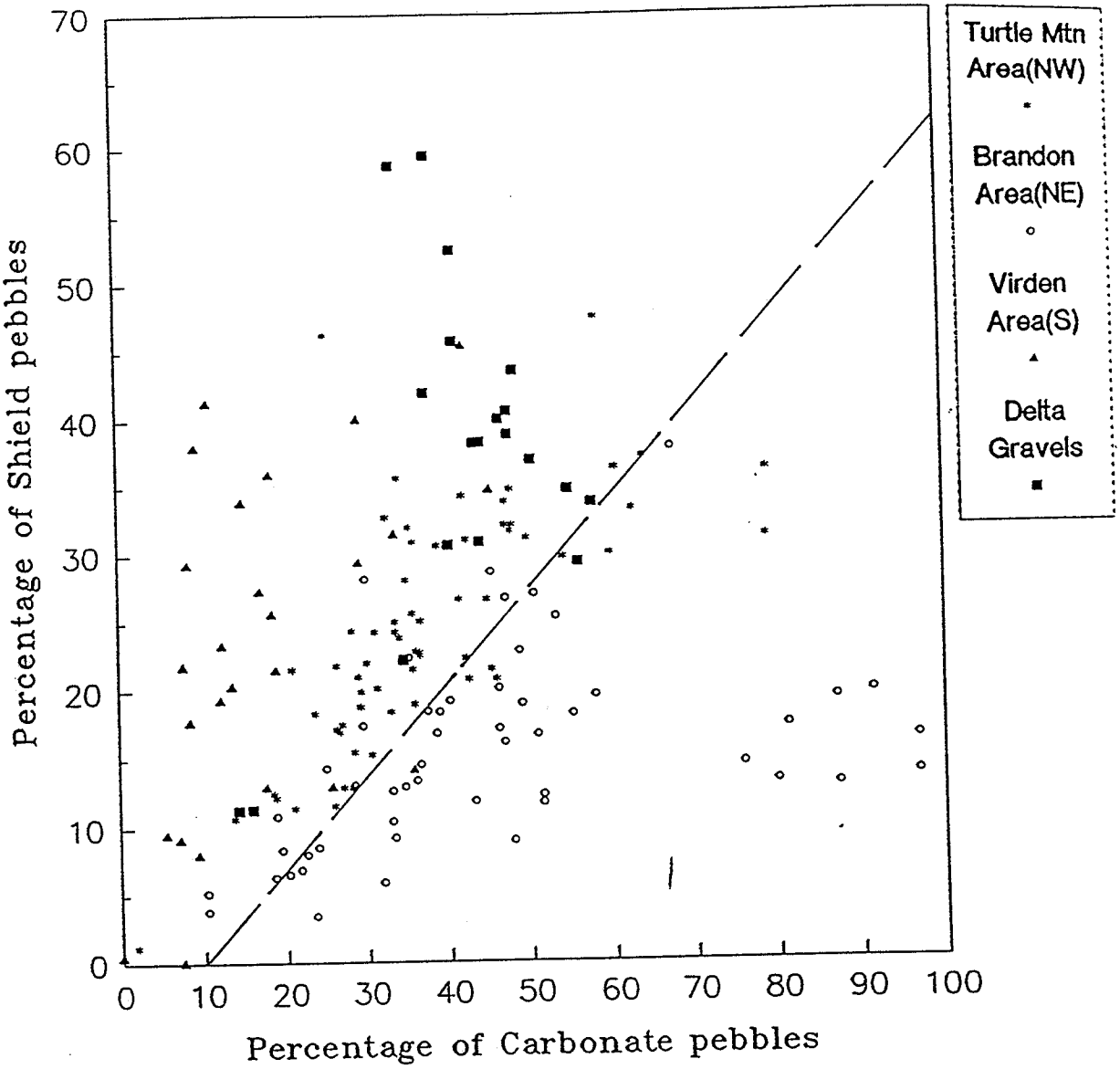

Fig. 3-3 Plot of percentages of carbonate pebbles against shield pebbles (granitic, metamorphic, and basaltic rocks). Notice 1) Surface till samples from the Brandon area (Dh) have higher percentages of carbonate rocks and lower percentages of shield rocks (Lower right half of the diagram) than till samples from the Virden and Turtle Mountain areas (Dl) (upper left half); 2) Deltaic gravels fall in the region of the Virden and Turtle Mountain tills (Dl), with the highest average percentage content of Shield rocks. The solid line indicates a carbonate/Shield rock ratio of 2:1.

content and low calcite/dolomite ratio. This subdivision can also be confirmed by using carbonate/Shield rock ratios.

Diamicton lithofacies with low carbonate (Dl sub-lithofacies)

Chittick analyses on silt and clay sized portion of this sub-lithofacies gives carbonate contents mostly from 17 to 28%, and a calcite/dolomite ratio from 0.2 to 1 (Fig. 3-2; Appendices IV, V). It consists of 34 to 60% sand, 25 to 51 % silt, 16 to 32% clay (Appendix III, Brandon area), and 5 to 15 % pebbles. Pebble counting results show a carbonate/Shield-rock ratio less than 2:1 (Fig. 3-3). In fresh exposures, the Dl sub-lithofacies is generally olive grey (5Y 5/2, 5Y 4/2) to olive (5Y 4/3, 5Y 4/4), which is lighter in color than the underlying tills. The base of this lithofacies is often marked by a boulder pavement, or lenses of sand and silt. Where a boulder pavement is exposed, striations on the boulders are oriented in a NW-SE direction.

Diamicton lithofacies with high carbonate (Dh sub-lithofacies)

This lithofacies is generally more clayey than the Dl sub-lithofacies, and is characterized by a higher carbonate content, which ranges from 24 to 58%, in contrast to the Dl sub-lithofacies, which has values of 17 to 28%. It commonly consists of 11-44% sand, 32-51% silt, 15-35% clay, (Appendix III, Virden and Boissevain areas) and 10 to 20% gravels. The carbonate/Shield rock ratio in pebbles ranges from 2:1 to 20:3, which means this lithofacies generally has many more carbonate pebbles than Shield pebbles (Fig. 3-3), in contrast to Dl sub-lithofacies which has values between 1:4 and

2:1. The oxidized surface of Dh lithofacies is generally more yellowish or pinkish than the Dl sub-lithofacies. Furthermore, a 0.5-m-thick, pinkish olive zone, which has a carbonate content over 60%, often exists at or near the surface of Dh sub-lithofacies (Fig. 3-1).

3.2.2 Gravel lithofacies (G)

The gravel lithofacies consists of poorly sorted to well sorted gravels, sandy gravels, pebbly sand, and boulder gravels. This lithofacies differs from the diamicton lithofacies because it has a low clay and silt content (<10%), it lacks reddish coloured silt clasts, and it differs from the finer-grained pebbly sand and sand lithofacies by having at least 20% gravels or boulder sizes. The lithological composition of pebbles of 4 mm to 16 mm in diameter is similar to that of the low-carbonate diamicton sub-lithofacies (Dl) (Fig. 3-3, Appendix II), and includes shale, carbonate, granitic, metamorphic, and basaltic pebbles. The average carbonate /Shield rock ratio is 1:1.

Based on the sedimentary structures and the percentage of fine matrix material, the gravel lithofacies can be subdivided into massive gravel sub-lithofacies (Gmm, Gmc, and Gms) and cross stratified gravel sub-lithofacies (Gx) (Table 3-1).

Massive gravel sublithofacies (Gmc, Gmm, and Gms)

This lithofacies has three subdivisions based on the amount of matrix and sorting: clast supported massive gravel sublithofacies (Gmc), matrix-supported massive gravel sublithofacies (Gmm), and pebbly sand sub-lithofacies.

The clast-supported massive gravel sublithofacies (Gmc) is composed of 50 to 100% clasts ranging in size from granules to boulders, up to 50% sand, and rare silt and clay sizes in the matrix. The majority of clasts are in contact, and are poorly sorted to well sorted. The matrix component can be moderately sorted or very poorly sorted sand, silt, and clay. Where there are no shale fragments, most clasts are well rounded and do not display any visible imbrication (Fig. 3-4).

Shale-fragment dominated gravel is a special kind of the clast supported massive gravel sublithofacies (Gmc), in which shale fragments make up 20 to 95% of the clasts; These fragments are pebble- to boulder-sized, subrounded to angular, with an open framework. Non-shale gravels are pebble- to granule-sized, well rounded, and are mostly carbonate and granitic rock types. The sand-sized matrix particles are also dominated by shale fragments, but with slightly more non-shale fragments than the gravel portion.

The matrix-supported massive gravel sublithofacies (Gmm) contains 50 to 80 % matrix material, which consists of poorly to moderately sorted fine to coarse sand, granules, and some silt and clay. The finer-than-sand content is generally less than 5 %. It is different from the clast-supported gravel sub-lithofacies by having more matrix content, and differs from the pebbly sand lithofacies by having 20% to 50% gravels (Fig. 3-5). Clast sizes range up to 20 cm in diameter and the majority are not in contact with one another; outsized clasts can be as large as 40 cm in diameter. There is no apparent imbrication, stratification, nor grading. This lithofacies is generally less than 6 m thick and in most cases it has no overlying fine-grained capping beds.

Fig. 3-4 Clast supported, massive gravel lithofacies (Gmc). This photograph was taken from a gravel pit at Sec.15-Tp12-R21W, in the proximal Little Saskatchewan delta (L of Fig. 2-3). Boulders are mostly 30 to 50 cm in diameter.

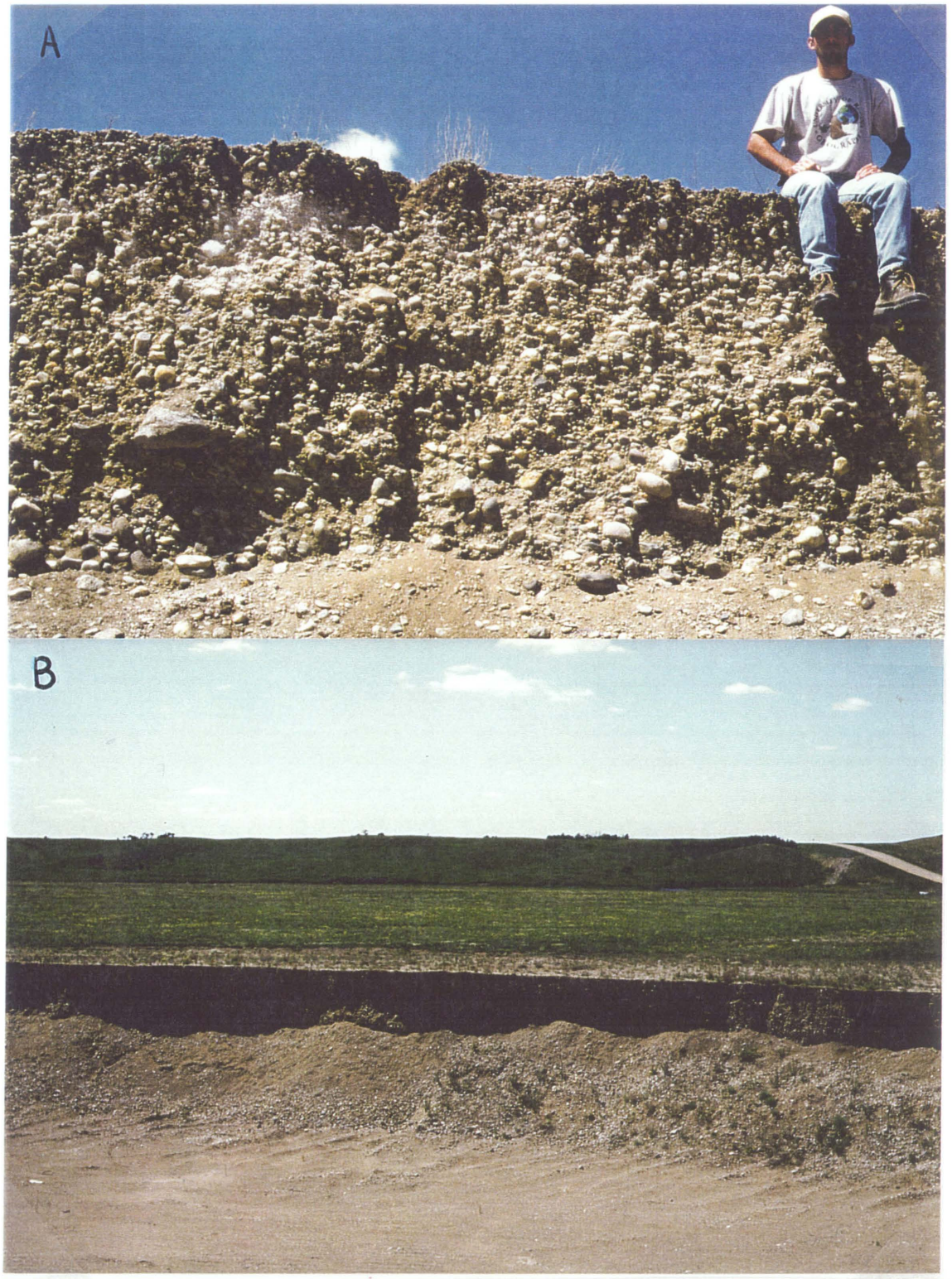

Fig. 3-5 Matrix-supported pebbly gravel lithofacies with dirty sand, and granule matrix (Gmm). These photographs were taken at the northern end of glacial Lake Arcola in southeastern Saskatchewan (Fig. 1-1) (Sec.36-Tp11-R9). A) a close view; B) Flat surface of Gmm on valley floor (no fine cap beds).

The pebbly sand sub-lithofacies (Gms) is a special case of matrix-supported gravel sub-lithofacies. It consists of mainly medium to coarse sand, and 5 to 20% granules and pebbles that are up to 10 cm in diameter (Fig. 3-6). Clasts are either dispersed in sand, or concentrated at the base of individual beds that are graded. Most sediments are massive and structureless in exposures (Fig. 3-6). This sub-lithofacies differs from the matrix-supported gravel lithofacies (Gmm) in that the pebbly sand lithofacies has finer and less gravel, and is better sorted than the matrix supported gravel lithofacies.

Cross-stratified gravel sublithofacies (Gx)

This lithofacies consists of cobbles, pebbles, granules, and coarse-grained sand that are planar cross-bedded, trough cross bedded, or hummocky cross-bedded. Gravels and granules are mainly clast supported, with an open framework or pores that are filled by sand. Most individual cross beds in this sub-lithofacies dip at an angle between 24 to 30 degrees (Fig. 3-7).

The hummocky cross-bedded gravels consist of cobbles and pebbles that are well sorted, with a hummocky surface. Fine gravels generally show trough and planar cross bedding, and have a flat surface that may be armoured by boulders near the surface. Coarse gravels and some boulders display hummocks and closed depression that have 5 to 15 m relief, whose cross bedding appears to conform to the hummocky surface (Fig. 3-8). Individual cross bedded units are 1 to 2 m-thick, and are separated from other units by a cobble layer that is about 0.2 m- thick.

Fig. 3-6 Pebbly sand lithofacies (Gms). This photo was taken from a gravel pit in the Bosshill delta at Sec.21-Tp10-R26W (G of Fig. 2-3), about 1.6 km west of the town of Virden.

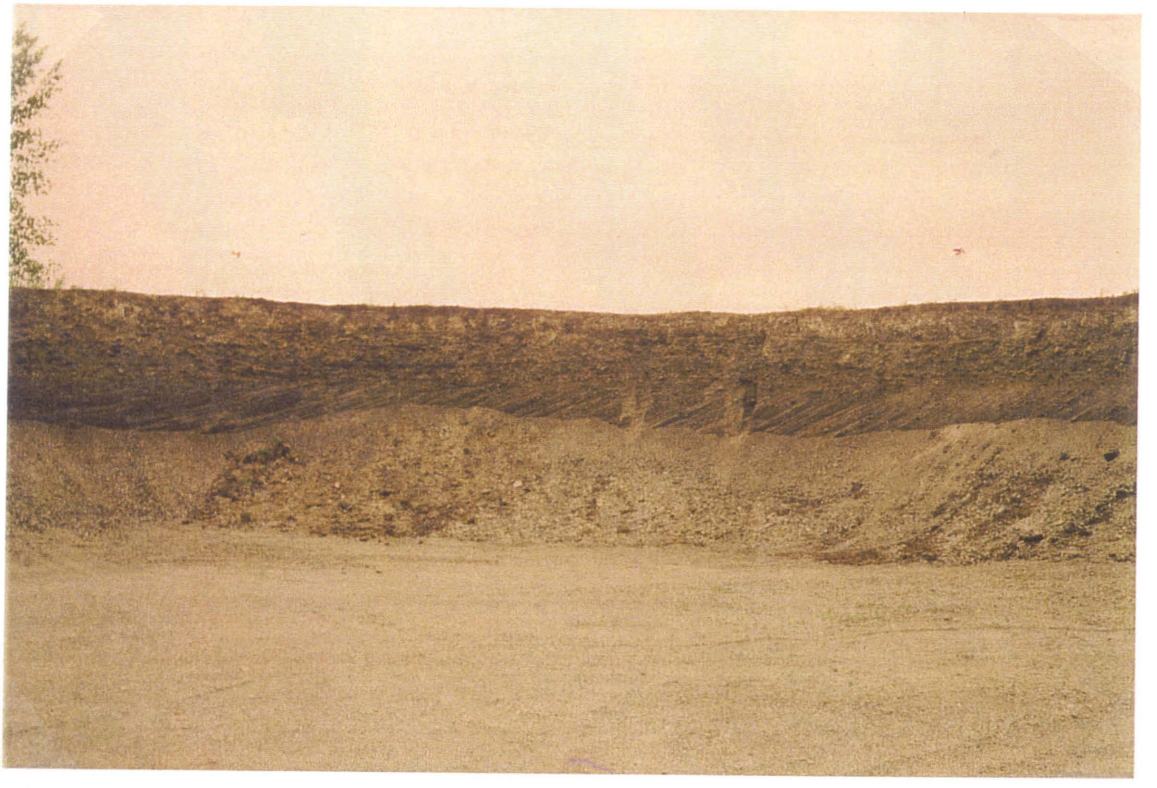

Fig. 3-7 Planar cross stratified gravel sub-lithofacies (Gx). This photograph was taken from a gravel pit in Sec.19-Tp6-R20W in the distal Dand delta (K of Fig.2-3). A 2 m-thick bed of massive shale-rich gravel overlies 4 + m-thick cross bedded fine sandy gravels. Photo looks northeast.

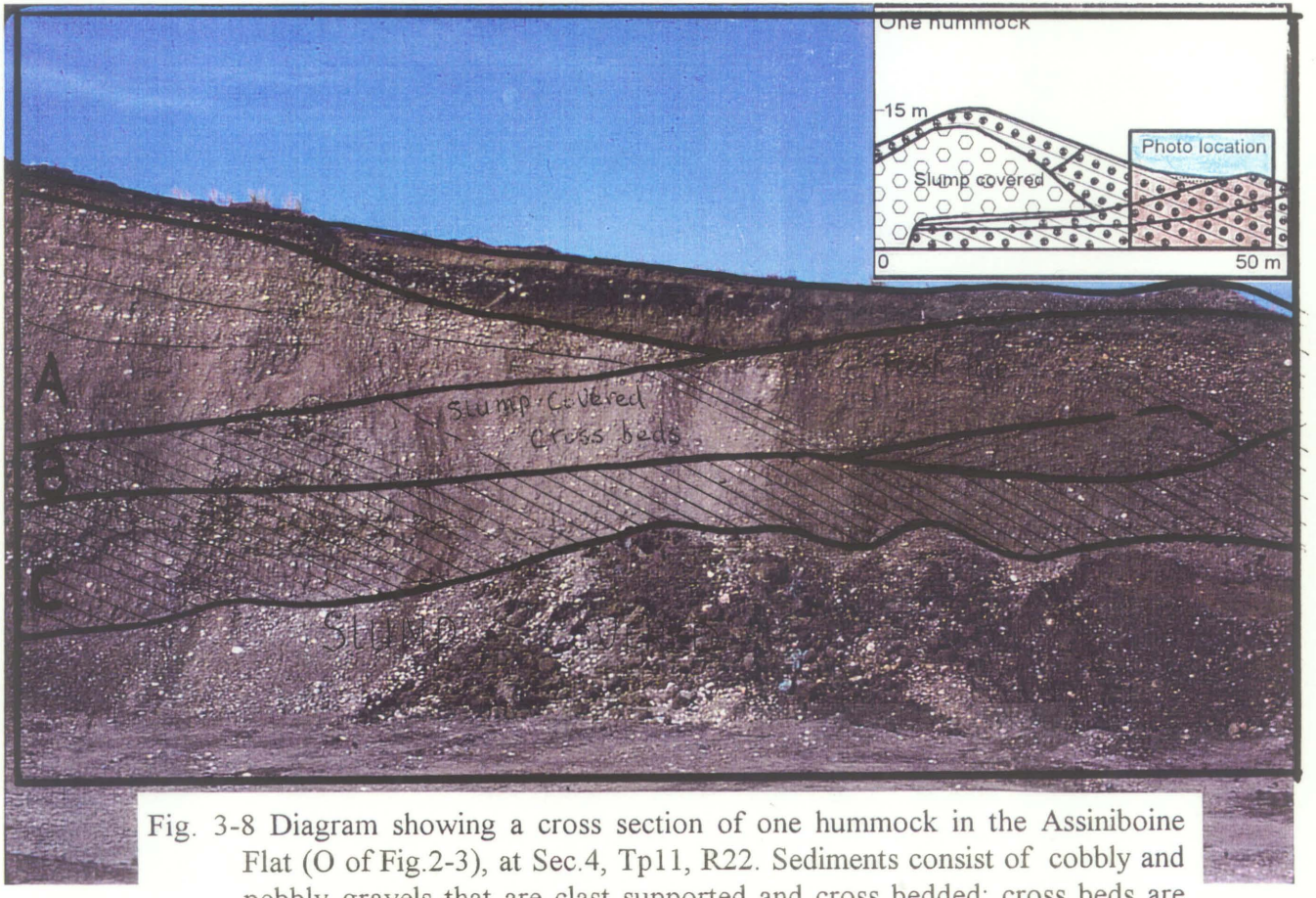

Fig. 3-8 Diagram showing a cross section of one hummock in the Assiniboine Flat (O of Fig.2-3), at Sec.4, Tp11, R22. Sediments consist of cobbly and pebbly gravels that are clast supported and cross bedded; cross beds are comformable to the surface of individual hummocks and are separated from each other by a 20 to 30-cm-thick layer of cobbles. See Fig. 4-1 for interpretation.

3.2.3 Sand lithofacies (Sm)

The sand lithofacies is comprised of coarse, fine, and silty sand that is moderately well sorted to very well sorted, and which is occasionally interbedded with thin gravel beds and silty beds. Most of the sand lithofacies from bore-holes and from dug-outs appear massive and non-graded, but some show horizontal bedding and ripples near river mouths. At one exposure a 0.5-m-thick fine sand unit at the top of a fining upward sequence displays climbing in-drift ripples that have fine internal cross lamination. Lignite, which commonly occurs in sand of the glacial Lake Souris basin in North Dakota (Lord, 1988), are rare in sand of the Sm lithofacies of the glacial Lake Hind basin.

3.2.4 Sand-mud couplet lithofacies (Sl)

This lithofacies is revealed only in bore-holes in central Lake Hind (Fig. 3-9). It consists of interbedded sand and mud beds. Sand beds are 0.1 to 1.8 m-thick and are composed of fine to medium grained sand that is laminated in the lower sequence and becomes massive in the upper sequence; mud beds are 0.3 to 1.6 m-thick and structureless. There is no sign of organisms or bioturbation in the silt and clay beds.

3.2.5 Mud lithofacies (F)

Homogeneous mud sub-lithofacies (Fm)

The mud lithofacies is comprised of silty clay, clayey silt, sandy silt, and sandy clay that is homogeneous, massive or subtly laminated. It occasionally contains granule-

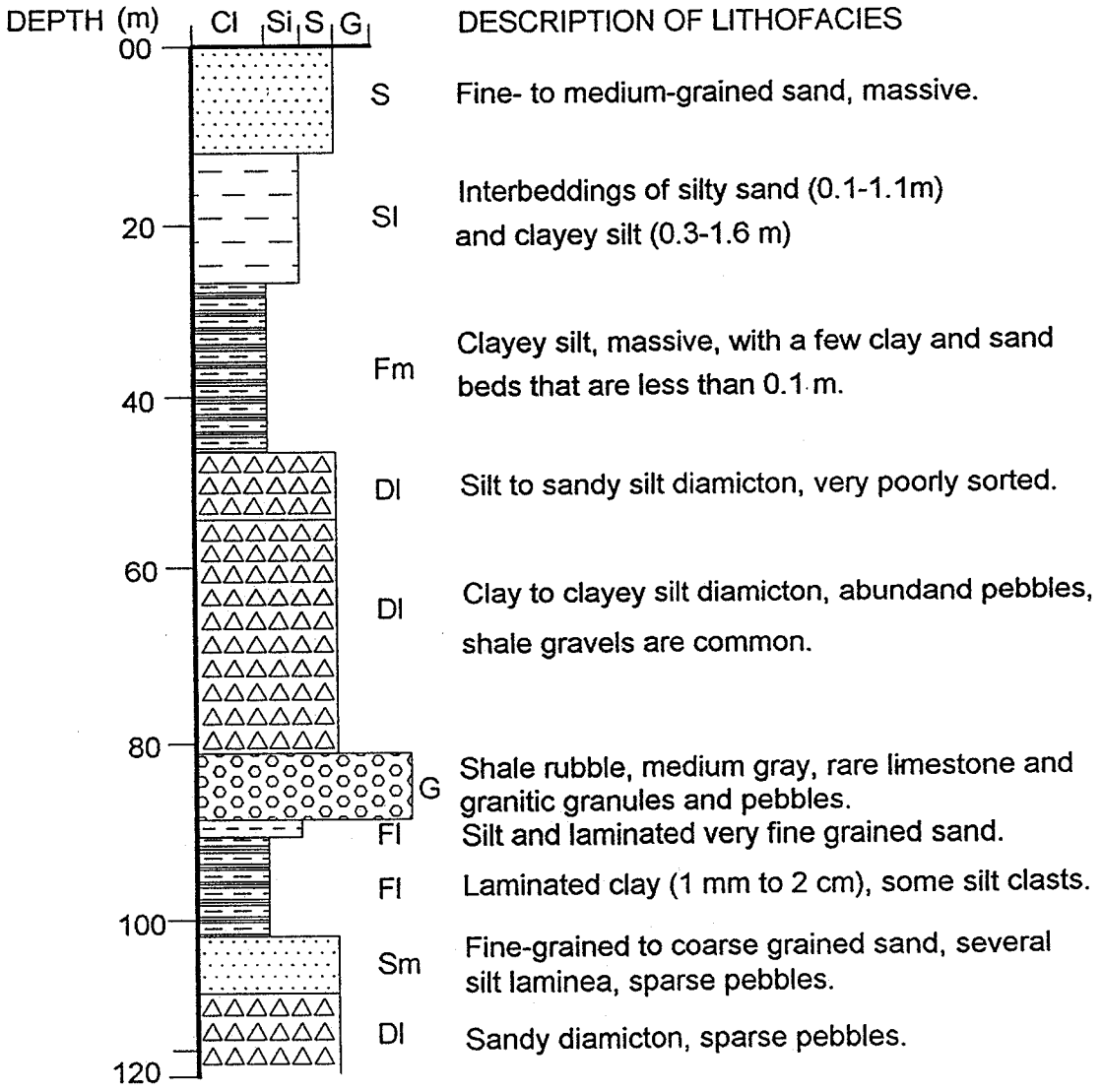

Fig. 3-9 Stratigraphic column of borehole 92TCA-DD. This borehole is located at Q1 of Fig.2-3, and is about 16 km east of the Pipestone delta (E of Fig.2-3). (after Matile, 1992, unpublished core descriptions of Virden area).

to pebble-sized dropstones and till clasts, and beds of sand, pebbly sand, and fine gravels that are massive, poorly sorted, and 1 cm to 10 cm thick. Interbedded sediments normally comprise no more than 10 % of the outcrop area of the mud lithofacies. The thickness of this lithofacies ranges from a few meters in exposures to 30 meters in well logs. Microscopic examination of the clayey silt and coarse silt samples at various depths from a core in the central glacial Lake Hind basin (borehole 92TCA-DD, Fig. 3-9) failed to find any diatoms or ostracodes.

Silt and clay rhythmites (Fl)

Rhythmitic silt and clay sublithofacies is exposed only in the southeastern and northeastern corners of the glacial Lake Hind basin. In Victoria Park of the town of Souris in the southeastern part of the basin, a 2-m-thick sequence of silt-clay rhythmites is overlain by 2-m-thick massive silt and clay, and is underlain by 4+ m of stratified gravels that contain pebble and cobble sized clasts of agate, petrified wood, and low grade coaly fragments (The Souris Gravels). The rhythmitic silt and clay sublithofacies here consists of 1 to 5-cm-thick clay beds and 5- to 50-cm-thick silt beds (Fig. 3-10). Sediments in the silty beds are massive, and contain lenses of poorly sorted gravel, sand, and till clasts. Where this sublithofacies is exposed in the northeastern corner of the glacial Lake Hind basin it is identical to that of the exposure in Victoria Park of Souris.

3.3 Geographic distribution and surface landforms of lithofacies

In this section I will first discuss the geographic distribution and surface

Fig.3-10 Laminated mud lithofacies (Fl). This photograph was taken from Victoria Park in the town of Souris (Sec.33-Tp7-R21W). Couplets consist of 1 to 5-cm-thick clay and 10 to 50-cm-thick silt. Dropstones and till clasts are common in the silt beds, and a large oval till clast can be seen below the knife. There is no till beneath the laminated silt and clay beds. The knife is 25 cm-long.

landforms of lithofacies. The purpose of these discussion is to pave the way for reconstruction of paleo-lake levels and deglaciation history.

From Figures 2-3, 3-11, and 3-12, and the surficial geological maps of Sun and Fulton (1995a, 1995b), it can be seen that the geographic distribution of diamicton, gravel, sand, and mud (silty clay) lithofacies follows a geographic pattern. In general, diamicton lithofacies occur peripheral to glacial Lake Hind basin; deltas occur along the western, southern, and northeastern margins of the lake basin; sand and most mud lithofacies occur within the basin.

3.3.1 Diamicton lithofacies

High-carbonate diamicton sub-lithofacies (Dh)

The high-carbonate diamicton sublithofacies is located in the Brandon area, east of the Alexander moraine (P of Fig. 2-3). A type section of the high-carbonate diamicton sub-lithofacies is located in the eastern town of Wawanesa, where a 40-m-high river-cut exposes two diamicton units and two lacustrine silt units that overly shale bedrock. The 3-m-thick high-carbonate diamicton sub-lithofacies, which is sandwiched in-between two 2-m-thick lacustrine silt units, includes a marker bed of light pinkish brown (5YR 6/4) till about 0.1 to 0.5 m-thick, whose carbonate content ranges from 35 to 53 %.

The high carbonate diamicton sub-lithofacies has three types of surface landforms: high ridges (end moraine), broad low ridges with potholes (end moraine), and flat till plains. Both the high ridges and broad low ridges with potholes are associated with the Alexander moraine. Flat till plains occur east of the end moraine.

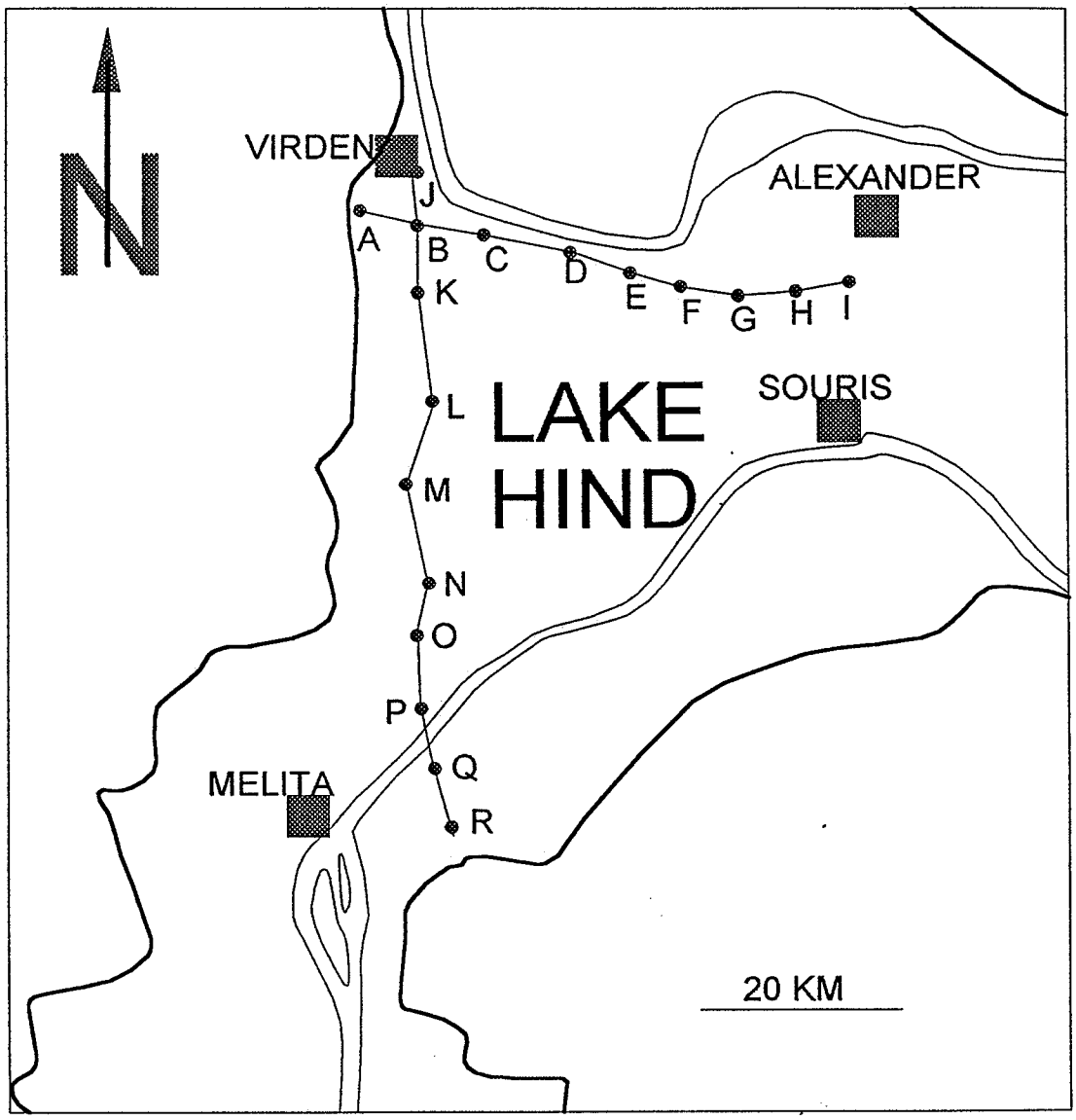

Fig.3-11A Location cross-sections shown in Fig.3-11B

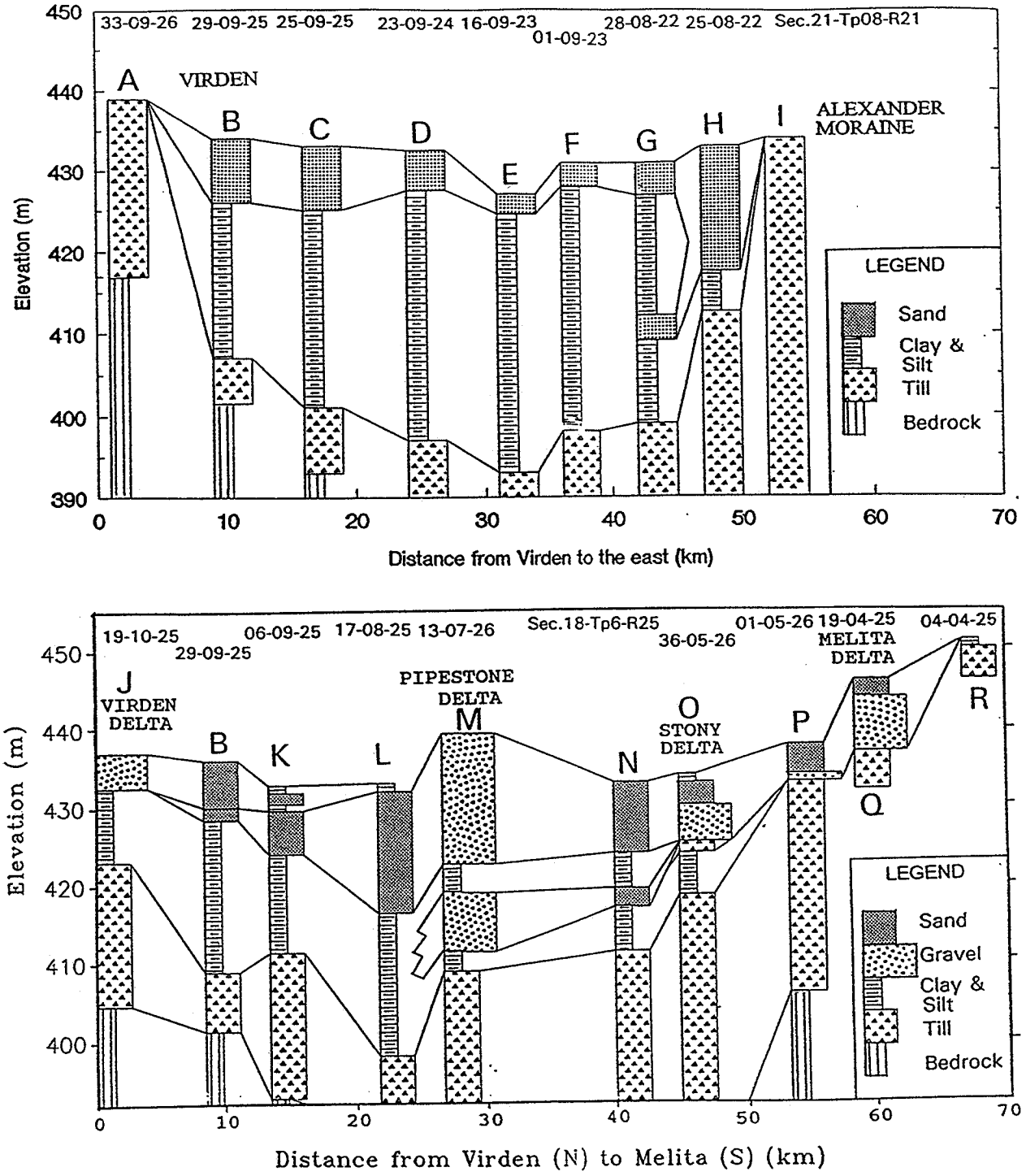

Fig.3-11B Sections across the glacial Lake Hind basin. A) a west-east section across the northern basin from Virden to the Alexander moraine. B) a north-south section across the western basin; Locations are shown as solid lines in Fig. 3-11A (log data from water well database of Manitoba Water Resources Branch).

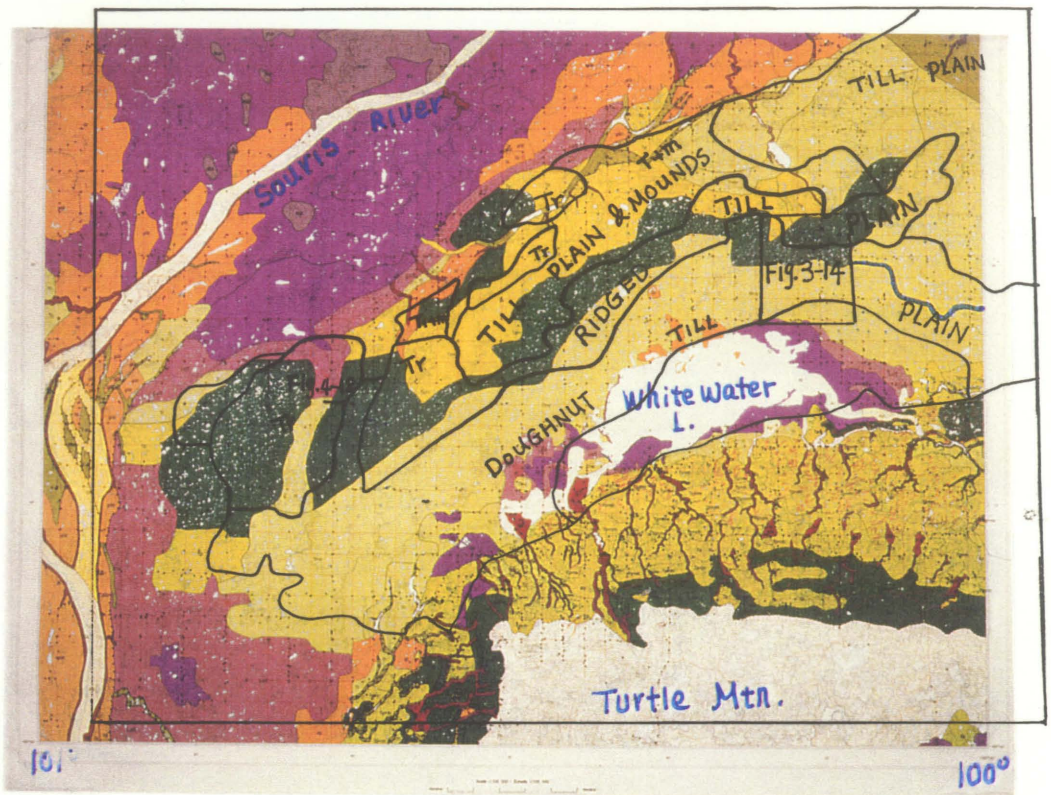

Fig.3-12 Surficial geology of SE1/4 of Virden sheet (62F), showing subparallel zones of ridged till plain and flat till plain with abundant doughnuts. White = Whitewater Lake, orange = deltaic gravels, purple = lacustrine sand and silt, green = tills. All tills are Dl sub-lithofacies, and are subdivided into three zones: Tr = ridged till plains and T+m = till plain with mounds (From Sun and Fulton, 1995b).

The Alexander moraine is composed of broad low ridges that are up to 8 km wide; this moraine stands 7 m higher than the lacustrine plains to the west and east. The ridge consists mainly of the glacial diamicton lithofacies (Dh), which is blanketed by a very thin bed of silt and clay at the northern end and on the flanks to the west and east. This broad low till ridge merges eastward into the Darlingford Moraine on the Tiger Hills Upland (Sun, 1993a; Conley, 1986), and is separated from a 15-m-high ridge (end moraine) to the north by the Assiniboine River.

Low-carbonate diamicton sublithofacies (Dl)

The low-carbonate diamicton sub-lithofacies has been identified west and south of the glacial Lake Hind basin. West of the basin in the Virden area, the surface of this diamicton sublithofacies is generally flat and scattered with broad, parallel, and arcuate ridges that are less than 5 m high and are oriented west-east (Fulton et al., 1994); this sublithofacies area is an extension of the corrugated moraine area mapped by Klassen (1979) in the Riding Mountain map area to the north.

South of the glacial Lake Hind basin in the Boissevain area, the surface of the low-carbonate diamicton sub-lithofacies (Dl) shows subparallel zonation toward the southeast: from till plain with low mounds (T+m), to ridged till plains (Tr), to silt-veneer over flat till plain with doughnuts (doughnut plain, Tl+C), and to level lacustrine plain at the Whitewater Lake (Fig. 3-12). The first zone south of the glacial Lake Hind basin is till plain with low mounds and superimposed short ridges that have a relief from 2 to 5 m and are oriented northwest-southeast. The second zone, the ridged till plain,

has two sets of perpendicular ridges. The higher ridges are oriented northeast-southwest and spaced at an interval of 250 m to 1 km. Each ridge is 0.5 to 10 km long, 50-175 m wide, and 5 to 10 m high. Sediments at the crest of these ridges can be till, sand, gravel, or sheared blocks of shale bedrock, while sediments in depressions are a veneer of silt over till. The second set of ridges are much narrower (10 to 40 m) and lower (2 to 5 m) than the high ridges, and are oriented perpendicular to the high ridges. Sediments in the surface 1 m of the minor ridges are mainly till. The third zone is a doughnut plain, where there are abundant closely spaced circular rim-ridges that are 0.5 to 1 m high and that typically outline shallow depressions (Fig. 3-13). A single depression and its rim-ridge is generally 200 to 400 m in diameter, consists dominantly of an admixture of silty clay and organic material in the central depressions, and diamicton or a silt veneer over diamicton in the rim-ridge. Farther to the south is the flat lacustrine plain (Fig. 3-12), which occurs mainly in the area around Whitewater Lake.

On the satellite image in Figure 3-14, doughnut landforms do not shown up and are replaced by narrow and paired ridges that are oriented in the same direction as the high ridges in the ridged till plain. Each pair of narrow ridges links with one high ridge in the ridged till plain and shows a smooth transition. In some cases a pair of narrow ridges in the doughnut till plain grades into a broad and low ridge first before it links to a single high ridge in the ridged till plain. The significance of this observation will be discussed in depositional environments of glacier deposits in Chapter 4.

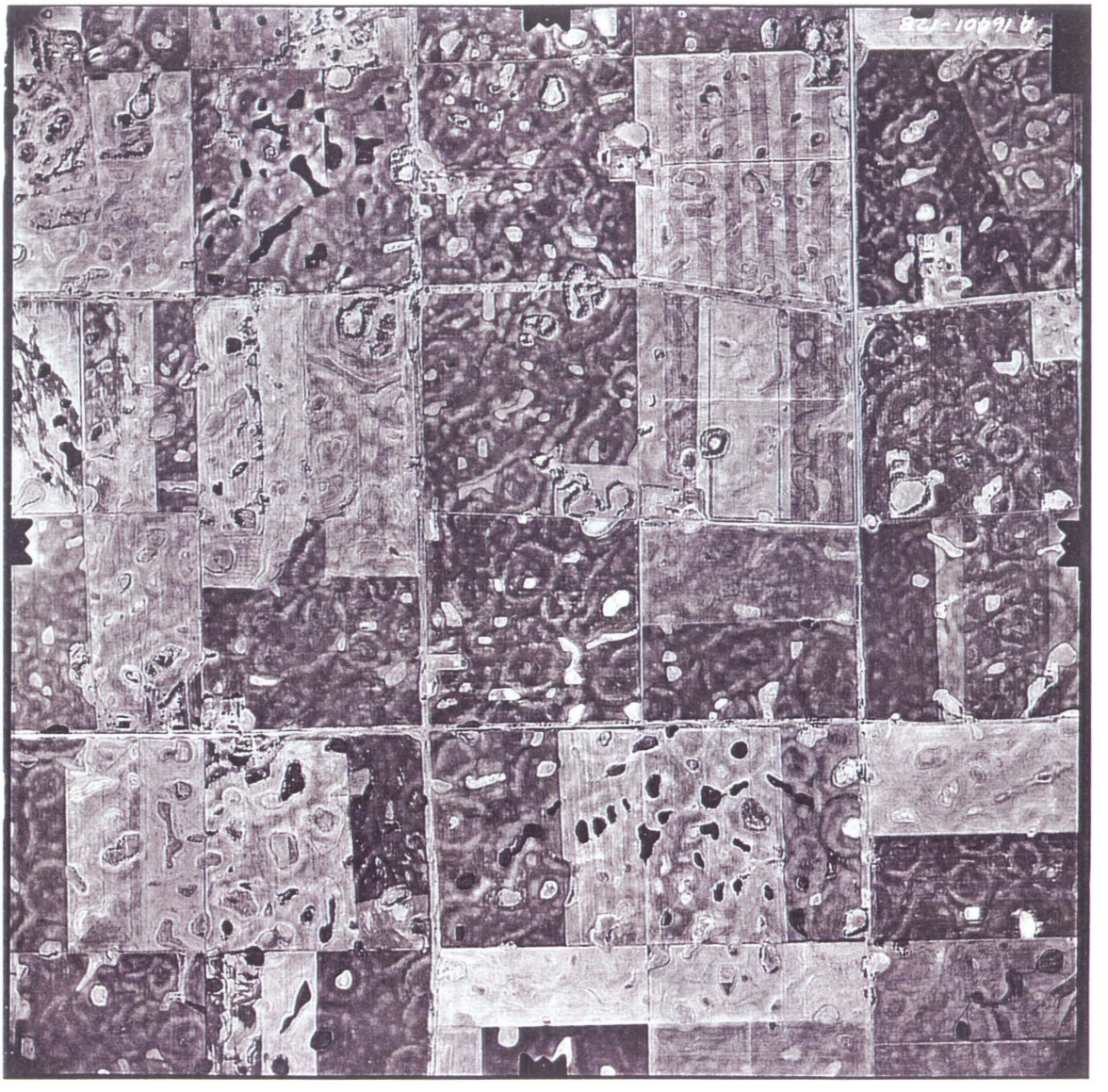

Fig.3-13 Air photo showing closely spaced doughnuts in the doughnut plain. Scale is about 1:26,400. Location of this air photo is shown in Fig. 3-14.

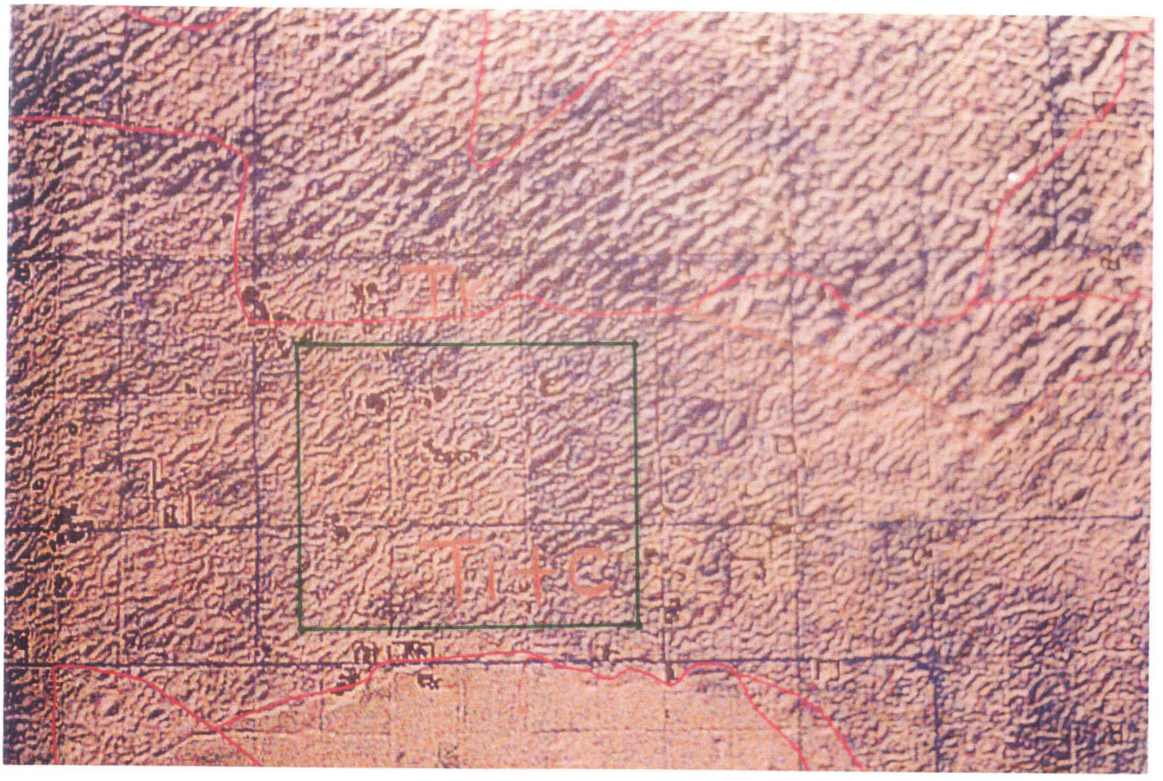

Fig. 3-14 Satellite image of the ridged till plain (Tr) and doughnut plain (Tl+C) of the Whitewater Lake area. Ridges are shown as shadows while depressions are shown as lighter color. Doughnuts that show very well in air photo (see Fig. 3-13) can not be identified. Instead, narrow ridges can be seen all over the doughnut plain (Tl+C) and are oriented in the same direction as the ridged till plain (Tr); Some broad ridges in the Tr plain continue into the doughnut plain and become paired-narrow ridges in the doughnut plain. One grid on the map is one mile. The square shows the location of Fig. 3-13.

3.3.2 Gravel lithofacies (G)

Of the four gravel sublithofacies, the matrix supported gravel sublithofacies occurs only in the northern end of glacial Lake Arcola (Figs. 1-1 and 3-5). The clast supported gravels occur in deltas, eskers, and bars; the pebbly sand sub-lithofacies dominated deltas lie along the western edge of Lake Hind basin; the cross bedded gravel sublithofacies occurs in deltaic foresets and in channel bars.

Massive gravel sub-lithofacies (Gmc, Gms)

The clast-supported massive gravel sub-lithofacies that lacks shale fragments (Gmc) is generally 2 to 6 m thick, and occurs in the Pipestone, Lauder, and Little Saskatchewan deltas (E, J, and L of Fig. 2-3). This sub-lithofacies also occur in the eastern half of the Dand delta (K of Fig. 2-3) and is the top-most unit of the Melita delta (I of Fig.2-3). The surface morphology of this sub-lithofacies is generally flat, and slopes toward the central basin. The shale-rich sub-division of this sub-lithofacies occurs in the Melita and Dand deltas (I and K in Fig. 2-3). These two deltas were deposited at the mouths of the Souris and Dand River valleys which were trenched into shale bedrock. In the Dand delta, shale-fragments dominate the proximal delta and the top-set beds of the distal delta (Fig. 3-7). In the Melita delta, the shale-rich massive gravel sub-lithofacies underlies the shale-deficient gravel sub-lithofacies in the proximal area. In addition, the shale-dominated massive gravel sublithofacies (Gmc) also composes the Arrow Hill Esker (N of Fig. 2-3, Fig. 3-15), which is about 21 km long, 0.5 to 3 km wide, and 20 to 50 m high, and forms a sharp high ridge in the downstream portion to

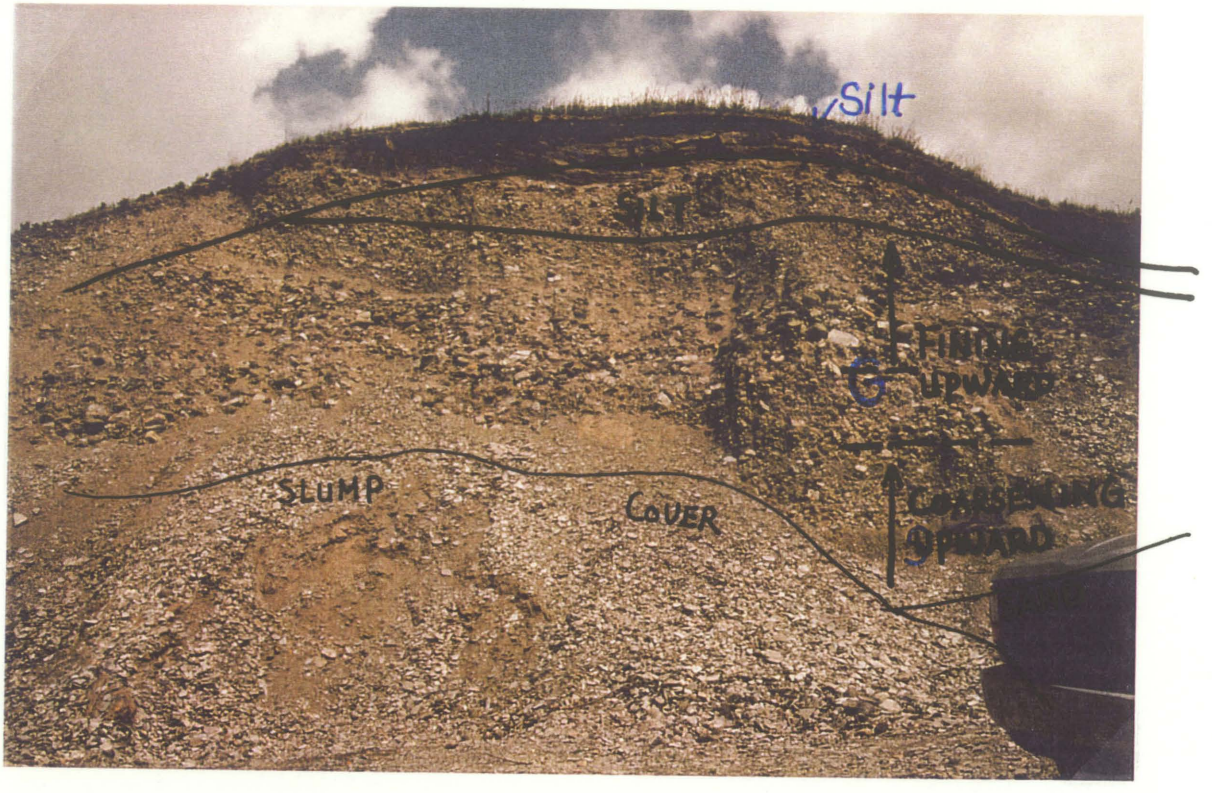

Fig. 3-15 Shale-rich gravel lithofacies (Gmc). This is a west-east cross section of the Arrow Hill Esker at Sec.23-Tp10-R24W. About 3.5 m of sand at the base (lower right) is overlain by 15+ m massive shale boulders and cobbles that show reverse grading to normal grading. The 2 m-thick silt on top of the esker is well sorted and laminated (1 mm to 5 mm thick). The front of my truck is in lower right corner as scale.

the south and multiple ridges with a hummocky topography in the upstream portion to the north. Glacial fluvial plains with low linear ridges to the west and north of the esker are also comprised mainly of shale gravels (Gmc)

Pebbly sand lithofacies (Gms) is the dominant lithofacies in the Antler, Graham, Jackson, Stony, Gopher, Bosshill, and Virden deltas (A, B, C, D, F, J, and H of Fig. 2-3). In other words, it dominates in all deltas except the Pipestone, Melita, and Lauder deltas in the western margin of the basin. This sub-lithofacies is generally less than 5 m thick, overlies low-carbonate diamicton lithofacies (Dl) or mud lithofacies (F). Its surface landform is flat to slightly rolling due to the presence of abandoned braid channels.

Matrix-supported massive gravel sub-lithofacies (Gmm) has not been found in the Lake Hind area. It is the main constituent in a gravel delta at the northern end of glacial Lake Arcola, Saskatchewan (Fig. 1-1). The channel that fed the delta is an under-fit channel that is about 1 to 1.6 km wide and 15 to 20 m deep, with steep-sided walls.

Cross bedded gravel sub-lithofacies (Gx)

Cross bedded gravel sub-lithofacies (Gx) occurs in the Pipestone, Melita, and Dand deltas (E, I, and K of Fig. 2-3). This sub-lithofacies commonly co-exists with and underlies the clast-supported gravel sub-lithofacies, forming the foreset beds of deltas. The content of shale fragments in this sub-lithofacies ranges from 0 to 50%: less than 5% in the Pipestone delta and more than 20% in the Melita and Dand deltas.

Cross bedded gravel sub-lithofacies also occurs at Assiniboine Flats, which is a 10 km-long, 4 km-wide Pleistocene gravel bar. The surface landform of this bar is flat

to hummocky in the upstream end, which has little obvious fluvial-dynamic streamlining, and lies 2 to 10 m higher than the comparatively flat downstream half. Only near the scalloped avalanche face that separates the upper half from the lower half of the bar is the downstream part covered with hummocks (Fig. 3-16).

3.3.3 Sand lithofacies

This lithofacies consists of sand and silty sand that is well to moderately well sorted, massive to laminated, and up to 20 m thick (Fig. 3-11). It occurs mainly in the central part of the glacial Lake Hind basin with a sharp contact to the underlying lacustrine clay and silt. The surface of the sand is generally flat, but in some areas has been reworked by wind into dunes up to 5 m high that are oriented northwest-southeast. Where there are no sand dunes, sand samples were collected for particle size analyses. Although this may still have been reworked by wind, the areal distribution of mean size shows that sands are coarser in the western basin near the Pipestone, Melita, and Virden deltas than the eastern basin. Medium-grained sand from the Assiniboine River was deposited as far east as the towns of Souris and Alexander (Fig. 3-17). There are broad, scoured channels on the surface that start from the Assiniboine River near Virden and extend southeast toward the Pembina Spillway.

3.3.4 Sand-mud couplet lithofacies (Sl)

The sand-mud couplet lithofacies is found in a core from central Lake Hind basin (Fig. 3-9) and in northern Lake Hind west of the Little Saskatchewan delta (L of Fig.

Fig. 3-16 Air photo shows the surface morphology of the Assiniboine Flat (O of Fig. 2-3). Sediments in the entire photo-area are dominated by cross bedded gravels (Gx), which can be subdivided into three units based on surface morphology: flat surface (Gl), flat to broad rolling surface (Gp), and hummocky surface (Gm). Most hummocks lie in the upstream part of the bar and near the scalloped avalanche face that separates the upper from the lower half of the bar. Scale is about 1:22,600.

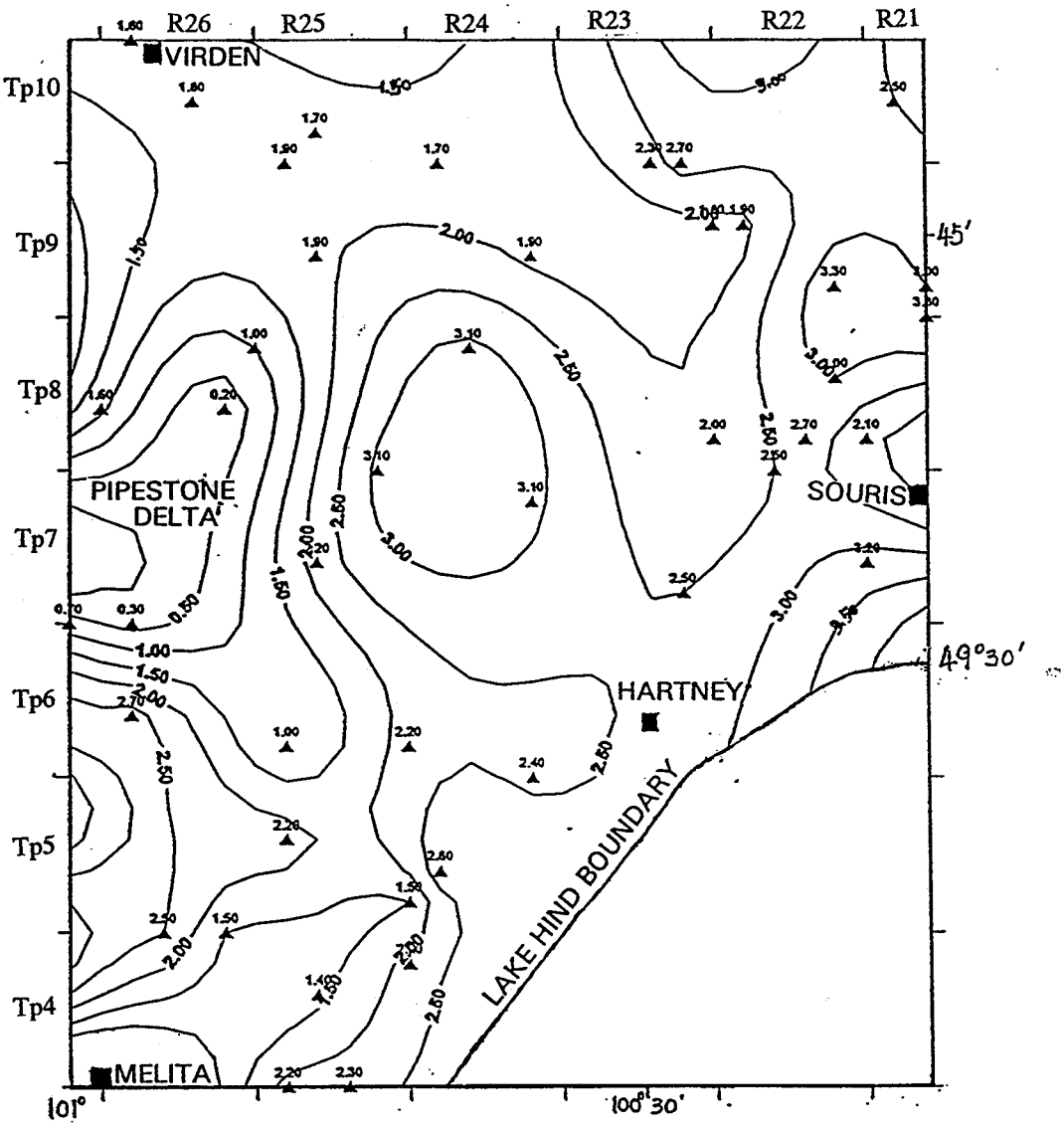

Fig. 3-17 Distribution of lacustrine sand (Sm) near the surface. Data used to plot this map include 37 surface samples taken from dune-free areas. Only the mean sizes are shown in this figure. The numbers in the map are mean size calculated by using Folk and Ward equation (1957). Coarse sand = >1phi, Medium sand = 1-2 phi, fine sand = 2-3 phi, very fine sand = 3-4 phi.

2-3). It is about 15 m thick, with a sand/mud ratio about 1:1. Laterally this sub-lithofacies grades to deltaic sand and lacustrine sand; vertically this overlies mud lithofacies (Fl and Fm) with a sharp contact, and is overlain by massive sand lithofacies in the central basin.

3.3.5 Mud lithofacies

This lithofacies includes fine-grained lacustrine deposits of silt, clay, and sandy silt (F lithofacies). The distribution of these sediments on the surface follows a geographic pattern. In the narrow southwestern end of the Lake Hind basin near the International Border, silt and clay occur at elevations up to 460 m. Northward along the southeastern edge of the basin, their uppermost elevation becomes gradually lower to 442 m. On the eastern side of the basin, silt and clay on the surface is everywhere below 434 m. In the western part of the basin, there are no fine lacustrine sediments above 442 m, and only a few patches of silt and clay occur below the level of most deltas (Fig. 2-3)

In the subsurface, this lithofacies overlies till, and is overlain by sand-mud couplets (Sl) or lacustrine sand (S lithofacies) and gravels (G lithofacies) (Figs. 3-9, 3-11). The thickness of the clayey silt unit ranges from a few meters to 30 m. It is thick in the northern end and thin near the Pipestone delta.

3.4 Description of stratigraphy

3.4.1 The sequence of sediments within the glacial lake basin

The sequence of sediments deposited in the Lake Hind basin during the last retreat

of ice can be generalized as the upper 80 m of sediment in Figure 3-9 and also is shown in the two cross sections in Figure. 3-11. There are four main stratigraphic units in the central lake basin, starting from the uppermost till (Fig. 3-9). The clayey silt and sandy silty diamicton units (Dl) are overlain by a coarsening upward sequence of silty clay unit (F lithofacies) to sand-mud couplets (Sl), and to sand lithofacies (S). A borehole that is located east of the Alexander moraine (Q2 of Fig. 2-3) also reveals a coarsening upward sequence, from silty clay to sandy silt, and to sand and silty sand (Fig. 3-18); at this location the sequence is only 25 m thick instead of the 45 m thick at the other borehole (Fig.3-9).

3.4.2 Stratigraphy of diamicton lithofacies adjacent to Lake Hind

The vertical sequence of diamicton lithofacies consists of at least four units based on their physical properties and carbonate factors at exposures. These are informally named Wawanesa, Souris, Fairfax, and Carroll tills. Only the Wawanesa till is part of the high carbonate sub-lithofacies (Dh); the others all contain less carbonate and have higher calcite/dolomite ratios and so belong to the low-carbonate lithofacies (Dl)

The Wawanesa till consists of high-carbonate lithofacies and occurs in the Brandon and Tiger Hills areas, east of the Alexander moraine (Figs. 2-3 and 1-1). A type section for the Wawanesa till is located at a 40-m-high river-cut east of Wawanesa (Figs. 3-1, 3-19). This unit is differentiated from any of the other tills in that it has a high carbonate content (>25%, Table 3-2), high carbonate pebble content, and low Shield pebble content. It can be identified in the field by a marker bed of light reddish brown

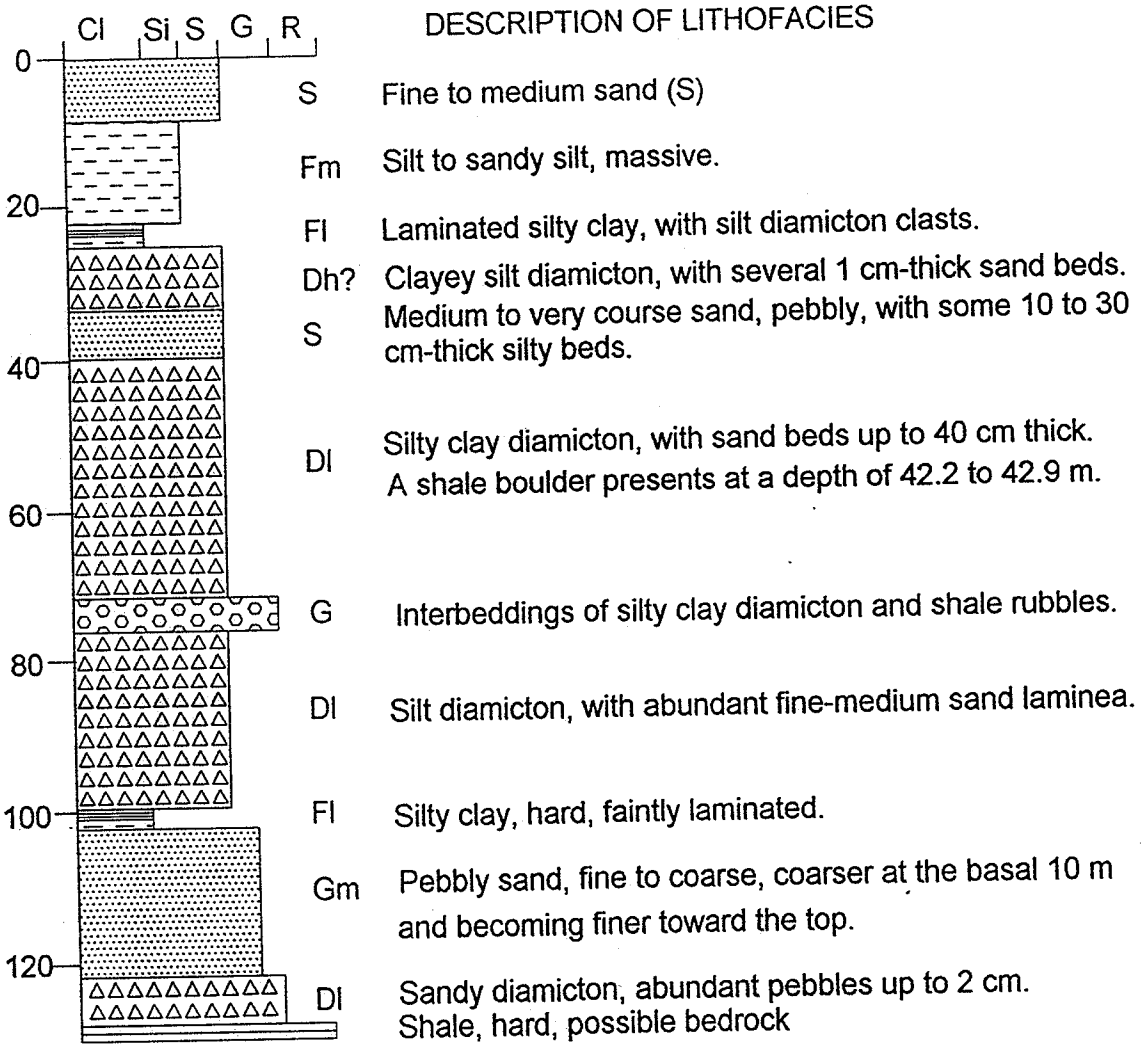

Fig. 3-18 Stratigraphic column of borehole 92TCA-CC. This borehole is located east of the Alexander moraine (Q2 of Fig. 2-3), and is about 2 km south and 8 km west of Brandon (Fig.2-3) (after Matile, 1992, unpublished core descriptions of Virden area).

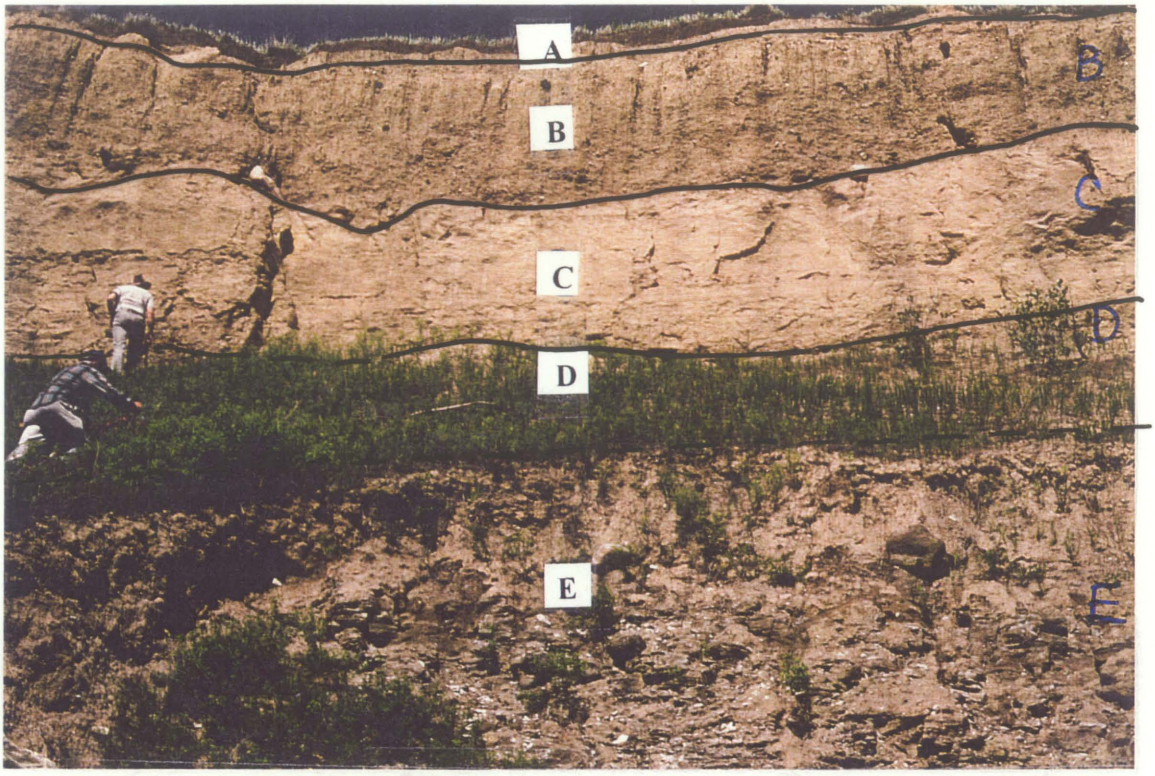

Fig. 3-19 A river-cut showing two till beds and two lacustrine silt beds at the southeastern town of Wawanesa at Sec.23 Tp7 R17W. The lower till unit (D) overlies shale bedrock (E) which is covered by slump; the upper till unit (B; Wawanesa till) is sandwiched by two silt beds (A and C). The bases of both till units are marked by scattered boulders. A close-look at a fresh face of the upper Wawanesa till (B) is shown in Fig. 3-1.

Table 3-2 Carbonate content based and textures of till units

UNITS	CARBONATE		SIZE ANALYSES			TILL FABRICS
	Content %	Calcite / Dolomite	Sand %	Silt %	Clay %	
Wawanesa	35 - 53 25 - 35	0.25 - 0.28 0.15 - 0.28	39 - 42	39 - 43	16 - 18	NE - SW
Souris	22 - 24	0.48 - 0.49	34 - 37	33 - 36	29 - 30	NW - SE* NW - SE**
Fairfax	21 - 26	0.40 - 0.88	34- 35	33 - 35	29 - 31	NE - SW
Carroll	17 - 20	0.29 - 0.30	30 - 32	36 - 38	30 - 32	NE - SW

* Near an end moraine
** Striation on boulders

(5YR 6/4) till about 0.1 to 0.5 m-thick, which is exposed at the surface in an area between Brandon, Souris, and Wawanesa only. The carbonate content ranges from 35 to 53 % in samples from the marker bed, and between 25 to 35% below the marker bed. In some places.

In the southern margin of the Darlingford Moraine at 15 km east and 10 km south of the town of Souris, two road cuts (Provincial Road 348) in the southern bank of the Souris River valley expose the Carroll, Fairfax, and Souris tills (Fig. 3-20). The Souris till is the uppermost till exposed and is identical to the underlying Fairfax till in total carbonate content, calcite/dolomite ratio, and gravel lithologies (Table 3-2), but is different in color. The Souris till is olive (5Y 5/4) and the Fairfax till is olive gray (5Y 3/2) in color (Fig. 3-21); they are separated by lenses of poorly sorted gravel, sand, and silt at the base of the Souris till (Fig. 3-20C). In addition, Fig.3-20C shows thrusted slabs of shale bedrock at the base of the Souris till; these slabs are 0.5 to 1 m thick, 2 to 3 m long. Till fabrics for the souris tills indicate northeast-southwest ice-flows (Fig. 3-22). But the validity of the till fabrics is questionable because this section is only 2 km west of the Darlingford moraine that was formed by the southwestly flowing Red River Lobe. Boulder lags at the base of the Souris till, which are not visible in the type section but can be seen at a river cut that is 10 km south and 5 km east of the town of Hartney, shows northwest-southeast striations. Till fabrics for the Fairfax till show a northwest-southeast direction (Fig. 3-22).

The Carroll till is the lowest till exposed in the region, and consists of silty diamicton that is a mixture of pale olive (5Y 5/4) and olive 5Y 4/3) materials, with 10

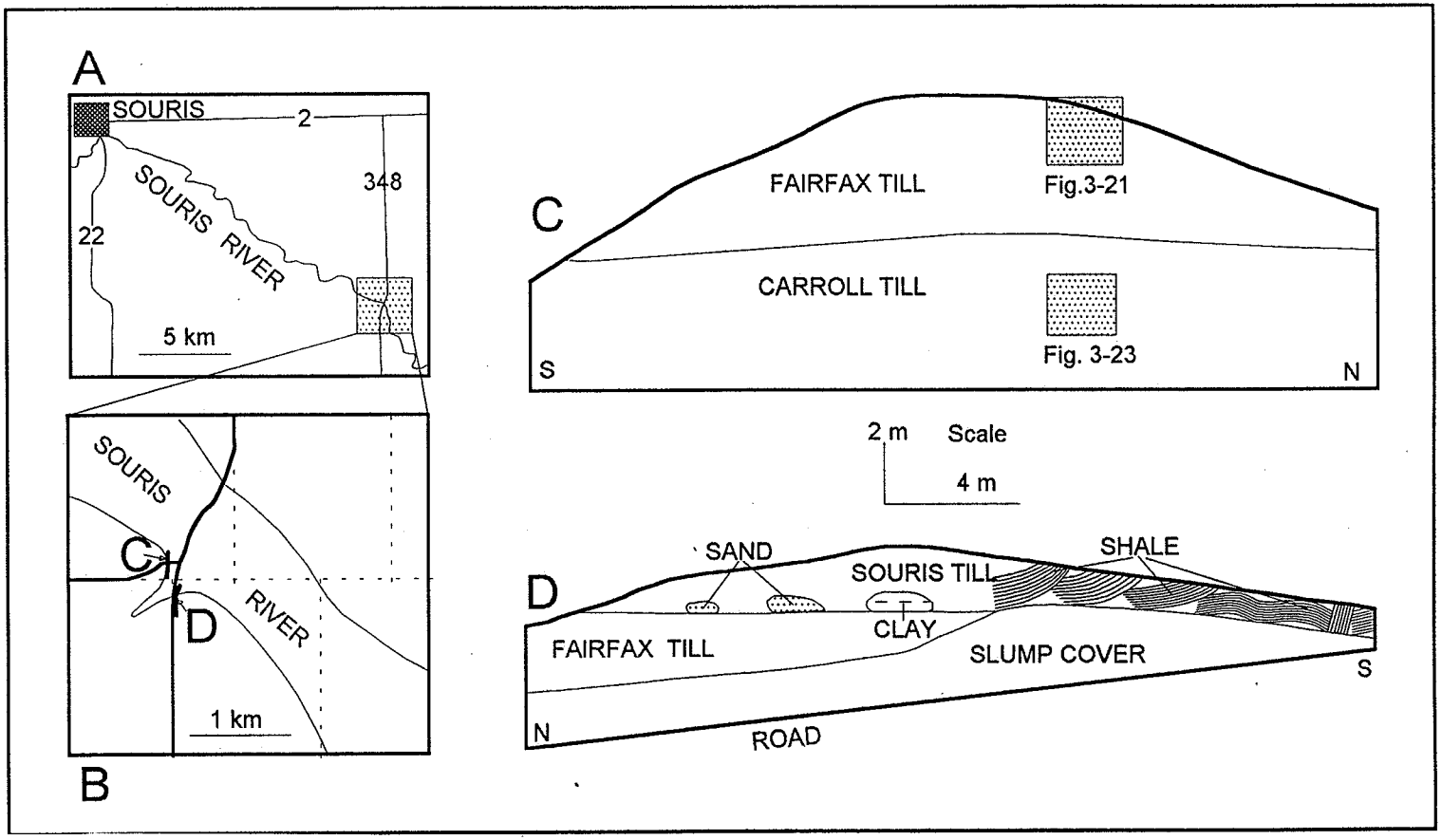

Fig. 3-20 Three diagrams showing relationship between the Souris, Fairfax, and Carroll tills and locations of exposures. A) Location of Fig.3-20B. B) Location of Figs.3-20C and 20D. C) Road-cut exposes the Souris and Fairfax till at Sec.36-Tp6-R20W. Shale slabs in the Souris till are indicative of north-south shear movements. D) the Fairfax and Carroll tills are exposed at Sec.1-Tp7-R20; See Figs. 3-21 and 3-23 for photos of the Fairfax and Carroll till.

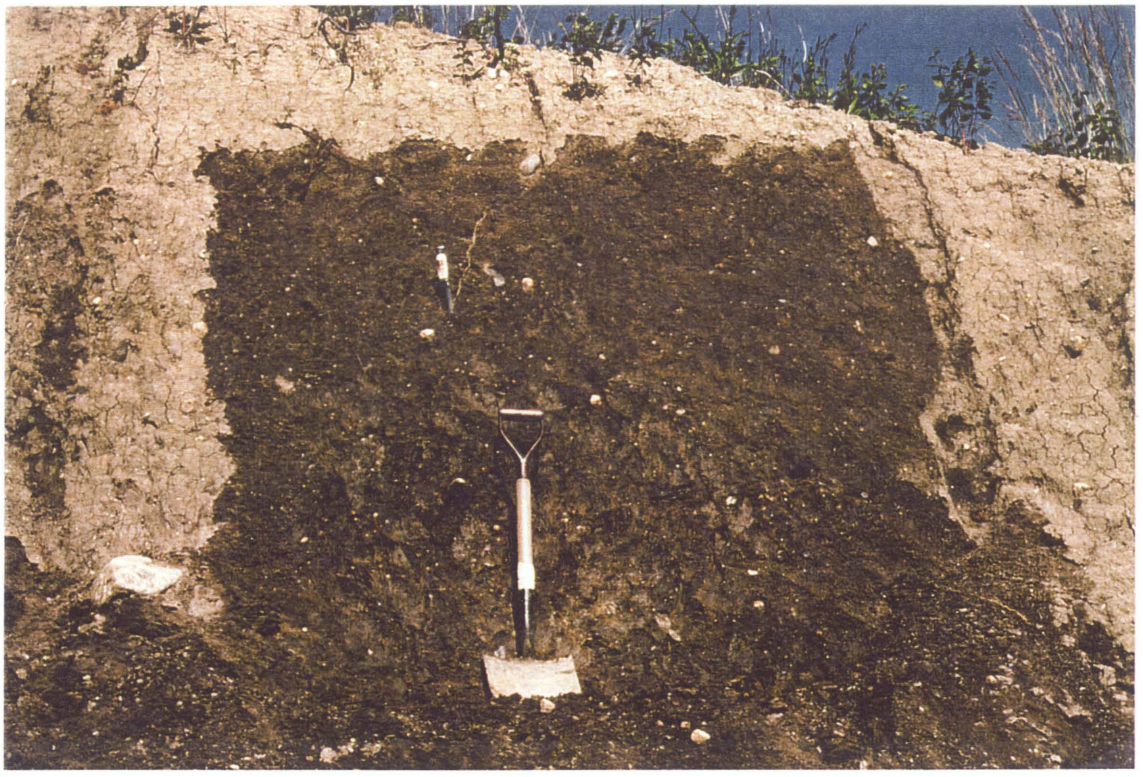

Fig. 3-21 A south-north section of the Fairfax till at the southeastern corner, Sec.1-Tp7-R20W. See Table 3-2 for composition and Fig.3-20 for location. The shovel handle is about 85 cm long.

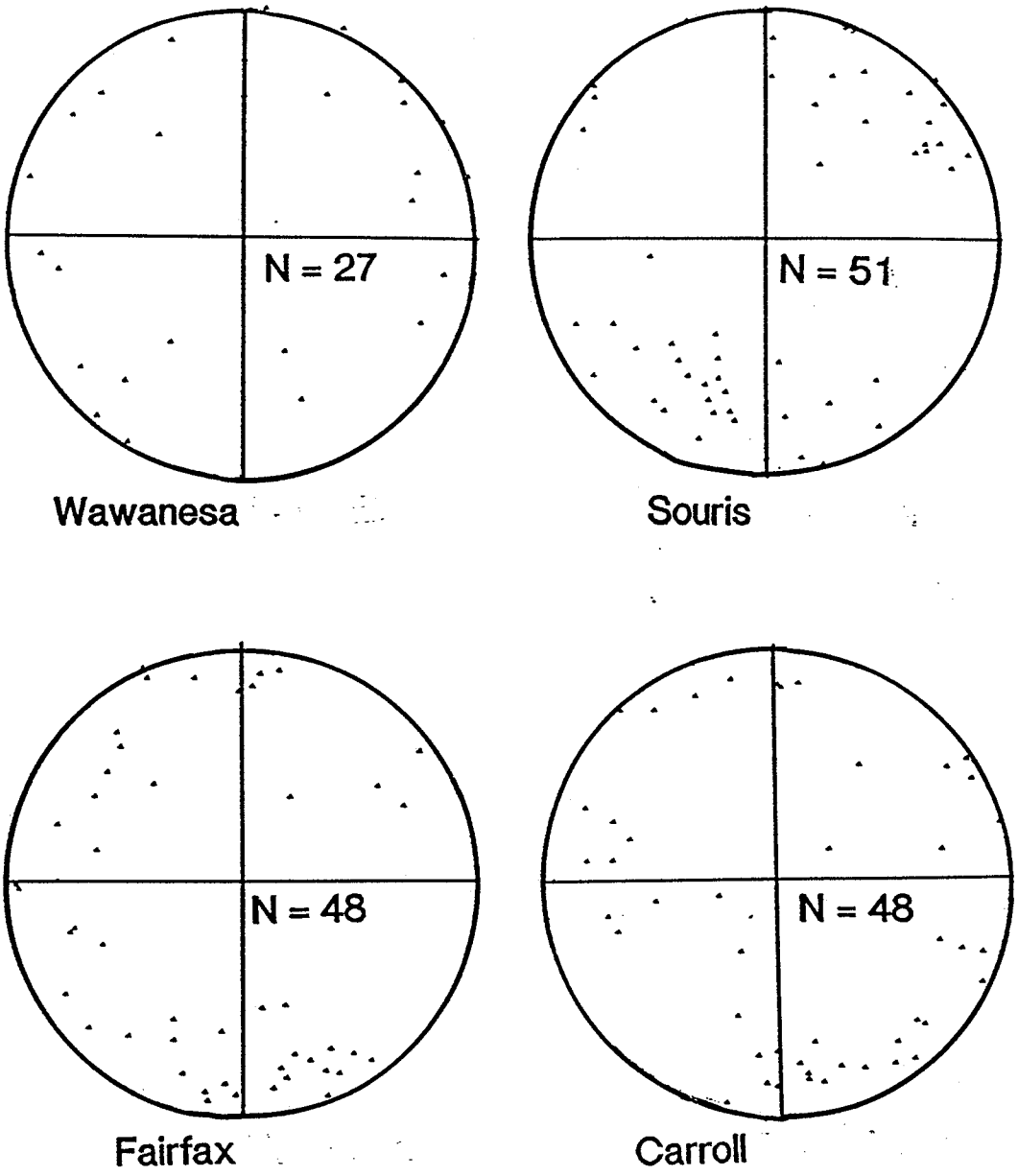

Fig. 3-22 Till fabric analyses. A) Wawanesa till southeast of Wawanesa at Sec.23 Tp7 R17W (See Fig.3-18 for stratigraphy); B) Souris till, C) Fairfax till, and D) Carroll till at 15 km east and 10 km south of the town of Souris (See Fig. 3-20 for stratigraphy).

Fig. 3-23 A south-north section of the Carroll till at the southeastern corner, Sec.1-Tp7-R20W. See Table 3-2 for composition and Fig. 3-20 for location. Notice abundant boulders in the exposure.

to 20 % gravels (Fig. 3-23). It differs from the Fairfax and Souris formations by its relatively low calcite/dolomite ratio (<3) (Table 3-2), and by its low carbonate content (<46 on AA results and <20% on Chittick analyses). Also, there are more boulders exposed in this till than any of the other two tills. Till fabrics studies suggest an ice flow from northwest toward southeast (Fig. 3-23).

3.4.3 Regional correlation

Stratigraphic correlation of tills in Manitoba, Saskatchewan, and North Dakota has been done by Christiansen (1992), Klassen (1989), Fenton et al.(1983), Teller and Fenton (1980), and Moran et al. (1976). It is not the intension of this thesis to discuss all of the correlations. Instead, I will simply discuss possible correlations of tills in the glacial Lake Hind region with adjacent areas in Riding Mountain (Klassen, 1979), Saskatchewan (Christiansen, 1992), and the northern North Dakota (Fenton et al., 1983). The correlation will be based on stratigraphic position, lithofacies, and carbonate content.

The **Wawanesa** till in southwestern Manitoba is very similar to the Arran and Zelena formations of Klassen (1979) in Riding and Duck Mountains. All are the uppermost tills, with relatively high carbonate contents (Table 3-3) and similar till fabric orientations.

The **Souris** till is similar to the Lennard Formation of Klassen (1979) in its low carbonate content (Table 3-3) and in being the topmost till in the Assiniboine River plain (Klassen, 1979) and glacial Lake Hind area. However, based on analyses in the Lake Hind basin, the Souris till has a slightly lighter color and is sandier than the Lennard

Table 3-3 Regional correlation of till stratigraphy based on the carbonate contents. (1) data from Christiansen (1992), (2) from Klassen (1979), (3) this study, (4) Teller (1976), Teller and Fenton (1980), and (5) Bluemle (1984), Conly (1986).

SASKATCHEWAN (1)		RIDING & DUCK MTN (2)		SW MANITOBA (3)		SE MANITOBA (4)	NORTH DAKOTA (5)
Formations	Carb. (%)	Formations	Carb. (%)	Units	Carb. (%)	Formations	Formations
Battleford	25.6	Arran	34-65	Wawanesa	35-53 (marker)	Marchand Whitemouth-L Roseau	Falconer Hansbora
		Zelena	26-36		25-35 (normal)		
		Lennard	14-19	Souris	21-24	Senkiw	Dahlem
Upper-floral	36.9	Minnedosa	18-24	Fairfax	21-26	Tolstoi Stuartburn	Gardar
Lower-floral	32.3	Shell	13-18* 24-36	Carroll	17-20	Woodmore	Vang
Warman	12.6	Tee Lake	20-26			Unnamed	Tiber
Dundurn	22.9	Largs	9 - 21	?		Rosa	Cando
Mennon	14.3						

* weathered

Formation mapped in Riding and Duck Mountains by Klassen (1979). Christiansen (1992) correlated the Arran, Zelena, and Lennard formations with the Battleford Formation in central Saskatchewan; Fenton et al. (1983) and Conley (1986) correlated Falconer, Hansboro, and Dahlen formations in North Dakota with the Arran, Zelena, and Lennard formations in Riding Mountains. The Marchand, Whitemouth Lake, Roseau, and Senkiw formations of Teller (1976) and Teller and Fenton (1980) in southeastern Manitoba has also been correlated to Arran, Zelena, and Lennard formations by Conley (1986). All of these formations are believed to be of late Wisconsinan age (Klassen, 1979, Fenton et al., 1983).

The **Fairfax** till underlies the Souris till, and has a similar carbonate content to the Souris till. But the unconformity between the two tills, especially where thrusted shale-slabs exist, is too obvious to be ignored. The stratigraphic position and the carbonate content of the Fairfax till are similar to that of the weathered Minnedosa Formation (Klassen, 1979), which underlies the Arran, Zelena, or Lennard formations (Table 3-3). Therefore, I believe the Fairfax till is correlative with the Minnedosa Formation of Klassen (1979) in Riding and Duck Mountains. Christiansen (1992) correlated the upper Floral Formation in central Saskatchewan with the Minnedosa Formation on the basis of stratigraphic position. A problem for this correlation is that the upper Floral Formation has a much higher carbonate content than the Minnedosa Formation and Fairfax till. These formations are assigned an early Wisconsinan age by Klassen (1979) and Christiansen (1992).

The **Carroll** till underlies the Fairfax till in the Lake Hind basin. The Shell

Formation underlies the Minnedosa Formation in the Riding and Duck Mountains, which I believe is correlative with the Fairfax till. The distinguishing characteristic of the Carroll till and the Shell Formation is that their carbonate contents are noticeably lower than that of the overlying Fairfax till and Minnedosa Formation. Therefore, the Carroll till is considered to be correlative with the Shell Formation (Tables 3-3).

CHAPTER 4

SEDIMENTOLOGY

4.1 Introduction

In this chapter, I will discuss the hydrodynamics and depositional environments of water-laid sediments (Gmm, Gmc, Gms, Gx, S, Sl, Fm, and Fl lithofacies), and the depositional environment of glacier-deposited sediments (Dl and Dh) lithofacies. For the purposes of reconstructing paleolake levels and the history of meltwater flows (in Chapter 6), the surface elevations of the twelve deltas in the Lake Hind basin will be discussed in detail in a separate section after the depositional environments of water-laid sediments.

4.2 Hydrodynamics of water-laid sediments

The water-laid sediments will be discussed in the following order: 1) massive gravel sub-lithofacies (Gm), 2) cross bedded gravel sub-lithofacies (Gx), 3) sand lithofacies (Sm), 4) Sand-mud couplet lithofacies (Sl), and 5) mud lithofacies (Fl, Fm). The massive gravel sub-lithofacies has been further divided into matrix-supported, clast-supported massive and pebbly sand sub-lithofacies in order to discuss their hydrodynamics in detail.

Before discussing the depositional mechanisms, I will first define some of the terms that will be used in the following sections, such as types of flows and grain-supporting mechanisms during sediment transportation.

Types of meltwater flows that are frequently used here are divided into three categories based on Costa's (1988) classification: water flood, hyperconcentrational flow, and debris flows (Table 4-1). Sediments in a water flood are supported mainly by turbulence and electrostatic forces. Sediments in a hyperconcentrational flow are supported by buoyancy, dispersive stress, and turbulence of water. In a debris flow, the supporting mechanisms are similar to those of the hyperconcentrational flows except that stress cohesion and structure-support becomes important while turbulence is depressed by the high sediment concentration (Lowe, 1982; Costa, 1988).

Supporting mechanism. The buoyancy of a flow is controlled by the density difference between submerged solids and the transporting fluid (Costa, 1988). It increases when the content of mud increases in a flow, such as in a debris flow. Dispersive stress (pressure) (Bagnold, 1954) results from the lift produced when forces are transmitted between particles in collision or near collision as one is sheared over another (Costa, 1988), such as in a grain flow. Structure-support, or grain-to-grain contact that lacks turbulent movements, occurs in debris flows and supports about one-third of the weight of coarse particles (Pierson, 1981)

4.2.1 Massive gravel lithofacies (Gm)

4.2.1.1 Matrix-supported massive gravel sub-lithofacies (Gmm, debris flow deposits)

The clasts in the matrix-supported massive gravel sub-lithofacies (Gmm) vary from pebbles to cobbles (Fig. 3-5); the matrix is poorly to moderately sorted coarse sand and pebbly sand with less than 5% mud. The matrix-supporting, massive sedimentary

Table 4-1 Sediment concentration and supporting mechanisms in water floods, hyper-concentrational flows, and debris flows (From Costa, 1988; Lowe, 1982).

FLOW	SEDIMENT CONTENTS (VOLUME %)	TYPE OF FLOWS	SUPPORTING MECHANISMS	SEDIMENTARY STRUCTURES & TEXTURES
Water Floods	0 - 20	Turbulent	Turbulent	-Well sorted -Graded -Bedded or massive -Gravels at basal layers
Hyper-concentrational flows	20 - 47	Turbulent	Dispersive stress Turbulence Buoyancy	-Fairly to poorly sorted -Clast supported -Graded or none-graded -Open frameworks
Debris Flows	40 - 77	Laminae	Buoyancy Cohesiveness Structure-support Dispersive stress	-very poorly sorted -Matrix supported -Out-sized clasts

structure, and lack of grading and imbrication indicate deposition from sediment gravity flows related to debris flows as described by others (Surlyk, 1984; Lowe, 1982; Nemec and Steel, 1984). The very low content of clay suggests that the sediment-laden flow was not viscous, therefore, the flow is not likely to have been a cohesive debris flow as discussed by Lowe (1982).

The matrix-supported gravel lithofacies here is massive, non-graded, and non-stratified, with a few outsized cobbles and boulders and abundant sand matrix (Fig. 3-5). A similar lithofacies with a sandy capping has been interpreted as deposition from a debris flow that evolved into a fully turbulent flow later (Lowe, 1982; Nemec and Steel, 1984). A similar section in east Greenland, which is matrix supported and low in clay, has been interpreted by Surlyk (1984) as having been deposited from inertial non-cohesive sandy debris flows. There is not a type section of this sub-lithofacies in the glacial Lake Hind basin, but there is an exposure at the mouth of Moose Mountain valley in the northern end of glacial Lake Arcola. The matrix-supported massive gravel sub-lithofacies at this site has a very flat surface, and shows no sandy capping (Fig. 3-5). The flow that deposited this matrix-supported massive gravel lithofacies was a high density turbulent flow, which may have dispersed rapidly upon entering lake water and deposited its bed-load. The turbulence in the flow prevented deposition of a sandy cap over the massive gravel bed.

4.2.1.2 Clast-supported massive gravel sub-lithofacies (Gmc, grain flow deposits)

The clast supported, massive boulders and coarse gravels (Gmc) (Fig. 3-4) occur

in the Lauder, Melita, Pipestone, Dand, and Little Saskatchewan deltas. They also occur widely in major meltwater channels (Kehew and Clayton, 1983; Kehew and Teller, 1994a). As described in Chapter 3, this sublithofacies consists of over 57% pebbles, cobbles, and boulders that are clast-supported, non-graded, and structureless. Lack of grading and stratification indicates that turbulence and dispersive pressure are not the only supporting mechanism during the transportation processes because sediments deposited from a flow that is supported mainly by dispersive pressure such as a grain flow will show clast-supporting and inverse grading at the base (Table 4-1) (Surlyk, 1984; Lowe, 1982; Nemec and Steel, 1984); deposition from a turbulent flow will normally result in a normal grading and good sorting (Surlyk, 1984 and Lowe, 1982). By comparison, a debris flow in which the flow volume is 47 to 70% of sediments (Costa, 1988) can deposit poorly sorted, massive, matrix-supported gravels (Pickering et al., 1986; Lowe, 1982). This is because the presence of mud and sand increases the specific gravity of the transporting media, thereby increasing the buoyancy of the flow (Lowe, 1982). Meanwhile, the high sediment load will depress the turbulence of the flow and maintain laminar flow. This, in turn, will reduce the chance of clast collision and therefore, reduce dispersive pressure generated from clast collisions (Costa, 1988).

In the clast-supported massive gravel sub-lithofacies (Gmc), the high clast content suggests that collisions between boulders and gravels were inevitable, i.e. dispersive pressure generated by collisions played a role in supporting clast-dispersion during transportation; therefore, the sediment-laden flow was similar to but not the same as the grain flows that have been described by Lowe (1982). Surlyk (1984) says that this type

of lithofacies is better described as a sandy debris flow transitional to a density modified grain flow. It is not a typical grain flow, nor a debris flow, but a density modified grain flow. Similar deposits in Watrous of central Saskatchewan has been described by Kehew and Teller (1994b) as hyperconcentrational flow deposits.

4.2.1.3 Pebbly sand sub-lithofacies (Gms, progradation of braided fluvial system)

As defined in section 3.2.4 of Chapter 3, the pebbly sand sub-lithofacies (Gms) has less than 10% pebbles. It is different from the matrix-supported massive gravel sub-lithofacies by lacking mud and being moderately sorted. Pebbly sand lithofacies are the dominant lithofacies in all but the Pipestone, Melita, and Lauder deltas in the western Lake Hind basin. This lithofacies is normally less than 5 m thick, with a flat to gently sloping surface, and is commonly associated with many shallow braid channels. One explanation is that it was deposited by the progradation of a braided fluvial system into a standing body of water (McPherson et al., 1987). The well-developed and abandoned braided river channels in the Antler, Graham, Jackson, and Stony deltas support this interpretation. Absence of grading and cross bedding, which are supposed to be the two common characteristics of braided delta deposits (McPherson et al., 1987), may be due to deposition into shallow lake water, on a low slope gradient, or due to reworking by waves and currents. An alternative explanation, provided by Pickering et al. (1986) for a similar lithofacies of disorganized pebbly sand, is the rapid collective grain deposition of a pebble-sand mixture from high-concentrational turbidity currents due to increased inter-granular friction. The common point of these two interpretations is that the sediment

load of the flows has to be high. The difference of the two is that in a braided channel, gravels and sands are transported mainly as bedload and dominate the deposits, while fine-grained sediments that are transported in suspension do not contribute greatly to sediment accumulation (Blatt et al., 1980). In contrast, in high-concentrational turbidity currents, a considerable proportion of sediment is deposited directly from suspension (Allen, 1990). Hiscott (1994) even suggested that the inertia layers (bedload) in a turbidity current are very thin and most massive sediments are deposited from suspension.

4.2.2 Cross-bedded gravel sub-lithofacies (Gx)

This lithofacies consists of cobbles, pebbles, and granules, and occurs in the Pipestone, Melita, Dand, and Little Saskatchewan deltas (Gx) (E, K, and L of Fig. 2-3). The presence of 2 to 4 m-thick, near angle-of-repose cross beds, and their association with massive to stratified gravels and sand caps suggest that this lithofacies may represent the forest beds of deltas (Rust and Koster, 1984). Normal grading across each foreset bed, such as is the case in the Dand delta (Fig.3-7), suggests that down-slope avalanching of coarse sediments from traction carpets were followed by suspension deposition of fine sediments from high-concentrational turbidity currents (Pickering et al., 1986). A water flood may also deposit cross bedded sediments. However, cross bedded gravels that are deposited from a waterflood will show better sorting and poorer grading than a hyperconcentrational flow due to stronger turbulence and less suspension load of coarse materials in a waterflood than a hyperconcentrational flow.

4.2.2.1 Large scale hummocky cross bedded gravels, a special case of Gx sub-lithofacies

The Assiniboine Flats (O of Fig. 2-3) is a special case of cross bedded gravel sub-lithofacies, in which the surface of this lithofacies displays hummocky topography (Fig. 3-16). The 16 km^2 gravel bar occurs in a broad bend of the Assiniboine channel (O of Fig. 2-3), and consists of a lower and an upper sequence (Fig. 4-1). The cross bedded fine gravels are overlain by scattered boulders in the upstream end, by hummocks in the upper sequence in the middle bar, and constitute the entire downstream half of the bar (Fig. 4-1; 3-8). This suggests that the bar was deposited by multiple events. The cross bedded gravels in the lower part of the sequence could be the result of gravel dune migration during floods or by lateral accretion. There are two possible explanations for the gravel hummocks of the upper sequence in the middle of the bar. One hypothesis is that the hummocks and associated closed depressions were the result of the collapse of stagnant ice after the deposition of gravel (Teller, personal commun. 1993). But my 4-year (1992-1995) continuous monitoring of an active gravel pit that is excavated from the center of a hummock to the adjacent closed-depressions found no sign of any collapse structures; ground penetrating radar surveys over this hummock and adjacent depressions found no sign of disturbance in the lower sequence, nor in the hummock. This suggests that this hummock and associated closed depressions did not result from collapse of stagnant ice after the deposition of gravels.

In a careful examination of this hummock it can be seen that this hummock consists of three to four sets of in-drift climbing mega-ripples (Fig. 3-8). Each set of mega-ripples has a wavelength of 25 to 60 m and is 4 to 6 m-high, and consists of a very

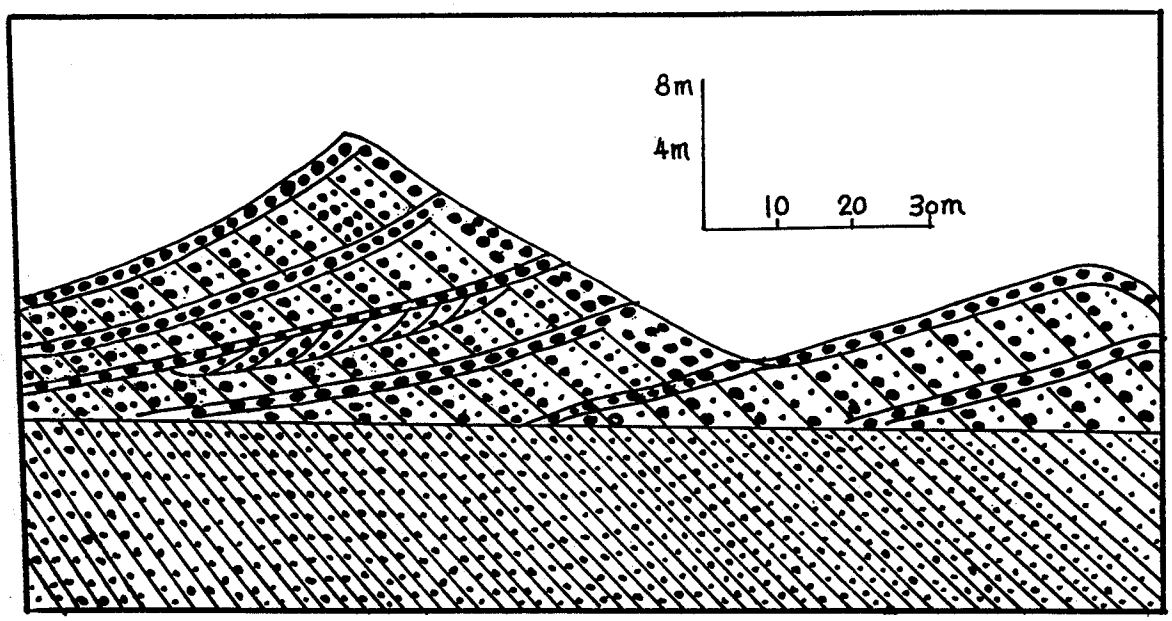

Fig. 4-1 A schematic interpretation of an exposure in the Assiniboune Flats(O of Fig. 2-3) based on Fig. 3-8 and ground penetrating radar surveys. Sediments in the upper sequence display hummocky topography and consist of cobbly and pebbly gravels that are clast supported and cross bedded (Gx sublithofacies); cross beds are separated from each other by a 20 to 30-cm-thick layer of cobbles, forming a non-graded bed unit. The low sequence consists of cross bedded fine gravels.

gentle slope to the stoss-side and a steep slope to the lee side (Fig. 4-1). All the beds are conformable to the surface of the hummock. My explaination of the deposition of hummocky cross beds is similar to that of the delta foresets discussed previously, where the cross beds were deposited by down-slope avalanching of coarse sediments from traction carpets which were followed by suspension deposition of fine sediments from high-concentrational turbidity currents (Pickering et al., 1986). The deposition of these hummocky cross beds was under the influence of persistent mega-turbulence, as evidenced by the non-streamlined hummocky landform (See map outlines in Fig. 4-1).

Because the gravel bar is located in a broad curved part of the Assiniboine valley between two large channels, Sun and Teller (1993) suggested that a chaotic megaturbulent flow may have occurred as a result of strong flow interference between the two channels during a catastrophic flood (Fig. 4-2); the irregular, vaguely streamlined hummocky bedforms were deposited at this time in the shallower turbulent floodwater over the bar (Figs. 3-8, 4-2). Meanwhile, in the upper head of the bar where the flow was uni-directional, previously-deposited gravel of the lower unit was reworked and eroded, leaving a lag of boulder on top of cross bedded fine gravels (Fig. 4-3).

4.2.3 Sand lithofacies (Sm, density flows and reworked by waves and wind)

Dunes are developed on a large portion of the surface of the sand lithofacies in glacial Lake Hind. Therefore, much of the near-surface sediment of this lithofacies has an eolian origin. Even in dune-free areas, well sorted eolian sand is common in the upper 0.5 m, showing an olive grey-colored mixture of sediment and soil. In order to get an

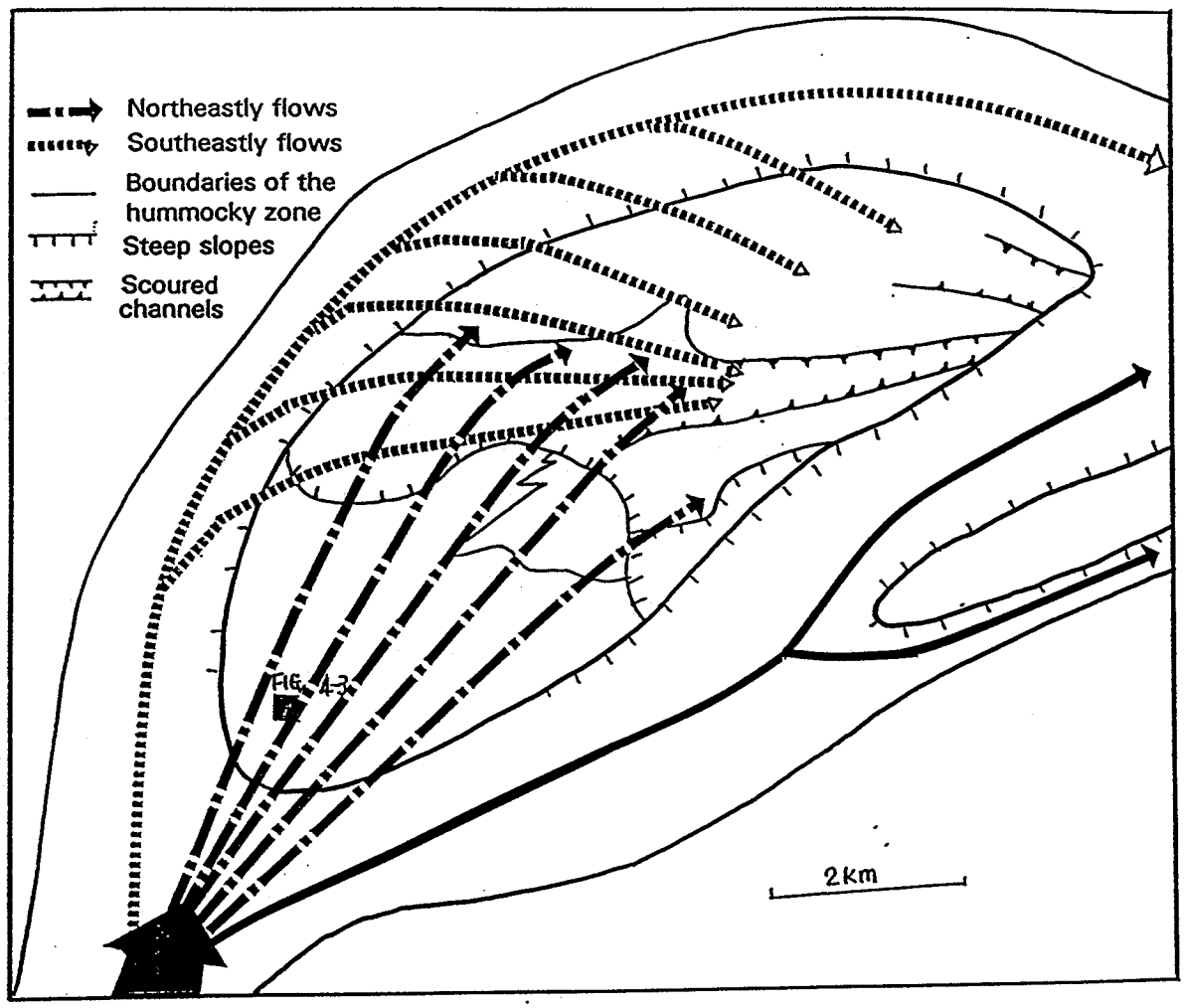

Fig. 4-2 Diagram Showing possible formation of megaturbulent flows along the slip-face of the migrating gravel unit, where the straight northeast flowing water met with the southeast-flowing water from the northern channel. Gravel hummocks were formed under the megaturbulent flows, in a way that the southeast-moving megaripples interfered with the northeastly migrating megarriples. Flat to level plains occur where unidirectional flow was dominant.

Fig. 4-3 Photo shows boulder lags over cross bedded fine gravels (Gx sub-lithofacies) in the upper head of the Assiniboine Flat (O of Fig. 2-3). Location of this photo is shown in Fig. 4-2.

aerial distribution of particle size of sand, samples were taken by a hand auger near the water table 1 to 1.5 m below the surface for size analyses.

As described in Chapter 3, sand of this lithofacies (Sm) at depth from auger and deep bore-holes (Figs. 3-9, 3-11) is generally moderately to well sorted, massive, and non-graded. Sedimentary structures are rarely seen in bore-holes in central Lake Hind, but horizontal bedding has been found at distal locations in the Melita delta (Fig. 4-4). This massive sand lithofacies is interpreted as having been deposited from underflow currents or turbidity currents and then reworked by waves. Similar disorganized sand lithofacies have been interpreted as rapid suspension deposition from turbidity currents by Postma (1990) and Pickering et al. (1986). Post-depositional liquefaction may be responsible for destroy sedimentary structures locally.

Fig. 3-17 shows that the surface particle size of sand in the Sm facies is coarser near the Pipestone, Melita, and Virden deltas in the western than the eastern glacial Lake Hind. This suggests that the turbidity flows and underflows mainly came from the Souris, Pipestone, and Assiniboine valleys, which have evidence of having been trenched by catastrophic floods (see Chapter 5). The surface sand in the northern part of the basin has shallow sub-parallel grooves that start from the Assiniboine River near Virden and extend southeastward to the outlets of the lake; this is interpreted as erosion by flows from the Assiniboine valley. Lack of fine sediments at the surface of the central basin suggests the basin was not a very effective sediment trap. Sand was deposited in shallow water and was probably reworked by waves and moved into the central part of the basin as the lake level fell; finer sediment remained in suspension and was carried out of the basin.

Fig. 4-4 A west-east section in the distal Melita delta (I in Fig. 2-3). Massive to faintly bedded fine gravels at the top 1-2 m (A) is underlain by a fining upward sequence of gravels (E), gravelly sand (D), coarse-grained sand (C), and very well sorted fine to medium sand (B). The basal unit (E) is covered by slump, and consists of cross bedded pebbles and cobbles, with abundant shale fragments.

4.2.4 Sand-mud couplet lithofacies (Sl)

This lithofacies (Sl) consists of interbedded sand and silty clay. This lithofacies is similar to the organized sand-mud couplets (C2) of Pickering et al. (1986), which was interpreted as deposition from high concentrational turbidity currents. The SI is different from the laminated mud lithofacies (Fl) by having up to 1.1 m silty sand beds. In lithofacies SI, each couplet consists of 0.1 to 1.1 m of silty sand separated from the next couplet by a 0.1 to 1.6 m silty clay unit. Deposition of each couplet occurred from one turbidity surge event which deposited the silty sand that was followed by silty clay after-surging. The transition from laminated silty sand beds in the lower sequence to massive sand beds in the upper sequence suggests that either the site was getting closer to the source area of turbidity flow (due to the prograding of delta fronts) or the energy of the turbidity flow became stronger (Lowe, 1982).

The lack of sand-mud couplets in the basin east of the Alexander moraine (Q2 of Fig. 2-3 and Fig. 3-18) can be explained by the eastern region being covered by ice at the time the SI lithofacies was deposited to the west (Sun and Teller, 1996), or because surging flows did not extend that far (after ice melting), or because of low surface gradients and shallow depths at the lake floor.

4.2.5 Mud lithofacies (Fl, Fm, suspension settling)

Rhythmite silt and clay lithofacies (Fl)

There are several interpretations for the rhythmite silt and clay lithofacies in glaciolacustrine environments. One mechanism involves seasonally controlled alternations

between the warmer melt season when coarse sediments were deposited from meltwater flows and the cold season when fine sediments were deposited from suspended particles in the water column (Wolfe and Teller, 1993). Here, one couplet of coarse and fine lacustrine sediment represents accumulation over a one year period. Alternative interpretations are slump-induced surge current deposits, fluctuations in runoff to the lake, or changes in wave energy. In these situations, the coarse-grained unit may form at any time of year, and may form a very irregular thickness of coarse sediment that displays a gradational upper silt contact (Smith and Ashley, 1985). Wolfe and Teller (1993) suggested that this gradational upper silt contact in the rhythmite silt and clay lithofacies could be used to distinguish a surge current-produced rhythmite from annual valves; they noted that a sharp upper silt contact in a varve would result from an abrupt break in deposition when the lake changed from ice-free to ice-covered. However, if a surge flow generated by spring melting or flooding from a river was very strong, it may have eroded the entire fine layer of winter deposits and resulted in a bi-annual couplet or multiple-year couplet of silt and clay beds.

In glacial Lake Hind, the 1- to 5-cm-thick clay laminae often show signs of erosion and disturbance, such as rip-up clay clasts, suggesting that the clay beds were disturbed by subsequent strong underflows probably generated from spring melting. The 1- to 10-cm-thick silty beds of this lithofacies probably were deposited by low density, quasi-continuous underflow currents generated from ice-marginal meltwater flows. Cross laminated beds of coarse sand and scattered gravels and till clasts support the view that underflows or turbidity currents were an important dispersal mechanism.

Homogeneous mud lithofacies (Fm)

This lithofacies is believe to have been deposited from suspension settling, in part from density current and turbulent suspension. In a glacial lake where inflow and outflow were high and depth of water ranged from 5 to 35 m, the key factors controlling mud deposition were wave energy, and water depth; the elevation of outlets played a key role in the latter. The 20 to 30 m-thick homogenous mud with subtle lamination in central glacial Lake Hind (Fig. 3-9) suggests continuous deposition with no disturbance. This lithofacies is thickest in the central deep basin, so it was certainly deposited in the deep water region below wave base.

4.3 Depositional environments of water-laid sediment

In this section I will discuss the depositional environments in the order from upstream to downstream, from esker to deltas, to lacustrine sand, silt, and clay. The depositional environments of glacier-deposited sediments will be discussed in the next section.

4.3.1 Depositional environments of eskers and low linear ridges

A glaciofluvial plain with low linear ridges occurs north of the Arrow Hill esker (Fig. 4-5). Sediment composition of the fluvial plain is similar to that of the esker, and is dominantly shale fragments. Adjacent to each of the low-linear ridges are channels scoured into shale bedrock. A similar landform in the Livingstone Lake area of northern Saskatchewan has been called a "drumlin" by Shaw (1983); these features are either spindle or streamlined in shape and consist of sand, pebbly sand, and sandy pebbly

Fig. 4-5 Glacial fluvial plains with low linear ridges and the Arrow Hill esker in the northern edge of the study area.

diamicton. These "drumlins" have been interpreted as having been deposited from suspension into basal cavities within the ice during catastrophic subglacial floods (Ashley, 1985; Shaw, 1991). In the early stage of these subglacial floods, the pressure generated by the flood was sufficiently high to lift large areas of the glacier from the ground. As the flood depth increased, erosional marks were sculpted in both the bedrock and overlying ice, producing large cavities in the base of ice. As the flood pressure fell the ice settled toward the ground. The cavities became areas of flow expansion where sediments were deposited from suspension. This may be the origin of subparallel low linear ridges north of the Assiniboine River.

All these low-linear-ridges converge downstream into the Arrow Hill esker. The esker consists of 15 to 20 m-thick massive beds of shale boulders and cobbles that are moderately sorted and clast-supported (Gmc) (Fig. 3-15), suggesting deposition from a hyperconcentrational flow (grain flow). The convergence of low linear ridges at the esker suggests that the subglacial flood that deposited these low-linear-ridges was confined within the Arrow Hill ice-walled channel. The catastrophic density flow swept weathered shale bedrock into the channel and transported the boulder- to cobble-sized shale fragments for a long distance before depositing them in the ice-walled channel.

4.3.2 Depositional environments and surface elevations of deltas

4.3.2.1 Definition:

An early description of deltas was made by Gilbert (1885) for Pleistocene fan-shaped coarse sediments deposited by glacial streams into Lake Bonneville. Based on

Gilbert's description, Barrell (1912) defined a delta as "deposits, partly subaerial, built by a river into or against a permanent body of water"; and he used topset, foreset, and bottomset to describe the structure of delta. Miall (1984) pointed out that deltaic sediments that are deposited subaerially and in shallow marine or lacustrine environments typically show a gradation into fine-grained offshore facies.

Fan delta is a subtype of delta. Holmes (1965) and McPherson et al. (1987) defined a fan-delta as an alluvial fan prograding directly into a standing body of water from an adjacent highland. This definition has been expanded to include deltas that are coarse-grained and bedload dominated (Gallway, 1976; Postma and Reop, 1985; Nilsen, 1985), and deltas deposited mainly by density underflow and braid flows (Sun, 1993a).

As described in Chapter 3, delta sediments in glacial Lake Hind area are coarse-grained, and consist mainly of pebbly sand, clast supported gravels, and cross bedded gravels. These deltas can be subdivided into two categories modified from Smith (1991) classification: a Gilbert-type fan delta and a braided delta. A Gilbert-type delta (fan-foreset delta of Smith, 1991) consists of a topset, a foreset, and a bottomset. A braid delta consists of a fan-shape sandar that has abundant shallow braided channels at the surface and lacks large scale foresets internally; it is different from the braid delta of Smith (1991) and McPherson (1987) by lacking visible subaqueous foreset slope deposits and by having fan shapes.

4.3.2.2 Gilbert-type fan delta

The deltaic model in Fig. 4-6 is constructed based on the fan-foreset delta model

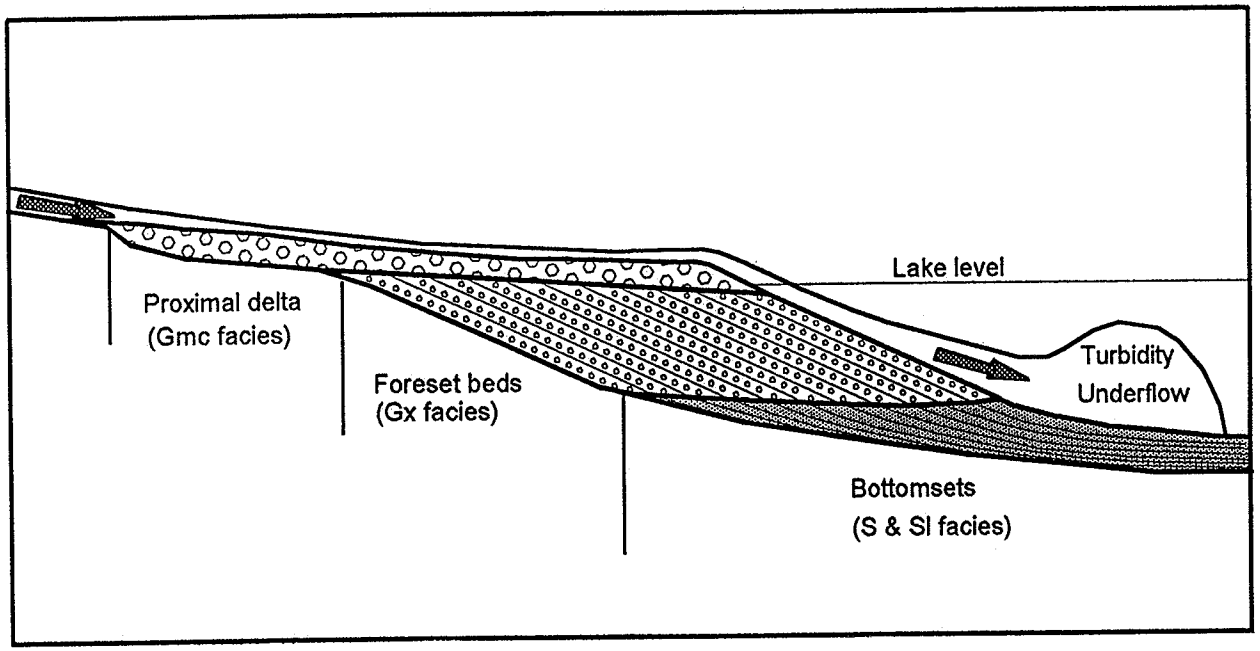

Fig. 4-6 A schematic diagram of Gilbert-type fan-foreset delta. Sediments are dominantly gravels and coarse-grained sand; Deposition was dominated by fequent hyperconcentrational underflows (modified after Smith, 1989).

of Smith (1991) and underflow delta model of Smith and Ashley (1985, their figure 4-29). This model reflects the fact that several exposures in deltas of the Lake Hind area (Figs. 3-8, 3-6, 3-11, 4-7) reveal massive cobbles and boulders in the proximal deltas and cobbly to pebbly gravel topsets that overlie finer gravel foreset in the delta fronts, which is similar to that of fan-foreset delta of Smith (1991).

Sediments in the topsets ranges from massive boulders to cobbles, and to pebbles that are clast supported and poorly sorted, with a sand and granule matrix. Cut and fill structures are rare, so is stratification. Furthermore, where a main-feeding channel trenched into shale, the proximal delta can be dominated by massive shale boulders and cobbles (Melita and Dand deltas); otherwise, carbonate rocks and Shield rocks are dominant (Pipestone and Little Saskatchewan deltas). It is clear that the sediments in the topsets are probably high energy, hyperconcentrational flow deposits.

Deltaic foresets occur in fan-foreset-deltas that have large feeding channels, such as the Souris valley and Dand valley that relate to hyperconcentrational floods (see next chapter) (Kehew and Teller, 1994a; Sun and Teller, 1996). The vertical sequences in this setting are similar to that of the deep-water fan-foreset delta of Smith (1991), i.e. cobbly and pebbly topset beds are underlain by gravel deltaic foreset beds, which in turn, are underlain by sandy bottomset beds (Fig. 4-7). According to Smith and Ashley (1985), meltwater deltas were mostly deposited by either quasi-continuous or surging-type underflows that were triggered by hyperconcentrational floods. The association of deltaic foresets with large meltwater spillways in Lake Hind suggests that sudden surging-type underflow were the dominant depositional mechanism.

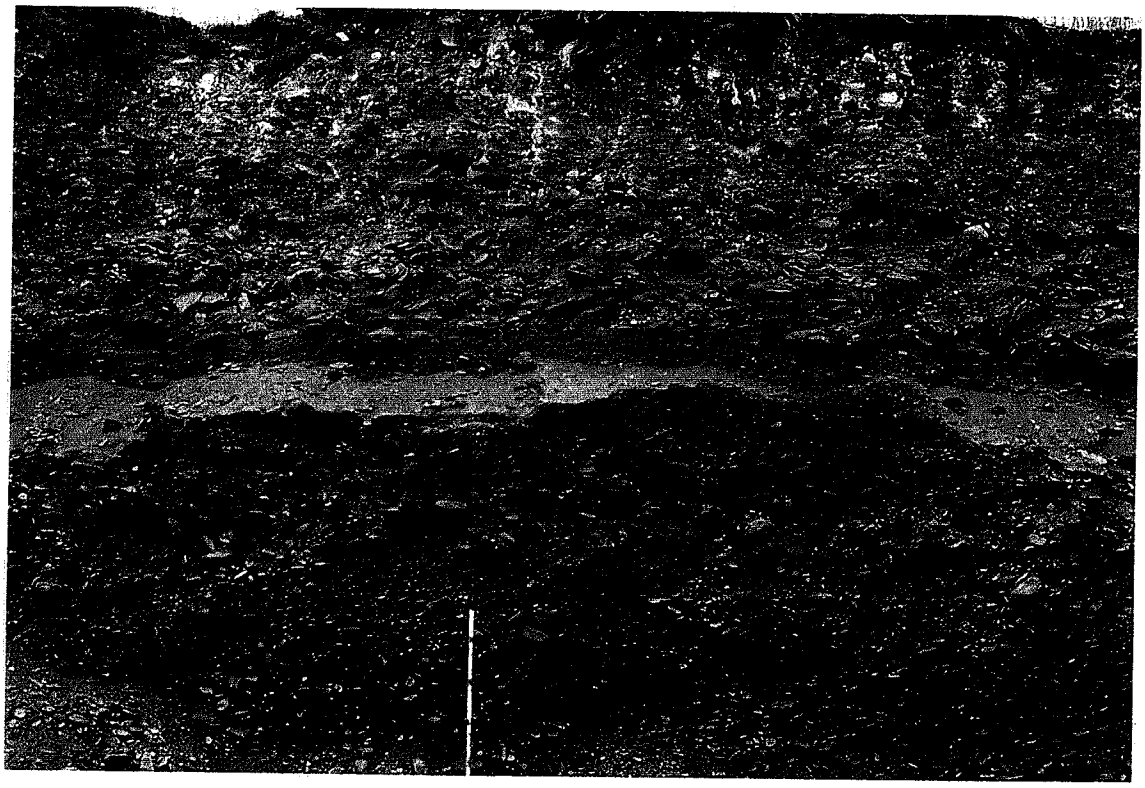

Fig. 4-7 A photograph of the massive shale fragments in the proximal Dand delta (K of Fig. 2-3) at 6.5 km west and 2 km south of the town of Elgin. Similar sediments also occur in the distal delta (see Fig. 3-7). The Auger is 1.2 m-long.

Deep-water bottomsets are not well exposed. Well logs reveal that there is a thick bed of fine to coarse grained sand adjacent to the deltas (Fig. 3-11), suggesting that the delta bottomset beds are dominated by sand (S) that was deposited from turbidity underflows.

4.3.2.3 Braid delta

The deltaic model in Fig. 4-8 (braid delta) is characterized by lacking deltaic foresets. Pebbly sand sub-lithofacies is the dominant lithofacies in the main-part of the delta and it generally is less than 5 m thick. Basinward the pebbly sand sub-lithofacies changes to shallow water lacustrine sand (S) and to mud (Fm) (Fig. 4-8). On the surface, abundant braided channels form inter-locked net works along a main channel. The main feeding channels are small (less than 500 m wide and less than 10 m deep) according to the 1:50,000 topographic maps. Examples of these deltas are the Antler, Gainsborough, Jackson, Stony, Bosshill, and Gopher deltas in the western Lake Hind basin.

Blatt et al. (1980) suggest that lack of stratification is the result of either rapid deposition from suspension or deposition from very high concentrated sediment dispersions caused by continuous meltwater flows, and by sheet floods during spring melting. For the braid deltas in the Lake Hind basin, lack of foreset beds may be explained by rapid deposition in broad shallow water zones during sheet floods. These sheet floods may be less turbulent, lower in sediment concentration, and smaller in magnitude than any of the hyperconcentrational and catastrophic floods that have been discussed by Kehew and Teller (1994a; 1994b), Kehew and Clayton (1983), and Lord

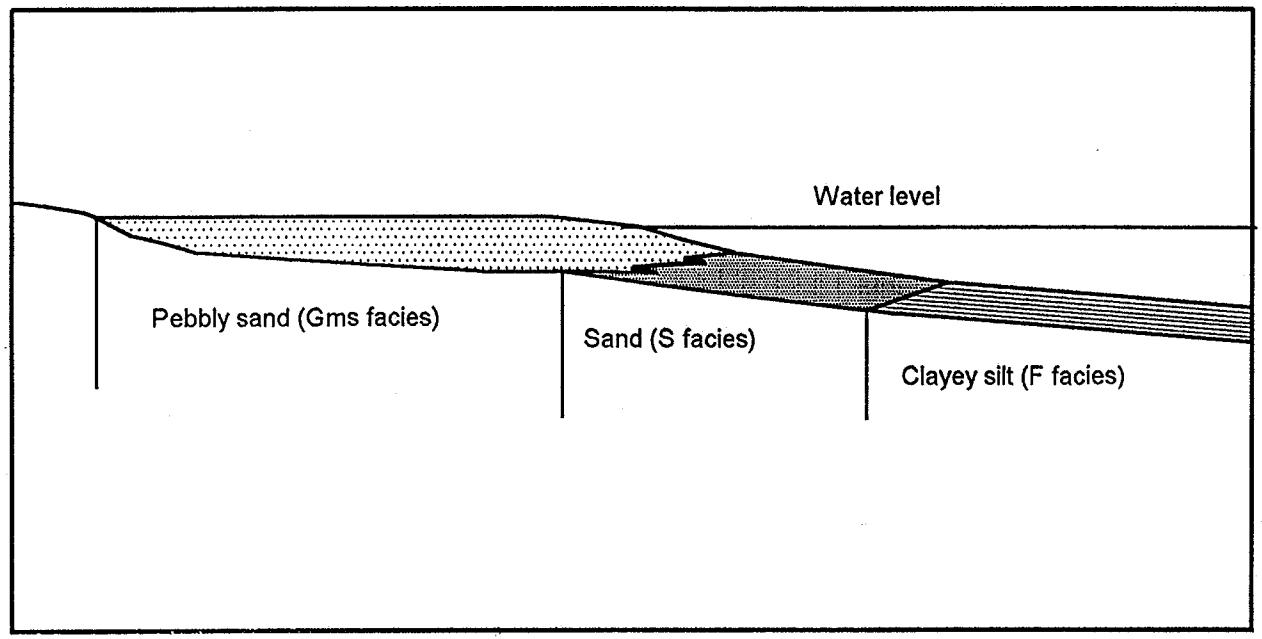

Fig. 4-8 A schematic diagram of braid delta. This type of delta is generally small, and is deposited in very shallow water (< 5 m). Sediments may be deposited by seasonal floods or quasi-continuous meltwater flows. It is different from the braid delta of McPherson et al. (1987) by lack foresets and having pebbly sand of density flow deposits.

(1991). In addition, these meltwater channels may have functioned for a short time period, so they could not have supplied enough sediments to allow the deltas to prograde across the a broad shallow-water zone into deep-water to form foreset beds.

4.3.3 Surface elevations of deltas

In this section the late glacial elevation of deltas during deposition will be discussed. This late glacial elevation is different from the modern elevation of deltas due to crustal tilting after the retreating of the ice. The purpose of this discussion is to link the paleo-lake level with the late glacial elevations of deltas.

There are 12 deltas along the margin of the glacial Lake Hind basin (A to L of Fig. 2-3). Of the 12 deltas, 9 form an irregular and nearly continuous fringe of coarse sediment between the higher elevation till to the west and the finer lacustrine sediments in the lake basin to the east (Fig. 2-3).

Figure 4-9 shows the modern surface elevation and the late glacial elevations of the 12 deltas. The modern elevation is corrected back to late glacial elevation by removing an amount of crustal rebound, which is derived from the isostatic tilting curves of Herman beach level of Teller and Thorleifson (1983, their figure 2), and extended lines of equal postglacial uplift (Teller and Thorleifson, 1983, their figure 1). The Herman Beach level of Lake Agassiz was choose because meltwater from glacial Lake Hind deposited the Pembina delta when glacial Lake Agassiz was at the Herman beach level (Kehew and Clayton, 1983). In Fig. 4-9, the late glacial elevations of the deltas gradually decrease toward north. The Dand delta and the Little Saskatchewan delta (K

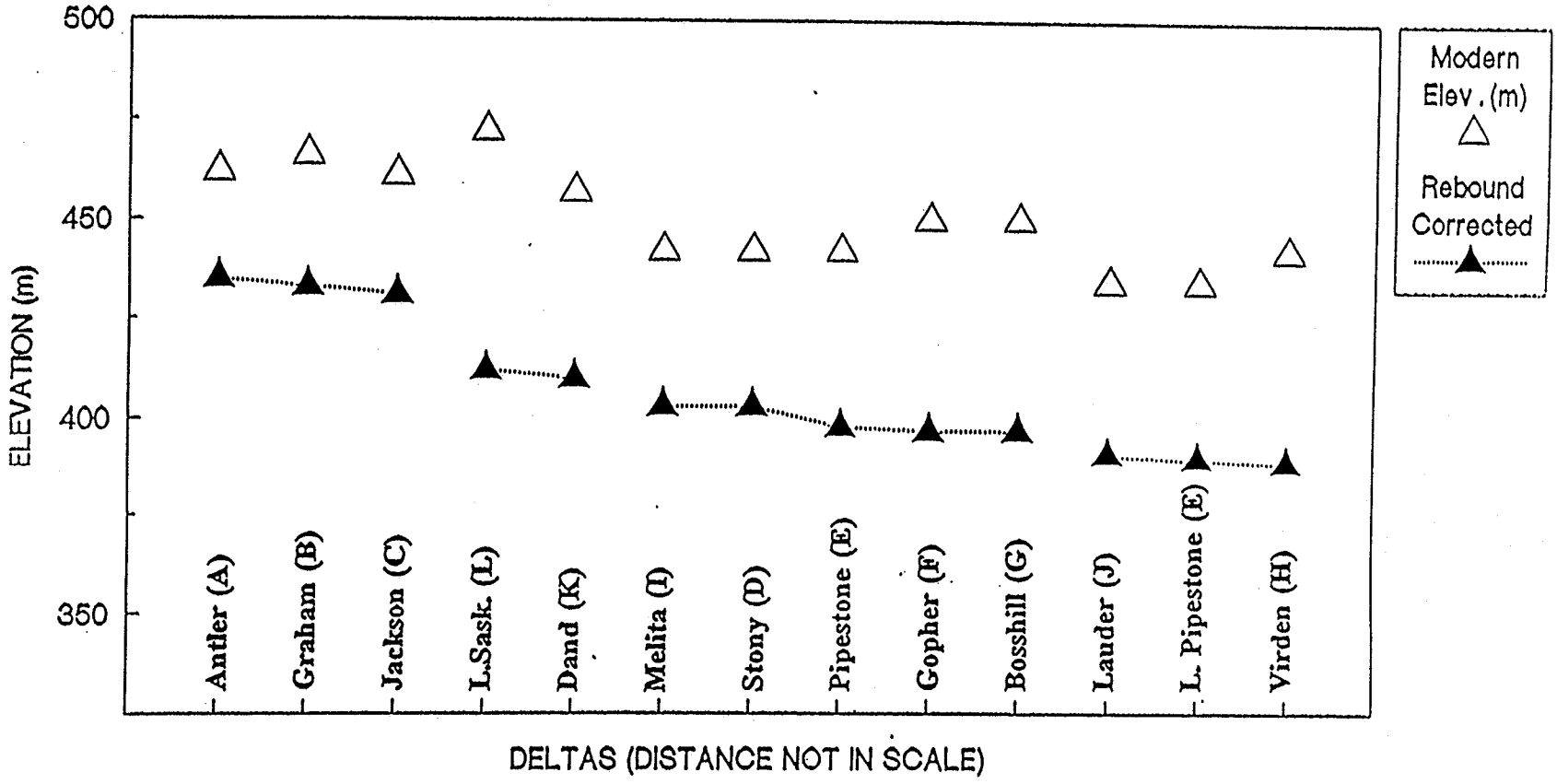

Fig. 4-9 Modern elevation and the corrected late glacial elevation of the delta surfaces. See Fig. 2-3 for locations of deltas. (From Sun and Teller, 1996, Fig.4)

and L in Fig. 2-3 and 4-9) on the eastern side of the basin are two exceptions. Based on the corrected late glacial elevation (in brackets) of deltas, the 12 deltas can be divided into 3 groups: 1) above 410 m (457 m modern); 2) between 403 (450) and 397 (442) m; and 3) below 391 (434) m.

Deltas with surface elevations above 457 m (paleoelevation of 410 m) are: Antler, Graham, and Jackson deltas in the narrow southwestern end of the basin (A, B, and C of Figs. 4-9 and 2-3), the Little Saskatchewan delta (L of Figs. 2-3 an 4-9) in the northeastern corner, and Dand delta (K of Figs. 2-3, 4-9) in the southeastern part of the basin. Sediments are dominated by pebbly sand sub-lithofacies (Gms) in the Antler, Graham, and Jackson deltas (braid deltas of Fig. 4-8), by clast supported gravel lithofacies (Gmc) with low shale content in the Little Saskatchewan Delta, and by clast-supported and shale-rich gravel sub-lithofacies (Gmc) overlying cross bedded gravel sub-lithofacies (Gx) in the Dand delta (fan-foreset deltas of Fig. 4-7).

Among these deltas, the Dand delta is special because of its surface slope and its feeding system. The Dand delta is a long and narrow delta. Its long-axis is oriented parallel with the southeastern edge of the basin (Fig. 4-10), and forms a 135° angle with its feeding channel, the Dand Channel. The surface elevation of the delta is 7 m higher in the eastern end (457 m) than the western end (450 m). The channel that leads to the delta is only 20 km long and 1 km wide. It starts at the southern edge of the Lake Hind basin, cuts across ridged till, and enters the same basin from the southwest with three branches (Figs. 4-10, 2-3). The western branch is at a lower elevation than the eastern two.

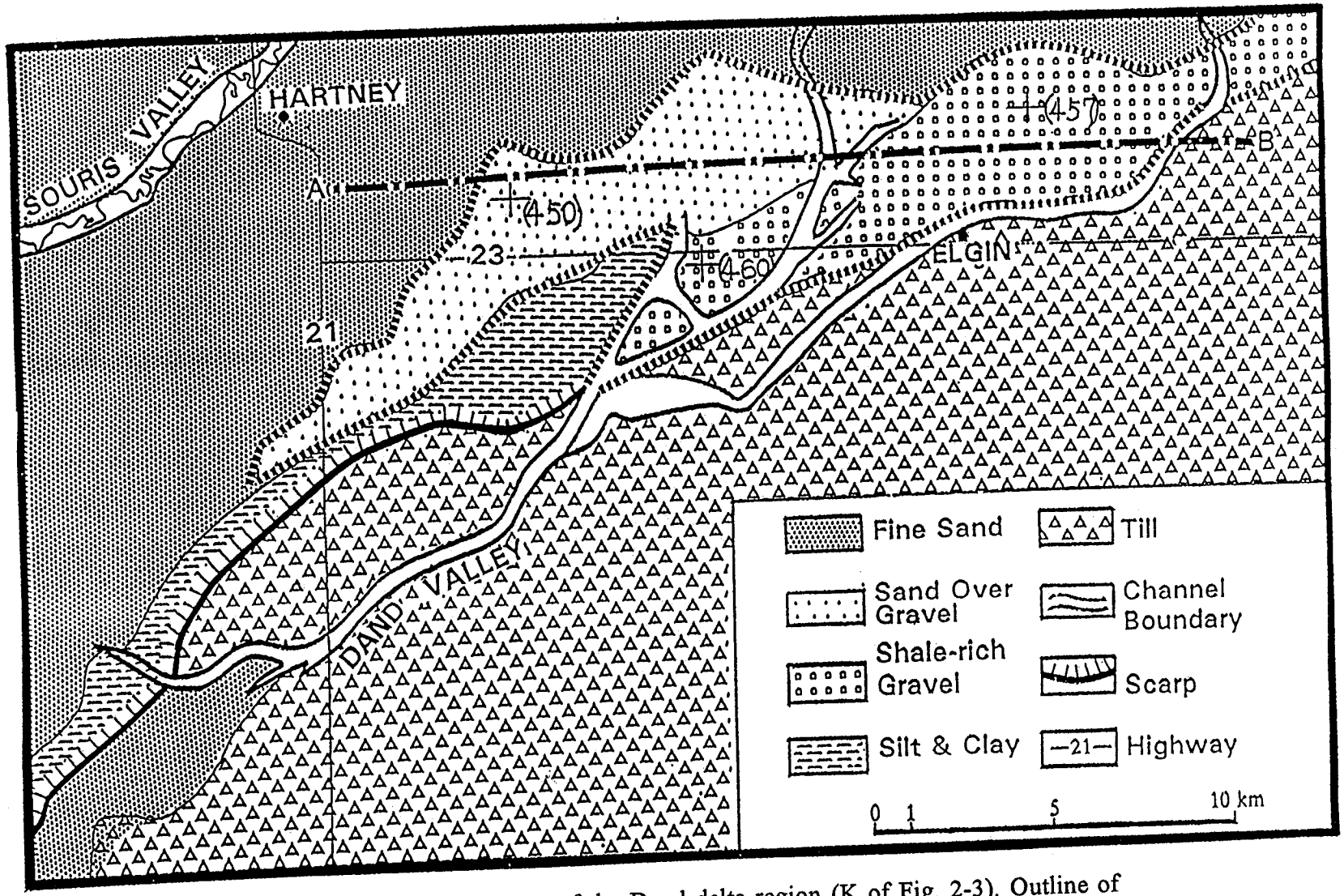

Fig. 4-10 Surficial geology of the Dand delta region (K of Fig. 2-3). Outline of the delta is shown by dotted lines. Numbers in bracket are surface elevations from topographic map (after Sun and Teller, 1996).

Along the western side of the basin from Melita to Virden, 4 deltas occur at an elevation between 403 and 397 m (450 to 442 modern). From south to north they are Melita, Stony, Pipestone, Gopher, and Bosshill deltas (I, D, E, F, G of Fig. 2-3). The Stony, Gopher, and Bosshill deltas are braid type deltas because they lack foreset beds. The Melita and Pipestone deltas are fan-foreset deltas. Among these deltas, Pipestone delta is the largest with the thickest deltaic sediment sequence, and is underlain by very thin lacustrine silt and clay (Fig. 3-11B).

The Virden and Lauder deltas are the two lowest deltas (Figs. 2-3, 4-9). The Virden delta is located adjacent to the Assiniboine River valley in the northwest corner of glacial Lake Hind and consists of mainly massive sandy pebbles. The proximal Virden delta is overlain by about 0.5 m till. The Lauder delta is located on the north side of the Souris River at 391 m (434 m modern), and consists of 6 m of massive, non-stratified, and clast supported cobbles (Gmc sub-lithofacies, underflow fan), underlain by till (Dl) and patches of well laminated clayey silt (Fl). This delta differs from the Melita delta (Gmc, Gx) by having much coarser gravels that are deficient in shale fragments, and by a lack of stratification.

4.3.4 Depositional environments of sand and mud in central Lake Hind basin

The borehole described on Fig. 3-9 from the central Lake Hind basin shows 20 m of clay and silt, overlain by 15 m of sand and mud couplets; which, in turn, is overlain by 12 m of sand. How did this 47-m-thick coarsening upward sequence get deposited in the short history of Lake Hind? I believe that, beside the large number of

feeding channels (11), underflows that were caused by periodic catastrophic floods from the Souris, Pipestone, and Qu'Appelle-Assiniboine spillways may have supplied most of the sediments into deep-water area.

How far can underflows go from the river mouths? Pickrill and Irwin (1982) detected underflows up to 40 km downlake from a stream mouth in Lake Wakatipu during a flood. It is reasonable to believe that a catastrophic flood, such as the one from the Souris River valley (Kehew, 1982; Kehew and Lord, 1986, 1987; Kehew and Clayton, 1983, Kehew and Teller, 1994a), may generate such a powerful underflow that it may continue more than 40 km from the river mouth. In the deep basin, sediments such as the massive sand lithofacies and the sand beds in sand-mud couplet lithofacies (Fig. 3-9) were probably deposited from sudden catastrophic surging flows. These deposits are separated by silt and clay of suspension deposits in low energy regions of a lake.

4.4 Depositional environments of glacier deposits

Glacier-deposits underlie lacustrine sediments (Figs. 3-9, 3-11) and are exposed in uplands peripheral to Lake Hind (Figs. 2-3, 3-12, 4-10). Detailed studies of lithofacies (Dl and Dh) and the stratigraphy of glacier deposits under lacustrine sediments are difficult because they are rarely exposed at the surface and, in borehole descriptions they are very similar in color and texture. Thus, my discussion in this section will be concentrated on the morphology and lithofacies of late Wisconsinan deposits near the surface.

The areal distribution of the carbonate content of till samples (Shown in Fig 4-11) suggests that Dl diamicton sub-lithofacies occurs south, west, and northwest of glacial Lake Hind, while Dh diamicton sub-lithofacies occurs only east of glacial Lake Hind. The Alexander moraine (P of Fig. 2-3) is roughly the divide between the two sub-lithofacies. The Alexander moraine is the northern extension of the Darlingford moraine in the Tiger Hills Upland (Sun, 1993a; Conley, 1986), and is characterized by low relief and abundant potholes-lakes; it is blanketed by 0.3-0.5 m of lacustrine deposits. Carbonate analyses of till samples from the ridge yielded high carbonate contents (Sun, 1993a), suggesting that the ridge is part of the high carbonate sub-lithofacies by ice flowing from the east. The abundance of pothole lakes in the Alexander moraine suggests that the moraine was formed in an ice marginal lake.

The Dl diamicton sub-lithofacies occurs to the west and south Lake Hind area (Fig. 4-11). The most notable glacial landforms in the Dl diamicton sub-lithofacies are the sub-parallel ridges and doughnut-till plain in the Boissevain area, south of glacial Lake Hind (see section 3.3.1 of Chapter 3) (Fig. 3-12). As described in Chapter 3, the doughnut landforms can be identified clearly in air photos (Fig. Fig. 3-13). However, the same doughnuts are not shown on the satellite images (Fig. 3-14); instead, the region appears to be covered by narrow-ridges (some are paired) that are oriented in the same direction as the ridges in the ridged till plain. In places one or two of the narrow ridges in the doughnut plain are linked with an ice ridge in the ridged till plain, and show a smooth transition. In some cases a pair of narrow ridges in the doughnut till plain grade into a broad and low ridge before linking to a single thrust-ridge in the ridged till plain.

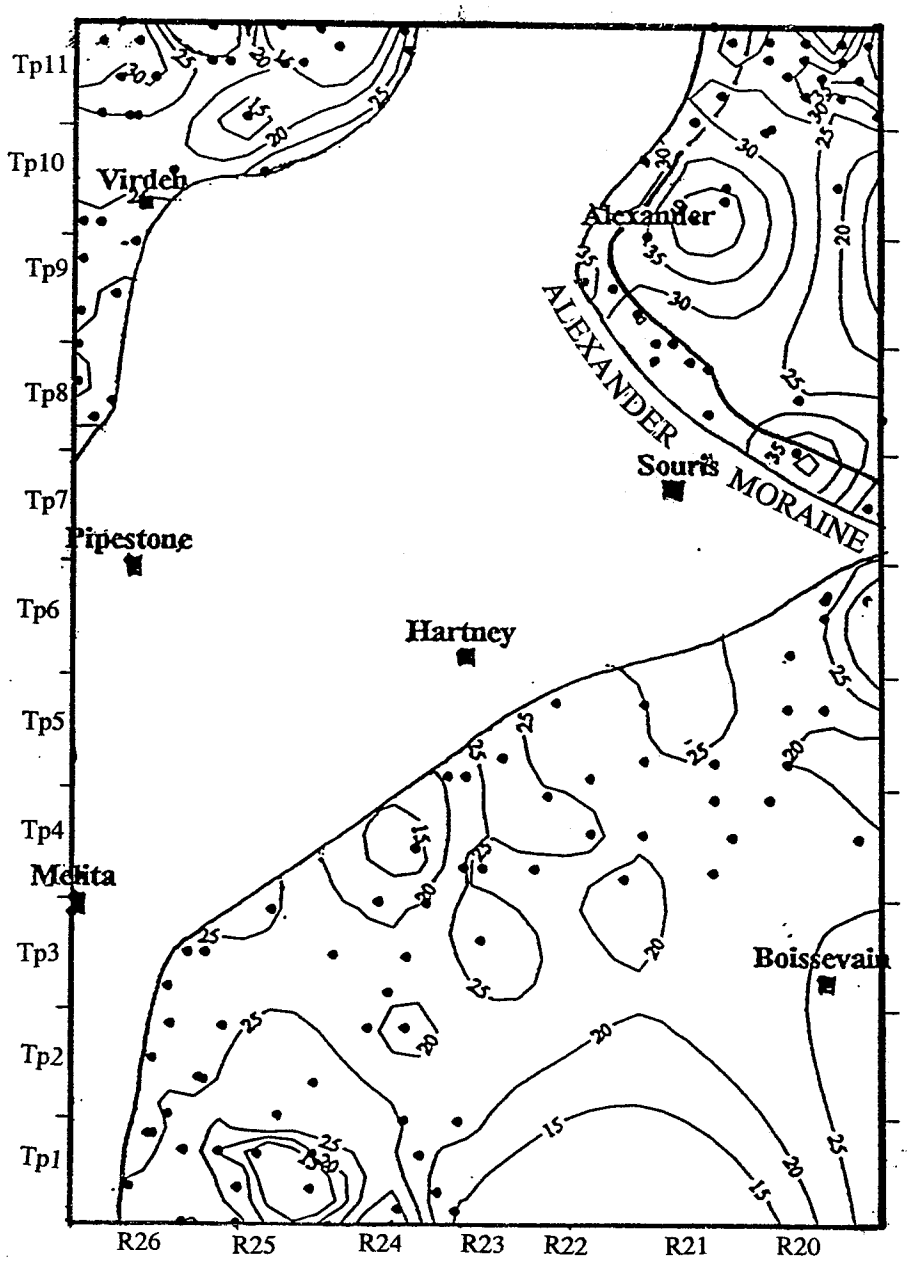

Fig. 4-11 Contour map of carbonate content of tills near the surface. This map is based on carbonate analysis on 90 till samples. The uncontoured area is covered by lacustrine and eolian sediments.

This suggests that the doughnuts and thrusted ridges are related.

There are three possible interpretations for sub-parallel ridges in a till plain: thrusted ridges, recession (annual) ridges, and filled crevasses. The presence of evidence of large blocks (>25 m^2) of shale bedrock in the study area suggests that the sub-parallel ridges are likely thrust-ridges in origin. Based on the low carbonate content of the tills and the orientation of these ridges, they were formed by a northwest to southeast advance of glacial ice.

Deal's (1972) model for similar sheared ridges (washboard moraines) in Rolette County of North Dakota can serve as an explanation in the Boissevain area. Fig. 4-12 shows how superglacial shear-ridges could form in the early stage of ice-melting by sediment being carried up shear-plains in the ice by compressional flow. Because these sediments were provided protections from solar radiation, ice under the thick drift near the debris ridges melted slower than ice in-between the shear-plains (Fig. 4-12). As the relief became accentuated, sediments in the ridges slumped into the adjacent depressions, resulting in thick drift in the inter-shear-plains areas; this exposed ice along the former shear-plains (Fig. 4-12). This process may have been repeated several times, resulting in sub-parallel and broad-ridges in a till plain. (Fig.4-12).

However, it is difficult, if not impossible, to use Deal's (1972) model to explain the large shale slabs on the crests of ridges and the occurrence of stratified gravels and sand in ridges (Fig. 4-13). An alternative interpretation is that the gravels and shale slabs were let-down vertically with little disturbance. In this model, the initial melting resulted in a blanket of drift over the ice. The effectiveness of solar radiation in melting ice

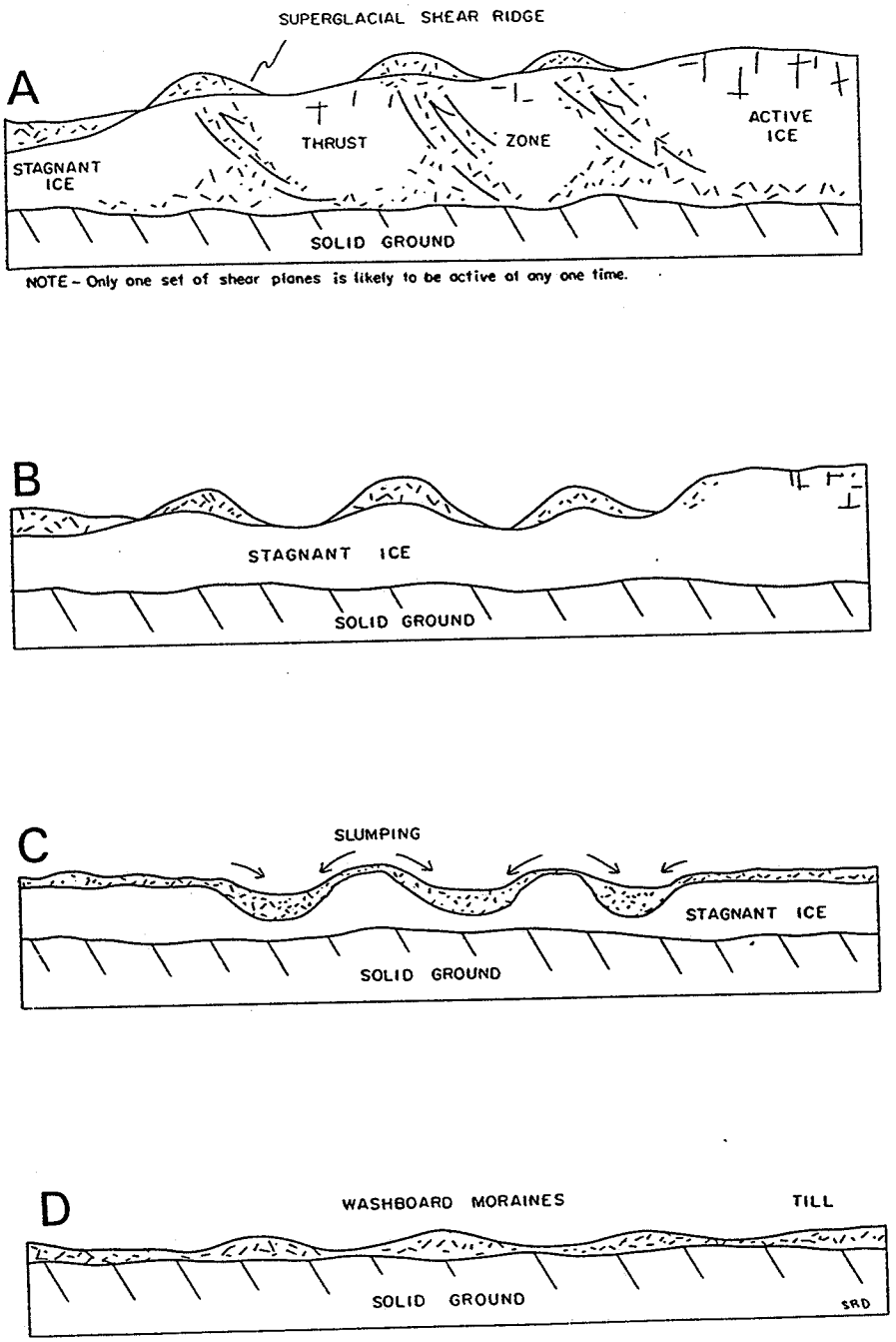

Fig. 4-12 Schematic diagram showing how subparallel ridges can be formed from superglacial shear ridges (after Deal, 1972).

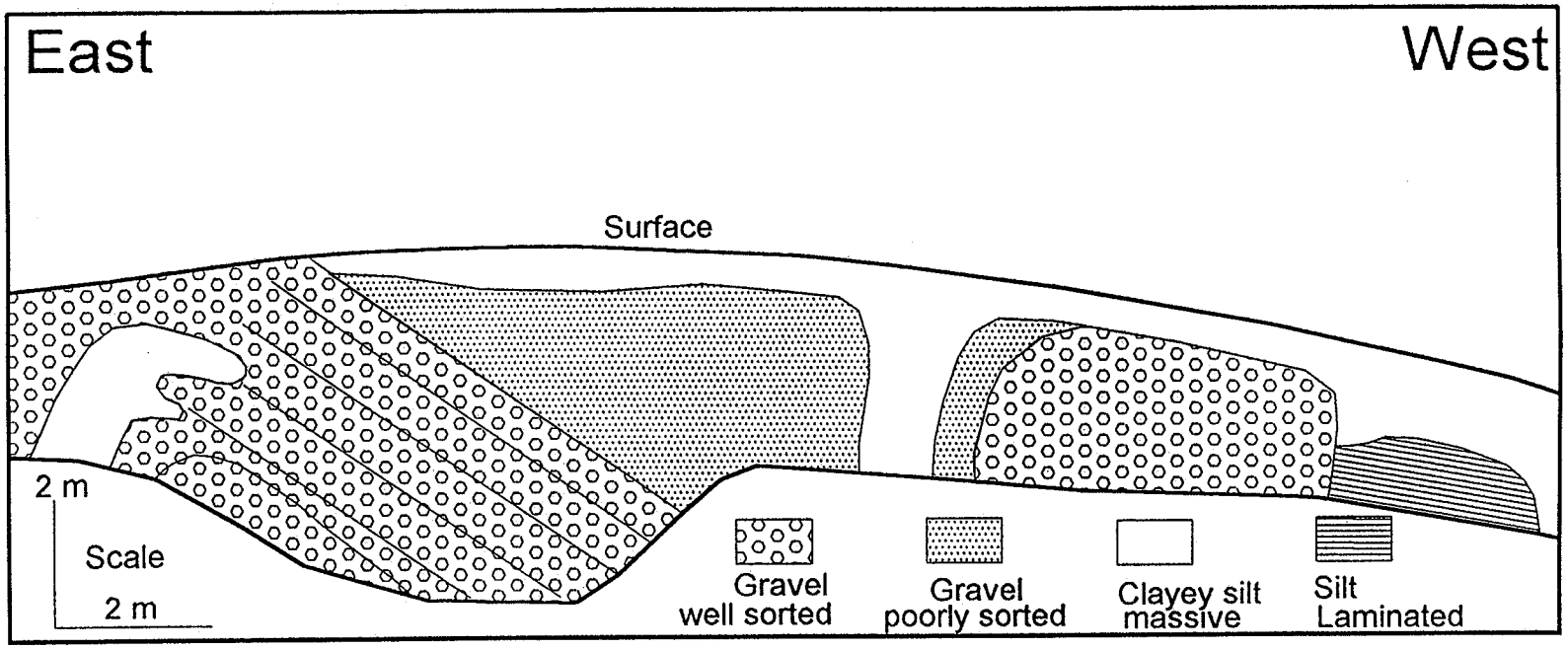

Fig. 4-13 A east-west cross section of a single ridge in the ridged plain. The inclined beds of silt and gravels are indicative of a thrust plain. Location of this figure is shown in Fig.3-12.

decreased as more and more sediments covered the ice. Meanwhile, down-ice percolation of rain water and meltwater along the shear-planes resulted in faster melting near the shear-plains than anywhere else, resulting in ridges along the former shear-plains, which contain well sorted material and large slabs of bedrocks.

What is the origin of doughnuts in till plains? Deal (1972) and Clayton (1967) proposed two models as shown in Fig. 4-14. But these two models can not explain why the doughnuts chain up along the thrust ridges and coincide with lacustrine deposits at the surface, and why there are no doughnuts in most parts of the ridged till plain where there are no silts or clays at the surface.

Maizels (1992) proposed a jökulhlaup flow model for boulder-rich rim structures. Boulder-rich rims consists of diamicton that overlie sandur gravels of catastrophic flood deposits in Myrdals sandur, south Iceland. The rim ridges (doughnuts) were produced by the melting of debris-rich ice blocks, which were transported on the surface of a hyperconcentrational flood surge (Maizels). Doughnuts in the Whitewater Lake area of southwestern Manitoba are not associated with any gravels from flood deposits. So Maizels model (1992) can not be used without modification.

The occurrence of thin lacustrine silt over the doughnut plains suggests that the doughnuts may have been related to a superglacial lake. The lake covered the southern half of the stagnant ice area that had been sheared (Fig. 4-15a). Thus, the processes operating in the shallow-water were probably different from those in the higher northern area where high sheared ridges were formed. In the shallow lake area, wave winnowing and storm washing resulted in thick sediment deposited along the shear plains (Fig. 4-

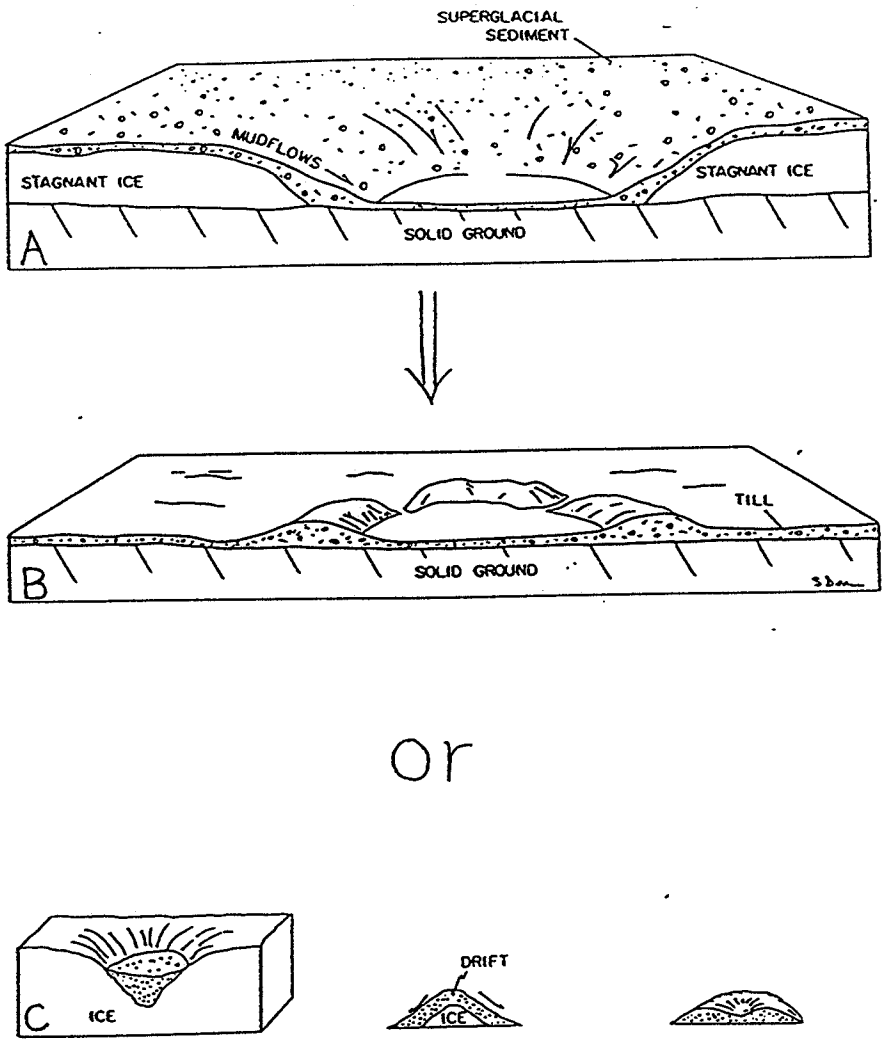

Fig. 4-14 Two traditional explanation for doughnuts in till plain. In these models, glacial fluvial and lacustrine sediments were deposited in ice-walled kettle lakes. Melting of ice resulted in large depressions and rim-ridges if the kettle lake was large and on solid ground (A and B). Otherwise melting of ice outside of kettle lakes would resulted in low mounds or kames with ice cores. Subsequent melting of ice cores resulted in potholes with rim-ridges around each potholes (C). In both cases, doughnuts will occur randomly, instead of line-up with sheared ridges (From Deal, 1972, Clayton, 1967).

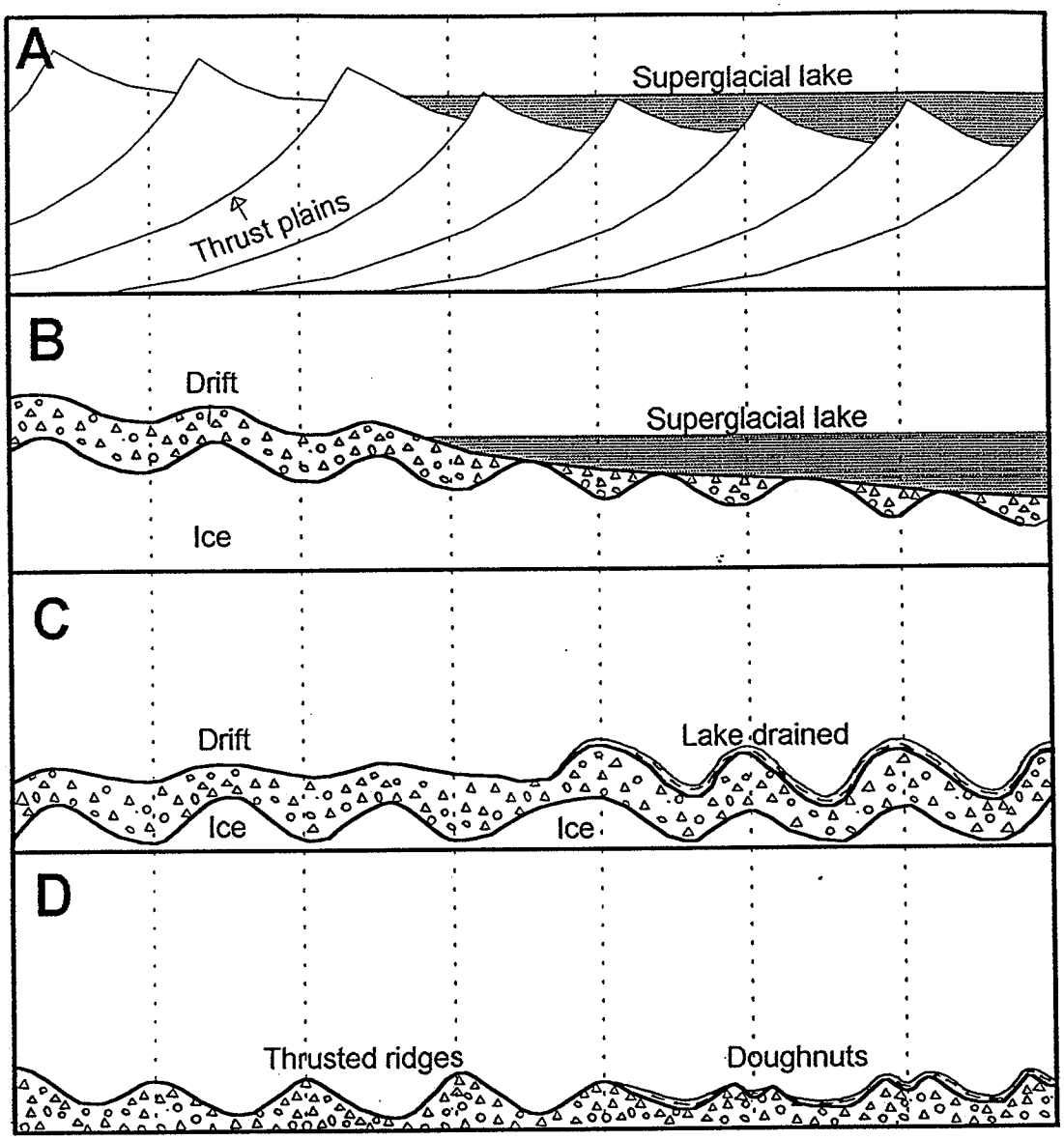

Fig. 4-15 A Model for subparallel ridges and associated doughnuts north and west of the Whitewater Lake area. A) Shear movements during glacial advance resulted in a series of subparallel thrust plains; subsequently a superglacial lake was formed in the lower southern end. B) In the superglacial lake, more drifts were deposited in depressions than in the hill of ice. C) The superglacial Lake drained; melting of ice in the former lake plain resulted in ice-cored hills along the thrust plains; but in the upland area, ice-cored hills were formed in-between the thrust plains. D) melting of ice resulted in potholes with rim-ridges in the former lake floor; and resulted in high ridges in onshore area.

15b). Next, the superglacial lake drained before the complete melting of ice; continuous melting of ice resulted in ice-cored ridges along the shear-plains (Fig. 4-15c). Each of the ice-cored ridge became a chain of ice-core hills as a result of uneven melting of ice cores. Subsequent melting of these stagnant ice left closely spaced potholes that are surrounded by 0.5 to 1 m-high circular rim-ridges.

CHAPTER 5

FLUVIAL GEOMORPHOLOGY AND PALEOHYDROLOGY

5.1 Introduction

Based largely on the study of the Souris River spillway, Kehew (1982), Kehew and Clayton (1983), Kehew and Lord (1986, 1987), Lord (1991), and Kehew and Teller (1994a) proposed criteria for identifying catastrophic floods that eroded large spillways over an initially flat lowland. These criteria include, but are not limited to, scoured sub-uplands adjacent to the inner spillways, boulder lags in the scoured sub-uplands and in the inner channels, residual hills within the spillways and in the scoured sub-uplands, and massive boulder and cobble deposits in the terraces. Sun and Teller (1996) suggest that scoured sub-uplands and boulder-lags may be missing if a channel was formed as the result of multiple flood events.

Among the 10 main drainage ways that enter Lake Hind (Fig. 2-3), the Souris-Moose Mountain spillway, Pipestone spillway, and Assiniboine-Qu'Appelle systems appear to have been formed by major floods (Kehew and Clayton, 1983; Kehew and Teller, 1994a; Sun and Teller, 1996). Other drainage ways immediately west of the Lake Hind basin probably began as subglacial valleys that carried mainly "normal" flows of meltwater (Fulton et al., 1994; Sun and Teller, 1996).

In the following sections I will describe channel morphologies, terraces, and gravel bars of the Moose Mountain spillway, Souris River spillway, Pipestone valley,

Assiniboine-Qu'Appelle River spillway, and Pembina River spillway. This is followed by a paleohydrological interpretation based largely on the morphology of these valleys and the sedimentary structures and grain size of materials in their terrace and bars.

5.2 Souris-Moose Mountain spillway system

5.2.1 Moose Mountain spillway and glacial lakes Indian Head and Arcola

The Moose Mountain spillway system includes glacial Lake Indian Head, Moose Mountain spillway, and glacial Lake Arcola. The Moose Mountain spillway joins with the Souris River spillway at the town of Oxbow (Fig. 1-1). The 2300 km^2 glacial Lake Indian Head basin is at the head of this system, lies at an elevation up to 640 m, and consists of up to 7 m thick lacustrine sediments. The basin has three outlets. These three outlets are Moose Mountain spillway, which lies at an elevation of 655 m at its upper end, Pipestone valley, which lies at 640 m at its upper end, and Qu'Appelle spillway, which everywhere lies below 579 m (Fig. 5-1).

The Moose Mountain Spillway originates at the southern end of glacial Lake Indian Head basin, and, en route to the Souris spillway, passes through glacial Lake Arcola, which covers 700 km^2. The upper 37 km of this spillway, just south of glacial Lakes Indian Head, is shallow and has a reversed-gradient toward the north, while the rest of the spillway downstream has a normal gradient; this "normal'' part of the spillway is about 1 km wide and 15 to 20 m deep, has steep side-walls, and lacks visible terraces or scoured sub-uplands adjacent to the spillway. Where the Moose Mountain spillway enters the northern end of glacial Lake Arcola, there is a large gravel delta (bar?).

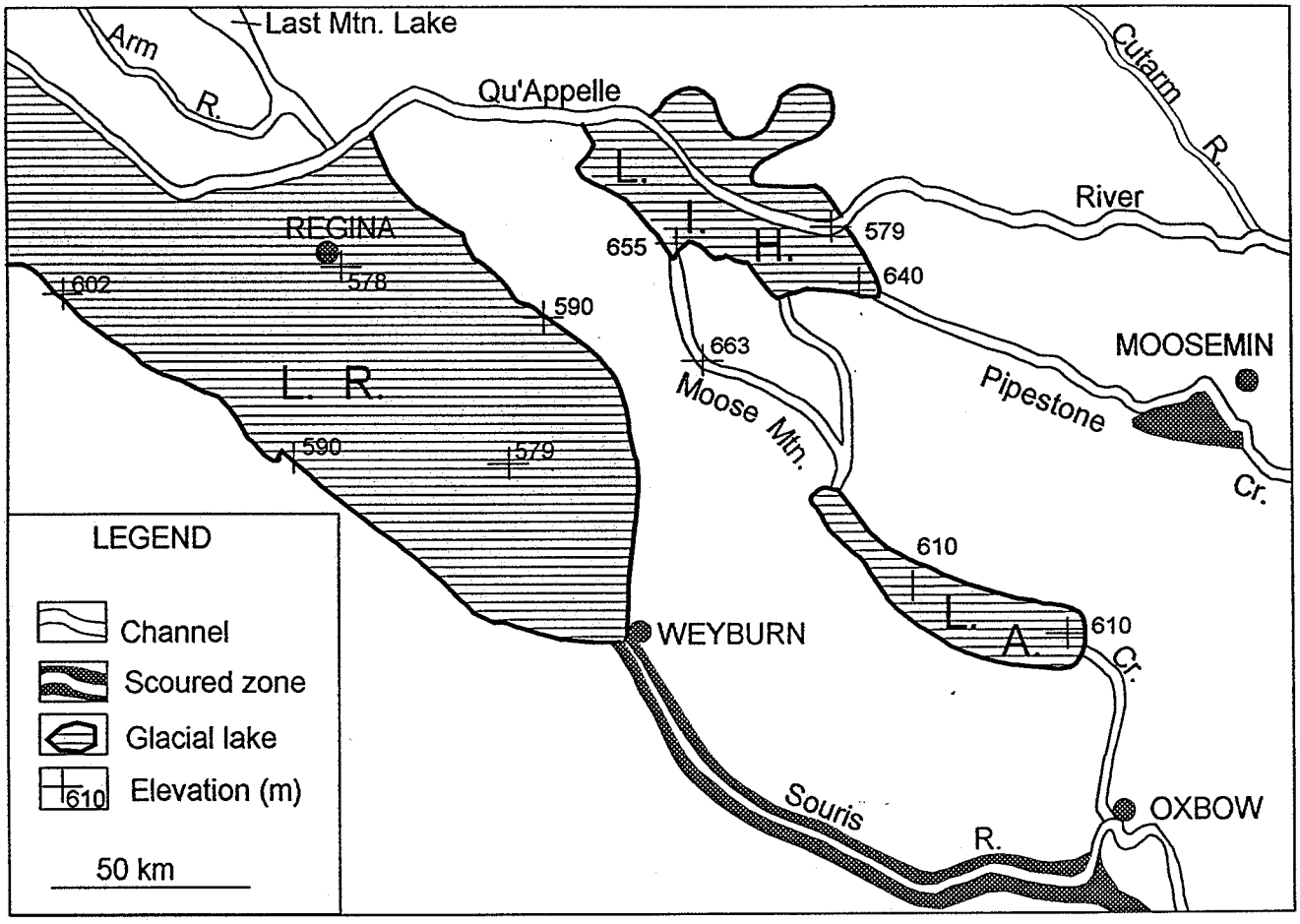

Fig. 5-1 Location of glacial lakes Regina (L.R.), Indian Head (L.I.H.), and Arcola (L.A.); with selected elevations on the lake floors and their outlets.

Sediments in this delta are dominated by massive, matrix supported, 5-m-thick beds of pebbles and cobbles (Gmm sub-lithofacies), with a sand and mud matrix, suggesting deposition from a high density turbulent flow or debris flow (see section 4.2.1 of Chapter 4) that originated in glacial Lake Indian Head.

The arcuate glacial Lake Arcola (Figs.1-1, 5-1) is located along the southern flank of Moose Mountain upland, and is surrounded by hummocky till deposits. The lake floor is generally flat except near the Kisbey Esker (Christiansen, 1956), which is located in the northern basin and is parallel with the long-axis of the lake; this esker rises 20 to 50 m above the lake floor. The Moose Mountain spillway, on the other hand, is no more than 50 m wide and 5 m deep in the central part of the Lake Arcola basin.

The spillway between glacial Lake Arcola and the Souris River spillway has a steep slope (0.15% vs 0.04-0.09%), with a V-shape cross section about 1 km wide and 10 to 50 m deep. There are 2- to 3-km-wide scoured sub-uplands areas adjacent to the eastern side of the spillway. Abundant potholes in till, a sign of deposits from stagnant ice (Deal, 1972), are present immediately to the west of the spillway and east of the scoured sub-uplands. Near the Souris valley junction, there are two distinctive terraces. The high terrace is developed on till (scoured sub-uplands), while the low terrace consists of a large bar of very coarse cobbly gravels. The massive, clast-supported, cobbly gravels in this bar also suggest deposition by a major flood (Facies Gmc).

5.2.2 Souris River spillway and glacial lakes Regina and Souris

The Souris River spillway system consists of, in downstream order, glacial Lake

Regina, the Souris River spillway, glacial Lake Souris, glacial Lake Hind, and the Pembina River spillway (Figs. 1-1). I will not discuss Lake Hind here because Lake Hind and its sediments have been discussed in the previous four chapters. The Pembina spillway will be discussed in a later section.

Glacial Lake Regina covered an area of about 9300 km^2 (Kehew and Clayton, 1983). The basin floor is flat along the northwest-southeast long-axis and rises about 12 m toward the southwestern and northeastern margins. The northwestern end of the basin near Regina is at an elevation of about 578 m, which is the same as the southeastern end near the town of Weyburn (Fig. 5-1). Sediments in this basin consist of up to 14 m of silt and clay (Regina Clay, Christiansen, 1960) in the central basin, which grade into silt and sand toward the higher southwestern and northeastern margin. The modern basin has two outlets: the Souris River valley and the Qu'Appelle River spillway. The Qu'Appelle River spillway cuts a 2-km-wide and 60-m-deep valley across the northern edge of Lake Regina (Christiansen, 1961). The Souris River spillway, on the other hand, originates from the southern tip of glacial Lake Regina at Weyburn (Fig. 1-1), and has no visible scoured channels extending into the basin.

Immediately downstream from the lake basin, the Souris River spillway has a small central channel within an 8-km-wide scoured zone that contains elliptical hills and boulder lags, as described in detail by Kehew (1982) and Kehew and Clayton (1983). The central inner channel becomes gradually deeper and wider downstream from less than 500 m wide and 15 m deep in the first 30 km downstream from Weyburn to 1.2 km-wide and 30 m-deep at 20 km upstream from the Moose Mountain junction (Fig. 5-

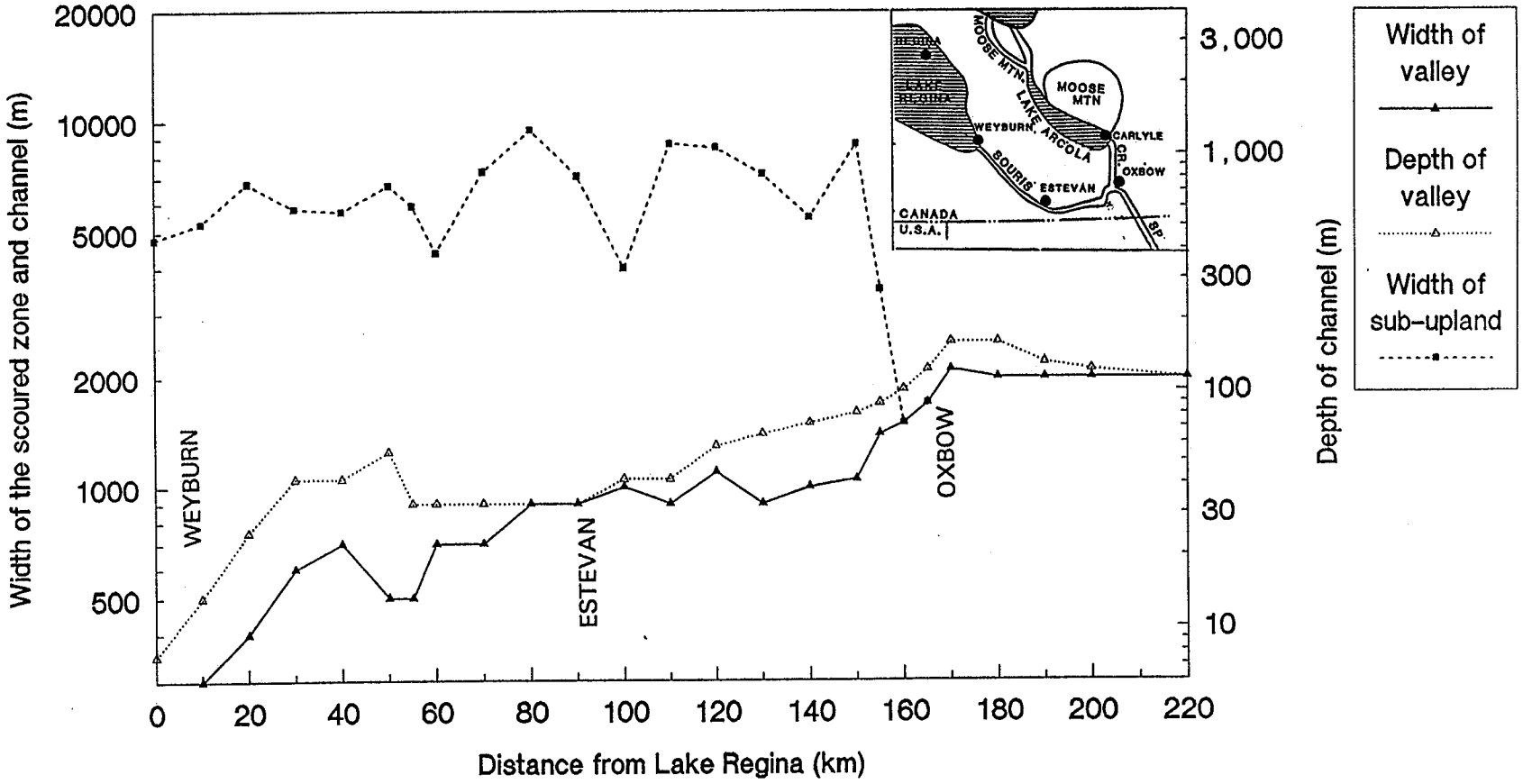

Fig. 5-2 Downstream variation of width of inner channel and of the channel when the scoured sub-uplands are included in the Souris River valley between Weyburn and Oxbow, Saskatchewan.

2). The inner channel enlarges sharply to 2 km wide and 50 m deep in the next 10 km to the Moose Mountain River spillway junction (Figs. 5-2). The width of the scoured zone varies from 4500 to 8000 m wide until 20 km upstream from the Moose Mountain junction at Oxbow (Fig. 5-2), where the scoured zone becomes abruptly narrower and disappears before reaching Oxbow (Fig. 5-2). Although the scoured channel continued for about 10 km southeast (Fig. 5-1) into the De Locs valley, the headwater of the De Locs valley is only about 10 m deep and 1 km wide, and is 35 m higher than the Souris River valley (Kehew and Clayton, their Figure 3).

From Oxbow downstream to glacial Lake Souris, the channel remains 2 to 3 km wide, and becomes gradually shallower, from 50 m deep near Oxbow to 25 m deep at the river mouth in the glacial Lake Souris Basin, and to less than 5 m-deep where the river crosses the lake floor (Kehew and Clayton, 1983). Along this part of the Souris Spillway, scoured subupland channels are rare. Upon entering the Lake Souris basin, two coarse-grained sediment fans with fining upward sequences were deposited (Lord, 1988, 1991); one of these is at the mouth of the Souris River and another one in the middle basin floor.

Glacial Lake Souris covers an area about 6000 km^2 and has three prominent strandlines at 472 m, 460 m, and 450 m in Rolette County, North Dakota (Deal, 1972). Sediments in the basin consist of up to 20 m of sand and 5 m silt and clay overlying till (Lord, 1988). There are two coarse-grained fans, the one near the glacial Lake Souris inlet is at an elevation between 457 and 466 m (Lord, 1988), and a smaller one in the deep basin is at an elevation of about 450 m (Lord, 1988; topographic maps). Both fans

consist of matrix-deficient gravels (Gmc) overlying lignite-rich gravels (Gmm) in the proximal fan and well sorted sand(s) overlying lignite-bearing sand in the middle and distal fan (Lord, 1988, his Fig. 39). The lake basin has two outlets: the southeastern outlet consists of a series lakes leading to the James Spillway and Sheyenne Spillway, ranging from 457 to 472 m in elevation (Lord, 1988); the Souris Spillway is at an elevation about 424 m and exits the basin northward to glacial Lake Hind (Fig.1-1).

In between glacial lakes Souris and Hind, the Souris River spillway has a slope-gradient of about 0.013%. The first 12 km of the spillway is a single channel that is about 2 km wide and 15 m deep, with its floor and scoured sub-uplands at about 434 m and 450 m respectively. In the next 18 km to glacial Lake Hind the channel is separated into three branches by two elliptical hills that are 8 to 15 km long and 2 to 3 km wide. Each of these Souris River spillway branches is about 15 m deep and 1 to 2 km wide. When the scoured zone bordering the entire entrenched spillway is included, the width is 10 km wide. The surface sediments in the scoured zone are either reworked (washed) tills (Dl lithofacies) or massive and cross stratified gravels and pebbly sand (Gmm, Gms, and Gx lithofacies) (Fig. 2-3). In contrast, sediments within the channels dominantly consist of scattered boulders and thin fluvial deposits of laminated fine sand and silty clay over shale bedrock (Fig. 2-3).

5.2.3 Paleohydrological interpretation

Moose Mountain spillway system

Because the Moose Mountain spillway is the highest outlet of glacial Lake Indian

Head (Fig.5-1), the lower Pipestone and Qu'Appelle outlets must have been blocked by ice when the lake discharged into Moose Mountain spillway. In addition, the reversed-gradient in the first 37 km of this spillway, leading from the lake basin, requires that glacial Lake Indian Head was either a subglacial lake or a superglacial lake. If it was a subglacial lake, meltwater could have flowed up-slope under high pressure beneath the ice (Fig. 5-3). Alternatively, glacial Lake Hind was a superglacial lake that was dammed to the south by stagnant ice (Fig. 5-4). The lake water found its way to the base of the ice and cut the Moose Mountain Spillway as pressurized outflow flowed upslope of the base of the glacier (Fig.5-4). The meltwater flow that trenched the spillway was a hyperconcentrational flow or debris flow, as evidenced by massive-matrix supported gravel deposits (Gmm) in the gravel delta at the northern end of glacial Lake Arcola (Fig. 3-5) (See 4.3.2 of Chapter 4). Lack of a scoured zone in the upland immediately adjacent to the spillway supports the superglacial lake theory, i.e. the uplands were protected by stagnant ice.

Once the hyperconcentrational flow entered glacial Lake Arcola, the flow dispersed rapidly and deposited a massive gravel delta (Gmm lithofacies). The hyperconcentrational flow did not erode a large channel across glacial Lake Arcola, suggesting that the lake was full of water, possibly dammed by stagnant ice, which acted as a buffer reducing the shear-stress of the incoming flow. At the southern margin of the stagnant ice where the flood water came out of the ice-walled channel, a cobbly gravel fan was deposited. Farther downstream the flood water may have followed an early ice marginal channel and enlarged it into the Moose Mountain spillway all the way to glacial

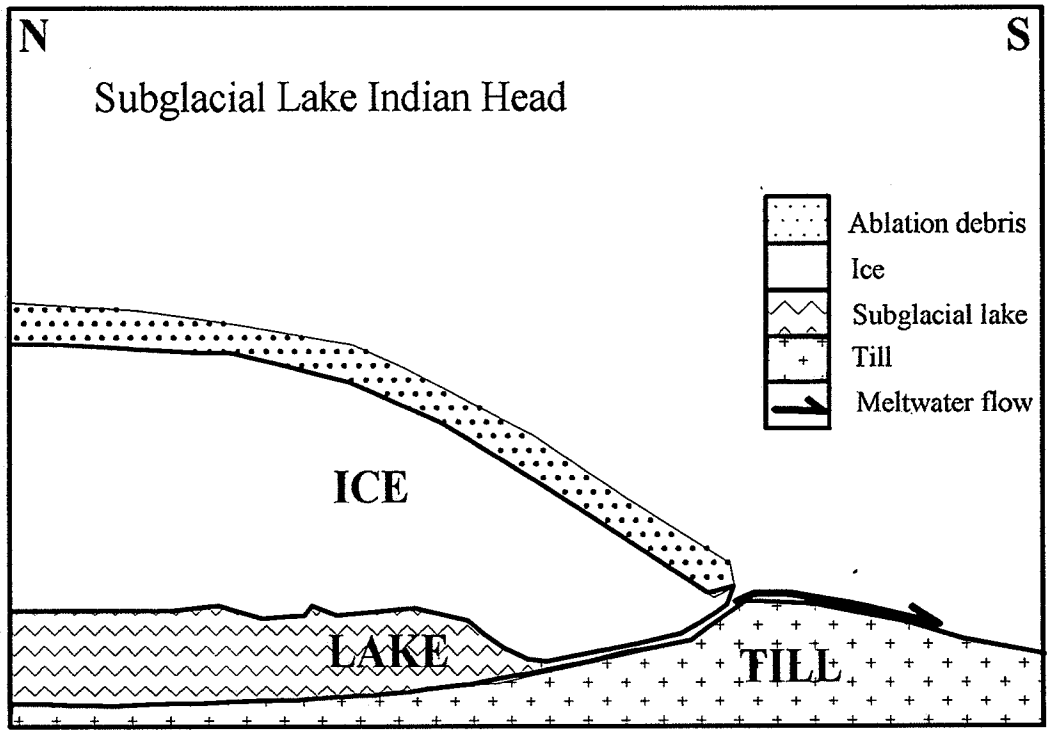

Fig. 5-3 Schematic diagram showing hypothesis I of glacial Lake Indian Head. The lake may be a subglacial lake. Under high pressure generated from upstream input, the meltwater may have flowed southward and eroded the Moose Mountain valley. Melting of ice would deposit till over lacustrine sediments.

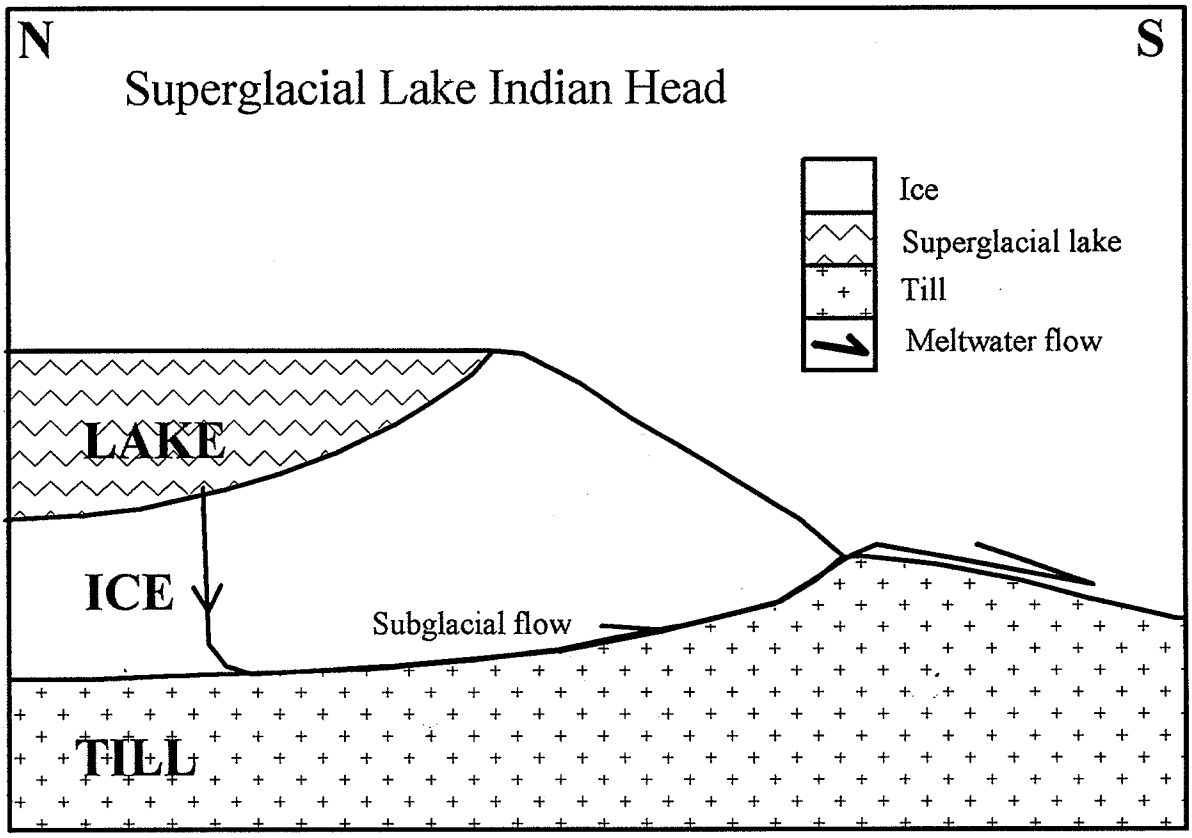

Fig. 5-4 Schematic diagram showing hypothesis II of glacial Lake Indian Head. The lake may be a superglacial lake that was dammed by ice to the south. Meltwaters found their way to the base of ice and burst southward. This eroded the Moose Mountain valley into ice and newly deposited till.

Lake Souris.

In glacial Lake Souris, the incoming flow deposited a high elevation fan at the mouth of the spillway at an elevation of 457-466 m (Lord, 1988), and caused a catastrophic drainage of the lake northward into glacial Lake Hind via the Souris Spillway (Lord, 1988; Kehew and Clayton, 1983). The northern outlet was chosen because it was lower than the southern outlet. In-between glacial lakes Souris and Hind, the flood water deeply entrenched the spillway, which branches into three spillways within a 5 to 10 km scoured zone. At the entrance in glacial Lake Hind, this flood deposited the shale-rich lower sequence of Melita delta at an elevation about 442 m (I of Fig. 2-3). As a result of rapid incision of the Pembina spillway, Lake Hind fell to about 434 m, as indicated by the surface elevation of next group of lower deltas at 434 m (Fig. 4-9).

Souris-River spillway system

Glacial Lake Regina was a 9300 km^2 ice marginal lake that was impounded by stagnant ice along the southeastern end (Kehew and Clayton, 1983). The absence of shorelines and presence of hummocky till plains in the southeastern end (Christiansen, 1960) (except in the Souris River spillway) support this interpretation. The catastrophic flood from glacial Lake Regina probably was started by the failure of this ice dam. A lack of scoured channels across the lake floor suggests that this was a one-time event and was not repeated, and indicates that subsequent overflow from this basin did not occur through the southern outlet (Kehew and Teller, 1994a)

The Souris River spillway is less than 700 m wide in the first 30 km downstream from the lake. In the next 110 km downstream, the width of the scoured zone ranges from 4700 to 8000 m wide while the depth and width of the inner channel increases gradually (Fig. 5-2). Similar inner channels within scoured zones have been produced in flume studies (Shepherd and Schumm, 1974) by sheet flows, which initially scoured a broad area and then incised a narrow inner channel. Kehew (1982), Kehew and Teller (1994a), and others have concluded that many steep-sided channels in the Canadian Prairies that have scoured zones along them (e.g. 5-10 km wide) were initiated by flood sheet flows that soon entrenched the scoured zones.

The abrupt increase in width and depth of the inner channel and the sudden termination of the scoured zone near the junction with the Moose Mountain spillway near the town of Oxbow (Fig. 5-2) suggests that the flow entered a pre-existing valley, probably the one formed by the flood burst from lakes Indian Head and Arcola. The pre-existing channel must have been enlarged by this second flood. Fig.5-1 shows that the scoured zone continues southeast into the De Locs valley (Kehew and Clayton, 1983). However, the De Locs valley could not have carried a significant amount of the Lake Regina flood because the headwater of the valley is only about 10 m deep and 1 km wide, and is 35 m higher than the Souris River valley.

In glacial Lake Souris, the sudden inflow eroded a 2-km-wide channel across the previously deposited delta (Lord, 1988) at an elevation between 457 and 466 m, and deposited the lower fan in the central basin at an elevation about 450 m. Lack of silt and clay sediments over sand at the surface (Lord, 1988, 1991) suggests that the basin was

no longer a good sediment trap. The flood water from this second flood flowed through the lake, further enlarging the pre-existing northern outlets, and discharging into next lake downstream, Lake Hind. In glacial Lake Hind, the flood waters deposited a shale-deficient massive gravel sub-lithofacies over the Melita delta at an elevation of 442 m (I of Fig. 2-3), eroded a shallow channel across southern Lake Hind, and deposited a small delta in the deep basin at an elevation of 434 m (J of Fig. 2-3).

This interpretation is different from previous hypotheses which suggests that the Souris River spillway was trenched by a single catastrophic flood from glacial Lake Regina, and that glacial lakes Souris and Hind were drained completely by this one flood (Kehew, 1982; Kehew and Clayton, 1983; Kehew and Lord, 1986, 1987; Kehew and Teller, 1994a). My interpretation can explain better the two drastically different sequences (Gmc and Gx sub-lithofacies) in the Melita delta. The presence of massive gravel lithofacies (Gmm and Gmc sub-lithofacies) along the Moose Mountain spillway supports the idea of a second hyperconcentrational flood. This hyperconcentrational flow had nowhere to go but into glacial lakes Souris and Hind. Therefore, it is logical to consider that some sediments in these two basins were deposited as a result of this flood.

5.3 Pipestone River valley

5.3.1 Geomorphology

The Pipestone River valley originates in glacial Lake Indian Head at an elevation about 15 m lower than the Moose Mountain Spillway outlet (Fig. 5-1). The system consists of four distinctive parts, from upstream to downstream. 1) glacial Lake Indian

Head, 2) a 150-km-long narrow valley, 3) a 30-km-long broad valley, and 4) the Pipestone delta (Figs.5-1, 5-5).

Glacial Lake Indian Head has been discussed in the last section as part of the Moose Mountain spillway system. The Pipestone River valley is the intermediate outlet of glacial Lake Indian Head at an elevation of about 640 m. From glacial Lake Indian Head to 150 km downstream near Cromer, the width of the Pipestone River valley increases gradually, while its depth varies between 21 and 42 meters (Fig. 5-5). The walls of the valley from 0 to 105 km downstream (A to D) are steep, except on the inside of a meander bend at 87 km (C in Fig. 5-5) where a massive cobbly gravel bar was deposited. Scoured channels and drumlines occur in a 22 km zone along the Pipestone valley between 60 and 105 km (B to D of Fig. 5-5).

At the distance of 105 to 150 km downstream from Lake Indian Head, the valley walls become irregular with abundant hummocks. Two types of terraces have been observed. One lies south of Moosemin (D of Fig. 5-5) and consists of residual hills and remnants of residual hills of till; the main valley here is 7 to 15 m lower than the terrace (Fig. 5-6). Two gravel terraces are found 11 km upstream from Cromer at elevations of about 488 m and 510 m (E of Fig.5-5). A gravel pit in the upper terrace exposes 4+ m of massive bouldery gravels (Gmc).

The lower 30 km of the valley between Cromer and glacial Lake Hind is 3 to 4 km wide and less than 25 m deep, with walls that gently slope toward the modern river (Figs. 5-7). There are no residual hills, nor boulder lags, nor major gravel deposits along the northeastern side of the valley, but abundant gravels and three gravel hills lie

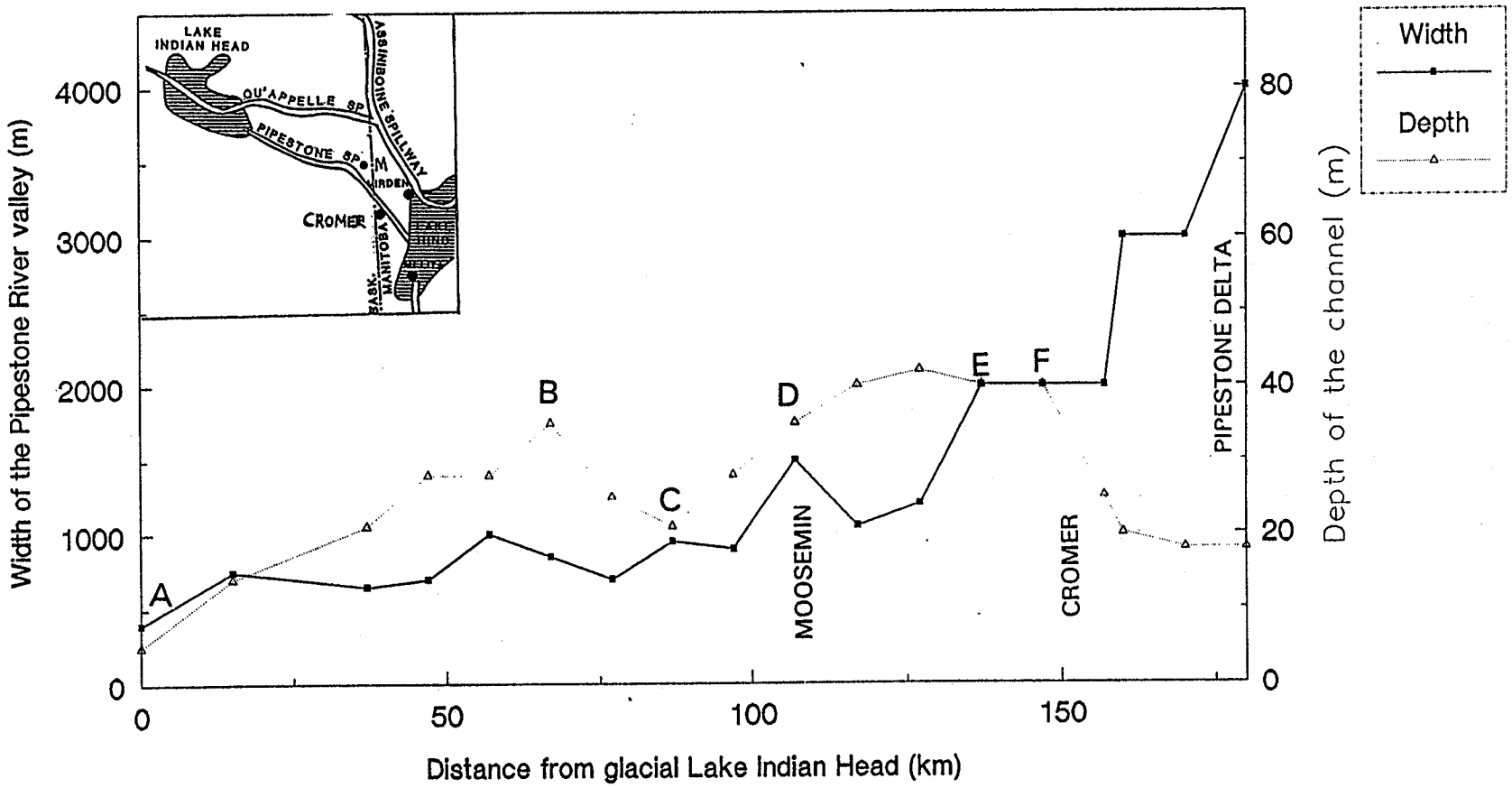

Fig. 5-5 Downstream variation of width and depth of the Pipestone River valley and the width of the scoured zone.

Fig.5-6 Photograph of former valley floor of the Pipestone valley at Sec.21-Tp12-R31W, south of Moosemin. Some streamlined hills are cut in half by the main deep valley, suggesting two flood events.

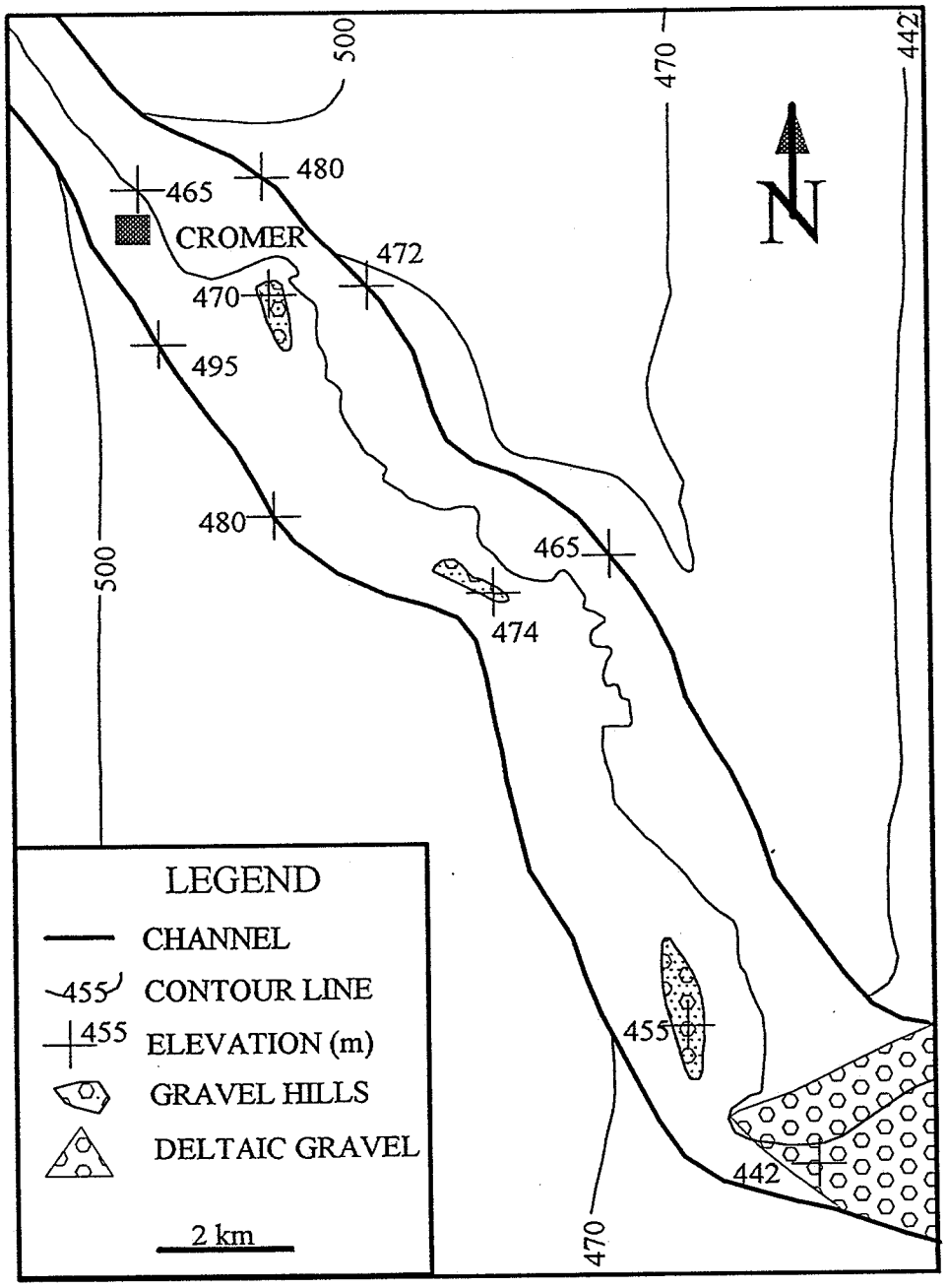

Fig.5-7 Pipestone River valley from the town of Cromer, Manitoba, to the Pipestone delta. Notice that gravel hills (kame-eskers) occur on the western side of the river only.

on the gentle slopes of the southwestern side (Fig. 5-7). The three gravel hills are 5 km apart; each is about 1 to 4 km long, 100 m to 1.5 km across. The one near Cromer (F) has a hummocky surface and the second hill 5 km downstream has a flat surface, both of which are at a surface elevation about the same as, or higher than, the upland till plains to the west and east (Fig. 5-7). A gravel pit in the second hill exposed 15 m of gravels, which consists of massive sandy fine gravels (Gms sub-lithofacies) in the basal 5 meters and massive cobbly gravels in the upper 10 meters (Gmc sub-lithofacies). The third hill near the delta has an elliptical shape and lies at an elevation at least 10 m higher than the modern river floor and delta surface.

Two deltas were deposited at the mouth of the Pipestone valley (Fig. 5-7, E in Fig. 2-3). The highest Pipestone delta lies at an elevation of about 442 m and consists of gravelly delta foreset beds that are capped by gravelly topset beds and are trenched by a 3-km-wide and 7-m-deep valley. A second delta lies at an elevation of about 434 m and consists of massive sandy gravels.

5.3.2 Paleohydrological Interpretation

The Pipestone valley may originally have been a subglacial channel, becoming an open channel later, as indicated by the hummocky side-wall from 105 to 150 km. The surface elevations of the three gravel ridges/hills in the lower part of the valley between Cromer and the Pipestone delta, which are as high as the till uplands just outside of the valley (Fig. 5-7), are indicative of a kame-esker origin rather than open channel deposition because confinement by ice walls seems necessary. The occurrence of gravel

deposits exclusively along the western side of the valley suggests that the ice-walled valley shifted eastward after deposition of these gravels. This preferred direction of channel migration probably relates to the eastward surface gradient Fig. 5-7); the Pipestone River valley is oriented northwest-southeast, which is oblique to the regional slope.

How many floods occurred in the Pipestone valley system? In the downstream end, the high Pipestone delta (E of Fig. 2-3) is a fan-foreset gravel delta that was deposited by high energy flows into glacial Lake Hind at an elevation of about 442 m, as indicated by gravel foreset beds (Gx) and massive gravel topset beds (Gmc sub-lithofacies); the same flow may have deposited the three kame-esker ridges between Cromer and the Pipestone delta (Fig. 5-7). The 3 km-wide broad valley across the higher delta and massive gravels in the lower Pipestone delta at an elevation about 434 m probably are indicative of a second flood; this flood probably was responsible for the eastward migration of the lower Pipestone valley.

In the upstream end of the Pipestone valley, the trench-like valley with uniform width from glacial Lake Indian Head to Moosemin, streamlined hills on a terrace near Moosemin (Fig. 5-6), and clast-supported massive cobbly gravels (Gmc) on the inside of a meander suggest a catastrophic flood from glacial Lake Indian Head. Evidence of more than one flood also lies at two gravel terraces at 10 km north of Cromer; 4+ meters of massive boulderly gravels were found at the higher terrace. If there are two floods where did the waters come from? Glacial Lake Indian Head seems to be the only source on surficial geological maps. Perhaps an unknown subglacial lake contributed to

one of the floods. The presence of kame-eskers in the lower Pipestone valley is indicative of a subglacial or superglacial flood.

5.4 The Qu'Appelle-Assiniboine River spillway system

5.4.1 Geomorphology

The Qu'Appelle-Assiniboine spillway system is one of the largest channels in the Canadian Prairies. At one time its headwaters extended west as far as the Rocky Mountains through the South Saskatchewan and Red Dear River valleys, a distance over 1300 km (Sun and Teller, 1995b). Thus, this glacial river crossed the provinces of Alberta, Saskatchewan, and Manitoba before reaching Lake Agassiz. The main valley and its branches drained a total area about 400,000 km^2 (Sun and Teller, 1995b), which was equivalent to about a fifth of the total drainage area of the Lake Agassiz basin.

The Assiniboine River spillway (Fig. 1-1) is a trench that is commonly 60 m deep and 2 km wide from its headwaters at Kamsack, Saskatchewan, to Brandon, Manitoba. The Qu'Appelle spillway has a similar profile which is about 80 m deep and 2 to 3 km wide (Klassen, 1983). En route to its junction with the Assiniboine River valley, the Qu'Appelle River spillway cuts across the basins of glacial Lakes Regina, Indian Head, and the Welby sand plain, and is joined by the Thunder, Last Mountain Lake, and Cutarm spillways in Saskatchewan (Figs. 1-1, 5-1) (Kehew and Teller, 1994a; Klassen, 1983). The valley fill beneath both the Qu'Appelle and Assiniboine spillways is composed of mainly clay, silt, and sand that is from 40 to 100 m thick (Klassen, 1983). Major coarse sediments deposited inside or adjacent to the valley downstream from

glacial Lake Regina include the 350 km^2 Welby sand plain at the mouth of the Cutarm valley near the Qu'Appelle and Assiniboine spillway junction (Klassen, 1979), a 4 km^2 gravel delta in the northwestern corner of glacial Lake Hind basin (Virden delta, H of Fig.2-3), a 16 km^2 gravel bar in the Assiniboine Flat (O of Fig.2-3), and a 6500 km^2 delta, the Assiniboine Delta, in the western Lake Agassiz basin near Brandon (Fig.1-1).

5.4.2 Interpretation

The Qu'Appelle and Assiniboine River spillways are examples of complex meltwater spillways. Kehew and Teller (1994a) propose that up to eight floods from the Qu'Appelle-Assiniboine spillway system may have reached Lake Agassiz; Wolfe and Teller (1995) suggest that a catastrophic flood from glacial Lake Assiniboine eroded the upper Assiniboine River spillway; Sun (1993a) concluded that at least three floods from the Assiniboine Spillway poured into Lake Agassiz and deposited coarse sediments in the Assiniboine delta. The lack of major deltaic deposits in glacial lakes Regina, Indian Head, and Hind suggests that these glacial lakes had drained prior to the time when floods from the next lake upstream reached them and entrenched their valleys across the drained lake floor.

The huge gravel bar with hummocky topography in the Assiniboine Flats is another example of multiple flood events as noted in Chapter 4 (section 4.2.2.1; see Figs.3-8, 4-1, 4-2). The Assiniboine River spillway in this area must have been eroded before deposition of this bar, and this must have been after Lake Hind drained because its location is in the northern (deeper) side of the lake basin. Several floods seem to have

been responsible for constructing this expansion bar in a broad part of the valley. The lower cross bedded gravels of the Assiniboine Flat bar were deposited first. The overlying coarse gravels on the upstream end of the bar appear to represent another flood event.

5.5 Pembina spillway

5.5.1 Geomorphology

The Pembina spillway is located along the southern side of the Tiger Hills upland and western side of the Pembina Mountain (Figs.1-1, 5-8), between the hummocky Darlingford moraine immediately to the north and till plains to the south. The spillway can be divided into three parts based on the morphology: from Lake Hind to the town of Ninette, from Ninette to the town of La Riviere, and from La Riviere to glacial Lake Agassiz.

From topographic and surface geological maps (Sun and Fulton, 1995a, 1995b; Manitoba Mines Mineral Resources Division, 1980), the Pembina spillway immediately east of Lake Hind is about 1.5 km wide and 60 m deep; As the valley expands to 3 km wide in the next 30 km to Ninette, the depth of the channel reduces to 30 m (Fig. 5-8). In this part there are several terraces. Two terraces at elevations of about 445 and 427 m respectively are well preserved along the northern side of the valley immediately downstream of the Souris Gorge. Paired terraces at 419 m are largely cut by the present meandering Souris River. No terraces have been found between the towns of Ninette and La Riviere; the valley in this part has a flat bottom and very steep side-walls (Elson,

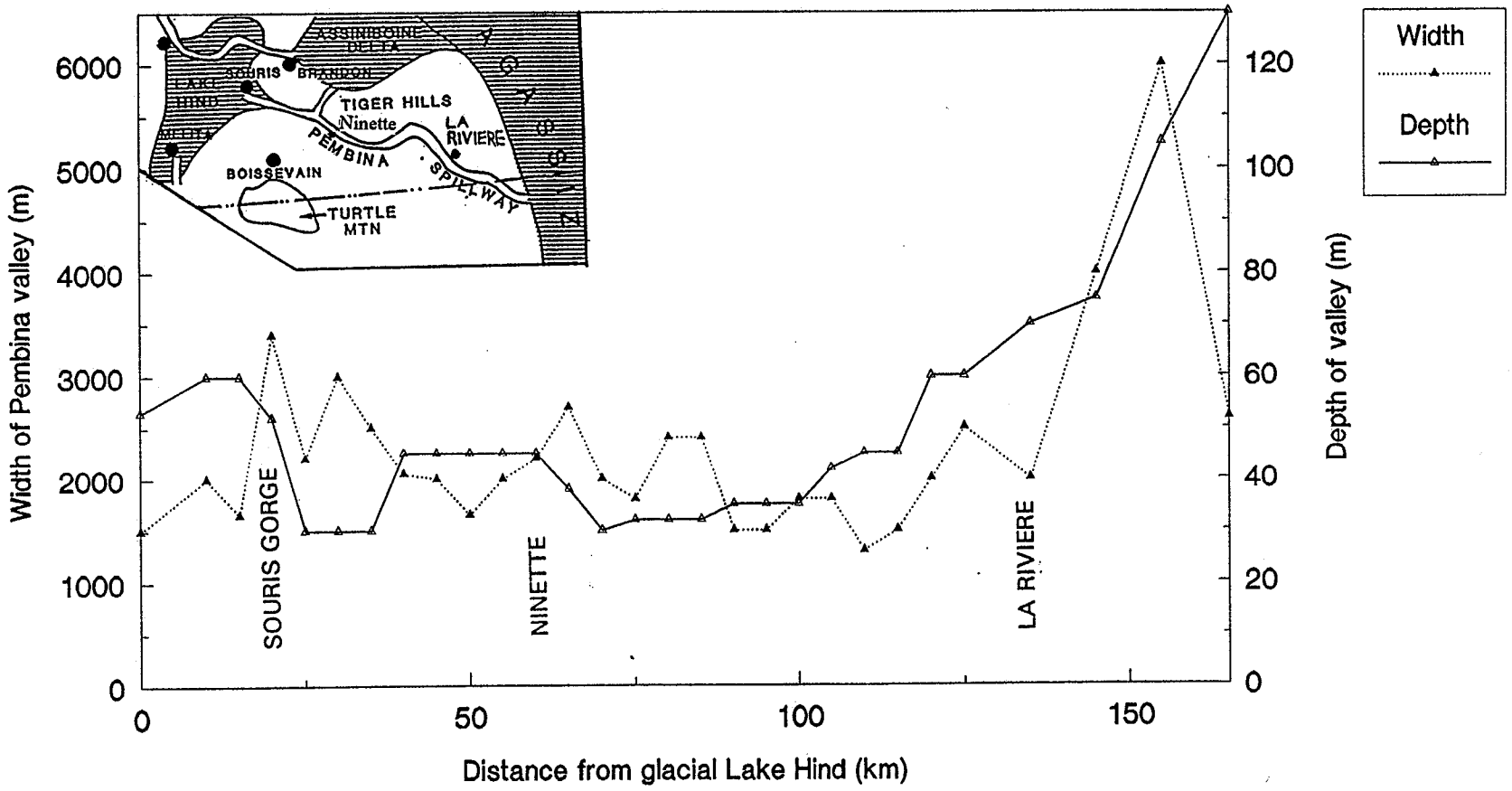

Fig. 5-8 Downstream variation of width and depth of the Pembina valley.

1956). East of La Riviere along the Pembina Mountains the valley is 2 to 5 km wide and 130 m deep (Fig. 5-8), with large terraces about 1 km wide (Elson, 1956, Manitoba Mineral Resources Division, 1980).

A scoured sub-upland surface occurs in places in the upper 30 km of the valley, at an elevation of up to 472 m. The scoured subupland is 4.5 km wide but contains no scoured channels, nor residual hills; boulder lags are rare. This is different from the scoured subupland zones along the entrenched upper Souris River spillway, which contains abundant scoured grooves, residual hills, and boulder lags (Kehew, 1982; Kehew and Lord, 1986, 1987; Kehew and Clayton, 1983; and Kehew and Teller, 1994a). There are no visible scoured subupland areas downstream from Ninette to La Riviere, nor from La Riviere to glacial Lake Agassiz

5.5.2 Interpretation

The Pembina spillway served as the outlet of glacial Lake Hind during most of its life; therefore, the elevation of this spillway controlled the water level in glacial Lake Hind. This Spillway began as an ice-marginal channel, and was enlarged in steps by multiple floods. This includes floods that trenched the Dand valley, Moose Mountain Spillway, Souris Spillway, and Pipestone Spillway. Because the last flood from the Souris Spillway was a catastrophic one, it erased all but a few terraces along the Pembina Spillway.

Kehew and Clayton (1983) suggest that the Pembina spillway and its scoured sub-upland zone were eroded in the same manner as the head of Souris River spillway and

by the a single catastrophic flood that was initiated from glacial Lake Regina. There are three lines of evidence against this suggestion. First, there are no visible scoured channels and residual hills, and rare boulder lags in the scoured zone, suggesting erosion by non-catastrophic events. Second, the scoured sub-upland zone downstream from Lake Hind extends only about 30 km, suggesting that the flood water downstream from this was confined within a pre-existing valley. By-passing through the Souris Gorge, which joins with the Pembina spillway 12 km downstream from glacial Lake Hind, can be ruled out because the large meanders and lack of floodplains in this Souris Gorge suggest that the discharge through this valley "was never much greater than it is at present" (Elson, 1956). Third, the scoured sub-uplands in the upper end of Pembina spillway is at an elevation up to 472 m, which is higher than all but the Little Saskatchewan delta in the lake Hind basin, and is about 30 m higher than the surface elevation of the Melita delta (60 km west of the Pembina spillway) which is interpreted to have been deposited by an early flood from the Souris River spillway (Sun and Teller, 1996).

It is possible that the sub-upland was scoured by early overflows when the lake level was higher than 457 m. Sun and Teller (1996) suggest an interlobate lake, proto glacial Lake Hind had overflowed into the Pembina spillway long before glacial Lake Souris could overflow through the Souris-Pembina spillway. Evidence of a pre-existing valley also occurs downstream. Between La Riviere and glacial Lake Agassiz the valley was so deep and wide (Fig. 5-8) that water of the last flood was largely confined below the level of high terraces (Kehew and Clayton, 1983).

CHAPTER 6

DELGLACIATION HISTORY

6.1 Introduction

During the late Wisconsinan, ice in the study area flowed from two ice centers: the Labradorean and Keewatin centers. Fenton et al. (1983) suggested that ice from the Labradorean center advanced southwestward as far as the western edge of glacial Lake Agassiz; ice flow from the Keewatin center advanced southward later and was deflected westward around the Labradorean ice. As the Labradorean ice began to waste back, Keewatin ice flowed southeastward into the area formerly covered by the Labradorean ice (Fenton et al., 1983). In the glacial Lake Hind region, two ice lobes covered the area at the end of the last glaciation: the Red River Lobe and the Assiniboine Ice Lobe (Elson, 1956), which were part of the Labrador and Keewatin ice sheets, respectively.

One of the last major readvances across the region by the Labradorean ice (Red River - Des Moines Lobe) reached its maximum in central Iowa between 13,500 and 14,000 BP (Ruhe, 1969). This date is supported by 16 radiocarbon dates on wood: 4 within the Cary till, one from the base of the upper till (Cary) unit, and the other 11 from Tazewell loess that underlies the Cary till (Ruhe, 1969) (Table 1-1). After a period of retreat, another major readvance sent the ice to the southern border of South Dakota at about 12,300 BP, as suggested by 8 radiocarbon dates on wood beneath and within till in southeastern South Dakota (Fenton et al., 1983; Clayton and Moran, 1982) (Table 1-2; Fig. 6-1). These radiocarbon dates indicate that the Lake Agassiz basin was covered by

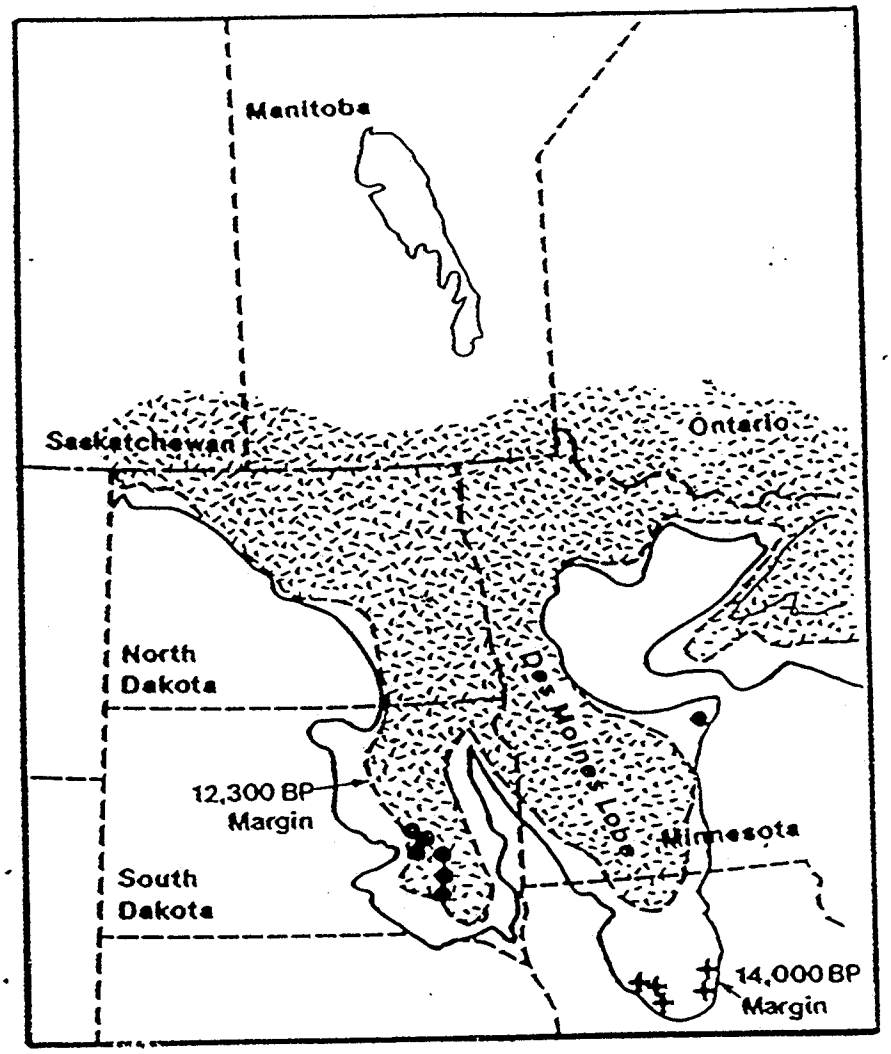

Fig.6-1 Ice marginal position at 14,000 BP and 12,300 BP. Solid black dotes indicate dates of 12,050-12,680 BP and plus signs indicate dates of 13,800 - 16,700 BP (from Fenton et al., 1983).

ice until after 12,300 BP.

The ice margin in South Dakota began to retreat shortly after the advance at 12,300 BP into southern South Dakota. By 11,700 BP, possibly as early as 12,000 BP (See Chapter 1), the Red River Lobe retreated into the glacial Lake Agassiz basin and, therefore, marks the birth of glacial Lake Agassiz (Fenton et al., 1983). To the west of this, retreat of the Assiniboine Lobe occurred at about the same time. Based on the approximate locations and ages of the ice marginal boundaries shown by Clayton and Moran (1982) and conclusions reached by Kehew and Teller (1994a), deglaciation of the glacial Lake Hind basin began after 12,000 BP and ended before 11,000 BP. This ice retreat can be divided into 6 phases based on the sedimentary and geomorphic record in the Lake Hind basin and in the major meltwater channels leading to this basin.

The Assiniboine Ice Lobe (Fig. 6-2), which was referred to as the Souris Ice Lobe by Elson (1956), flowed from the north or northwest and met the Red River Ice Lobe in the eastern glacial Lake Hind basin (Klassen, 1975, 1983; Elson, 1956; Sun, 1993a). Near the southern margin of glacial Lake Hind, flow of the local upslope-flowing ice became compressive, and shearing formed a series of thrust planes in the ice between glacial Lake Hind and the Turtle Mountain upland. This compressional flow resulted in the formation of ridges, where shale blocks overlie till and massive silt beds (Fm) overlie cross bedded gravels (Gx). Farther south, the ice split into two sublobes and flowed around Turtle Mountain (Fig. 6-2); the Souris sublobe to the west and the Leeds sublobe to the east (Lemke and Colton, 1958; Deal, 1972). The Assiniboine Lobe deposited the till of the Souris Formation, which has a low carbonate content, higher shale content, and

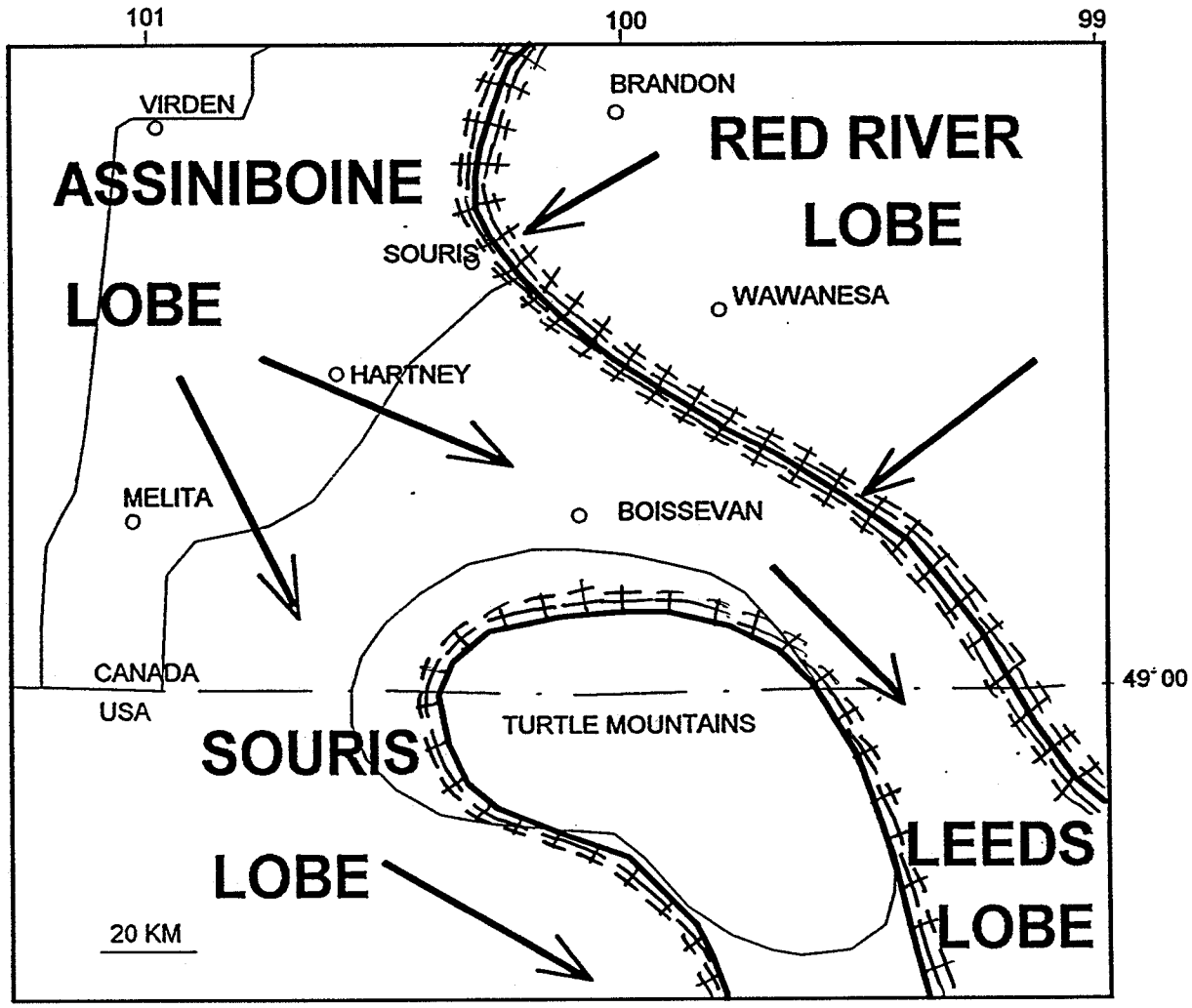

Fig.6-2 Phase 1: map showing the lobes of ice in the Lake Hind region about 12,000 BP and Superglacial Whitewater Lake north of the Turtle Mountain. The lake probably overflowed east through an ice-wall channel to the Mather outwash plain (Conley, 1986).

higher calcium/dolomite ratio than the Wawanesa formation in the glacial Lake Hind basin, because it flowed mainly across shale bedrock.

Ice of the Red River Lobe (Fig. 6-2), which was named the Sub-Assiniboine Ice Lobe by Klassen (1975, 1983), flowed into the Lake Hind basin from the northeast and advanced as far as the Tiger Hills upland in southern Manitoba. It built the Darlingford Moraine (Elson, 1956, 1967; Conley, 1986) and its northwestern extension, the Alexander Moraine (Sun, 1993a, 1993b). The Red River Lobe deposited the light-coloured diamicton of the Wawanesa Formation, which has a high carbonate content and low calcium/dolomite ratio because it flowed mainly across the carbonate bedrocks.

6.2 Phase 1, Superglacial Whitewater Lake

The Turtle Mountain upland was the place where an unusual thickness of stagnant dirty ice accumulated (Deal, 1972). During deglaciation, many superglacial lakes formed on the Turtle Mountain upland, which overflowed downslope on either side of the mountain to superglacial lakes in the lower land (Deal, 1972). On the northern and western sides meltwater accumulated in superglacial Whitewater Lake (Fig. 6-2). The presence of superglacial Whitewater Lake is evidenced by a 0.5 to 1 m cap of clayey silt on top of the till plain that covers the Boissevain plain. This superglacial lake probably overflowed east, and incised an outlet channel (a preaccessor of the Pembina River channel) that is now 24 to 38 m higher than any point of the till plain north and west of the Turtle Mountain upland.

The aerial distribution of silt and clay cap over till coincides with the occurrence

of doughnuts. All doughnuts that can be seen on air photos (Fig. 3-13) are shown on a satellite image as part of the sheared ridge systems that is oriented northeast-southwest (Fig. 3-14). Fig. 3-14 shows that linear ridges in the ridged till plain extend into the doughnut plain, and many of them spit into paired narrow ridges, suggesting that these doughnuts relate to sheared ice. Why, along the same continuous thrust ridges, were doughnuts developed in the southern part that has a cap of silt and clay, and high ridges were formed in the northern part where till is at the surface? Perhaps wave action in the once superglacial lake made the difference. The process that formed these doughnuts may be similar to Deal's (1972) model (See Section 4.4 of Chapter 4), with the addition of wave winnowing in the shallow water area of superglacial Whitewater Lake. On the higher ice north of superglacial Whitewater Lake, a thick blanket of debris over ice reduced the effectiveness of solar radiation; meltwater and precipitation runoff along the thrust plains resulted in deposition of gravels (Fig. 4-15) and more rapid melting of the ice than of the inter-ridge areas.

In the later part of this phase, superglacial Whitewater Lake became smaller as deglaciation continued and its eastern outlet was more deeply incised. To the south, proto-Lake Souris was a small ice marginal lake along the eastern margin of the Lake Souris basin (Fig. 6-3).

6.3 Phase 2, Glacial Lake Souris

Glacial Lake Souris began as a small ice marginal lake at the southern edge of the ice that lay to the north and west (Deal, 1972), overflowing south-southeastward into the

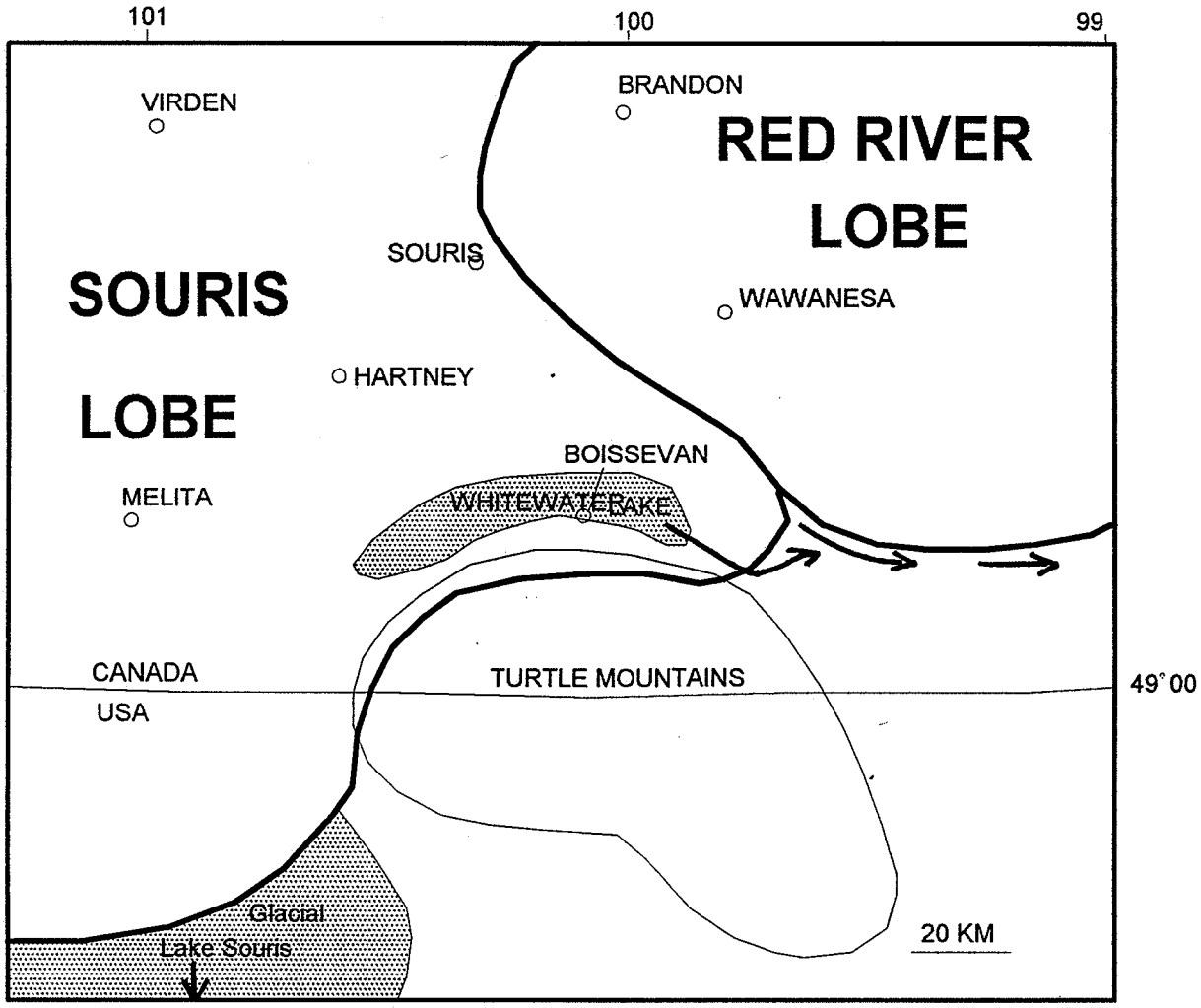

Fig.6-3 Phase 1: Superglacial Whitewater Lake became smaller as its eastern outlet incised deeper.

James River valley leading to Lake Dakota (Kehew and Teller, 1994a; Kehew and Clayton, 1983). The lake expanded northward along what is today the Souris River spillway in North Dakota as the ice margin wasted back. The lake level at the upper end of the James River was at an elevation of about 472 m, which is the same as the highest strandline of glacial Lake Souris of Deal (1972) in the Rollete County, North Dakota. Subsequently, as the lake abandoned the James River valley for the Sheyenne River valley, which also overflowed southeastward (Fig.1-1), lake level fell to an elevation between 457 and 466 m, which is roughly the same elevation as the second highest strandline identified in the Souris basin by Deal (1972); meltwater from glacial Lake Souris discharge through Sheyenne River valley into glacial Lake Agassiz until about 11,400 BP (Kehew and Teller, 1994a).

As the southern margin of the Assiniboine Lobe retreated northward, glacial Lake Souris extended an 'arm' northward into the narrow southern end of the Lake Hind basin (Figs.1-1, 2-3, 6-4). The lake level near the International border was probably at an elevation of 462 to 466 m (a paleo-elevation of between 425 and 436 m), as indicated by the reconstructed elevations of three deltas on the western side of the basin (Antler, Jackson, and Graham deltas, A, B, and C of Figs. 2-3, 4-9, 6-4) and the fine lacustrine deposits at the same elevation along the eastern side.

6.4 Phase 3, Proto-glacial Lake Hind

Meanwhile, as the eastern margin of the Assiniboine Lobe wasted back, a long and narrow interlobate lake (proto glacial Lake Hind) was formed between the Red River

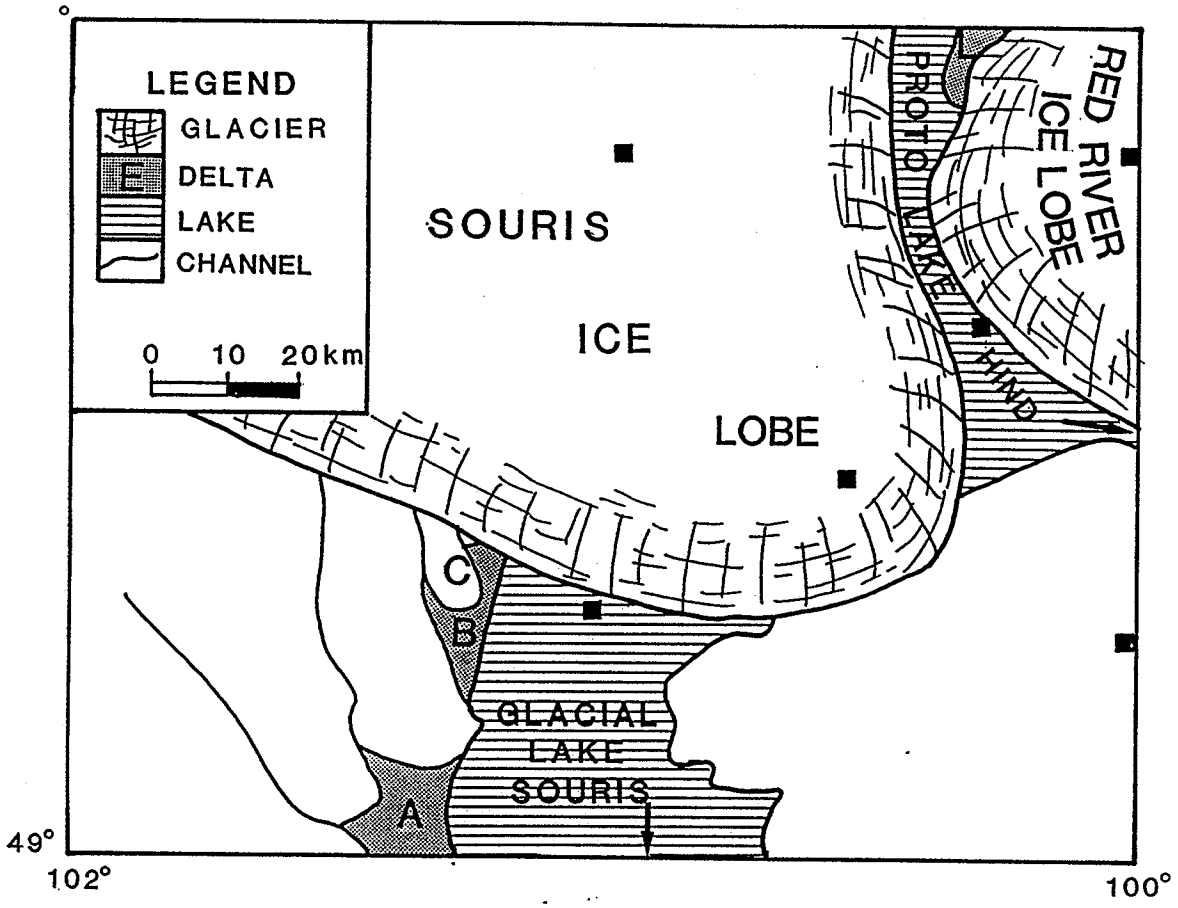

Fig.6-4 Phase 3 of glacial Lake Hind. Figure shows the location of the two ice lobes, glacial Lake Souris, and proto glacial Lake Hind. Meltwater from the west deposited Antler, Gainsborough, and Jackson deltas (A, B, and C respectively) into glacial Lake Souris; while meltwater from the north deposited the Little Saskatchewan delta (L) into the northern proto Lake Hind (From Sun and Teller, 1996, Fig.8).

Lobe and the Assiniboine Lobe in the eastern part of the glacial Lake Hind basin (Fig. 6-4). The level of this lake, which drained eastward along the ice margin to the Pembina spillway (Fig. 1-1), was at about 457 to 472 m (paleo-elevation of 410 to 425 m) at the north end, as evidenced by the elevation of the Little Saskatchewan River delta (L of Figs. 2-3, 4-9, 6-4). The central glacial Lake Hind basin was still occupied by the Assiniboine Lobe, which separated proto glacial Lake Hind to the east from glacial Lake Souris to the southwest. By this time, Whitewater Lake was roughly the same size as it is today.

Proto Lake Hind is different from Elson's (1956) Lake Carroll although both of them were interlobate lakes. Elson's (1956) Lake Carroll occupied only the southeastern corner of Lake Hind basin near the Dand delta. The surface elevation of the Little Saskatchewan delta (475 m, late glacial elevation of 410 m, Fig.4-9) indicates the presence of an early interlobate lake near the mouth of the Little Saskatchewan River valley. Thus, the proto Glacial Lake Hind is proposed here to be an elongated lake that extended from the Little Saskatchewan delta south to the Dand delta, including Elson's Lake Carroll (1956).

6.5 Phase 4, Early glacial Lake Hind

Continued retreat of the Assiniboine Lobe permitted ice marginal drainage to cut the Dand valley (Figs. 2-3, 6-5). Meltwater from Lake Souris eroded the Dand valley into shale bedrock and deposited the shale-rich eastern half of the Dand delta (Fig. 3-7)) into the southern end of the proto glacial Lake Hind (K of Figs. 2-3 and 6-5). With the

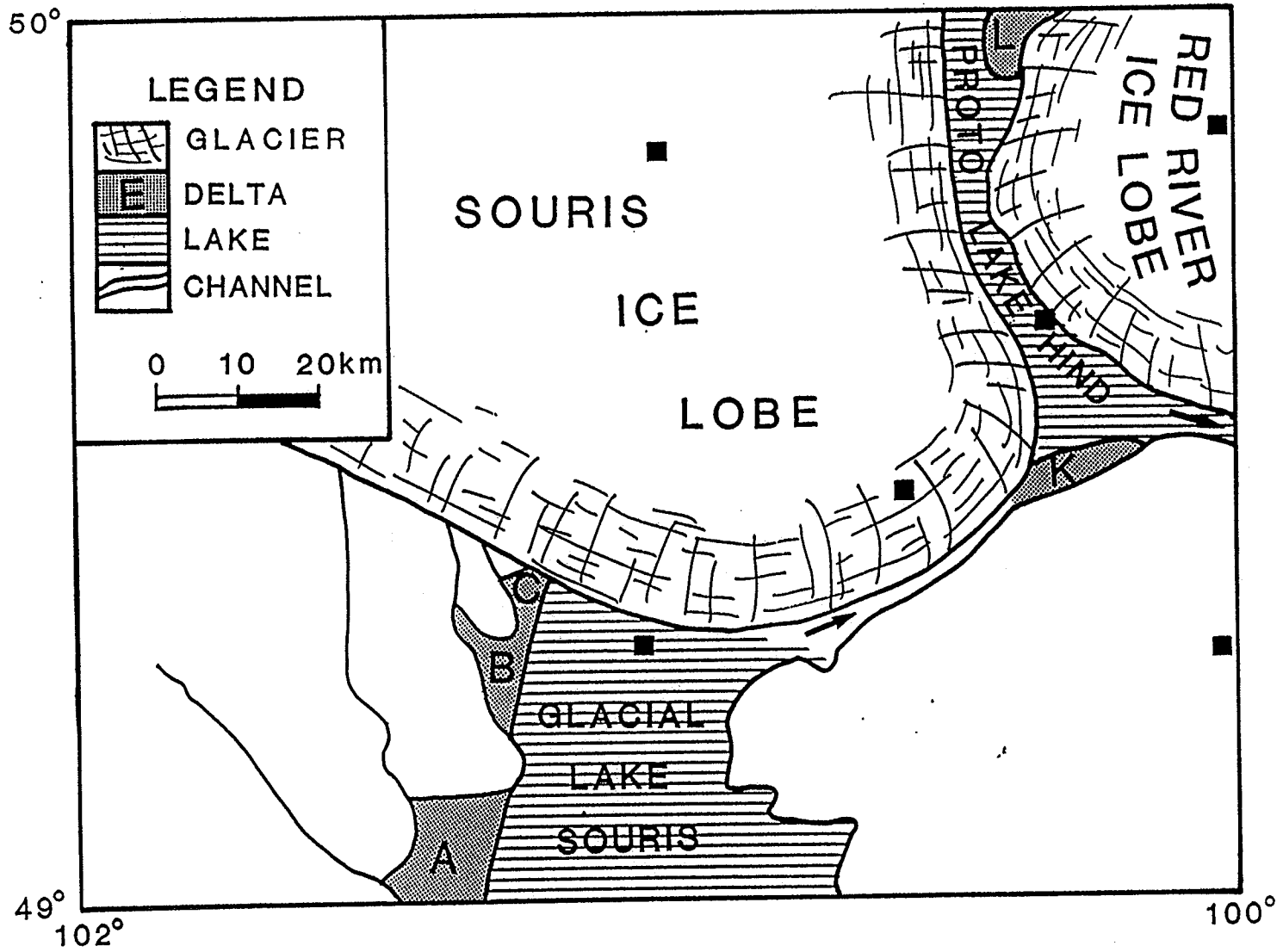

Fig. 6-5 Phase 4 of glacial Lake Hind. Waters from glacial Lake Souris overflow into proto glacial Lake Hind and deposited Dand delta (K at the eastern end of the Dand channel) at a modern elevation about 457 m. (From Sun and Teller, 1996, Fig. 9)

opening of this lower outlet, the level of glacial Lake Souris began to drop and its Sheyenne River outlet to the south (Fig. 1-1) was eventually abandoned. Meanwhile, as the Assiniboine Lobe retreated farther into the Lake Hind basin, meltwater abandoned the Dand valley and cut a lower channel between the ice margin to the north and the southern margin of the lake basin and deposited the western Dand delta that is deficient in shale fragments (Figs. 4-10 and 2-3). With further ice retreat, glacial Lake Hind came into existence by the merger of proto glacial Lake Hind with the northern 'arm' of glacial Lake Souris (Fig. 6-6), which became isolated from Lake Souris in North Dakota when the water level declined during formation of the new lower overflow routes east around the end of the Red River Lobe. The water level in glacial Lake Hind dropped to 445 m (a paleo-elevation of about 403 m) with the cutting of the deeper eastern outlets to the Pembina Spillway by meltwater exclusively from glacial Lake Souris. Meltwater from the west began to build the Stony and Pipestone deltas (D and E of Fig. 6-6). The newly formed glacial Lake Hind was now separated from glacial Lake Souris by newly exposed high ground near the International Border, linked only by a 10-km-wide broad depression (Fig. 6-6) at an elevation of 450 m (a paleo-elevation of about 405 m) in the upper end. Thus, the lake level related to this outlet was at an elevation of about 450 m. Strandlines at this level have been reported as the lowest strandline of glacial Lake Souris by Deal (1972), and have been regarded as the level of Lake Souris II by Lord (1988).

6.6 Phase 5, Subglacial meltwater flowing into glacial Lake Hind

As the Assiniboine Lobe retreated across the glacial Lake Hind basin, the lake

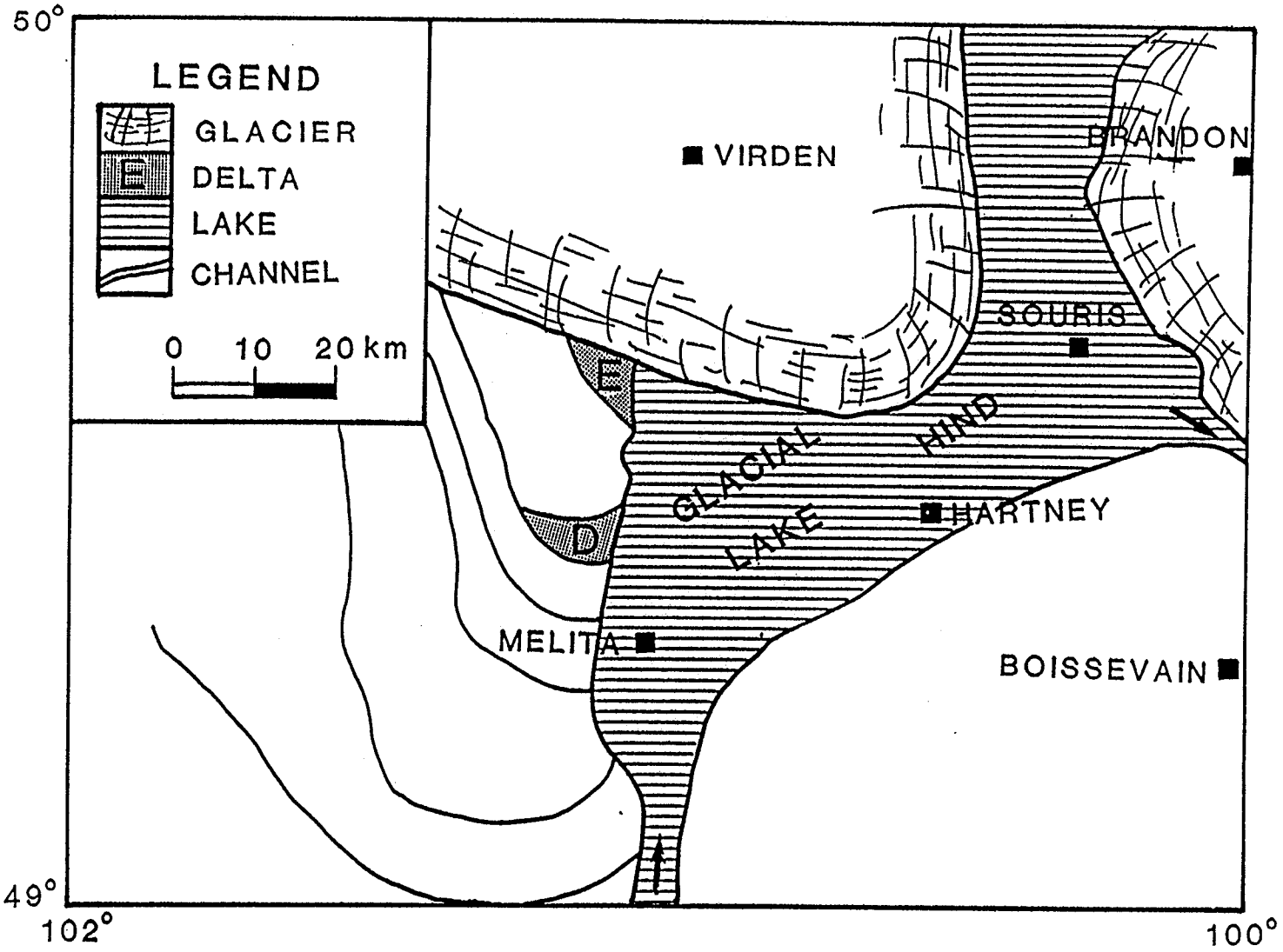

Fig. 6-6 Phase 4, early stage of glacial Lake Hind. Meltwater from the Pipestone and Stony River valleys began to build the Stony and Pipestone deltas (D and E respectively) (From Sun and Teller, 1996, Fig.10).

expanded northward while lake level stayed at 445 m (a paleo elevation of 403 m). During this period, the Arrow Hills Esker and associated low linear ridges (see section 4.3.1; Fig. 4-5; N of Fig. 2-3) were deposited north of the Lake Hind basin by subglacial meltwater flows. West of glacial Lake Hind, meltwater eroded a series of sub-parallel meltwater channels as the ice retreated, and deposited the Stony, Pipestone, Gopher, and Bosshill deltas (D, E, F, G of Figs. 2-3, 6-7). These channels probably started as subglacial channels that were oriented northwest-southeast, oblique to the ice margin (Fig. 6-7). Among these channels, the Pipestone Channel was the longest and deepest, and supplied the most sediment to glacial Lake Hind. At least two flood events occurred along the Pipestone valley (See section 5.3). The first flood occurred possibly from a subglacial lake, which formed linear grooves and drumlins west of Moosemin and flooded into the Pipestone River valley through eight braided channels. This early flood deposited the kame-eskers near the ice margin, and deposited the higher Pipestone delta of clast-supported pebbly gravels; the second flood occurred during phase 7 (see section 6.8)

Throughout this period, when deltas in the western lake basin were deposited, Lake Hind was at an elevation about 442 m (400 m during the late glacial). In the central part of the basin, a 30-m-thick unit of silty clay was deposited (Fig. 3-11). However, Kehew and Teller (1994a) only assigned Lake Hind a total of 200 years of life. There are three possibilities that may explain this: 1) Kehew and Teller's (1994a) time estimate was incorrect; 2) some of the silt and clay seen in borehole logs are pre-Wisconsinan in age; 3) sedimentation rates were very high, with more than 20 cm of silt and clay being

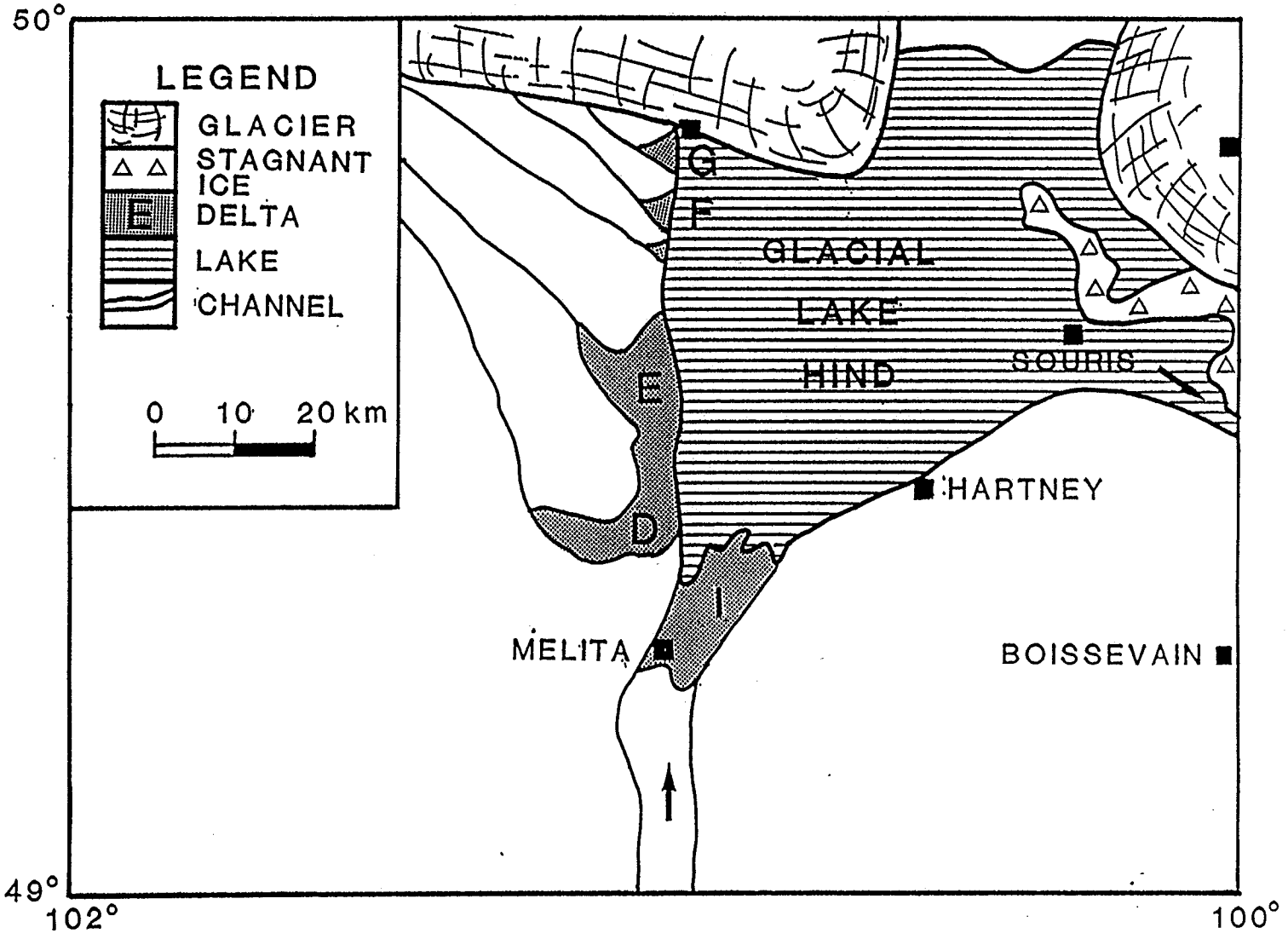

Fig. 6-7 Phase 5 of glacial Lake Hind: Lake Hind was at an elevation about 445 m (397 m of late glacial elevation). Meltwater from the west had built the Stony, higher Pipestone, Gopher, and Bosshill deltas (D, E, F, G respectively) before the first catastrophic flood from glacial Lake Regina.

deposited in glacial Lake Hind each year; It is unlikely that some of the silt and clay are pre-Wisconsinan deposits because the clay beds that immediately overlie the top till are uniform in lithology with subtle laminae, suggesting continuous deposition without major interruptions. In addition, Fig. 3-9 shows that the upper 47 m sediments of the core from central Lake Hind basin, which overlies the uppermost till, consists of a single coarsening upward sequence grading from silty clay to sand-mud couplets and then to massive sand; there was only one pebble (1 cm) found in the entire 47 m sequence. If some of the lower silty clay sequence is pre-Wisconsinan in age, I would expect to see at least some remnants of glacial deposits, such as gravels or tills in this succession. Lacking this, it seams likely that they were all deposited after the last deglaciation.

It is difficult to accurately estimate the age of glacial lakes in the prairie region where radiocarbon control is limited. Kehew and Teller (1994a) established their chronology of events in the eastern Prairies through the relationship between meltwater channel and glacial lakes, constrained by a starting age of 12.3 and ending age of 10.9 BP. Kehew and Teller (1994) assigned 600 to 700 years for Lake Souris, and 200 years for lakes Hind, Regina, and Indian Head. But Lake Hind has the thickest sediments among these four lakes (See section 5.2.1 and 5.2.2). It is my believe that glacial Lake Hind may have a longer life than 200 years.

There are up to 25-m-thick sand overlying 30-m-thick of silt and clay in the Lake Hind basin (Figs. 3-11B, 3-9, 3-18). How long it taken to deposit these sediments is depend on the sedimentation rates. However, it is difficult to estimate a depositional rate in a glacial lake, especially one like glacial Lake Hind, which had 11 inlets and received

the waters from several catastrophic floods. There are no clay and silt rhythmites found in cores from the central part of the basin (Fig.3-9) and those seen in exposure. The clay and silt rhythmites that are exposed in the Victoria Park at the town Souris may not be annual rhythmites. Previous studies in adjacent ice marginal lakes indicate that a sedimentation rate of 10 to 20 cm/years was common. In the 1500 km^2 glacial Lake Assiniboine that is about 200 km north of glacial Lake Hind, Wolfe and Teller (1993) reported varves that were up to 19 cm in thickness, with an average of about 10 cm. Teller and Last (1989) estimated that sedimentation rates in glacial Lake Agassiz exceeded 15 cm/year.

6.7 Phase 6, The Moose Mountain spillway flood from glacial Lake Indian Head

Several glacial lakes near the Moose Mountain upland were formed at this time. A superglacial (or subglacial) lake, glacial Lake Indian Head, was formed north of the Moose Mountain Upland; glacial Lake Arcola was dammed by stagnant ice in the southern Moose Mountain upland; and glacial Lake Regina was impounded in the area between Regina and Weyburn (Figs. 1-1, 5-1, 6-8).

When the meltwater in superglacial Lake Hind found it way to escape subglacially (see Fig. 5-4), it eroded a deep spillway into the newly-deposited drift as far south as to glacial Lake Hind. Hairpin-type drumlins have been found immediately north of glacial Lake Arcola and west of the Moose Mountain spillway by Christiansen (1958), suggesting erosion by this flood. Alternatively, this flood may have originated as a subglacial outburst (see Fig. 5-3). In glacial Lake Arcola, the incoming flood deposited

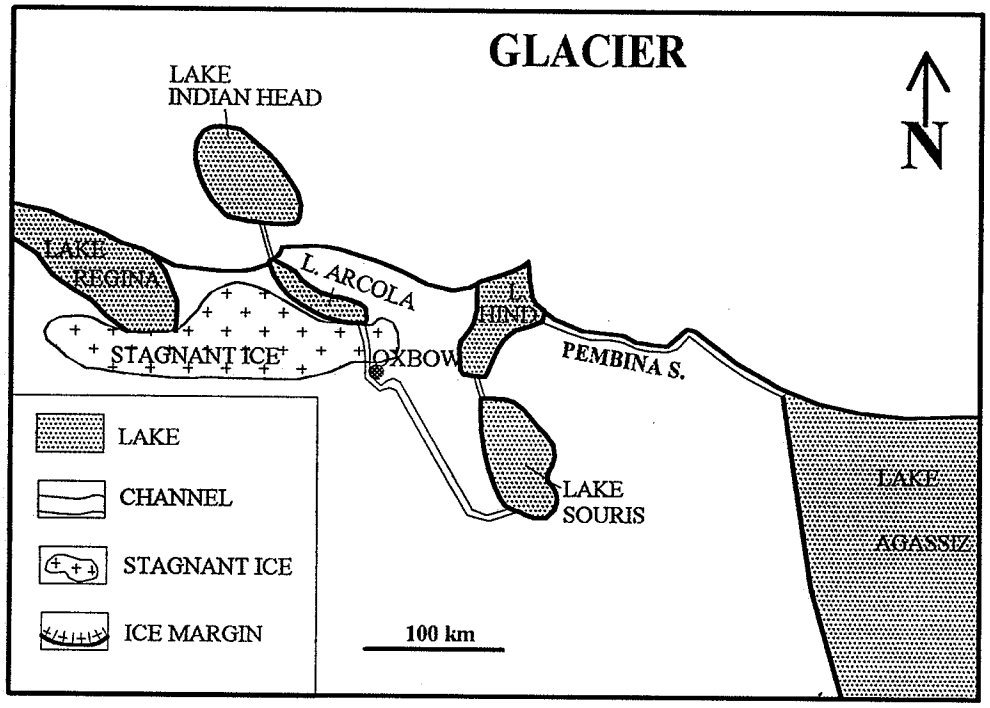

Fig. 6-8 Phase 6. The first catastrophic flood from superglacial Lake Indian Head to glacial lakes Arcola, Souris, Hind, and Agassiz through the Moose Mountain, Souris, and Pembina Spillways.

the massive, matrix-supported gravel lithofacies (Gmm) into the northern end. Because the initial inflow exceeded outflow, the lake level rose quickly until a series of scoured channels and the main Moose Mountain outlet channels had been eroded. This catastrophic flood deposited the cobbly massive gravels (Gmc) west of Oxbow and incised the Moose Mountain channel from glacial Lake Indian Head to Oxbow (Fig.5-1) and the ancestor of the Souris River spillway between the town of Oxbow and glacial Lake Souris (Fig. 6-8). In turn, this flood deposited a fan at an elevation of 455 to 466 m at the inlet to glacial Lake Souris. The same flood deposited the shale-rich gravel lithofacies (Gmc) in the lower sequence of the Melita delta in glacial Lake Hind. The shale boulders in the lower Melita delta were eroded from bedrocks along the Souris Spillway between lakes Souris and Hind (Sun and Teller, 1996). This suggests that the Souris Spillway between glacial lakes Souris and Hind was trenched into the shale bedrock at this time, possibly below 440 m because, based on the bedrock topography in Fig. 2-2, the surface of bedrock south of Melita is at an elevation between 420 and 440 m. If this is true, glacial Lake Souris may have been drained completely because the floor of Lake Souris basin is at the same elevation as its northern outlet.

6.8 Phase 7, glacial Lake Hind and Lake Brandon

Because of the erosion of the outlet to the Pembina Spillway by the Lake Indian Head flood from glacial lakes Indian Head, Arcola, and Souris, the level of Lake Hind dropped to about 434 m (a late glacial elevation of 390 m); the region east of the Alexander moraine became a separated lake at this time, forming another glacial lake that

was named Lake Brandon by Elson (1956) (Fig. 6-9). This lake overflowed westward across the moraine through the Alexander Channel and possibly through the Assiniboine Channel into Lake Hind; these two lakes probably were at about the same elevation.

In the western Lake Hind basin, meltwater from glacial Lake Indian Head (Fig.1-1) enlarged the Pipestone valley, eroded a wide channel across the previous delta, and deposited a lower delta into Lake Hind at about 434 m (a paleo-elevation of 390 m) (E of Fig. 6-9). Meanwhile, meltwater from the north deposited the Virden delta (H of Fig.2-3). Strong wave action in the shallowing Lake Hind basin carried sand from the deltas into the central lake and transported the silty and clayey portion to the next lake downstream, Lake Agassiz.

6.9 Phase 8, the Souris flood from glacial Lake Regina

Shortly after the floods through Moose Mountain and Pipestone River valleys, there was a catastrophic flood from glacial Lake Regina (see section 5.2.3). This further enlarged and deepened the Moose Mountain spillway downstream from Oxbow, and was the primary cause for the formation of the upper Souris River spillway. The flood from Lake Regina may have been much larger than the flood from the glacial Lake Indian Head, because 1) an inner channel within an 8-km-wide scoured zone was eroded in the upper Souris River spillway downstream as far as the town of Oxbow (Figs. 5-2), 2) the Souris River spillway is about 50% wider than Moose Mountain spillway near Oxbow, and 3) glacial Lake Regina was at least triple the combined size of glacial Lake Indian Head and glacial Lake Arcola. Evidence that the first flood came from Moose Mountain,

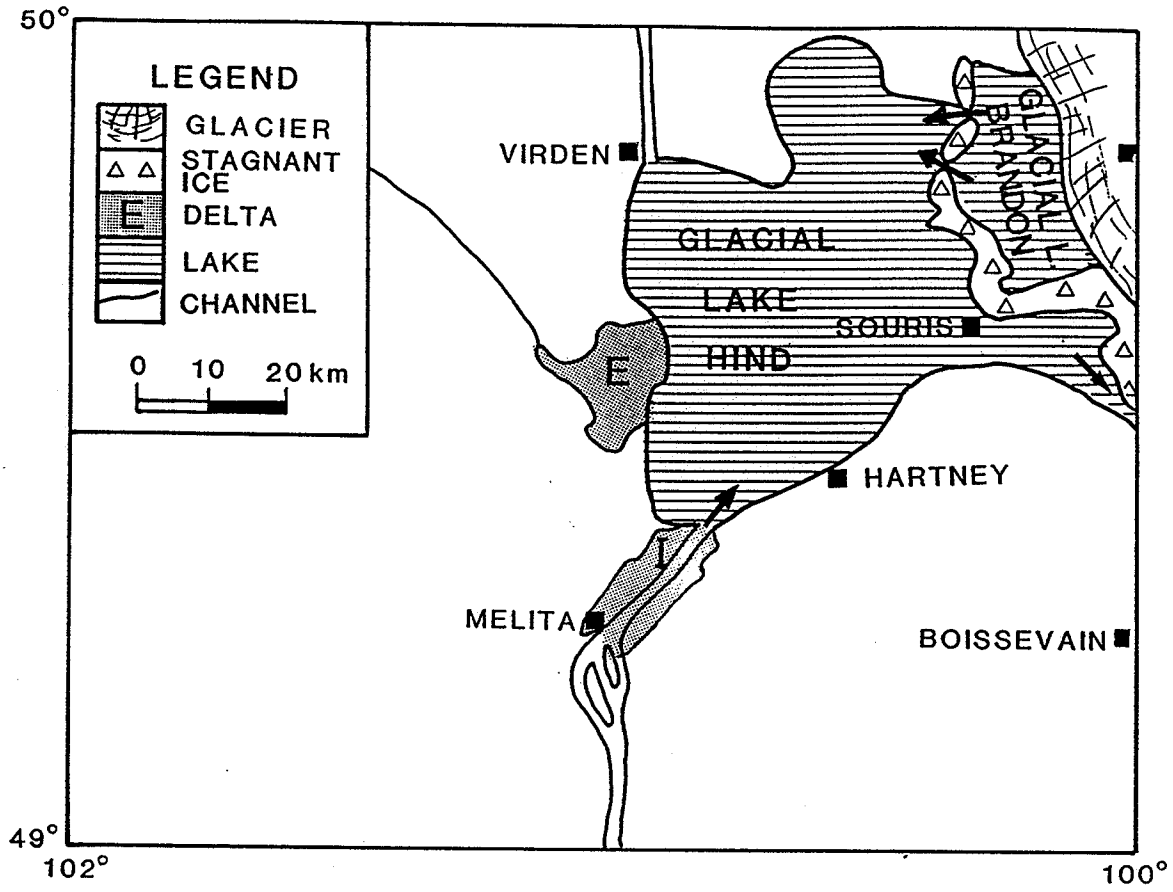

Fig. 6-9 Phases 7. Figure shows the formation of Lake Brandon after the first flood from glacial Lake Indian Head (After Sun and Teller, 1996). The flood deposited the Melita delta (I) and incised the outlet to an elevation about 434 m (about 390 m of late glacial elevation). Overflow from Lake Brandon was west through the Alexander moraine.

and the second flood from glacial Lake Regina, lies in the distribution of scoured sub-upland valleys. The broad and scoured sub-upland area adjacent to the deeper inner channel was described by Kehew (1982) as one of the three main criteria for identifying the occurrence of a catastrophic flood. This scoured sub-upland zone is present only along the Souris River spillway from its outlet at glacial Lake Regina downstream to Oxbow (Figs. 5-1, 5-2) (Kehew and Clayton, 1983). This suggests that the flood water from glacial Lake Regina eroded the upper reach of the Souris spillway from Weyburn to Oxbow. But the absence of this scoured sub-upland zone downstream from Oxbow (Figs. 5-2) suggests that 1) the flood water from glacial Lake Regina, which was probably much larger in magnitude than the Moose Mountain flood, utilized and enlarged the Moose Mountain spillway from Oxbow to glacial Lake Souris, and 2) the subupland zone scoured previously by the Moose Mountain flood was destroyed by the Lake Regina flood.

In glacial Lake Souris, this flood eroded a 2- to 4-km-wide channel into the higher fan and across the lake floor, and deposited a smaller fan in the central basin. Lord (1988) suggests that this flood from glacial Lake Regina deposited both the higher and lower fans, which have identical sedimentary sequences (see Section 5.2.3 of Chapter 5) but lie at different elevations. If this "one flood'' scenario was the case, there was no sedimentary record left by the Moose Mountain flood, which seems unlikely. As I pointed out above, there is evidence that the Moose Mountain flood preceded the Souris flood from glacial Lake Regina, thus, it is logical to assume that the higher fan in glacial Lake Souris was deposited by the early flood, and that the lower fan was deposited by

the second flood.

When the glacial Lake Regional flood waters reached glacial Lake Hind, they deposited the upper sequence of the Melita delta (A in Fig.4-4), and the Lauders delta (J of Figs. 2-3 and 6-10) at an elevation of 434 m (a paleo-elevation of 390 m). Because of the resistance from the shallow lake water, the flood water only eroded a shallow channel in the southern end of the basin. The shallow channel was subsequently occupied by the Souris River when glacial Lake Hind because smaller (Fig.6-10). Because this flood was largely confined within a previously existing channel (the one that was cut by the Moose Mountain flood), the Lauder delta is small, and contains less shale fragments than the delta deposited by the previous Moose Mountain flood. In the Pembina spillway, this catastrophic flood was responsible for deepening and widening the spillway; remnants of the older valley fill remain as a terrace at an elevation of about 445 m in a broad part of the spillway near the Souris Elbow. Because of this downcutting of outlet, most of glacial Lake Hind drained except the deeper northern half.

Shortly after the glacial Lake Regina flood, the northeastward retreat of the Red River Lobe allowed glacial Lake Brandon to overflow east into Lake Agassiz through a series of shallow channels south of the city of Brandon. As the level of glacial Lake Brandon dropped, it resulted in a reversal of outflow across the Alexander moraine, and glacial Lake Hind overflowed eastward for a short time both across the former glacial Lake Brandon basin and through the long-standing outlet from the southeastern corner into the Pembina spillway (Fig. 6-10).

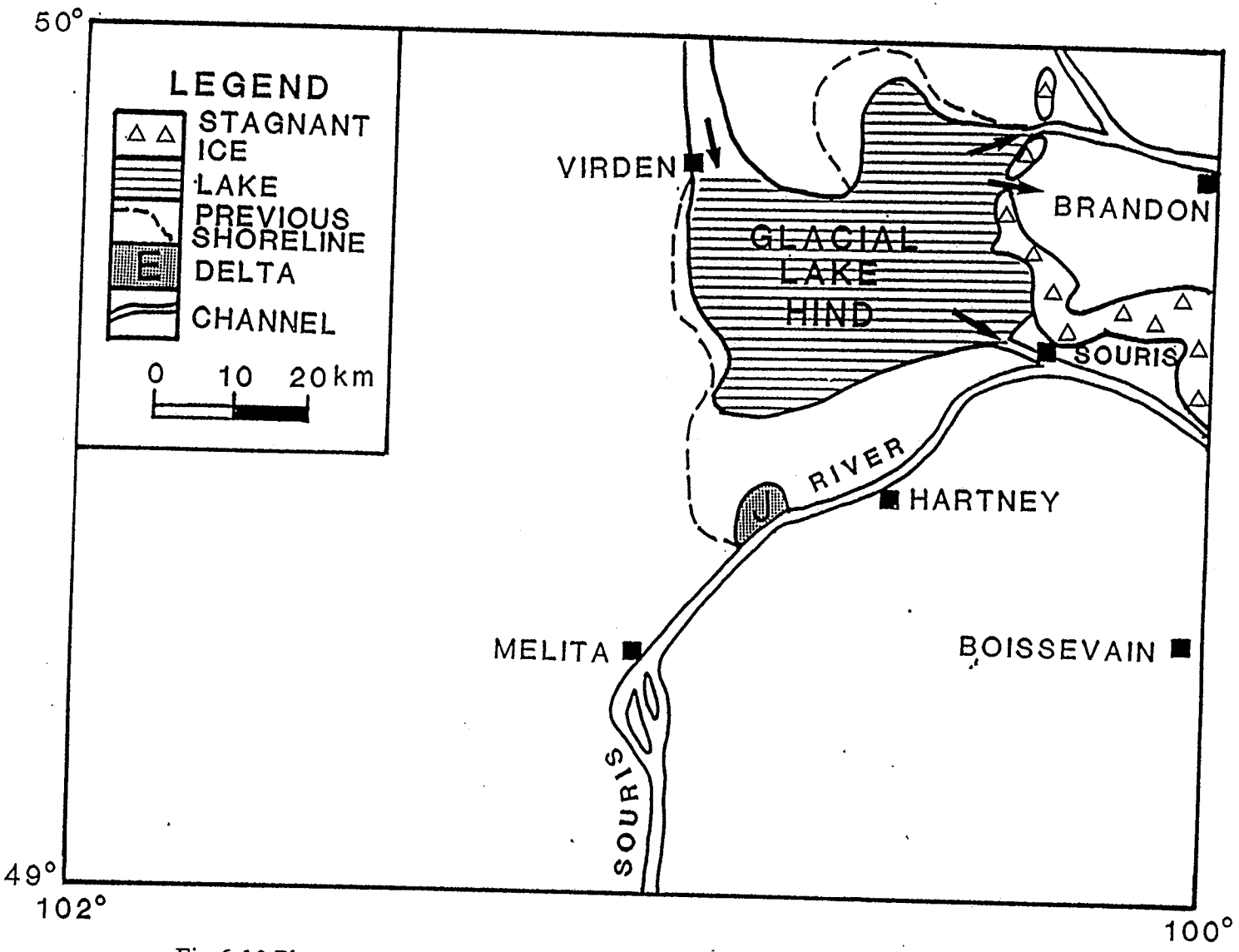

Fig.6-10 Phase 9. Glacial Lake Hind during the flood from the Assiniboine valley. Arrows show possible contemporaneous routing of water across the Lake Hind Basin to two different route to Lake Agassiz. (From Sun and Teller, 1996). J is the Lauder delta, deposited during Phase 8.

6.10 Phase 9, the Qu'Appelle-Assiniboine floods

As ice retreated northeastward, a flood from the Qu'Appelle-Assiniboine Spillway system trenched across the glacial Lake Hind basin into glacial Lake Agassiz. The flood appears to have originated from glacial Indian Head, which eroded an early shallow Qu'Appelle spillway. Subsequently, another flood originated in the upper reaches of the Qu'Appelle basin and passed through glacial Lake Indian Head (Kehew and Teller, 1994a). In glacial Lake Hind, this incoming flood eroded many shallow sub-parallel grooves and deposited sand on the lake floor. Lack of fine lacustrine sediments in the central part of the lake basin suggests that the basin was not a very effective sediment trap. Fine sediment remained in suspension and was carried out of the basin into glacial Lake Agassiz through the Pembina, Alexander, and Assiniboine Channels. Subsequently, there were several additional floods from the Qu'Appelle and Assiniboine spillways that reached Lake Agassiz (Kehew and Teller, 1994a; Wolfe, 1993; Wolfe and Teller, 1993, 1995) through the newly incised Assiniboine Spillway. These floods passed through the newly drained Lake Hind in the Assiniboine spillway without leaving a sedimentary record, depositing their sediment loads in the Assiniboine delta of Lake Agassiz (Fig. 1-1). Based on sedimentary records in the Assiniboine delta, Sun (1993a) suggested that at least three floods from the Assiniboine Spillway had poured into Lake Agassiz depositing coarse sediments in the delta. Evidence in the Assiniboine flat (O of Fig. 2-3) is also indicative of at least two flood events (Sun and Teller, 1993a) after the formation of the Assiniboine River spillway, and these appear to be related to the last Assiniboine-Qu'Appelle spillway floods shortly after 10,800 BP (Kehew and Teller, 1994a).

SUMMARY OF HISTORY

During late Wisconsinan time, there were two ice lobes in the glacial Lake Hind area. The Red River Lobe advanced as far west as the Alexander moraine and the Assiniboine Lobe occupied most of the basin to the west. At the Turtle Mountain upland, the Assiniboine Lobe split into two sublobes, the Souris Sublobe to the west and the Leeds Sublobe to the east.

After about 12,000 BP, deglaciation in the Turtle Mountain area resulted in the formation of superglacial Whitewater Lake north and west of the Turtle Mountain Upland. This superglacial lake became smaller as the ice margin withdrew from Turtle Mountain and as its eastern outlet were cut deeper. Meanwhile, glacial Lake Souris formed in the Souris Basin in North Dakota, expanding northward as far as the southern end of the glacial Lake Hind basin; the Antler, Graham, and Jackson deltas were deposited into the Lake Hind basin along the western margin at this time. During this phase, glacial Lake Souris overflowed south first through the James Spillway into Lake Dakota and then through the Sheyenne Spillway in North Dakota into glacial Lake Agassiz. Meanwhile, a second lake was forming in the eastern Lake Hind basin between the Assiniboine and Red River Lobes, into which the Little Saskatchewan delta was built; overflow from this lake was east into glacial Lake Agassiz through the early Pembina Spillway.

As the Assiniboine Lobe retreated and Lake Souris expanded, a lower northern outlet was opened, and glacial Lake Souris abandoned its southern route through the Sheyenne Spillway. The Dand delta was deposited at this time, and rapid incision of the

Pembina spillway occurred. Further retreat of ice allowed the formation of glacial Lake Hind by merging the northern arm of glacial Lake Souris with proto glacial Lake Hind. The water level in glacial Lake Souris was at about 445 m while the water level in Lake Hind was at about 442 m. Glacial Lake Hind may have stayed at this level for at least 200 years, and a 30-m-thick silt and clay sequence was deposited in the central Lake Hind basin. The Stony, Pipestone, Gopher, Bosshill, and Melita deltas were deposited into glacial Lake Hind at this time. The Virden, lower Pipestone, and Lauder deltas were deposited at the next lower lake level, which formed as a result of a catastrophic flood from the Moose Mountain spillway.

Of the 12 deltas deposited in Lake Hind, the Antler, Graham, Jackson, Stony, Gopher, Bosshill, and Virden deltas are braid deltas that are less than 5 m thick and lack foreset beds. The Melita, Dand, and Pipestone deltas are fan-foreset deltas that were deposited by meltwater floods. The surface elevations of deltas in the western lake basin, after correcting for differential isostatic tilting, suggest an episodic falling of water level due to the incision of the outlet by floods.

Two catastrophic floods were responsible for the formation of the Souris River Spillway; both of these impacted on the history of Lake Hind. The first flood came from glacial Lake Indian Head, via the Moose Mountain Spillway and the lower Souris spillway; this deposited a fan in glacial Lake Souris and deposited the Melita delta in glacial Lake Hind, and resulted in the complete drainage of glacial Lake Souris. The second flood came from glacial Lake Regina, eroded the upper Souris Spillway, enlarged the lower Souris Spillway, and resulted in deposition of the Lauder delta in glacial Lake

Hind.

There were two floods into Lake Hind from the Pipestone valley as well; the first one was probably from a subglacial lake, which deposited three kame-eskers and the high Pipestone delta in glacial Lake Hind. The second flood came from glacial Lake Indian Head after the Moose Mountain spillway flood.

An early flood from glacial Lake Indian Head through the Assiniboine River spillway deposited sand-sized materials into the Virden delta and across the Lake Hind floor; this flood probably entered glacial Lake Agassiz via the Pembina Spillway, Alexander 'channel, and the Assiniboine channel. Subsequent floods from the upper reaches of Qu'Appelle-Assiniboine River spillways enlarged the valley, deposited gravel bars in the Assiniboine Flat, and deposited the Assiniboine delta into Lake Agassiz. These floods left no records in the sediments of glacial Lake Hind.

REFERENCES CITED

Allen, J.R.L., 1990. The Bouma division A and the possible duration of turbidity currents. Journal of Sedimentology Petrology, v.61, p.291-295.

Ashley, G.M., Shaw, J., and Norman, D.S., 1985. Glacial sedimentary environments. SEPM Short Course No.16. Society of Economic Paleontologists and Mineralogists, Tulsa. 246p.

Bagnold, R.A. 1954. Experiments on a gravity-free dispersion of large solid spheres in a Newtonian fluid under shear. Proceeding of Royal Society of London Series A225, p.49-63.

Bamburak, J.D., 1978. Stratigraphy of the Riding Mountain, Boissevain, and Turtle Mountain Formations in Turtle Mountain area, Manitoba. Manitoba Department of Mines, Resources and Environmental Management, Mineral Resources Division, Geological Survey, Geological Report 78-2, 47p.

Barrell, J. 1912. Criteria for the recognition of ancient delta deposits. Geological Society of America Bulletin, v.23, p.377-446.

Betcher, R.N, 1983. Groundwater availability map series, Virden area (62-F). Manitoba Natural Resources, Water Resources. 10 figures and 1 table.

Blatt, H., Middleton, G., and Murry, R., 1980. Origin of sedimentary rocks. Prentic-Hall inc., Englewood Cliffs, New Jersey, 782p.

Bluemle, J.P., 1984. Geology of Towner County, North Dakota: North Dakota Geological Survey Bulletin 79, North Dakota State Water Commission, County Groundwater Studies 36, part 1, 44p.

Christiansen, E.A., 1992. Pleistocene stratigraphy of the Saskatoon area, Sasktchewan, Canada: an update. Canadian Journal of Earth Sciences, v.29, p1767-1778.

Christiansen, E.A., 1979. The Wisconsinan deglaciation of southern Saskatchewan and adjacent areas. Canadian Journal of Earth Sciences, v.16, p.913-938.

Christiansen, E.A., 1961. Geology and ground-water resources of the Regina area Saskatchewan. Saskatchewan Research Council Geology Division, Report No.2, 72p.

Christiansen, E.A., 1960. Geology and ground-water resources of the Qu'Appelle area, Saskatchewan. Saskatchewan Research Council Geology Division, Report No.1,

53p.

Christiansen, E.A., 1956. Glacial geology of the Moose Mountain area, Saskatchewan. Department of Mineral Resources, Report no. 21, 35p.

Clayton, L., 1983. Chronology of Lake Agassiz drainage to Lake Superior. In Teller, J.T. and Clayton, L. (eds): Glacial Lake Agassiz. Geological Association of Canada Special Paper 26, p.291-307.

Clayton, L., 1967. Stagnant-glacial features of the Missouri Coteau in North Dakota. In Glacial geology of the Missouri Coteau and adjacent area, North Dakota Geological Survey Miscellaneous Series 30, p.25-46.

Clayton, L., and Moran, S.R., 1982. Chronology of late Wisconsinan glaciation in middle north America. Quaternary Science Reviews, v.1, p.55-82.

Conley, G.G., 1986. Surficial geology and stratigraphy of the Killarney-Holmfield area, southwestern Manitoba. M.Sc Thesis, University of Manitoba, Winnipeg, Manitoba, 168p.

Costa, J.E., 1988. Rheologic, geomorphic, and sedimentologic differentiation of water floods, hyperconcentrated flows, and debris flows. In: Baker V.R., Kochel, and Patton P.C. (eds): Flood geomorphology, p.113-122.

Deal, D.E., 1972. Geology of Rolette County, North Dakota. North Dakota Geological Survey Bulletin 58, 89p.

Dreimanis, A., 1962. Quantitative gasometric determination of calcite and dolomite by using Chittick apparatus. Journal of Sedimentary Petrology, v.32, p.520-529.

Dreimanis, A., and Lundquist, J., 1984. What should be call till? in Konigsson, L.K.(ed): 10 years of nordic research, Striae, v.20, p.5-10.

Eilers, R.G., 1978. Soils of the Boissevain-Melita area. (Winnipeg) Manitoba Department of Agriculture, Soil Report no.20, Canada-Manitoba Soil Survey no.20, 204p.

Elson, J.A., 1967, Geology of glacial Lake Agassiz. In W.J. Mayer-oakes (ed): Life, land, and water. University of Manitoba Press, Winnipeg: 36-95.

Elson, J.A., 1956. Surficial geology of the Tiger Hills regions. Unpublished Ph.D. Thesis, Yale University. New Haven, Connecticut, 316p.

Ehrlich, W.A., Pratt, L.E., and Poyser, E.A., 1956. Report of Reconnaissance soil

survey of Rossburn and Virden map sheet areas. Manitoba Soil Survey, 121p.

Fenton, M.M., Moran, S.R., Teller, J.T., and Clayton, L., 1983. Quaternary stratigraphy and history in southern part of the Lake Agassiz Basin. In J.T. Teller & L. Clayton (eds), Glacial Lake Agassiz. Geological Association of Canada Special Paper 26: 49-74.

Fulton, R.J., Thorleifson, L.H., Matile, M., and Blais, A., 1994. Prairie NATMAP field work and field database structure. In Current Research 1994-B. Geological Survey of Canada: 69-72.

Gallway, W.E., 1976. Sediments and stratigraphic framework of the Copper River fan-delta, Alaska. Journal of Sedimentary petrology, v.46, p.726-737

Gilbert, G.K., 1885. The topographic features of lake shores. U.S. Geological Survey Fifth Annual Report, 1883-84, p.64-123.

Groom, H.D., 1988. Surficial geology and aggregate deposits in the R.M. of Edward, Manitoba. Manitoba Energy and Mines; preliminary map number: 1988 ED.

Halstead, E.C., 1959. Ground-water resources of Brandon map area, Manitoba. Geological Survey of Canada Memoir 300, 67p.

Hiscott, R.N., 1994. Loss of capacity, not competence, as the fundamental process governing deposition from turbidity currents. Journal of Sedimentary Research, v.A64, p.209-214.

Holmes, A., 1965. Priciples of physical geology. London, England, Thomas Nelson and sons Ltd., 1288 p.

Jenkins, R., 1989. Instrumentation. In Bish, D.L. and Post, J.E. (eds): Modern powder diffraction. Reviews in mineralogy, v.20, Mineral Society of America, Washington D.C., p.19-45.

Jopling, A.V., and Walker, R.G., 1968. Morphology and origin of ripple-drift cross-lamination, with example from the Pleistocene of Massachusetts. Journal of Sedimentary Petrology, v.38, p.971-984.

Kehew, A.E., 1982. Catastrophic flood hypothesis for the Souris Spillway, Saskatchewan and North Dakota. Geological Society of America Bulletin. 93: 1051-1058.

Kehew, A.E., and Clayton, L., 1983. Late Wisconsinan floods and developments of Souris-Pembina Spillway system in Saskatchewan, North Dakota, and Manitoba. In J.T. Teller & L. Clayton (eds), Glacial Lake Agassiz. Geological Association

of Canada Special Paper 26: 187-210.

Kehew, A.E. and Lord, M.L., 1987. Glacial-lake outbursts along the mid-continent margins of the Laurentide Ice Sheet. In L. Mayer & D. Nash (eds), Catastrophic flooding. Allen & Unwin, Boston: 95-120.

Kehew, A.E., and Lord, M.L., 1986. Origin and large-scale erosional features of glacial lake spillways in the northern great plains. Geological Society of America Bulletin. 97: 162-177.

Kehew, A.E. and Teller, J.T., 1994a. History of late glacial runoff along the southwestern margin of the Laurentide Ice Sheet. Quaternary Science Reviews, v.13, p.859-877.

Kehew, A.E. and Teller, J.T., 1994b. Glacial-lake spillway incision and deposition of a coarse-grained fan near Watrous, Saskatchewan. Canadian Journal of Earth Sciences, v.31, p.544-553.

Klassen, R.W., 1989. Quaternary geology of the southern Canadian interior plains. In R.J. Fulton (ed), Quaternary geology of Canada and Greenland, Geological Survey of Canada, Geology of Canada. no.1: 138-173.

Klassen, R.W., 1983a. Assiniboine Delta and the Assiniboine-Qu'Appelle valley system-implications concerning the history of Lake Agassiz in southwestern Manitoba. In J.T. Teller & L. Clayton (eds), Glacial Lake Agassiz. Geological Association of Canada Special Paper 26: p.211-230.

Klassen, R.W., 1983b. Lake Agassiz and the late glacial history of Northern Manitoba. In J.T. Teller & L. Clayton (eds), Glacial Lake Agassiz. Geological Association of Canada Special Paper 26: p.97-115.

Klassen, R.W., 1979. Pleistocene geology and geomorphology of the Riding Mountain and Duck Mountain areas, Manitoba-Saskatchewan. Geological Survey of Canada Memoir 396: 52p.

Klassen, R.W., 1975. Quaternary geology and geomorphology of Assiniboine and Qu'Appelle valley of Manitoba and Saskatchewan. Geological Survey of Canada, Bulletin 228: 61p.

Klassen, R.W., Wyder, J., and Bannatyne, B.B., 1970. Bedrock topography and geology of southern Manitoba. Geological Survey of Canada Paper 70-51.

Last, W.M., 1980. Sedimentology and postglacial history of Lake Manitoba. Ph.D Thesis, University of Manitoba, Winnipeg, 686p.

Lemke, R.W. & Colton, R.B., 1958. Summary of the Pleistocene geology of North Dakota. In Guidebook, Ninth Annual Field Conference, Mid-western Friend of the Pleistocene. North Dakota Geological Survey, Miscellaneous Series No.10, p.47-57

Lord, M.L., 1991. Depositional record of a glacial-lake outburst: glacial Lake Souris, North Dakota. Geological Society of America Bulletin, v.103, p. 290-299.

Lord, M.L., 1988. Glacial Lake Souris--the history and sedimentology of a lake inundated by discharges from a glacial-lake outburst. Ph.D. dissertation. University of North Dakota, Grandforks, 196p.

Lord, M.L., and A.E. Kehew, 1987. Sedimentology and paleohydrology of glacial-lake outburst deposits in southeastern Saskatchewan and northwestern North Dakota. Geological Society of America Bulletin. v.99, p.663-673.

Lowe, D.R., 1982. Sediment gravity flows: II. Depositional models with special reference to the deposits of high-density turbidity currents. Journal of Sedimentary Petrology, v.52, p.279-297.

Maizels, J., 1992. Boulder ring structures produced during jökulhlaup flows. Gepgrafiska Annaler, v.74A, p.21-33.

Manitoba Energy and Mines, 1988. Aggregate resources compilation series, Map AR88-1-4, Virden, NTS 62F, 1:250,000.

Manitoba Mineral Resources Division, 1980. Quaternary Geological Map, southern Manitoba 62F, Virden. Geological Map AR80-6, scale 1:250,000.

Manitoba Mineral Resources Division, 1979. Geological Map of Manitoba. Map 79-2, scale 1:1,000,000.

Manitoba Water Resources Division, 1976. Groundwater resources in the Souris Basin in Manitoba.

Mayboom, P., van Everdingen, R.O., and Freeze, R.A., 1966. Patterns of groundwater flow in seven discharge areas in Saskatchewan and Manitoba. Geological Survey of Canada Bulletin 147, 57p.

McCabe, H.R., 1971. Stratigraphy of Manitoba, and introduction and review. In Turnock, A.C. (ed), Geoscience studies in Manitoba. Geological Association of Canada Special Paper 9, p.167-187.

McPherson, G.H., Shanmugam, G. and Moiola, R.J., 1987. Fan-deltas and braid deltas:

varieties of coarse-grained deltas. Geological Society of America Bulletin. 99: 331-340.

McNeil, D.H. and Caldwell, W.G.H., 1981. Cretaceous rocks and their foraminifera in the Manitoba Escarpment. Geological Association of Canada, St.John's, Newfoundland. Geological Association of Canada Special Paper 21: 439p.

Miall, A.D., 1984. Deltas. In Walker, R.G. (ed), Facies models, second edition. Geoscience Canada, p.105-118.

Moran, S.R., Arndt, B.M., Bluemle, J.P., Camara, M., Clayton, L., Fenton, M.M., Marris, K.L., Hobb, H.C., Keating, R., Sackreiter, D.K., Saloman, N.L., and Teller, J.T., 1976. Quaternary stratigraphy and history of North Dakota, Southern Manitoba, and Northwestern Minnesota. In Mahaney, W.C. (ed), Quaternary stratigraphy of North America. stroidsburg, Pennsylvania, Dowden, Hutchinson and Ross, p.133-158.

Nambudiri, E.M.V., Teller, J.T., and Last, W.M., 1980. Pre-Quaternary microfossils-A guide to errors in radiocarbon dating. Geology, v.8, p.123-126.

Nilsen, T.H., 1985. Modern and ancient alluvial fan deposits. A Hutchinson Ross Benchmark Book. Van Nostrand Reinhold Company, New York, 372p.

Nemec W. and Stell, R.J., 1984. Alluvial and coastal conglomerates: their significance features and some comments on gravelly mass-flow deposits. In Koster, E.H. and Steel, R.J. (eds), sedimentology of gravels and conglomerates. Memoir of Canadian Society of Petroleum Geology, No.10, P.1-31.

Perkin, E.H., and Dyck, J.H., 1973. Heinz gas--volugraph. Saskatchewan Research Council Report P73-6, 89p.

Pickering, K., Stow, D., Watson, M., and Hiscott, R., 1986. Deep-water facies, processes and models: A review and classification scheme for modern and ancient sediments. Earth Sciences Review, v.23, p.75-174.

Pickrill, R.A., and Irwin, J. , 1982. Predominant headwater inflow and its control of lake-river interactions in Lake Wakatipu. New Zealand Journal of Freshwater Research, v.16, p.201-213.

Pierson, T.C., 1981. Dominant particle-support mechanisms in debris flows at Mount Thomas, New Zealand, and implications for flow mobility. Sedimentology, v.28, p.48-60.

Podolsky, G., 1985. Soils of Souris, Virden and Wawanesa Town-sites. Manitoba

Department of Agriculture, Agriculture Canada, Soils Report No.D56, 138p.

Postma, G., 1990. Depositional architecture and facies of river and fan delta: a synthesis. In Colella, A. and Prior, D.B. (eds), Coarse-grained delta. Blackwell Scientific Publications, Cambridge Massachusetts, P.13-28.

Postma, G., and Roep, T.B., 1985. Resedimented conglomerates in the bottomsets of Gilbert-type gravel deltas. Journal of sedimentary petrology, v.55, p.874-885.

Potts, P.J., 1987. Handbook of silicate rock analysis. New York, Chapman and Hall, 622p.

Ruhe, R.V., 1969. Quaternary landscapes in Iowa. Ames, Iowa, Iowa State University Press, 255p.

Ross, W.C., 1986. Atomic absorption methods for quantitative determination of carbonates in tills. Saskatchewan Research Council, Technical Report 214, 19p.

Ruhe, R.V., 1969. Quaternary landscapes in Iowa: Ames, Iowa. Iowa State University Press, 255p.

Rust, B.R. and Koster, E.H., 1984. Coarse alluvial deposits. In Walker. R.G. (ed), Facies models, GeoScience Canada Reprint Series 1, p.53-71.

Schreiner, B.T., 1990. Lithostratigraphic correlation of Saskatchewan tills, a mirror image of Cretaceous bedrock. Ph.D thesis, University of Saskatchewan, Saskatoon, Saskatchewan. 401p.

Schultz, L.G., 1964. Quantitative interpretation of mineralogical composition from X-ray and chemical data for the Pierre Shale. U.S. Geological Survey Professional Paper 391-C, 31P.

Shaw, J., 1991. Hairpin erosional marks, horseshoe vortices and subglacial erosion. Sedimentary Geology, v.91, p.269-283.

Shaw, J. 1983. Drumlins formation related to inverted meltwater erosional marks. Journal of Glaciology, v.29, p.461-479.

Shepherd, R.G. and Schuman, S.A., 1974. Experimental study of river incision. Geological Society of America Bulletin, v.85, p.257-268.

Smith, D, G., 1991. Canadian landform examples--22. The Canadian Geographer, v.35, p.311-316.

Smith, N.D., and Ashley, G., 1985. Chapter 4, proglacial lacustrine environments. in Ashley, G.M., Shaw, J., and Norman, D.S.(Eds), Glacial sedimentary environments. SEPM Short Course No.16. Society of Paleontologists and Mineralogists, Tulsa. p.135-215.

Sun, C., 1993a. Quaternary geology and deglaciation history of Assiniboine Fan-Delta area, southwestern Manitoba. Unpublished M.Sc Thesis, University of Manitoba, Winnipeg, Manitoba: 180p.

Sun, C.S., 1993b. Preliminary study of the surficial geology of Virden area, southwestern Manitoba: in Current Research, Part B; Geological Survey of Canada, Paper 93-B, p.57-61.

Sun, C.S., and Fulton, R.J., 1995a. Surficial geology of Oak Lake area, Manitoba (62F/NE), 1 colour map, scale 1:100,000: Geological Survey of Canada Map Open File 3065.

Sun, C.S. and Fulton, R.J., 1995b. Surficial geology of Whitewater Lake area, Manitoba (62F/SE), 1 colour map, scale 1:100,000: Geological Survey of Canada Map Open File 3056.

Sun, C.S. and Fulton, R.J., 1994. Surficial geology, Virden (62F/15) and Alexander (62F/16), Manitoba, 2 colour maps, scale 1:50,000: Geological Survey of Canada Open File 2962.

Sun, C.S., and Teller, J.T.. in press (1996). Reconstruction of glacial Lake Hind in southwestern Manitoba, Canada. Journal of Paleolimnology, v.17.

Sun, S., and Teller, J.T., 1995a. Reconstruction of paleo-lake level of glacial Lake Hind based on perched deltas and fine lacustrine deposits: in: Abstracts with Programs, Geological Society of America 29th North-Central and South-Central Meeting, Nebraska, p.88.

Sun, S. and Teller, J.T., 1995b. The route of meltwater discharges from Lake Agassiz and their impact on the global climate. *in*: Proceedings of the Second Academic Conference of Young Scientists, Volume of Environmental and Natural Resource, p.295-300 (published in Chinese).

Sun, S. and Teller, J.T., 1993. Sedimentology of a large Pleistocene gravel bar produced by flooding: in American Quaternary Association Program and Abstract of the 13th biennial meeting, Minneapolis, p.251.

Surlyk, F., 1984. Fan-delta to submarine fan conglomerates of the Volgian-Valanginian Wollaston Foreland Group, eastern Greenland. In Koster, E.H. and Steel, R.J.

(eds): Sedimentology of gravel and conglomerates. Canadian Society of Petroleum Geologists Memoir 10, p.359-382.

Teller, J.T., 1989. Importance of the Rossendale site in establishing a deglacial chronology along the southwestern margin of the Laurentide Ice Sheet. Quaternary Research 32, p.12-23.

Teller, J.T., 1987. Proglacial lakes and the southern margin of Laurentide Ice Sheet. In W.F. Ruddiman & H.E. Wright, Jr. (eds), North America and adjacent oceans during the last deglaciation. The Geological Society of America. k-3: 39-69.

Teller, J.T., 1985. Glacial Lake Agassiz and its influence on the greet Lakes. In P.F. Karrow & P.E. Calkin (eds), Quaternary evolution of the Great Lakes. Geological Association of Canada Special Paper 30: 1-16.

Teller, J.T., 1980, Radiocarbon dates in Manitoba. Mineral Resources Division Geological Report GR80-4, 61p

Teller, J.T., and Bannatyne, B., 1976. Geology and topography of the buried bedrock surface of southern Manitoba. Manitoba Mineral Resources Division Surficial Map 76-3, Scale 1:500,000.

Teller, J.T., Bannatyne, B., Large, P., and Ringrose, S., 1976. Quaternary sediment, bedrock topography and geology of southern Manitoba. Manitoba Mineral Resource Division Surface Map Series, 76-1, 76-2, 76-3, and 76-4, scale 1:500,000.

Teller, J.T. and Bluemle, J.P., 1983. Geological setting of the Lake Agassiz region. In Teller, J.T. and Clayton, L.(eds): Glacial Lake Agassiz. Geological Association of Canada Special Paper 26, p.7-20.

Teller, J.T., and Fenton, M.M., 1980. Late Wisconsinan glacial stratigraphy and history of southeastern Manitoba. Canadian Journal of Earth Sciences, v.17, p.19-35.

Teller, J.T., Moran, S.R., and Clayton, Lee, 1980. The Wisconsinan deglaciation of southern Saskatchewan and adjacent areas: Discussion: Canadian Journal of Earth Sciences, v.17, p.539-541.

Teller, J.T. and Thorleifson, L.H., 1983. The Lake Agassiz-Lake Superior connection. In Teller, J.T. and Clayton, L.(eds): Glacial Lake Agassiz. Geological Association of Canada Special Paper 26, p.261-290.

Tholeifson, L.H., 1983. The eastern outlets of Lake Agassiz. M.Sc Thesis, University of Manitoba, Winnipeg, 87p.

Vincent, J-S., 1989. Quaternary geology of the southeastern Canadian Shield. In Chapter 3 of Quaternary Geology of Canadian and Greenland: R.J. Fulton (ed), Quaternary geology of Canada and Greenland, Geological Survey of Canada, Geology of Canada, no.1: 249-275.

Warman, T.A., 1991. Sedimentology and history of deglaciation in the Dryden Ontario area, and their bearing on the history of Lake Agassiz. MSc Thesis, University of Manitoba, Winnipeg, 256p.

Weirich, F.H., 1984. Turbidity currents: monitoring their occurrence and movement with a three dimensional sensor network. Science, v.224, p.384-387.

Wickenden, R.T.D., 1945. Mesozoic stratigraphy of eastern plains, Manitoba and Saskatchewan. Geological Survey of Canada Memoir 239.

Wolfe, B., 1993. Geological history of glacial Lake Assiniboine, Saskatchewan. M.Sc Thesis, University of Manitoba, Winnipeg, 391p.

Wolfe B. and Teller, J.T., 1995. Sedimentation in Ice-dammed glacial Lake Assiniboine, Saskatchewan, and catastrophic drainage down the Assiniboine valley. Géographie Physique et Quaternaire, v.49, p.251-263.

Wolfe, B. and Teller, J.T., 1993. Sedimentological and stratigraphic investigations of a sequence of 106 varves from glacial Lake Assiniboine, Saskatchewan. Journal of Paleolimnology, v.9, p.253-273.

Wright, Jr, H.E., 1972. Quaternary history of Minnesota. In Sims, P.K. and Morey, G.B. (eds): Geology of Minnesota: a centennial volume. Minnesota Geological Survey, p.515-547.

APPENDICES

CANADA 62F UTM 14U

EDITION 3

62

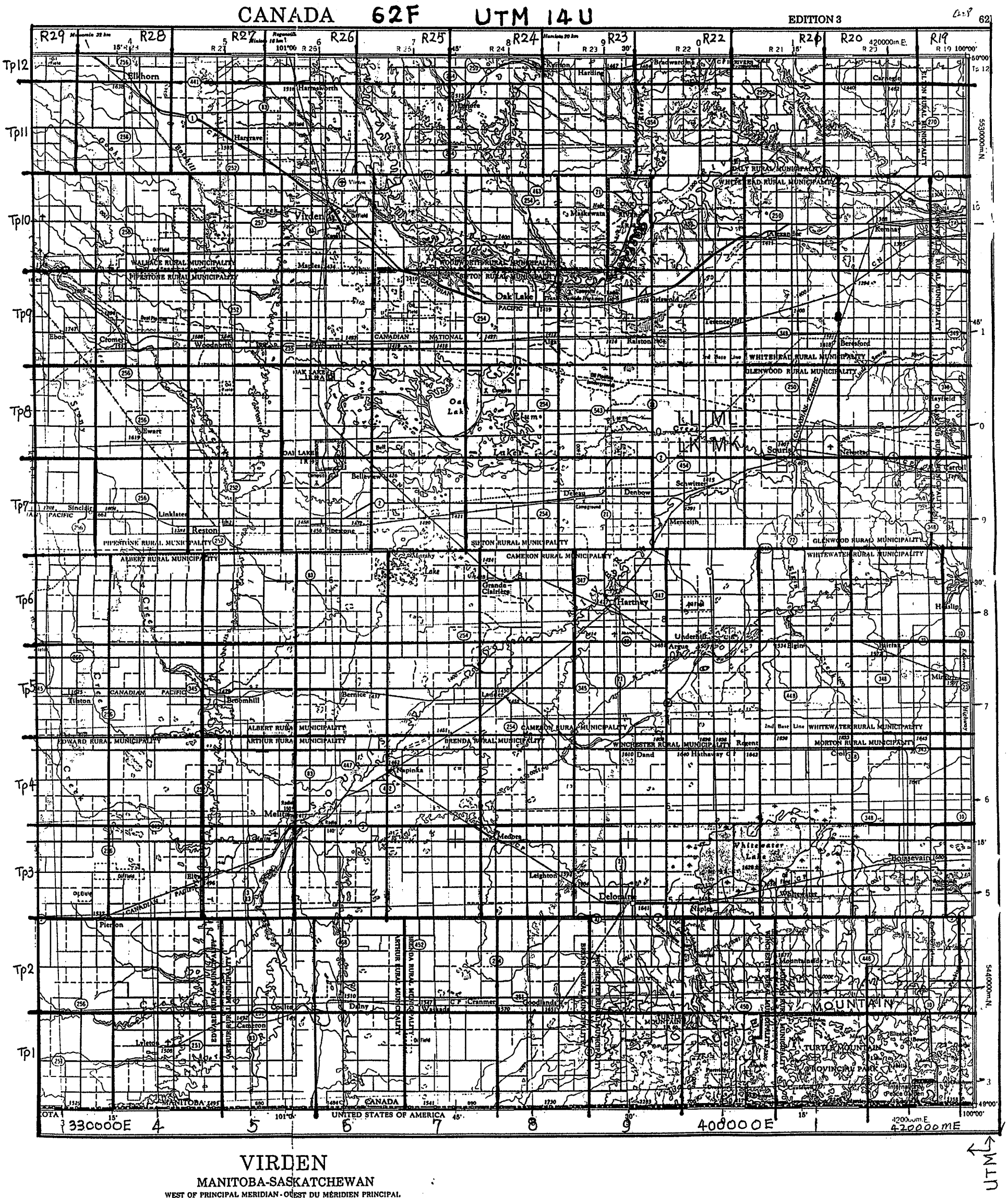

VIRDEN

MANITOBA-SASKATCHEWAN

WEST OF PRINCIPAL MERIDIAN - OUEST DU MÉRIDIEN PRINCIPAL

Scale 1:250,000 Échelle

MILES
KILOMETRES.

UTM

Appendix I Sieve analysis of sand

Site	Easting	Northing	<-1 (g)	-0.5 (g)	0 phi (g)	0.5 (g)	1 phi (g)	1.5 (g)	2 phi (g)	2.5 (g)	3 phi (g)	3.5 (g)	4 phi (g)	>4 phi (g)	Weight (g)	Mean Phi	Stnd D. Phi
92SFI228	388300	5513850					0.25	15.2	130.5	251.8	150	58.2	27.5	25.6	659.05	2.25	0.66
92SFI229	391350	5513800							5	10	47.5	42.5	22.5	12	139.5	2.75	0.53
92SFI231	378400	5514100					4.7	29.3	145.1	93.7	26.2	4.7	2.4	2.2	308.3	1.71	0.48
92SFI236	370200	5514350							20.4	35.4	26.5	8.9	5.4	3	99.6	1.87	0.35
92SFI238	365450	5517700					2	21.4	87.7	58.5	29.3	7.4	1.3	0.2	207.8	1.77	0.53
92SFI238	365400	5520950					2.9	32.5	106.5	22.7	49	12.5	4.5	0.9	231.5	1.82	0.65
92SFI242	362200	5520950					2	21.4	49.8	31	13.5	1.2	0.5	0.2	119.6	1.64	0.54
92SFI275	359950	5501400				0.2	0.6	1.5	3	8.4	24.3	16.5	14.3	14	82.8	2.95	0.83
92SFI278	365000	5501400	68.4	28	43.5	75.3	111.7	76.8	50.5	15.1	4.9	1.1	0.5	0.4	476.2	0.15	1.16
92SFI293	361300	5489900	11.5	15	46.3	125.5	226.5	95.9	28.6	12	6	1	0.9	3.2	572.4	0.28	0.68
92SFI304	368200	5504500					32.5	31.3	16.5	6.4	2.1	0.5	0.1	0.1	89.5	1	0.55
92SFI365	383750	5496800				0.9	0.4	1.4	13.2	24.6	26.6	43.5	55	40.7	206.3	3.08	0.91
92SFI370	389400	5490850					0.4	4.6	30.6	49	43.8	24.8	24.8	13.2	191.2	2.47	0.84
93SFI203	396200	5510450						41.5	169.5	113	64.5	31.2	21.4	22.6	463.7	1.92	0.76
93SFI206	393000	5510500					1.5	10	26.5	22	9.5	2.8	1.2	0.4	73.9	1.78	0.57
93SFI218	392800	5499900					2.5	5.1	17	19.2	13.3	3.5	1.9	1.8	64.3	2.01	0.79
93SFI225	399500	5507050						2	5.7	13	18.8	17.5	21.3	34.7	113	3.31	0.92
93SFI233	396050	5497300							7	40	61	16	9.5	7	140.5	2.53	0.59
93SFI236	397800	5498900					1	3.5	13	32.5	51	24.6	21.7	18.9	166.2	2.73	0.87
93SFI256	399350	5499800						6	24.5	32	28	9	5.5	2.5	107.5	2.14	0.65
93SFI258	399400	5502150						3.3	7.5	9.9	14.3	21.3	23.3	13.4	93	2.95	0.91
93SFI259	402800	5505400					2.6	3.8	5.9	9.6	25.1	30.5	43.3	40.2	161	3.29	0.92
93SFI261	402700	5502100						1.6	36.5	109.4	146.5	79.8	35.5	15.5	424.8	2.53	0.69
93SFI262	405900	5500400							0.9	8	27.1	25.2	22.7	9.3	93.2	3.02	0.63
93SFI275	404500	5507000	0.5	0.2	0.4	1.3	5.1	15.4	40.4	24.1	6.9	1.5	1.3	3	100.1	1.64	0.66
93SFI290	398900	5487300	20.6	13.4	17.6	32.5	54	67	48.5	22	8.5	2	1.5	2	289.6	0.7	1.12
93SFI313	412700	5503700					7.1	22.5	34.9	24.5	12.2	3	2	2.5	108.7	1.68	0.7
93SFI485	369250	5483100			2.5	24	119.5	284.6	146	34.5	9.8	2.2	1	2	626.1	0.95	0.42
94SFI004	355300	5448800	26	15.3	32.5	103.4	215	72.5	26.5	6.5	3	1.2	1	2	504.9	0.41	0.73
94SFI328	379050	5476300						1.2	7	15.4	21.3	14.8	11.9	10.5	82.1	2.77	0.89
94SFI329	377300	5474700					39.5	26.5	25.5	24.5	22.5	6.5	1.2	1	147.2	1.51	0.86
94SFI336	377200	5471400						3	20.6	49	49.5	10	1.5	1.2	134.8	2.22	0.5
94SFI362	368850	5464900					0.3	4.1	38.3	38.5	32	16.7	7.7	3	140.6	2.2	0.69
94SFI363	372200	5464950				0.2	1.5	5	12.3	20.5	20.5	9.1	5.5	3.2	77.8	2.3	0.82
94SFI364	377050	5464800						1.5	6	15.5	20.8	11.8	9.9	7.2	72.7	2.7	0.84
94SFI346	383550	5459750	5.7	4.8	7.5	16.9	40.9	31.8	12.5	3.9	1.5	0.8	1	3.1	130.4	0.62	0.9
94SFI371	370600	5469850		0.2	0.2	1.7	19.5	123.3	220.8	40.3	6.8	1.1	0.9	3.2	418	1.38	0.42

APPENDIX II PEBBLE COUNTING RESULTS

A. PEBBLES FROM TILL SAMPLES

STATION I.D.	Carb. tan %	Carb. gray %	Metam -orphic %	Granit %	Basalt %	Shale %	Qtzite fine %	Qtzit c.g %	Chert %	Sdstn %	Ironst %	TOTAL COUNT
A1) BOISSEVAIN AREA												
SFI940074	3.5	47.9	18.3	4.2	9.9	10.6	0.7	1.4	1.4	1.4	0.7	142.0
sFI940020	5.7	38.9	15.3	10.2	12.7	9.6	1.3	1.9	1.9	2.5	0.0	157.0
SFI940025	1.9	24.8	22.9	14.3	11.4	5.7	3.8	1.0	11.4	1.0	1.9	105.0
SFI940028	3.6	37.1	25.3	7.2	9.3	9.3	0.5	1.5	5.7	0.0	0.5	194.0
SFI940034	6.5	38.9	12.0	12.0	13.0	4.6	2.8	0.0	4.6	0.0	5.6	108.0
SFI940037	1.6	45.5	15.8	8.7	7.1	15.0	0.8	0.0	2.8	1.6	1.2	253.0
SFI940039	4.8	38.7	19.4	6.5	8.9	15.3	0.8	0.0	2.4	1.6	1.6	124.0
SFI940040	6.1	42.0	10.7	8.4	10.7	14.5	2.3	0.0	0.0	2.3	3.1	131.0
SFI940043	3.6	43.6	20.0	5.0	10.0	10.0	2.1	1.4	0.0	2.9	0.7	140.0
SFI940047	4.1	44.8	20.7	6.2	8.3	11.7		1.4	0.7	0.0	2.1	145.0
SFI940048	5.5	46.4	21.8	10.9	4.5	5.5	0.0	0.9	0.9	0.9	1.8	110.0
SFI940050	2.0	51.0	16.3	4.8	6.8	12.2	1.4	0.7	0.7	0.7	3.4	147.0
SFI940053	4.0	41.3	27.8	2.4	8.7	9.5	0.8	1.6	2.4	0.8	0.8	126.0
SFI940058	3.9	41.9	22.5	4.7	14.0	7.8	0.8	0.0	2.3	1.6	0.8	129.0
SFI940064	3.4	47.1	16.8	13.4	6.7	5.9	0.0	0.0	2.5	2.5	1.7	119.0
SFI940064	2.8	47.2	19.8	8.5	5.7	11.3	1.9	0.0	2.8	0.0	0.0	106.0
SFI940066	4.7	46.2	20.8	6.6	6.6	11.3	0.9	0.0	0.9	1.9	0.0	106.0
SFI940068	1.7	45.0	22.5	6.7	7.5	7.5	0.8	0.8	4.2	2.5	0.8	120.0
SFI940074	3.5	47.9	18.3	4.2	9.9	10.6	0.7	1.4	1.4	1.4	0.7	142.0
SFI940221	1.5	39.3	19.3	1.5	8.9	26.7	0.7	0.7	0.7	0.7	0.0	135.0
SFI940231	4.3	42.1	12.9	3.6	9.3	25.0	0.7	0.0	0.7	1.4	0.0	140.0
SFI940235	2.8	36.6	9.7	2.1	6.9	34.5	0.7	0.0	0.0	2.8	4.1	145.0
SFI940237	2.6	43.4	18.4	5.3	3.9	23.7	0.0	0.0	0.0	0.0	2.6	76.0
SFI940242	3.0	44.4	21.2	6.1	7.1	15.2	2.0	0.0	0.0	0.0	1.0	99.0
SFI940246	2.8	50.0	19.8	3.8	9.4	5.7	1.9	0.0	1.9	0.9	3.8	106.0
SFI940247	2.6	42.6	23.2	6.3	5.3	14.7	0.0	0.5	1.6	0.0	3.2	190.0
SFI940251	3.1	35.1	20.6	3.1	3.8	28.2	0.8	1.5	0.0	0.8	3.1	131.0
SFI940254	3.5	49.0	20.3	5.6	6.3	9.8	1.4	0.0	2.1	0.7	1.4	143.0
SFI940148		51.2	27.9	2.3	16.3			0.0	0.0	0.0	2.3	43.0
SFI940153	4.6	53.8	17.7	9.2	7.7	4.6		0.0	1.5	0.8	0.0	130.0
SFI940156	6.0	50.7	15.7	4.5	9.7	7.5	1.5	0.0	0.7	0.0	3.7	134.0
SFI940159	3.1	46.9	27.5	5.0	6.3	3.1	0.6	1.3	3.8	0.6	1.9	160.0
SFI940161	3.6	49.5	20.7	5.4	9.0	5.4	1.8	0.0	0.9	0.9	2.7	111.0
SFI940163	2.0	59.2	17.3	4.1	11.2	3.1		1.0	0.0	2.0	0.0	98.0
SFI940164	1.9	56.1	21.5	5.6	4.7	0.0		1.9	0.0	0.9	5.6	107.0
SFI940169	2.4	50.0	20.7	4.9	4.9	8.5	1.2	1.2	0.0	1.2	4.9	82.0
SFI940171	1.6	43.2	19.2	5.6	7.2	17.6	0.0	0.8	0.8	1.6	2.4	125.0
SFI940175		28.0	20.7	6.1	2.4	39.0	1.2	0.0	0.0	0.0	2.4	82.0
SFI940178	2.3	52.3	18.8	3.9	3.9	11.7	1.6	0.0	0.8	0.8	3.9	128.0
SFI940179	1.6	38.1	12.7	3.2	9.5	24.6	0.0	4.8	0.8	0.0	4.8	126.0
SFI940180	0.8	31.1	14.3	2.5	3.4	44.5	0.0	0.0	0.0	0.0	3.4	119.0
SFI940181	2.7	38.9	15.0	6.2	7.1	12.4	1.8	0.0	0.9	3.5	10.6	113.0
SFI940183	2.1	34.5	16.0	4.6	3.1	36.1	0.5	0.0	0.5	0.5	1.5	194.0
SFI940188	1.4	36.1	11.8	3.5	1.4	41.7	0.7	0.0	1.4	0.7	1.4	144.0
SFI940190	1.4	40.4	13.7	3.4	5.5	32.2	0.7	0.7	1.4	0.0	0.7	146.0
SFI940192	2.0	44.4	11.9	2.6	8.6	25.8	1.3	0.0	1.3	0.7	1.3	151.0

SFI940194		43.2	16.2	16.2	2.7	16.2	0.0	2.7	0.0	0.0	2.7	74.0
SFI940196	2.7	30.4	10.7	4.5	7.1	41.1	0.0	1.8	0.0	1.8	0.0	112.0
SFI940263	1.7	51.7	17.2	4.3	2.6	7.8	1.7	0.0	0.9	0.0	12.1	116.0
SFI940265	0.8	41.5	16.1	2.5	6.8	28.8	0.8	0.0	0.8	0.0	1.7	118.0
SFI940274	1.8	34.8	23.2	4.5	8.9	21.4	0.9	0.9	1.8	0.0	1.8	112.0
SFI940276	0.9	46.0	16.8	7.1	6.2	15.0	0.0	0.0	1.8	0.0	6.2	113.0
SFI940283	2.6	29.4	16.5	3.9	4.3	39.4	0.4	0.0	1.7	0.4	1.3	231.0
SFI940283	0.3	5.3	1.7	1.3	0.7	87.8	0.3	0.0	0.7	0.7	0.7	303.0
SFI940291		61.5	12.8	6.4	5.1		2.6	2.6	2.6	3.8	2.6	78.0
SFI940296	3.8	59.0	18.1	6.7	6.7		0.0	0.0	1.0	1.9	2.9	105.0
SFI940354	0.9	50.9	14.9	3.5	6.1	20.2	0.0	0.9	0.9	0.9	0.9	114.0
SFI940345	4.2	33.6	14.7	4.2	5.6	32.2	1.4	0.7	0.7	2.1	0.7	143.0
SFI940347	2.8	49.2	18.3	3.7	6.1	10.6	2.4	2.0	2.4	0.8	1.6	246.0
SFI940349	2.6	59.0	14.1	7.7	6.4	2.6	2.6	0.0	2.6	0.0	2.6	78.0
SFI940385	1.3	50.7	25.7	4.6	5.9	3.9	2.0	0.0	2.6	1.3	2.0	152.0
SFI940386	1.8	60.3	18.7	4.6	5.0	2.3	1.8	0.9	0.9	0.5	3.2	219.0
SFI940387	1.3	39.2	20.3	7.2	5.9	14.4	2.6	1.3	1.3	2.6	2.6	153.0
SFI940388	1.6	54.0	23.3	4.8	7.4		0.0	0.0	1.6	2.6	4.8	189.0
SFI940389	2.6	39.4	16.8	4.5	5.8	23.9	1.3	1.3	0.6	0.6	3.2	155.0

STATION I.D.	Carb. %	Metam -phic %	Granit %	Basalt %	Shale %	Qtzite %	Chert %	Sdstn %	Ironst %	TOTAL COUNT
A2) BRANDON AREA										
SFI93004	51	9	9		19	10	1	2	1	87
SFI93006	46	15	7		15	2	0	11	3	123
SFI93007	50	16	8		18	3	0	4	0	125
SFI93009	55	7	9		13	6	2	5	3	165
SFI93011	59	10	4		18	5	0	3	1	114
SFI93136	74	8	8		5	2	0	1	1	85
SFI93198	74	6	9		6	3	0	1	1	100
SFI93199	39	13	8		34	5	0	1	0	77
SFI93026	38	27	8		14	11	0	2	0	125
SFI93030	50	20	9		18	4	0	0	0	106
SFI93032	57	15	7		10	4	0	6	2	115
SFI93039	50	8	13		17	4	0	6	3	107
SFI93095	74	7	9		3	3	0	5	0	81
SFI93096	57	11	8		18	3	2	1	1	112
SFI93096	53	19	10		15	3	0	0	0	78
SFI93313	47	15	7		17	8	0	4	2	96
SFI93323	53	11	9		18	7	0	2	0	159
SFI93339	66	17	5		0	11	0	2	0	113
SFI93352	82	3	10		1	4	0	0	0	73
SFI93359	57	17	10		8	6	0	3	0	107
SFI93376	51	8	11		20	7	0	1	2	142
SFI93388	54	7	11		14	11	0	3	0	114
SFI93407	57	13	8		7	11	0	3	1	123
SFI93408	42	9	6		37	5	0	1	0	187
SFI93408	23	6	3		65	2	0	1	0	223
SFI93408	19	7	2		66	6	0	0	0	181
SFI93408	41	6	7		40	4	0	2	0	124
SFI93408	37	7	5		42	6	1	1	1	183
SFI93408	41	9	6		37	5	0	2	1	171
SFI93408	42	9	5		39	5	0	1	0	194

SFI93409	38	4	1	53	4	0	0	0	161
SFI93409	33	10	5	48	4	0	1	0	114
SFI93409	36	6	6	46	5	0	2	0	191
SFI93413	78	9	9	0	1	0	1	2	152
SFI93413	32	12	7	43	5	0	1	0	169
SFI93413	48	12	7	20	8	0	5	0	131
SFI93074	45	14	14	21	3	0	3	0	127
SFI93080	83	7	7	1	3	0	0	0	103
SFI93085	50	19	12	11	4	0	2	3	109
SFI93040	80	7	5	4	3	0	0	0	92
SFI93041	55	18	6	16	4	0	2	0	142
SFI93044	56	14	6	14	4	0	4	1	160
SFI93052	56	9	6	20	3	0	5	0	130
SFI93053	64	8	5	16	2	0	5	1	134
SFI93074	48	19	9	17	3	0	4	0	161
SFI93425	69	3	10	8	8	0	1	1	91
SFI93479	64	9	12	2	9	0	5	0	115
SFI93499	78	8	8	1	1	0	1	2	96
SFI93409	38	9	8	40	5	0	1	0	196
SFI93410	46	17	9	19	7	0	2	1	183
SFI93413	62	6	6	17	8	0	2	1	193
SFI93205	82	8	4	4	1	0	1	0	85
SFI93251	76	8	5	6	4	0	1	0	78
SFI93304	51	16	8	10	14	0	2	0	130

STATION I.D.	Carb. %	Metam -phic %	Granit %	Basalt %	Shale %	Qtzite %	Chert %	Sdstn %	Ironst %	TOTAL COUNT
A3) VIRDEN AREA										
SFI92001	27	25	0	15	12	0	16	0	0	197
SFI92002	13	1	0	10	15	56	0	0	0	138
SFI92005	13	4	0	41	19	20	0	0	0	154
SFI92006	31	0	0	0	2	65	0	0	0	419
SFI92007	23	28	0	11	4	29	1	0	0	412
SFI92008	29	27	0	0	1	40	1	0	0	86
SFI92011	34	0	0	26	5	33	0	0	0	75
SFI92024	32	12	0	4	1	42	0	0	0	124
SFI92040	12	22	0	23	0	40	0	0	0	109
SFI92043	19	37	0	0	3	33	2	0	0	103
SFI92045	20	27	0	18	0	32	2	0	0	133
SFI92047	17	18	0	17	6	37	1	0	0	198
SFI92048	27	21	0	13	0	36	0	0	0	373
SFI92063	9	16	0	9	13	47	2	0	0	115
SFI92069	22	22	0	0	16	0	0	0	38	75
SFI92091	11	28	0	16	10	33	0	0	0	116
SFI92116	14	14	0	8	20	39	0	0	0	114
SFI92122	0	1	0	0	96	2	0	0	0	229
SFI92267	41	3	0	41	0	14	0	0	0	97
SFI92270	17	1	0	26	5	50	0	0	0	99
SFI92271	33	0	0	13	14	39	0	0	0	92
SFI92389	22	0	0	16	24	36	0	0	0	124
SFI92389	22	1	0	40	3	31	0	0	0	176
SFI92389	22	0	0	30	1	45	0	0	0	75
SFI92389	31	0	0	35	7	23	0	0	0	163

SFI92432	24	0	0	33	13	28	0	0	0	129

STATION I.D.	Carb. %	Metam -phic %	Granit %	Basalt %	Shale %	Qtzite %	Chert %	Sdstn %	Ironst %	TOTAL COUNT
B. DELTAIC GRAVELS										
SFI940007	108	24	41	14	5	16	2	2	2	214
SFI940143	74	15	42	8	21	9	1	0	0	170
SFI940387	66	10	40	7	22	0	1	3	0	149
SFI930470	76	25	52	20	0	6	0	4	2	185
SFI930470	49	9	22	13	3	2	0	0	3	101
SFI940007	101	22	28	9	1	9	2	1	2	175
PIPESTON	63	18	53	27	0	2	1	0	1	165
SFI940129	28	9	11	2	131	14	0	0	0	195
SFI920VIR	79	10	30	10	7	7	1	0	0	144
SFI940051	137	10	61	25	62	14	0	0	2	311
SFI930461	77	21	25	20	6	12	1	0	3	165
21-10-R20	107	16	35	5	16	4	2	4	2	191
09-11-R20	63	20	36	14	13	6	0	0	1	153
SFI940289	75	12	38	7	42	11	0	0	1	186
SFI940064	81	20	41	8	8	10	0	0	2	170
SFI940013	61	16	42	10	24	7	1	0	1	162
SFI940012	45	37	31	10	3	5	1	1	0	133
SFI940007	92	26	41	8	6	20	0	0	0	193
SFI940141	17	2	8	2	77	0	0	0	0	106
SFI940129	50	6	23	3	62	0	0	0	0	144

APPENDIX III TEXTURE COMPOSITION OF TILL SAMPLES

1) BOISSEVAIN AREA

STATION I.D.	SAMPLE NUMBER	EASTING	NORTHING	SAND%	SILT%	CLAY%
SFI940020	94SFI0002	360200	5452050	43.61	32.29	24.09
SFI940025	94SFI0003	366800	5443600	41.03	32.81	26.15
SFI940028	94SFI0004	362100	5445500	41.93	34.12	23.94
SFI940034	94SFI0005	366900	5455200	35.11	36.21	28.67
SFI940037	94SFI0006	368500	5448500	34.34	41.68	23.96
SFI940039	94SFI0007	368250	5437000	36.48	36.87	26.63
SFI940040	94SFI0008	365050	5437100	39.32	32.67	28.00
SFI940043	94SFI0009	361850	5438650	37.88	35.93	26.18
SFI940047	94SFI0010	365350	5455200	38.45	32.82	28.72
SFI940048	94SFI0011	363500	5452150	43.53	31.82	24.63
SFI940050	94SFI0012	366350	5443750	36.65	33.44	29.90
SFI940053	94SFI0013	364900	5430500	37.42	35.90	29.66
SFI940058	94SFI0014	360100	5433800	37.72	35.94	26.32
SFI940064	94SFI0015	355400	5441400	39.72	36.26	24.00
SFI940064	94SFI0016	355400	5441400	39.63	36.01	24.34
SFI940066	94SFI0017	363600	5440400	39.21	33.99	26.78
SFI940068	94SFI0018	363750	5448700	34.76	38.93	26.29
SFI940074	94SFI0019	354850	5458700	39.26	34.48	26.24
SFI940077	94SFI0020	369800	5430400	37.02	33.79	29.18
SFI940082	94SFI0021	387850	5433250	37.76	34.46	27.77
SFI940086A	94SFI0022	389500	5431500	30.71	37.42	31.86
SFI940090	94SFI0023	369950	5433650	42.50	35.10	22.38
SFI940092	94SFI0024	376500	5433500	39.06	32.01	28.91
SFI940094	94SFI0029	378135	5430200	42.55	34.36	23.08
SFI940099	94SFI0030	384400	5431700	43.45	33.10	23.43
SFI940102	94SFI0031	371850	5455000	41.31	32.94	25.43
SFI940111	94SFI0032	371700	5436750	43.18	34.80	22.01
SFI940115	94SFI0033	383000	5433300	40.53	35.67	23.78
SFI940120	94SFI0034	386300	5436600	37.39	33.86	28.73
SFI940148	94SFI0034	393650	5472700	36.68	37.06	26.25
SFI940153	94SFI0035	401700	5470900	39.38	34.71	25.90
SFI940156	94SFI0036	405150	5470700	39.21	35.04	25.73
SFI940159	94SFI0037	413200	5469000	27.71	46.61	25.66
SFI940161	94SFI0038	413250	5472300	41.52	36.22	22.25
SFI940163	94SFI0039	406750	5472450	41.26	37.42	21.31
SFI940164	94SFI0040	410150	5475650	39.28	31.90	28.81
SFI940385	94SFI0041	383300	5442100	49.22	31.60	19.16
SFI940386	94SFI0042	389800	5443050	43.61	33.10	23.27
SFI940387	94SFI0043	389800	5448000	45.95	36.54	17.50
SFI940169	94SFI0044	391700	5456300	37.29	35.24	27.46
SFI940171	94SFI0045	391850	5462850	36.97	39.06	23.96
SFI940175	94SFI0046	397800	5469300	38.84	36.79	24.35
SFI940178	94SFI0047	398350	5466000	34.37	36.45	29.16
SFI940179	94SFI0048	401750	5466000	44.85	33.60	21.53
SFI940180	94SFI0049	419900	5477100	43.49	38.87	17.62

SFI940181	94SFI0050	423200	5477100	41.61	31.55	26.82
SFI940183	94SFI0051	419900	5472250	43.34	39.14	17.51
SFI940188	94SFI0052	418250	5469000	40.96	36.56	22.46
SFI940190	94SFI0053	426300	5465600	42.15	37.52	30.32
SFI940192	94SFI0054	414850	5465700	42.40	37.35	20.23
SFI940196	94SFI0056	396600	5462800	39.82	36.83	23.34
SFI940221	94SFI0057	404900	5461900	42.51	36.25	21.23
SFI940231	94SFI0058	413100	5462500	40.79	36.03	23.16
SFI940235	94SFI0059	322900	5459100	39.34	36.69	23.95
SFI940237	94SFI0060	389650	439750	28.83	36.86	34.30
SFI940242	94SFI0061	384800	5439850	39.31	35.26	25.41
SFI940246	94SFI0062	373300	5440200	33.47	37.12	29.39
SFI940247	94SFI0063	376650	5436750	40.38	34.21	25.39
SFI940251	94SFI0064	384900	5448300	35.19	38.36	26.44
SFI940254	94SFI0065	376700	544330	42.61	36.18	21.19
SFI940263	94SFI0066	381600	5448300	36.55	37.13	26.30
SFI940265	94SFI0068	383400	5451600	38.16	37.81	24.01
SFI940274	94SFI0069	378500	5455000	43.27	32.70	24.01
SFI940276	94SFI0070	385050	5454800	41.15	34.79	24.04
SFI940283	94SFI0071	385850	5464650	41.19	31.70	27.10
SFI940283	94SFI0072	385850	5464650	22.86	38.82	38.31
SFI940291	94SFI0073	388700	5471100	42.11	36.88	21.00
SFI940296	94SFI0074	390350	5471100	39.25	36.14	24.59
SFI940388	94SFI0075	419600	5457400	41.18	36.82	21.99
SFI940389	94SFI0076	416350	5459200	42.18	33.33	24.47
SFI940345	94SFI0077	382550	5459800	39.48	34.58	25.93
SFI940347	94SFI0078	390150	5462900	44.39	33.89	21.71
SFI940349	94SFI0079	386750	5459700	35.58	38.13	26.28
SFI940354	94SFI0080	362250	5438650	40.31	33.66	26.01

2) VIRDEN AREA

STATION I.D.	SAMPLE NUMBER	EASTING	NORTHING	SAND	SILT	CLAY
SFI92001	92SFI001-01	410000	5710000	46.18	37.78	16.04
SFI92002	92SFI002-02	428500	5503400	45.54	35.78	18.67
SFI92004	92SFI004-03	355200	5509900	60.39	27.1	12.51
SFI92005	92SFI005-04	358600	5514600	44.88	33.48	21.63
SFI92006	92SFI006-05	355400	5513000	46.03	34.25	19.72
SFI92008	92SFI008-06	355600	5517800	45.45	31.91	22.64
SFI92011	92SFI011-07	360400	5519400	44.31	32.18	23.5
SFI92033	92SFI033-08	357200	5521150	3.74	82.72	13.54
SFI92034	92SFI034-09	355600	5521200			
SFI92040	92SFI040-10	359100	5539200	37.91	38.09	24
SFI92043	92SFI043-11	357370	5537500	47.74	29.26	22.99
SFI92045	92SFI045-12	360700	5537500	36.46	42.19	21.35
SFI92047	92SFI047-13	359000	5534250	48.45	35.21	16.33
SFI92048	92SFI048-14	362200	5534200	73.63	16.73	9.64
SFI92062	92SFI062-15	360500	5530800	15.65	63	21.35
SFI92063	92SFI063-16	359800	5530800	48.92	34.57	16.51
SFI92064	92SFI064-17	357250	5531000	47.97	34.18	17.85
SFI92068	92SFI068-18	363800	5525800	44.44	50.32	5.24

SFI92077	92SFI077-19	384650	5538500	38.42	35.41	26.17
SFI92077	92SFI077-01A	384650	5538500	44.91	33.46	21.62
SFI92077	92SFI077-02A	384650	5538500	43.49	32.36	24.14
SFI92077	92SFI077-03A	384650	5538500	43.33	35.03	21.64
SFI92077	92SFI077-04A	384650	5538500	41.99	34.7	23.31
SFI92086	92SFI086-20	377100	5538600	34.1	39.54	26.36
SFI92088	92SFI088-21	373500	5538850	16.12	52.29	31.58
SFI92091	92SFI091-22	370500	5538950	49.28	31.89	18.82
SFI92094	92SFI094-23	367350	5538850	50.74	32.32	16.93
SFI92105	92SFI105-24	378750	5537000	50.03	31.42	18.55
SFI92108	92SFI108-25	385000	5536800	61.74	25.85	12.41
SFI92115	92SFI115-27	367300	5535700	67.37	19.16	13.47
SFI92116	92SFI116-28	368900	5535600	45.71	51.16	3.13
SFI92121	92SFI121-29	373750	5535400	34.01	35.57	30.42
SFI92122	92SFI122-30	375500	5535500	39.08	41.66	19.27
SFI92150	92SFI150-31	370450	5530650	21.45	49.8	28.75
SFI92209	92SFI209-32	372000	5525700	76.38	14.38	9.24
SFI92267	92SFI267-33	355200	5506500	34.98	44.22	20.81
SFI92270	92SFI270-34	358400	5504750	23.92	58.36	17.72
SFI92271	92SFI271-35	356750	5503200	44.37	34.63	20.99
SFI92389	92SFI389A-36	331500	5518600	40.28	36.35	23.37
SFI92389	92SFI389B-37	331500	5518600	38.9	38.32	22.78
SFI92389	92SFI389C-38	331500	5518600	42.5	34.71	22.79
SFI92389	92SFI389D-39	331500	5518600	42.8	35.56	21.64
SFI92389	92SFI389E-40	331500	5518600	42.26	37.27	20.47
SFI92389	92SFI389F-41	331500	5518600	42.21	36.82	20.97
SFI92389	92SFI389G-42	331500	5518600	41.43	36.28	22.29
SFI92389	92SFI389H-43	331500	5518600	41.75	37.81	20.44
SFI92389	92SFI389I-44	331500	5518600	41.33	36.54	22.13
SFI92389	92SFI389J-45	331500	5518600	41.38	34.24	24.38
SFI92389	92SFI389K-46	331500	5518600	41.96	33.9	24.14
SFI92389	92SFI389M-47	331500	5518600	41.57	35.16	23.27
SFI92389	92SFI389N-48	331500	5518600	45.53	37	17.47
SFI92421	92SFI421-49	411350	5530400	57.45	31.13	11.42
SFI92432	92SFI432-50	417750	5529500	32.55	44.28	23.17

3) BRANDON AREA

STATION I.D.	SAMPLE NUMBER	EASTING	NORTHING	SAND	SILT	CLAY
SFI93002	93SFI001	427200	5537750	39.53	36.08	24.39
SFI93004	93SFI002	424800	5537800	34.60	37.30	28.10
SFI93006	93SFI006	418200	5537850	25.26	43.22	31.52
SFI93007	93SFI008	414800	5537800	24.09	43.30	32.60
SFI93011	93SFI010	413100	5539200	34.59	55.19	10.22
SFI93030	93SFI014	424850	5536150	34.60	37.73	27.66
SFI93032	93SFI017	421400	5536300	23.78	45.02	31.20
SFI93039	93SFI018	419850	5534700	28.31	44.35	27.33
SFI93040	93SFI021	423000	5534600	14.57	80.19	5.24
SFI93041	93SFI022	426400	5534500	15.10	45.01	39.89
SFI93044	93SFI025	428000	5531200	21.99	48.17	29.84
SFI93052	93SFI026	424750	5532800	32.63	37.31	30.06

SFI93053	93SFI029	421450	5532900	22.22	48.61	29.17
SFI93057	93SFI030	413850	5532850	31.89	39.73	28.38
SFI93074	93SFI032.3	418300	5529800	33.92	38.72	27.36
SFI93074	93SFI034	418300	5529800	35.83	36.74	27.43
SFI93080	93SFI033.6	424350	5524600	10.66	29.78	59.56
SFI93085	93SFI035	406800	5526700	38.19	39.15	22.66
SFI93095	93SFI037	414100	5523200	30.91	36.33	32.75
SFI93096	93SFI038	414200	5524400	35.86	43.62	20.52
SFI93096	93SFI040	414200	5524400	40.08	40.64	19.28
SFI93110	93SFI042	411200	5521500	15.86	49.16	34.97
SFI93136	93SFI043	401100	5515800	19.06	47.34	33.60
SFI93144	93SFI045	406150	5512900	35.55	40.22	24.23
SFI93198	93SFI047	409400	5510200	14.24	78.22	7.54
SFI93199	93SFI049	407850	5510200	17.75	50.77	31.48
SFI93205	93SFI051	407800	5508600	11.06	39.36	49.58
SFI93251	93SFI053A	411000	5508500	20.62	40.97	38.41
SFI93304	93SFI055A	412680	5507800	29.14	48.24	22.61
SFI93313	93SFI056A	412700	5503700	25.11	47.89	27.00
SFI93323	93SFI057A	411800	5498500	41.27	38.30	20.43
SFI93339	93SFI058A	420750	5500200	33.09	37.57	29.34
SFI93352	93SFI059A	420900	5505100	10.69	79.78	9.53
SFI93376	93SFI061A	427250	5495200	39.80	44.25	15.95
SFI93388	93SFI062A	427150	5486900	35.12	40.35	24.52
SFI93407	93SFI063A	423300	5485250	38.85	32.89	28.26
SFI93408	93SFI064A	423500	5487200	35.84	33.60	30.55
SFI93408	93SFI065A	423500	5487200	34.65	35.69	29.66
SFI93408	93SFI066A	423500	5487200	35.82	34.87	29.31
SFI93408	93SFI067A	423500	5487200	34.68	35.72	29.60
SFI93408	93SFI068A	423500	5487200	30.73	36.64	32.63
SFI93408	93SFI069A	423500	5487200	32.33	37.42	30.25
SFI93408	93SFI080A	423500	5487200	35.47	37.68	26.84
SFI93409	93SFI070A	423300	5486850	34.31	35.88	29.81
SFI93409	93SFI071A	423300	5486850	36.46	33.33	30.20
SFI93409	93SFI072A	423300	5486850	35.54	34.75	29.71
SFI93409	93SFI073A	423300	5486850	36.30	34.11	29.59
SFI93410	93SFI074A	423400	5486900	44.11	32.82	23.07
SFI93413	93SFI075A	451100	5493000	43.30	39.33	17.37
SFI93413	93SFI076A	451100	5493000	41.99	41.36	16.65
SFI93413	93SFI077A	451100	5493000	49.39	41.92	8.69
SFI93413	93SFI078A	451100	5493000	39.40	43.28	17.31
SFI93425	93SFI081A	355700	5462000	38.02	39.44	22.54
SFI93479	93SFI082A	365450	5461750	38.74	35.52	25.74
SFI93499	93SFI083A	403750	5515200	15.19	45.74	39.06

APEXDIX IV CARBONATE ANALYSIS RESULTS.

STATIONID	SMPLNUM	EASTING	NORTHING	ATOMIC ABSORPT. TOTAL	ATOMIC ABSORPT. CAL/DO	CHITTICK ANALYSES TOTAL	CHITTICK ANALYSES CAL/DO	XRD Carb%	XRD Cal/dol	XRD Total
								Include		Exclude
BRANDON AREA								everything		Gypsum
SFI93002	93SFI001	427200	5537750	69.51	0.46	35.72	0.53	identified		Claymin
SFI93004	93SFI002	424800	5537800	52.9	0.59	25.11	0.58			and
SFI93006	93SFI004	421500	5537800	50.88	0.45	25.56	0.58			hydroma
SFI93007	93SFI006	418200	5537850	74.14	0.4	35.33	0.41			
SFI93009	93SFI008	414800	5537800	84.75	0.41	38.55	0.67			
SFI93011	93SFI010	413100	5539200			30.45	0.38	25.66	0.24	60.57
SFI93026	93SFI012	418100	5536200	53.9	0.59	34.43	0.57	28.72	0.44	56.30
SFI93030	93SFI014	424850	5536150	52.97	0.52	24.91	0.61	25.55	0.58	48.55
SFI93032	93SFI016	421400	5536300	79.61	0.44	40.88	0.42	45.58	0.22	77.13
SFI93039	93SFI018	419850	5534700	62.88	0.3	33.07	0.36	30.04	0.16	62.61
SFI93040	93SFI020	423000	5534600	77.02	0.21	36.8	0.23	34.91	0.18	72.94
SFI93041	93SFI022	426400	5534500	78.37	0.33	36.42	0.56	37.19	0.30	61.87
SFI93044	93SFI024	428000	5531200	68.22	0.25	26.42	0.34	34.34	0.32	66.72
SFI93052	93SFI026	424750	5532800	58.25	0.26	25.97	0.33	26.17	0.61	56.46
SFI93053	93SFI028	421450	5532900	77.55	0.25	35.72	0.37	50.07	0.28	52.10
SFI93057	93SFI030	413850	5532850	51.84	0.28	27.23	0.28	47.32	0.30	47.32
SFI93074	93SFI032	418300	5529800	55.36	0.5	27.12	0.59	25.89	0.44	51.59
SFI93074	93SFI034	418300	5529800	53.14	0.55	24.84	0.52	28.24	0.37	54.31
SFI93080	93SFI033.5	424350	5524600					35.08	0.33	62.59
SFI93085	93SFI034	406800	5526700	46.07	0.39	23.5	0.28	28.93	0.36	56.86
SFI93085	93SFI035	406800	5526700	79.23	0.43					
SFI93095	93SFI036	414100	5523200	82.95	0.2	58.51	0.5			
SFI93096	93SFI038	414200	5524400	63.45	0.32	30.38	0.33	23.11	0.31	42.68
SFI93096	93SFI040	414200	5524400	60.2	0.35	31.72	0.35	42.85	0.40	44.10
SFI93110	93SFI042	411200	5521500	111.52	0.23	44.21	0.57			
SFI93136	93SFI043	401100	5515800	77.69	0.23	35.85	0.35	33.80	0.23	59.39
SFI93144	93SFI045	406150	5512900	55.93	0.26	24.53	0.27	25.89	0.50	51.67
SFI93198	93SFI047	409400	5510200	61.41	0.21	25.74	0.38	33.71	0.24	54.31
SFI93199	93SFI049	407850	5510200	60.99	0.09	27.66	0.2			
SFI93205	93SFI051	407800	5508600	63.81	0.41	30.43	0.5	28.27	0.24	59.15
SFI93251	93SFI053A	411000	5508500	65.69	0.25	26.71	0.48			
SFI93266	93SFI054A	409100	5496100	68.42	0.36	30.43	0.33			
SFI93304	93SFI055A	412680	5507800	61.38	0.45	28.4	0.43			
SFI93313	93SFI056A	412700	5503700	49.52	0.4	26.06	0.48			
SFI93323	93SFI057A	411800	5498500	54.84	0.4	24.63	0.35			
SFI93339	93SFI058A	420750	5500200	79.41	0.09	42.01	0.19	31.08	0.32	34.86
SFI93352	93SFI059A	420900	5505100	62.13	0.48	24.66	0.62	31.10	0.08	73.51
SFI93376	93SFI061A	427250	5495200	53.57	0.33	23.76	0.35	23.05	0.38	42.15
SFI93388	93SFI062A	427150	5486900	71.94	0.37	33.59	0.61			
SFI93407	93SFI063A	423300	5485250	53	0.61	41.26	0.35	30.00	0.45	41.40
SFI93408	93SFI064A	423500	5487200	48.72	0.74	22.05	0.64	28.36	0.34	58.32
SFI93408	93SFI065A	423500	5487200	48.52	0.63	21.44	0.41	22.26	0.44	42.49
SFI93408	93SFI066A	423500	5487200	45.89	0.51	23.82	0.41	21.44	0.47	46.44

STATIONID	SMPLNUM	EASTING	NORTHING	ATOMIC ABSORPT.		CHITTICK ANALYSES				
				TOTAL	CAL/DO	TOTAL	CAL/DO			
SFI93408	93SFI067A	423500	5487200	47.87	0.56	26.06	0.48	18.30	0.54	45.94
SFI93408	93SFI068A	423500	5487200	46.69	0.32	19.39	0.3	22.03	0.24	48.50
SFI93408	93SFI069A	423500	5487200	29.51	0.31	17.88	0.29	15.21	0.27	34.30
SFI93408	93SFI080A	423500	5487200	52.93	0.68	20.65	0.88	27.55	0.37	52.84
SFI93409	93SFI070A	423300	5486850	39.64	0.67	22.8	0.48	23.31	0.29	52.75
SFI93409	93SFI071A	423300	5486850	44.19	0.54	23.24	0.49	24.66	0.39	53.23
SFI93409	93SFI072A	423300	5486850	43.7	0.62	21.06	0.47	18.01	0.46	29.26
SFI93409	93SFI073A	423300	5486850	44.94	0.58	21	0.4			
SFI93410	93SFI074A	423400	5486900	50.1	0.48	24.99	0.49	45.70	0.39	47.66
SFI93413	93SFI075A	451100	5493000	67.46	0.33	35.09	0.28	29.53	0.28	54.76
SFI93413	93SFI076A	451100	5493000	19.24	0.21	52.89	0.25	45.58	0.16	72.98
SFI93413	93SFI077A	451100	5493000	41.92	0.5	20.62	0.23	18.05	0.29	38.97
SFI93413	93SFI078A	451100	5493000	50.4	0.34	25.66	0.15	47.50	0.28	50.53
SFI93425	93SFI081A	355700	5462000	49.29	0.54	25.56	0.66	49.32	0.55	52.12
SFI93479	93SFI082A	365450	5461750	59.59	1.49	31.24	1.33	27.34	1.09	56.43
SFI93499	93SFI083A	403750	5515200	69.37	0.16	31.53	0.2	26.84	0.21	58.00
VIRDEN AREA										
SFI92001	92SFI001	410000	5710000	41.43	0.58	19.93	0.44			
SFI92002	92SFI002	428500	5503400	51.77	0.35	27.36	0.43			
SFI92004	92SFI004	355200	5509900	44.46	0.47	24.32	0.74			
SFI92005	92SFI005	358600	5514600	44.2	0.44	22.49	0.37			
SFI92006	92SFI006	355400	5513000	56.89	0.57	28.02	0.66			
SFI92008	92SFI008	355600	5517800	52.49	1.02	28.98	1.1			
SFI92011	92SFI011	360400	5519400	55.25	1.14	30.28	1.48			
SFI92033	92SFI033	357200	5521150	62.19	0.21	25.64	0.27			
SFI92034	92SFI034	355600	5521200	59.98	0.53	27.57	0.65			
SFI92040	92SFI040	359100	5539200	64.74	1.23	38.61	1.56			
SFI92043	92SFI043	357370	5537500	71.21	1.12	43.25		17.89	0.40	27.10
SFI92045	92SFI045	360700	5537500	65.78	1.07	32.56	1.57			
SFI92047	92SFI047	359000	5534250	56.54	0.73	28.05	1.04			
SFI92048	92SFI048	362200	5534200	52.79	0.96	32.83	1.2			
SFI92062	92SFI062	360500	5530800	57.68	0.81	24.38	0.83			
SFI92063	92SFI063	359800	5530800	47.32	0.63	24.71	0.66			
SFI92064	92SFI064	357250	5531000	48.68	0.65	24.4	0.86			
SFI92068	92SFI068	363800	5525800	45.41	0.68	21.79	0.58			
SFI92077	92SFI077A	384650	5538500	44.04	0.39	17.42	0.31			
SFI92077	92SFI077B	384650	5538500	47.29	0.74	17.84	0.3			
SFI92077	92SFI077C	384650	5538500	34.89	0.31	17.46	0.35			
SFI92077	92SFI077D	384650	5538500	35.34	0.39	16.14	0.34			
SFI92077	92SFI077E	384650	5538500	33.81	0.43	15.95	0.38			
SFI92086	92SFI086	377100	5538600	7.69	0.59	4.95	1.79			
SFI92088	92SFI088	373500	5538850			1.99	0.79			
SFI92091	92SFI091	370500	5538950	56	1.49	29.99	1.33			
SFI92094	92SFI094	367350	5538850			1.57	1.35			

STATIONID	SMPLNUM	EASTING	NORTHING	ATOMIC ABSORPT. TOTAL	ATOMIC ABSORPT. CAL/DO	CHITTICK ANALYSES TOTAL	CHITTICK ANALYSES CAL/DO			
SFI92105	92SFI105	378750	5537000	73.81	0.92	3.91	0.26			
SFI92108	92SFI108	385000	5536800	36.7	0.62	33.61	0.53	10.49	0.41	24.10
SFI92115	92SFI115	367300	5535700	38.83	0.82	30.82	0.58			
SFI92116	92SFI116	368900	5535600	27.56	0.83	16.18	0.82			
SFI92121	92SFI121	373750	5535400	27.54	0.74	19.82	1.84			
SFI92122	92SFI122	375500	5535500	20.01	0.21	14.94	0.53			
SFI92150	92SFI150	370450	5530650	5.11	0.03	9.4	1.35			
SFI92209	92SFI209	372000	5525700	40.22	1.09	30.27	3.39			
SFI92267	92SFI267	355200	5506500	59.78	1.07	27.18	1.07			
SFI92270	92SFI270	358400	5504750	53.77	0.2	24.21	0.18			
SFI92271	92SFI271	356750	5503200	43.05	0.43	20.93	0.32			
SFI92389	92SFI389A	331500	5518600	53.08	0.53	22.04	0.35			
SFI92389	92SFI389B	331500	5518600	57.89	0.82	21.37	0.33			
SFI92389	92SFI389C	331500	5518600	50.43	0.53	22.67	0.34			
SFI92389	92SFI389D	331500	5518600	53.63	0.45	22.99	0.45			
SFI92389	92SFI389E	331500	5518600	51.38	0.56	24.93	0.43			
SFI92389	92SFI389F	331500	5518600	47.68	0.57	21.94	0.49			
SFI92389	92SFI389G	331500	5518600	55.67	0.5	22.6	0.5			
SFI92389	92SFI389H	331500	5518600	45.31	0.58	25.6	0.42			
SFI92389	92SFI389I	331500	5518600	47.75	0.47	23.67	0.46			
SFI92389	92SFI389J	331500	5518600	53.2	0.61	22.66	0.92			
SFI92389	92SFI389K	331500	5518600	52.95	0.7	23.63	0.69			
SFI92389	92SFI389M	331500	5518600	66.3	0.33	24.23	0.6			
SFI92389	92SFI389N	331500	5518600	52.83	0.66	24.09	0.45			
SFI92421	92SFI421	411350	5530400	57.62	0.39	33.77	0.32			
SFI92432	92SFI432	417750	5529500	55.78	0.46	25.6	0.42			
BOISSEVAIN/TURTLE MOUNTAIN AREA										
SFI94025	94SFI003	366800	5443600	48.28	0.49	20.14	0.43			
SFI94028	94SFI004	362100	5445500	56.61	0.72	22.16	0.49			
SFI94034	94SFI005	366900	5455200	62.04	0.39	22.93	0.38			
SFI94037	94SFI006	368500	5448500	50.08	0.84	23.43	0.73			
SFI94039	94SFI007	368250	5437000	55.34	0.63	19.64	0.36			
SFI94040	94SFI008	365050	5437100	47.34	0.38	27.59	1.00			
SFI94043	94SFI009	361850	5438650	54.87	0.63	21.96	0.52			
SFI94047	94SFI010	365350	5455200	49.25	0.49	21.96	0.52			
SFI94048	94SFI011	363500	5452150	57.20	0.67	22.95	0.67			
SFI94050	94SFI012	366350	5443750	53.85	0.45	25.26	0.80			
SFI94053	94SFI013	364900	5430500	52.08	0.55	24.36	0.80			
SFI94058	94SFI014	360100	5433800	40.08	0.45	24.58	0.80			
SFI94064	94SFI015	355400	5441400	46.92	0.37	19.06	0.45			
SFI94064	94SFI016	355400	5441400	49.75	0.67	20.34	0.41			
SFI94066	94SFI017	363600	5440400	48.46	0.27	26.51	0.70			
SFI94068	94SFI018	363750	5448700	49.72	0.36	20.55	0.40			
SFI94074	94SFI019	354850	5458700	56.35	0.59	23.24	0.77			

STATIONID	SMPLNUM	EASTING	NORTHING	ATOMIC ABSORPT. TOTAL	ATOMIC ABSORPT. CAL/DO	CHITTICK ANALYSES TOTAL	CHITTICK ANALYSES CAL/DO			
SFI94077	94SFI020	369800	5430400	32.61	0.31	25.62	0.70			
SFI94082	94SFI021	387850	5433250	38.92	0.57	15.50	0.79			
SFI94086	94SFI022	389500	5431500	43.26	0.52	14.72	1.14	13.51	0.67	29.69
SFI94090	94SFI023	369950	5433650	28.73	0.3	22.87	0.91	15.85	0.51	28.69
SFI94092	94SFI024	376500	5433500	57.88	0.7	6.75	0.32	3.82	0.89	6.98
SFI94094	94SFI025	378135	5430200	48.61	0.7	21.15	0.34	19.44	0.45	32.52
SFI94099	94SFI026	384400	5431700	55.69	0.76	32.04	1.00	33.40	0.67	38.67
SFI94111	94SFI027	371700	5436750	52.23	0.73	5.21	0.75	13.03	0.61	34.00
SFI94115	94SFI028	383000	5433300	51.58	0.72			23.98	0.42	39.63
SFI94120	94SFI029	386300	5436600	57.82	0.35	21.94	0.50	16.03	0.71	20.53
SFI94121	94SFI030			55.62	0.54	25.99	0.60	17.24	0.46	27.42
SFI94125	94SFI031	420100	5482000	50.02	0.69	20.06	1.10	19.22	0.42	19.22
SFI94134	94SFI032	406800	5477500	49.76	0.53	23.34	0.59	46.82	0.30	48.00
SFI94144	94SFI033	398600	5477600	49.36	0.63	23.07	0.53	27.70	0.65	32.81
SFI94148	94SFI034	393650	5472700	47.82	0.48	26.75	0.73	19.91	0.58	31.42
SFI94153	94SFI035	401700	5470900	46.47	0.26	21.66	0.41	42.27	0.44	44.17
SFI94156	94SFI036	405150	5470700	56.39	0.93					
SFI94159	94SFI037	413200	5469000	60.41	1.26	21.07	0.51	25.06	0.38	29.30
SFI94161	94SFI038	413250	5472300	47.91	0.64	20.71	0.33	20.34	0.33	38.73
SFI94163	94SFI039	406750	5472450	49.80	0.27	20.64	0.28			
SFI94164	94SFI040	410150	5475650	64.45	1.19	31.55	1.16	37.05	0.95	43.22
SFI94165	94SFI041			55.33	0.7	24.21	0.89	36.67	0.73	36.67
SFI94169	94SFI044	391700	5456300	56.16	0.67	29.71	1.60	34.44	1.43	35.22
SFI94171	94SFI045	391850	5462850	71.26	0.76	22.20	0.55	29.52	0.29	45.81
SFI94175	94SFI046	397800	5469300	54.92	0.43	25.11	0.90			
SFI94178	94SFI047	398350	5466000	40.52	0.44	32.82	1.44			
SFI94179	94SFI048	401750	5466000	50.98	0.65	27.70	1.13			
SFI94180	94SFI049	419900	5477100	44.32	0.4	21.77	0.56	18.09	0.45	21.58
SFI94181	94SFI050	423200	5477100	44.24	0.32	20.56	0.21			
SFI94183	94SFI051	419900	5472250	44.08	0.51	19.97	0.27	36.38	0.39	37.79
SFI94188	94SFI052	418250	5469000	43.26	0.34	24.37	0.49	23.36	0.32	37.12
SFI94190	94SFI053	426300	5465600	51.05	0.48	21.65	0.42			
SFI94192	94SFI054	414850	5465700	52.86	0.6	20.91	0.33			
SFI94194	94SFI055	406600	5465900	49.52	0.43	20.60	0.48			
SFI94196	94SFI056	396600	5462800	53.10	0.51	21.91	0.46			
SFI94221	94SFI057	404900	5461900	43.67	0.78	18.29	0.36	15.39	0.69	17.72
SFI94231	94SFI058	413100	5462500	57.26	0.6	23.12	0.58	33.56	0.40	34.94
SFI94235	94SFI059	322900	5459100	61.42	0.61	25.89	0.72			
SFI94237	94SFI060	389650	439750	48.43	0.42	20.86	1.58	57.59	3.02	57.97
SFI94242	94SFI061	384800	5439850	40.11	0.36	26.30	1.02			
SFI94246	94SFI062	373300	5440200	43.66	0.43	28.89	1.26	24.36	0.80	32.29
SFI94247	94SFI063	376650	5436750	53.23	0.57	21.32	0.56	33.06	0.40	34.47
SFI94251	94SFI064	384900	5448300	50.08	0.34	18.35	0.43	37.08	0.30	38.53
SFI94254	94SFI065	376700	544330	43.76	0.53	27.70	1.13	13.66	0.55	23.60

STATIONID	SMPLNUM	EASTING	NORTHING	ATOMIC ABSORPT. TOTAL	ATOMIC ABSORPT. CAL/DO	CHITTICK ANALYSES TOTAL	CHITTICK ANALYSES CAL/DO			
SFI94263	94SFI066	381600	5448300	41.00	0.34	21.51	0.52	16.66	0.39	34.99
SFI94265	94SFI068	383400	5451600	47.58	0.65	21.56	0.32	44.82	1.95	44.82
SFI94274	94SFI069	378500	5455000	14.55	0.04	21.13	0.33	31.61	0.36	32.74
SFI94276	94SFI070	385050	5454800	46.97	0.38	20.01	0.59	21.16	0.27	37.21
SFI94283	94SFI071	385850	5464650	57.06	0.63	18.96	0.36			
SFI94283	94SFI072	385850	5464650	62.97	1.01	6.84	0.39	3.81	0.00	11.34
SFI94291	94SFI073	388700	5471100	48.97	0.67	19.87	0.41	32.60	0.59	33.27
SFI94296	94SFI074	390350	5471100	44.59	0.42	23.25	0.48	18.97	0.38	30.41
SFI94362	94SFI075			47.42	0.57	26.58	0.48	30.81	0.25	36.68
SFI94382	94SFI076			49.06	0.42	20.85	0.27	27.23	0.12	58.34
SFI94345	94SFI077	382550	5459800	46.43	0.52	19.79	0.60	13.80	0.88	30.02
SFI94347	94SFI078	390150	5462900			25.44	0.72	16.05	0.80	29.11
SFI94349	94SFI079	386750	5459700			20.66	0.30	11.90	0.41	32.55
SFI94354	94SFI080	362250	5438650			19.78	0.30	14.27	0.45	26.38
FI93004	93FI001T	356100	5539100	49.2	0.71	21.16	0.36			
FI93010	93FI002T	352500	5534400	39.41	0.62	20.79	0.44			
FI93014	93FI003T	345400	5539400	42.69	0.61					
FI93018	93FI004T	348200	5534600	46.45	0.5	21.33	0.58			
FI93024	93FI005T	339400	5540800	42.66	0.4	22.97	0.42			
FI93035	93FI006T	345900	5533100	45.3	0.47	23.24	0.47			
FI93037	93FI007T	342500	5533100	47.07	0.55	27.33	0.4			
FI93042	93FI008T	349500	5528800	41.47	0.48	21.75	0.53			
FI93043	93FI009T	354500	5526100	46.31	0.74	20.69	0.33			
FI93044	93FI010T	347200	5523500	46.98	0.58	45.24	0.52			
FI93044	93FI011T	347200	5523500	46.71	0.46					
FI93048	93FI012T	325500	5542600	49.45	0.77					
FI93049	93FI013T	354100	5523900	50.98	0.5					
FI93050	93FI014T	354100	5523900	45.77	0.4					
FI93053	93FI015T	347300	5519800	44.6	0.38	20.08	0.39			
FI93057	93FI016T	335800	5520200	63.09	0.73	37.82	1.11			
FI93059	93FI017T	324600	5522300	46.75	0.52	23.96	0.53			
FI93062	93FI018T	352900	5519700	53.4	0.58	27.06	0.8			
FI93063	93FI019T	341600	5516800	44.13	0.48	24.97	0.43			
FI93069	93FI021T	329600	5528300	47.18	0.38	23.37	0.37			
FI93070	93FI022T	321300	5520700	46.59	0.83	23.79	0.94			
FI93072	93FI023T	327600	5517700	50.68	0.33	23.35	0.35			
FI93076	93FI024T	336200	5538700	47.19	0.64	23.96	0.53			
FI93080	93FI025T	332600	5534200	50.85	0.53	24.08	0.41			
FI93082	93FI026T	329700	5539900	47.12	0.52					
FI93085	93FI027T	321000	5532800	46.24	0.81	25.87	0.7			
FI93090	93FI028T	337700	5524800	49.87	0.51	23.37	0.37			
FI93093	93FI029T	332500	5530300	44.87	0.7	23.37	0.63			
FI93095	93FI030T	323000	5526000	42.1	0.59	19.87	0.41			
FI93099	93FI031T	355550	5534300	51.34	0.6	22.75	0.41			
FI93119	93FI032T	355400	5517900	40.07	0.54	19.95	0.51			
FI93146	93FI033T	319700	5536200	78.75	0.96	35.69	1.79			
FI93146	93FI034T	319700	5536200	45.5	0.63	24.92	0.37			
FI93153	93FI035T	319800	5541200	45.77	0.55	26.24	0.6			
FI93154	93FI036T	330800	5515400	51.1	0.55	25.91	0.75			

APPENDIX V CARBONATE ANALYSIS BY CHITTICK METHOD

Sample Number	W gm	V ml.	1 st. Reading Corr. Fact.	1 st. Reading Corr ml	2nd Reading ml.	2nd Reading Corr. Fact.	2nd Reading Corr. ml	% CO2 From Calcite	%CO2 From dolomite	Calcite %	Dolomite %	Total Car-bonate	Cal/ Dolo
93SFI-02	1	57	1.03	58.7	161	1.03	165.83	54.43	111.40	12.38	23.34	35.72	0.53
93SFI-04	1	42	1.03	43.3	113	1.03	116.39	40.33	76.06	9.18	15.93	25.11	0.58
93SFI-06	1	43	1.03	44.3	115	1.03	118.45	41.32	77.13	9.40	16.16	25.56	0.58
93SFI-07	4	12	1.03	12.4	40	1.03	41.20	11.21	29.99	10.20	25.13	35.33	0.41
93SFI-09	1	70	1.03	72.1	173	1.03	178.19	67.86	110.33	15.44	23.11	38.55	0.67
93SFI-11	2	20	1.03	20.6	69	1.03	71.07	18.58	52.49	8.45	21.99	30.45	0.38
93SFI-26	1	57	1.03	58.7	155	1.03	159.65	54.67	104.98	12.44	21.99	34.43	0.57
93SFI-30	1	43	1.03	44.3	112	1.03	115.36	41.45	73.91	9.43	15.48	24.91	0.61
93SFI-32	1	57	1.03	58.7	185	1.03	190.55	53.44	137.11	12.16	28.73	40.88	0.42
93SFI-39	6	7	1.03	7.2	25	1.03	25.75	6.47	19.28	8.83	24.24	33.07	0.36
93SFI-40	1	35	1.03	36.1	168	1.03	173.04	30.57	142.47	6.95	29.85	36.80	0.23
93SFI-41	1	60	1.03	61.8	164	1.03	168.92	57.52	111.40	13.08	23.34	36.42	0.56
93SFI-44	4	8	1.03	8.2	30	1.03	30.90	7.33	23.57	6.67	19.75	26.42	0.34
93SFI-52	1	31	1.03	31.9	118	1.03	121.54	28.35	93.19	6.45	19.52	25.97	0.33
93SFI-53	1	46	1.03	47.4	162	1.03	166.86	42.60	124.26	9.69	26.03	35.72	0.37
93SFI-57	1	30	1.01	30.3	124	1.03	127.72	26.40	101.32	6.01	21.23	27.23	0.28
93SFI-74	1	47	1.01	47.5	122	1.03	125.66	44.34	81.32	10.09	17.04	27.12	0.59
93SFI-74	1	40	1.01	40.4	112	1.03	115.36	37.40	77.96	8.51	16.33	24.84	0.52
93SFI-85	1	26	1.01	26.3	107	1.03	110.21	22.90	87.31	5.21	18.29	23.50	0.28
93SFI-95	4	23	1.01	23.2	66	1.03	67.98	21.44	46.54	19.51	39.00	58.51	0.50
93SFI-96	1	37	1.01	37.4	138	1.03	142.14	33.18	108.96	7.55	22.83	30.38	0.33
93SFI-96	2	20	1.01	20.2	72	1.03	74.16	18.04	56.12	8.21	23.51	31.72	0.35
93SFI-11	1	75	1.01	75.8	199	1.03	204.97	70.58	134.39	16.06	28.15	44.21	0.57
93SFI-13	1	45	1.01	45.5	166	1.01	167.66	40.56	127.10	9.23	26.63	35.85	0.35
93SFI-14	1	26	1.01	26.3	114	1.01	115.14	22.70	92.44	5.17	19.37	24.53	0.27
93SFI-19	1	34	1.01	34.3	119	1.01	120.19	30.91	89.28	7.03	18.70	25.74	0.38
93SFI-19	1	24	1.01	24.2	129	1.01	130.29	20.00	110.29	4.55	23.11	27.66	0.20
93SFI-20	4	12	1.01	12.1	35	1.01	35.35	11.19	24.16	10.18	20.25	30.43	0.50
93SFI-25	1	41	1.01	41.4	123	1.01	124.23	38.10	86.13	8.67	18.04	26.71	0.48
93SFI-30	1	37	1.01	37.4	141	1.01	142.41	33.17	109.24	7.55	22.89	30.43	0.33
93SFI-31	1	41	1.01	41.4	131	1.01	132.31	37.77	94.54	8.59	19.81	28.40	0.43
93SFI-32	2	20	1.01	20.2	60	1.01	60.60	18.58	42.02	8.46	17.60	26.06	0.48
93SFI-33	1	31	1.01	31.3	114	1.01	115.14	27.96	87.18	6.36	18.26	24.63	0.35
93SFI-35	2	18	1.01	18.2	98	1.01	98.98	14.95	84.03	6.80	35.21	42.01	0.19
93SFI-35	1	44	1.01	44.4	113	1.01	114.13	41.65	72.48	9.48	15.18	24.66	0.62
93SFI-37	1	30	1.01	30.3	110	1.01	111.10	27.07	84.03	6.16	17.60	23.76	0.35
93SFI-38	1	59	1.01	59.6	154	1.01	155.54	55.75	99.79	12.68	20.91	33.59	0.61
93SFI-40	1	52	1.01	52.5	191	1.01	192.91	46.90	146.01	10.67	30.59	41.26	0.35
93SFI-40	1	40	1.01	40.4	101	1.01	102.01	37.94	64.07	8.63	13.42	22.05	0.64
93SFI-40	1	30	1.01	30.3	99	1.01	99.99	27.51	72.48	6.26	15.18	21.44	0.41
93SFI-40	1	33	1.01	33.3	110	1.01	111.10	30.22	80.88	6.87	16.94	23.82	0.41
93SFI-40	4	10	1.01	10.1	30	1.01	30.30	9.29	21.01	8.46	17.60	26.06	0.48

93SFI-40	1	22	1.01	22.2	90	1.01	90.90	19.47	71.43	4.43	14.96	19.39	0.30
93SFI-40	1	20	1.01	20.2	83	1.01	83.83	17.65	66.18	4.02	13.86	17.88	0.29
93SFI-40	1	35	1.01	35.4	105	1.01	106.05	32.52	73.53	7.40	15.40	22.80	0.48
93SFI-40	1	36	1.01	36.4	107	1.01	108.07	33.49	74.58	7.62	15.62	23.24	0.49
93SFI-40	1	32	1.01	32.3	97	1.01	97.97	29.69	68.28	6.76	14.30	21.06	0.47
93SFI-40	1	29	1.01	29.3	97	1.01	97.97	26.54	71.43	6.04	14.96	21.00	0.40
93SFI-41	1	39	1.01	39.4	115	1.01	116.15	36.32	79.83	8.26	16.72	24.99	0.49
93SFI-41	1	38	1.01	38.4	163	1.01	164.63	33.33	131.30	7.58	27.51	35.09	0.28
93SFI-41	2	27	1.01	27.3	123	1.01	124.23	23.39	100.84	10.64	42.25	52.89	0.25
93SFI-41	1	20	1.01	20.2	96	1.01	96.96	17.13	79.83	3.90	16.72	20.62	0.23
93SFI-41	1	19	1.01	19.2	120	1.01	121.20	15.11	106.09	3.44	22.23	25.66	0.15
93SFI-40	1	44	1.01	44.4	94	1.01	94.94	42.42	52.52	9.65	11.00	20.65	0.88
93SFI-42	1	47	1.01	47.5	117	1.01	118.17	44.64	73.53	10.16	15.40	25.56	0.66
93SFI-42	1	80	1.01	80.8	141	1.01	142.41	78.34	64.07	17.82	13.42	31.24	1.33
93SFI-49	1	28	1.01	28.3	147	1.01	148.47	23.47	125.00	5.34	26.19	31.53	0.20
SFI-1	1	29	1.01	29.3	91	1.02	92.82	26.75	66.07	6.09	13.84	19.93	0.44
SFI-2	1	39	1.01	39.4	125	1.02	127.50	35.87	91.63	8.16	19.20	27.36	0.43
SFI-4	1	47	1.02	47.9	110	1.02	112.20	45.37	66.83	10.32	14.00	24.32	0.74
SFI-5	1	29	1.02	29.6	103	1.02	105.06	26.56	78.50	6.04	16.45	22.49	0.37
SFI-6	1	51	1.02	52.0	127	1.02	129.54	48.92	80.62	11.13	16.89	28.02	0.66
SFI-8	1	68	1.02	69.4	130	1.02	132.60	66.83	65.77	15.20	13.78	28.98	1.10
SFI-11	1	80	1.02	81.6	135	1.02	137.70	79.36	58.34	18.05	12.22	30.28	1.48
SFI-33	1	27	1.02	27.5	118	1.02	120.36	23.83	96.53	5.42	20.22	25.64	0.27
SFI-34	1	50	1.02	51.0	125	1.02	127.50	47.94	79.56	10.91	16.67	27.57	0.65
SFI-40	4	26	1.02	26.5	43	1.02	43.86	25.83	18.03	23.50	15.11	38.61	1.56
SFI-43	1	146	1.02	148.9	190	1.02	193.80	147.12	46.68	33.47	9.78	43.25	3.42
SFI-45	1	88	1.02	89.8	145	1.02	147.90	87.43	60.47	19.89	12.67	32.56	1.57
SFI-47	1	64	1.02	65.3	126	1.02	128.52	62.75	65.77	14.28	13.78	28.05	1.04
SFI-48	1	80	1.02	81.6	147	1.02	149.94	78.87	71.07	17.94	14.89	32.83	1.20
SFI-62	1	50	1.02	51.0	110	1.02	112.20	48.55	63.65	11.05	13.33	24.38	0.83
SFI-63	1	45	1.02	45.9	112	1.02	114.24	43.17	71.07	9.82	14.89	24.71	0.66
SFI-64	1	51	1.02	52.0	110	1.02	112.20	49.61	62.59	11.29	13.11	24.40	0.86
SFI-69	1	37	1.02	37.7	99	1.02	100.98	35.21	65.77	8.01	13.78	21.79	0.58
SFI-77-1	1	20	1.02	20.4	80	1.02	81.60	17.95	63.65	4.08	13.33	17.42	0.31
SFI-77-2	1	20	1.02	20.4	82	1.02	83.64	17.87	65.77	4.07	13.78	17.84	0.30
SFI-77-3	2	11	1.02	11.2	40	1.02	40.80	10.04	30.76	4.57	12.89	17.46	0.35
SFI-77-4	1	20	1.02	20.4	74	1.02	75.48	18.20	57.28	4.14	12.00	16.14	0.34
SFI-77	1	21	1.02	21.4	73	1.02	74.46	19.30	55.16	4.39	11.56	15.95	0.38
SFI-86	1	14	1.02	14.3	22	1.02	22.44	13.95	8.49	3.17	1.78	4.95	1.79
SFI-88	1	4	1.02	4.1	9	1.02	9.18	3.88	5.30	0.88	1.11	1.99	0.79
SFI-91	1	76	1.02	77.5	134	1.02	136.68	75.15	61.53	17.10	12.89	29.99	1.33
SFI-94	1	4	1.02	4.1	7	1.02	7.14	3.96	3.18	0.90	0.67	1.57	1.35
SFI-105	1	4	1.02	4.1	18	1.02	18.36	3.51	14.85	0.80	3.11	3.91	0.26
SFI-104	1	54	1.02	55.1	153	1.02	156.06	51.04	105.02	11.61	22.00	33.61	0.53
SFI-108	1	21	1.02	21.4	76	1.02	77.52	19.18	58.34	4.36	12.22	16.59	0.36
SFI-115	4	13	1.03	13.4	35	1.02	35.70	12.50	23.20	11.37	19.44	30.82	0.58
SFI-116	1	33	1.02	33.7	73	1.02	74.46	32.03	42.43	7.29	8.89	16.18	0.82
SFI-121	4	14	1.03	14.4	22	1.02	22.44	14.10	8.34	12.83	6.99	19.82	1.84

SFI-122	4	6	1.02	6.1	17	1.02	17.34	5.67	11.67	5.16	9.78	14.94	0.53
SFI-150	6	4	1.02	4.1	7	1.02	7.14	3.96	3.18	5.40	4.00	9.40	1.35
SFI-209	1	102	1.02	104.0	133	1.02	135.66	102.78	32.88	23.38	6.89	30.27	3.39
SFI-267	1	63	1.02	64.3	122	1.02	124.44	61.85	62.59	14.07	13.11	27.18	1.07
SFI-271	1	20	1.01	20.2	113	1.01	114.13	16.44	97.69	3.74	20.47	24.21	0.18
SFI-271	1	25	1.01	25.3	97	1.01	97.97	22.34	75.63	5.08	15.84	20.93	0.32
SFI-389A	1	28	1.01	28.3	102	1.01	103.02	25.29	77.73	5.75	16.28	22.04	0.35
SFI-389B	1	26	1.01	26.3	99	1.01	99.99	23.31	76.68	5.30	16.06	21.37	0.33
SFI-389C	1	28	1.01	28.3	105	1.01	106.05	25.17	80.88	5.73	16.94	22.67	0.34
SFI-389D	1	34	1.01	34.3	106	1.01	107.06	31.43	75.63	7.15	15.84	22.99	0.45
SFI-389E	1	36	1.01	36.4	115	1.01	116.15	33.17	82.98	7.55	17.38	24.93	0.43
SFI-389F	1	34	1.01	34.3	101	1.01	102.01	31.63	70.38	7.20	14.74	21.94	0.49
SFI-389G	1	35	1.02	35.7	103	1.02	105.06	32.93	72.13	7.49	15.11	22.60	0.50
SFI-389H	1	36	1.02	36.7	117	1.02	119.34	33.42	85.92	7.60	18.00	25.60	0.42
SFI-389I	1	35	1.02	35.7	108	1.02	110.16	32.72	77.44	7.44	16.22	23.67	0.46
SFI-389J	1	49	1.02	50.0	102	1.02	104.04	47.82	56.22	10.88	11.78	22.66	0.92
SFI-389K	1	44	1.02	44.9	107	1.02	109.14	42.31	66.83	9.63	14.00	23.63	0.69
SFI-389M	1	42	1.02	42.8	110	1.02	112.20	40.07	72.13	9.11	15.11	24.23	0.60
SFI-389N	1	35	1.02	35.7	110	1.02	112.20	32.64	79.56	7.43	16.67	24.09	0.45
SFI-421	1	40	1.02	40.8	155	1.02	158.10	36.11	121.99	8.21	25.56	33.77	0.32
SFI-437	1	36	1.02	36.7	117	1.02	119.34	33.42	85.92	7.60	18.00	25.60	0.42
SFI-93-4	1	44	1.01	44.4	123	1.01	124.23	41.25	82.98	9.38	17.38	26.77	0.54
SFI-93-2	1	30	1.02	30.6	85	1.02	86.70	28.36	58.34	6.45	12.22	18.67	0.53
SFI-93-8	4	12	1.02	12.2	50	1.02	51.00	10.69	40.31	9.73	33.78	43.51	0.29
SFI-93-3	6	12	1.01	12.1	29	1.01	29.29	11.43	17.86	15.61	22.45	38.05	0.70

APPENDIX VI CARBONATE ANALYSIS BY ATOMIC ABSORPTION

1 %Ca BY AA
2 %Mg BY AA
3 Wt% DOLOMITE=COL.2.5852
4 Wt% CALCITE=(COL.1COL.2*1.6486)) *2.4973
5 TOTAL Wt% CO3 (COL+COL.4)
6 WT%DOLOMITE/Wt% CAITE (COL.3/COL .4)
7 CO2 FROM CALCITE=C.4*2.238
8 CO2 FROM DOLOMITE=L.3*2.429
9 TOTAL CO2=COL.7+CO8

	%Ca	%Mg	WT%DO	WT%CAL	CO3TOT	DO/CAL	CO2CAL	CO2DOL	CO2TOT
94SF-100 1	5.94	1.76	13.35	7.59	20.94	1.76	16.98	32.43	49.41
94SF-100 2	5.95	1.70	12.89	7.86	20.75	1.64	17.59	31.32	48.91
94SF-100 3	6.19	2.48	18.81	5.25	24.06	3.58	11.75	45.69	57.44
94SF-100 4	5.64	1.82	13.81	6.59	20.40	2.09	14.75	33.53	48.28
94SF-100 5	7.08	1.85	14.03	10.06	24.10	1.39	22.52	34.09	56.61
94SF-100 6	7.03	2.47	18.74	7.39	26.12	2.54	16.53	45.51	62.04
94SF-100 7	6.44	1.53	11.61	9.78	21.39	1.19	21.90	28.19	50.08
94SF-100 8	6.77	1.90	14.41	9.08	23.50	1.59	20.33	35.01	55.34
94SF-100 9	5.34	1.90	14.41	5.51	19.93	2.61	12.34	35.01	47.34
94SF-100 10	6.72	1.88	14.26	9.04	23.30	1.58	20.24	34.64	54.87
94SF-100 11	5.78	1.84	13.96	6.86	20.82	2.03	15.35	33.90	49.25
94SF-100 12	7.07	1.92	14.56	9.75	24.31	1.49	21.82	35.37	57.20
94SF-100 13	6.24	2.06	15.63	7.10	22.73	2.20	15.89	37.95	53.85
94SF-100 14	6.22	1.88	14.26	7.79	22.05	1.83	17.44	34.64	52.08
94SF-100 15	4.65	1.53	11.61	5.31	16.92	2.18	11.89	28.19	40.08
94SF-100 16	5.28	1.89	14.34	5.40	19.74	2.65	12.10	34.82	46.92
94SF-100 17	6.15	1.67	12.67	8.48	21.15	1.49	18.98	30.77	49.75
94SF-100 18	5.21	2.10	15.93	4.37	20.29	3.65	9.77	38.69	48.46
94SF-100 19	5.55	2.03	15.40	5.50	20.90	2.80	12.31	37.40	49.72
94SF-100 20	6.82	1.98	15.02	8.88	23.90	1.69	19.87	36.48	56.35
94SF-100 21	3.56	1.38	10.47	3.21	13.68	3.26	7.18	25.43	32.61
94SF-100 22	4.69	1.38	10.47	6.03	16.50	1.74	13.50	25.43	38.92
94SF-100 23	5.12	1.59	12.06	6.24	18.30	1.93	13.97	29.29	43.26
94SF-100 24	3.13	1.22	9.25	2.79	12.05	3.31	6.25	22.48	28.73
94SF-100 29	5.55	1.65	12.52	7.07	19.58	1.77	15.82	30.40	46.22
94SF-100 30	6.73	2.20	16.69	7.75	24.44	2.15	17.34	40.53	57.88
94SF-100 31	6.06	1.60	12.14	8.55	20.68	1.42	19.13	29.48	48.61
94SF-100 32	7.03	1.78	13.50	10.23	23.73	1.32	22.89	32.80	55.69
94SF-100 33	6.56	1.69	12.82	9.42	22.24	1.36	21.09	31.14	52.23
94SF-100 34A	6.46	1.68	12.74	9.22	21.96	1.38	20.63	30.95	51.58
94SF-100 34B	6.44	2.37	17.98	6.33	24.30	2.84	14.16	43.67	57.82
94SF-100 35	6.64	2.01	15.25	8.31	23.55	1.84	18.59	37.03	55.62
94SF-100 36A	6.23	1.65	12.52	8.77	21.28	1.43	19.62	30.40	50.02
94SF-100 36B	5.92	1.81	13.73	7.33	21.06	1.87	16.41	33.35	49.76
94SF-100 37	6.03	1.70	12.89	8.06	20.95	1.60	18.04	31.32	49.36
94SF-100 38	5.59	1.80	13.65	6.55	20.20	2.08	14.66	33.16	47.82
94SF-100 39	4.97	2.03	15.40	4.05	19.45	3.80	9.07	37.40	46.47
94SF-100 40	7.37	1.65	12.52	11.61	24.13	1.08	25.99	30.40	56.39
94SF-100 41	8.32	1.51	11.45	14.56	26.01	0.79	32.59	27.82	60.41

94SF-100 42	5.87	1.64	12.44	7.91	20.35	1.57	17.70	30.22	47.91
94SF-100 43	5.35	2.16	16.38	4.47	20.85	3.67	10.00	39.80	49.80
94SF-100 44	8.78	1.67	12.67	15.05	27.72	0.84	33.68	30.77	64.45
94SF-100 45	6.90	1.82	13.81	9.74	23.54	1.42	21.79	33.53	55.33
94SF-100 46	6.95	1.88	14.26	9.62	23.88	1.48	21.52	34.64	56.16
94SF-100 47	9.01	2.27	17.22	13.15	30.37	1.31	29.44	41.82	71.26
94SF-100 48	6.30	2.14	16.23	6.92	23.15	2.34	15.49	39.43	54.92
94SF-100 49	4.68	1.56	11.83	5.26	17.10	2.25	11.78	28.74	40.52
94SF-100 50	6.27	1.73	13.12	8.54	21.66	1.54	19.10	31.87	50.98
94SF-100 51	5.03	1.76	13.35	5.32	18.67	2.51	11.90	32.43	44.32
94SF-100 52	4.85	1.86	14.11	4.45	18.56	3.17	9.97	34.27	44.24
94SF-100 53	5.20	1.63	12.36	6.28	18.64	1.97	14.04	30.03	44.08
94SF-100 54	4.79	1.79	13.58	4.59	18.17	2.96	10.28	32.98	43.26
94SF-100 56	5.97	1.92	14.56	7.00	21.57	2.08	15.68	35.37	51.05
94SF-100 57	6.41	1.85	14.03	8.39	22.42	1.67	18.78	34.09	52.86
94SF-100 58	5.68	1.93	14.64	6.24	20.88	2.35	13.96	35.56	49.52
94SF-100 59	6.27	1.96	14.87	7.59	22.46	1.96	16.98	36.11	53.10
94SF-100 60	5.54	1.38	10.47	8.15	18.62	1.28	18.25	25.43	43.67
94SF-100 61	6.95	2.00	15.17	9.12	24.29	1.66	20.42	36.85	57.26
94SF-100 62	7.48	2.13	16.16	9.91	26.07	1.63	22.18	39.24	61.42
94SF-100 63	5.55	1.89	14.34	6.08	20.41	2.36	13.60	34.82	48.43
94SF-100 64	4.49	1.63	12.36	4.50	16.87	2.75	10.08	30.03	40.11
94SF-100 65	5.01	1.70	12.89	5.51	18.41	2.34	12.34	31.32	43.66
94SF-100 66	6.41	1.89	14.34	8.23	22.56	1.74	18.41	34.82	53.23
94SF-100 68	5.55	2.07	15.70	5.34	21.04	2.94	11.95	38.14	50.08
94SF-100 69	5.21	1.59	12.06	6.46	18.53	1.87	14.47	29.29	43.76
94SF-100 70	4.55	1.69	12.82	4.40	17.22	2.91	9.86	31.14	41.00
94SF-100 71	5.86	1.61	12.21	8.01	20.22	1.53	17.92	29.66	47.58
94SF-100 72	1.35	0.76	5.76	0.24	6.01	23.78	0.54	14.00	14.55
94SF-100 73	5.29	1.89	14.34	5.43	19.77	2.64	12.15	34.82	46.97
94SF-100 74	6.98	1.96	14.87	9.36	24.23	1.59	20.95	36.11	57.06
94SF-100 75	8.35	1.77	13.43	13.57	26.99	0.99	30.36	32.61	62.97
94SF-100 76	6.06	1.64	12.44	8.38	20.82	1.48	18.76	30.22	48.97
94SF-100 77	5.11	1.74	13.20	5.60	18.80	2.36	12.53	32.06	44.59
94SF-100 78	5.70	1.69	12.82	7.28	20.10	1.76	16.29	31.14	47.42
94SF-100 79	5.63	1.91	14.49	6.20	20.68	2.34	13.87	35.19	49.06
94SF-100 80	5.49	1.71	12.97	6.67	19.64	1.94	14.93	31.51	46.43

BRANDON AREA									
SFI930001	8.0	2.65	20.10	2.17	0.00	9.24	20.69	48.82	69.51
SFI930002	6.4	1.86	14.11	1.6	0.00	8.33	18.63	34.27	52.90
SFI930004	5.89	1.95	14.79	2.21	0.00	6.68	14.95	35.93	50.88
SFI930006	8.42	2.94	22.30	2.50	0.00	8.92	19.97	54.17	74.14
SFI930008	9.66	3.34	25.33	2.44	0.00	10.37	23.21	61.54	84.75
SFI930010	7.24	2.16	16.38	1.78	0.00	9.19	20.56	39.80	60.36
SFI930026	6.48	1.92	14.56	1.76	0.00	8.28	18.53	35.3	53.90
SFI930030	6.2	1.94	14.72	1.91	0.00	7.70	17.22	35.74	52.97
SFI930032	8.6	3.37	25.56	3.27	0.00	7.83	17.52	62.09	79.61
SFI930039	6.8	2.67	20.25	3.31	0.00	6.11	13.68	49.19	62.88
SFI930040	8.0	3.49	26.47	4.66	0.00	5.68	12.72	64.30	77.02
SFI930041	8.6	3.26	24.73	3.02	0.00	8.18	18.31	60.06	78.37

SFI930044	7.2	3.02	22.91	4.07	0.00	5.62	12.58	55.64	68.22
SFI930052	6.2	2.55	19.34	3.84	0.00	5.03	11.27	46.98	58.25
SFI930053	8.2	3.42	25.94	3.99	0.00	6.50	14.54	63.01	77.55
SFI930057	5.6	2.23	16.91	3.52	0.00	4.80	10.75	41.09	51.84
SFI930074	6.5	2.06	15.63	2.01	0.00	7.78	17.40	37.95	55.36
SFI930074	6.3	1.91	14.49	1.81	0.00	8.02	17.95	35.19	53.14
SFI930080	9.1	3.08	23.36	2.33	0.00	10.04	22.48	56.75	79.23
SFI930085	5.2	1.84	13.96	2.57	0.00	5.44	12.16	33.90	46.07
SFI930095	8.5	3.80	28.82	4.99	0.00	5.78	12.94	70.01	82.95
SFI930096	6.9	2.66	20.18	3.13	0.00	6.45	14.45	49.01	63.45
SFI930096	6.7	2.47	18.74	2.85	0.00	6.56	14.69	45.51	60.20
SFI930110	11.7	4.99	37.85	4.33	0.00	8.75	19.58	91.94	111.52
SFI930136	8.1	3.49	26.47	4.42	0.00	5.98	13.39	64.30	77.69
SFI930144	5.9	2.45	18.58	3.85	0.00	4.82	10.79	45.14	55.93
SFI930198	6.3	2.79	21.16	4.73	0.00	4.47	10.01	51.40	61.41
SFI930199	5.8	3.06	23.21	11.26	0.00	2.06	4.61	56.38	60.99
SFI930205	7.2	2.51	19.04	2.43	0.00	7.85	17.56	46.25	63.81
SFI930251	6.99	2.89	21.92	3.94	0.00	5.56	12.44	53.25	65.69
SFI930304	7.66	2.78	21.09	2.74	0.00	7.68	17.20	51.22	68.42
SFI930313	7.11	2.35	17.83	2.21	0.00	8.08	18.08	43.30	61.38
SFI930323	5.63	1.96	14.87	2.48	0.00	5.99	13.41	36.11	49.52
SFI930339	6.22	2.18	16.54	2.52	0.00	6.56	14.68	40.17	54.84
SFI930352	7.65	3.98	30.19	11.11	0.0	2.7	6.08	73.33	79.41
SFI930354	7.26	2.34	17.75	2.09	0.00	8.50	19.02	43.11	62.13
SFI930376	5.91	2.23	16.91	3.03	0.00	5.58	12.48	41.09	53.57
SFI930388	8.06	2.92	22.15	2.73	0.00	8.11	18.14	53.80	71.94
SFI930407	6.45	1.84	13.96	1.64	0.00	8.53	19.10	33.90	53.00
SFI930408A	6.13	1.57	11.91	1.35	0.00	8.84	19.79	28.93	48.72
SFI930408B	5.93	1.67	12.67	1.60	0.00	7.93	17.76	30.77	48.52
SFI930408C	5.41	1.70	12.89	1.98	0.00	6.51	14.57	31.32	45.89
SFI930408D	5.73	1.72	13.05	1.80	0.00	7.23	16.18	31.69	47.87
SFI930408E	5.14	1.95	14.79	3.08	0.00	4.81	10.76	35.93	46.69
SFI930408F	3.22	1.25	9.48	3.28	0.00	2.89	6.48	23.03	29.51
SFI930408G	6.57	1.76	13.35	1.46	0.00	9.16	20.50	32.43	52.93
SFI930409A	4.90	1.33	10.09	1.49	0.00	6.76	15.13	24.50	39.64
SFI930409B	5.27	1.60	12.14	1.85	0.00	6.57	14.71	29.48	44.19
SFI930409C	5.33	1.51	11.45	1.61	0.00	7.09	15.88	27.82	43.70
SFI930409D	5.42	1.59	12.06	1.73	0.00	6.99	15.64	29.29	44.94
SFI930410E	5.85	1.89	14.34	2.10	0.00	6.83	15.28	34.82	50.10
SFI930413A	7.44	2.81	21.31	3.04	0.00	7.01	15.69	51.77	67.46
SFI930413B	12.37	5.44	41.26	4.86	0.00	8.49	19.01	100.23	119.24
SFI930413C	4.93	1.56	11.83	2.01	0.00	5.89	13.18	28.74	41.92
SFI930413D	5.59	2.08	15.78	2.92	0.00	5.40	12.08	38.32	50.40
SFI930425	5.87	1.79	13.58	1.86	0.00	7.29	16.31	32.98	49.29
SFI930429	8.42	1.36	10.32	0.67	0.00	15.43	34.53	25.06	59.59
SFI930499	6.99	3.29	24.96	6.38	0.00	3.91	8.75	60.62	69.37

VIRDEN AREA

		%Mg	WT%DO	DO/CAL		WT	CO2CAL	CO2DOL	CO2TOT
SF1920001	4.9	1.45	11.00	1.71	0.00	6.44	14.42	26.72	41.13
SF1920002	5.7	2.12	16.08	2.83	0.00	5.68	12.71	39.06	51.77

SF1920004	5.1	1.69	12.82	2.15	0.00	5.95	13.32	31.14	44.46
SF1920005	5.0	1.71	12.97	2.29	0.00	5.67	12.69	31.51	44.20
SF1920006	6.8	2.02	15.32	1.74	0.00	8.79	19.67	37.22	56.89
SF1920008	6.9	1.47	11.15	0.98	0.00	11.35	25.41	27.08	52.49
SF1920011	7.48	1.46	11.07	0.87	0.00	12.6	28.35	26.90	55.25
SF1920033	6.48	2.82	21.39	4.68	0.00	4.57	10.23	51.96	62.19
SF1920034	7.14	2.18	16.54	1.87	0.00	8.86	19.82	40.17	59.98
SF1920040	8.88	1.64	12.44	0.81	0.00	15.42	34.52	30.22	64.74
SF1920043	9.61	1.90	14.41	0.89	0.00	16.18	36.20	35.01	71.21
SF1920045	8.82	1.79	13.58	0.93	0.00	14.66	32.80	32.98	65.78
SF1920047	7.10	1.83	13.88	1.36	0.00	10.20	22.82	33.72	56.54
SF1920048	6.94	1.52	11.53	1.04	0.00	11.07	24.78	28.01	52.79
SF1920062	7.37	1.79	13.58	1.23	0.00	11.04	24.70	32.98	57.68
SF1920063	5.78	1.63	12.36	1.60	0.00	7.72	17.29	30.03	47.32
SF1920064	5.99	1.65	12.52	1.53	0.00	8.17	18.27	30.40	48.68
SF1920069	5.62	1.52	11.53	1.48	0.00	7.78	17.40	28.01	45.41
SF1920077	3.89	1.31	9.94	2.3	0.00	4.32	9.67	24.14	33.81
SF1920077-1	4.98	1.76	13.35	2.57	0.00	5.19	11.62	32.43	44.04
SF1920077-2	5.9	1.53	11.61	1.36	0.00	8.53	19.10	28.19	47.29
SF1920077-3	3.8	1.47	11.15	3.20	0.00	3.49	7.8	27.08	34.8
SF1920077-4	4.0	1.41	10.70	2.56	0.00	4.18	9.31	25.98	35.3
SF1920086	0.93	0.27	2.05	1.7	0.00	1.21	2.71	4.97	7.68
SF1920088	0.17	0.37	2.81	-2.55	0.00	-1.10	-2.46	6.82	4.36
SF1920091	7.91	1.28	9.71	0.67	0.00	14.48	32.41	23.58	56.00
SF1920094	0.34	0.23	1.74	-17.83	0.00	-0.10	-0.22	4.24	4.02
SF1920104	9.63	2.17	16.46	1.09	0.00	15.12	33.83	39.98	73.81
SF1920105	0.35	0.21	1.59	1.68	0.00	0.01	0.02	3.87	3.89
SF1920108	4.49	1.26	9.56	1.59	0.00	6.03	13.48	23.21	36.70
SF1920115	4.97	1.20	9.10	1.22	0.00	7.47	16.72	22.11	38.83
SF1920116	3.53	0.85	6.45	1.21	0.00	5.32	11.90	15.66	27.56
SF1920121	3.46	0.89	6.75	1.36	0.00	4.98	11.14	16.40	27.54
SF1920122	2.08	0.91	6.90	4.77	0.00	1.45	3.24	16.77	20.01
SF1920150	0.47	0.27	2.05	32.96	0.00	0.06	0.14	4.97	5.11
SF1920209	5.40	1.09	8.2	0.92	0.00	9.00	20.14	20.08	40.22
SF1920267	8.01	1.63	12.36	0.93	0.00	13.29	29.75	30.03	59.72
SF1920270	5.55	2.47	18.74	5.08	0.00	3.69	8.26	45.51	53.77
SF1920271	4.95	1.67	12.67	2.31	0.00	5.49	12.28	30.77	43.05
SF1920389A	6.30	1.94	14.72	1.90	0.00	7.75	17.34	35.74	53.08
SF1920389B	7.02	1.70	12.89	1.22	0.00	10.53	23.57	31.32	54.89
SF1920389C	5.99	1.84	13.96	1.89	0.00	7.38	16.52	33.90	50.43
SF1920389D	6.20	2.0	15.63	2.23	0.00	7.00	15.67	37.95	53.63
SF1920389E	6.16	1.84	13.96	1.79	0.00	7.81	17.47	33.90	51.38
SF1920389F	5.73	1.70	12.89	1.76	0.00	7.31	16.36	31.32	47.68
SF1920389G	6.55	2.07	15.70	2.00	0.00	7.84	17.53	38.14	55.67
SF1920389H	5.47	1.60	12.14	1.72	0.00	7.07	15.83	29.48	45.31
SF1920389I	5.56	1.81	13.73	2.13	0.00	6.43	14.40	33.35	47.75
SF1920389J	6.47	1.85	14.03	1.64	0.00	8.54	19.11	34.09	53.20
SF1920389K	6.59	1.75	13.27	1.43	0.00	9.25	20.71	32.24	52.95
SF1920389M	7.33	2.75	20.86	2.99	0.00	6.98	15.63	50.67	66.30
SF1920389N	6.52	1.78	13.50	1.51	0.00	8.95	20.04	32.80	52.83
SF1920421	6.5	2.30	17.45	2.56	0.00	6.81	15.25	42.38	57.62
SF1920432	6.4	2.13	16.16	2.19	0.00	7.39	16.53	39.24	55.78

APPENDIX VII XRD ANALYSIS ON SELECTED TILL SAMPLES

SITE SAMPLE	QUARTZ %	K-SPAR %	PLAG %	CALC %	DOLO %	TOTAL Clay	GYPSUM %	HYDRO-Mag. %	Total Carb.	Calc/ Dolo.
T11R20NE7	37.38	10.14	15.07	9.87	24.67	0.00	0.00	2.87	34.55	0.40
925fi143	27.93	7.39	12.81	5.09	12.80	30.40	0.00	3.58	17.89	0.40
94382.76	12.18	2.84	4.43	2.92	24.31	0.00	51.63	1.69	27.23	0.12
94362.75	31.26	6.48	15.43	6.13	24.68	0.00	13.44	2.58	30.81	0.25
94354.80	18.80	11.40	9.64	4.45	9.83	0.00	44.51	1.38	14.27	0.45
94349.79	13.04	2.98	8.63	3.48	8.42	0.00	63.45	0.00	11.90	0.41
94347.78	18.39	7.22	13.46	7.12	8.92	28.52	14.69	1.67	16.05	0.80
94345.77	16.98	4.36	10.83	6.46	7.34	51.88	0.00	2.15	13.80	0.88
94296.74	24.51	6.23	12.67	5.25	13.72	29.06	8.56	0.00	18.97	0.38
94291.73	43.45	7.58	14.36	12.16	20.44	0.00	0.00	2.01	32.60	0.59
94283.72	18.11	4.62	7.03	0.00	3.81	64.50	0.00	1.94	3.81	0.00
94276.70	19.35	4.56	11.79	4.52	16.63	40.70	0.00	2.45	21.16	0.27
94274.69	40.86	7.06	17.01	8.44	23.17	0.00	0.00	3.45	31.61	0.36
94265.68	31.61	9.09	14.48	29.60	15.22	0.00	0.00	0.00	44.82	1.95
94263.66	18.43	4.43	8.09	4.67	11.99	35.43	14.88	2.07	16.66	0.39
94254.65	27.91	6.21	10.10	4.86	8.79	32.48	8.24	1.40	13.66	0.55
94251.64	34.60	9.12	15.43	8.64	28.44	0.00	0.00	3.76	37.08	0.30
94247.63	36.45	8.24	18.17	9.37	23.69	0.00	0.00	4.09	33.06	0.40
94246.62	31.32	6.42	13.33	10.86	13.49	0.00	21.28	3.29	24.36	0.80
94237.60	20.23	10.68	11.12	43.56	14.41	0.00	0.00	0.00	57.97	3.02
94231.58	34.71	8.75	19.04	9.63	23.94	0.00	0.00	3.94	33.56	0.40
94221.57	23.28	33.02	15.13	6.28	9.11	0.00	13.17	0.00	15.39	0.69
94201.43	40.54	8.54	17.04	8.28	23.03	0.00	0.00	2.56	31.31	0.36
94188.52	23.52	8.51	7.55	5.68	17.68	37.06	0.00	0.00	23.36	0.32
94183.51	30.27	8.21	21.42	10.22	26.17	0.00	0.00	3.71	36.38	0.39
94180.49	20.01	8.74	37.00	5.63	12.46	0.00	13.66	2.50	18.09	0.45
94171.45	17.37	5.92	11.63	6.61	22.92	32.97	0.00	2.58	29.52	0.29
94169.44	18.52	6.78	38.04	20.28	14.16	0.00	0.00	2.21	34.44	1.43
94165.41	33.20	6.13	24.01	15.52	21.14	0.00	0.00	0.00	36.67	0.73
94164.40	27.36	8.88	12.44	18.04	19.01	0.00	14.27	0.00	37.05	0.95
94161.38	18.27	7.03	6.87	5.08	15.25	0.00	45.48	2.01	20.34	0.33
94159.37	31.11	6.56	22.81	6.88	18.19	0.00	11.37	3.09	25.06	0.38
94153.35	37.15	0.00	16.28	12.95	29.31	0.00	0.00	4.30	42.27	0.44
94148.34	27.12	6.10	10.24	7.34	12.57	34.88	0.00	1.76	19.91	0.58
94144.33	32.46	6.45	17.81	10.92	16.77	0.00	12.70	2.89	27.70	0.65
94134.32	27.61	12.01	11.10	10.92	35.90	0.00	0.00	2.45	46.82	0.30
94125.31	41.76	22.40	16.62	5.66	13.56	0.00	0.00	0.00	19.22	0.42
94121.30	19.80	10.00	15.82	5.45	11.79	37.14	0.00	0.00	17.24	0.46
94120.29	37.46	7.19	17.37	6.64	9.39	0.00	19.26	2.69	16.03	0.71
94115.28	18.08	5.10	13.35	7.12	16.86	0.00	37.89	1.61	23.98	0.42
94111.27	14.46	4.67	6.17	4.92	8.11	0.00	60.06	1.61	13.03	0.61
94102.27	24.96	5.18	37.56	5.84	11.83	0.00	14.64	0.00	17.67	0.49
94099.26	25.63	6.55	20.81	13.46	19.94	0.00	13.61	0.00	33.40	0.67
94094.25	27.04	0.00	13.29	6.06	13.38	0.00	40.23	0.00	19.44	0.45
94092.24	14.49	17.72	18.75	1.79	2.03	45.22	0.00	0.00	3.82	0.89

94090.23	22.35	4.21	12.83	5.36	10.49	33.51	11.25	0.00	15.85	0.51
94085.22	17.92	5.36	8.71	5.44	8.06	54.51	0.00	0.00	13.51	0.67
93499.83	11.04	3.66	4.74	4.75	22.09	50.27	0.00	3.46	26.84	0.21
93479.82	15.24	0.00	5.88	14.23	13.11	51.55	0.00	0.00	27.34	1.09
93425.81	24.86	7.38	13.07	17.53	31.78	0.00	0.00	5.37	49.32	0.55
93413.78	29.51	6.42	10.58	10.30	37.20	0.00	0.00	5.99	47.50	0.28
93413.78	29.71	6.47	10.66	10.38	37.47	0.00	0.00	5.31	47.84	0.28
93413.77	18.16	3.86	6.25	4.05	14.00	52.03	0.00	1.66	18.05	0.29
93413.76	9.49	2.91	4.48	6.38	39.20	19.64	14.37	3.54	45.58	0.16
93413.75	14.27	3.87	6.26	6.47	23.06	43.59	0.00	2.47	29.53	0.28
93410.74	23.42	10.05	16.72	12.85	32.85	0.00	0.00	4.11	45.70	0.39
93409.72	30.19	3.38	9.99	5.70	12.31	36.62	0.00	1.81	18.01	0.46
93409.71	15.35	0.00	6.32	6.93	17.73	50.22	0.00	3.44	24.66	0.39
93409.70	12.47	0.00	8.41	5.17	18.14	53.07	0.00	2.74	23.31	0.29
93408.80	12.03	6.65	5.90	7.46	20.07	42.30	5.59	0.00	27.53	0.37
93408.69	15.95	4.04	9.16	3.20	12.01	38.25	15.27	2.12	15.21	0.27
93408.68	13.28	3.62	6.49	4.25	17.77	45.70	6.66	2.24	22.03	0.24
93408.67	10.88	3.45	7.21	6.40	11.90	58.36	0.00	1.80	18.30	0.54
93408.66	12.58	3.62	8.52	6.89	14.55	51.79	0.00	2.04	21.44	0.47
93408.65	16.52	3.51	10.09	6.79	15.47	47.62	0.00	0.00	22.26	0.44
93408.64	13.79	0.00	6.48	7.12	21.24	48.60	0.00	2.77	28.36	0.34
93407.63	19.97	7.44	15.06	9.34	20.66	0.00	24.66	2.87	30.00	0.45
93376.61	18.94	4.83	7.86	6.36	16.68	43.70	0.00	1.62	23.05	0.38
93352.59	6.01	0.00	5.19	2.35	28.75	41.56	13.08	3.05	31.10	0.08
93339.58	38.63	6.88	12.56	7.46	23.62	0.00	10.85	0.00	31.08	0.32
93205.52	11.07	3.18	5.27	5.39	22.88	49.54	0.00	2.67	28.27	0.24
93198.48	14.31	5.56	8.48	6.55	27.15	23.22	11.28	3.44	33.71	0.24
93144.46	12.16	3.57	8.49	8.63	17.26	47.83	0.00	2.06	25.89	0.50
93136.44	10.55	3.69	8.87	6.43	27.38	40.68	0.00	2.40	33.80	0.23
93096.41	37.93	3.04	13.35	12.24	30.61	0.00	0.00	2.83	42.85	0.40
93096.39	11.79	2.84	16.42	5.53	17.58	43.76	0.00	2.08	23.11	0.31
93085.35	12.91	3.62	5.43	7.67	21.26	46.37	0.00	2.75	28.93	0.36
93080.33	12.98	3.30	4.69	8.73	26.35	41.08	0.00	2.88	35.08	0.33
93074.32	14.74	3.56	6.00	7.89	18.00	46.73	0.00	3.08	25.89	0.44
93074.32	13.99	4.09	5.68	7.70	20.54	45.86	0.00	2.14	28.24	0.37
93057.31	30.69	6.68	15.31	11.04	36.28	0.00	0.00	0.00	47.32	0.30
93053.29	27.99	7.80	10.23	10.86	39.21	0.00	0.00	3.91	50.07	0.28
93052.27	11.92	3.33	4.93	9.96	16.21	42.68	8.70	2.28	26.17	0.61
93044.25	12.32	0.00	4.80	8.27	26.06	39.89	6.02	2.63	34.34	0.32
93041.23	12.12	4.11	6.69	8.57	28.62	37.37	0.00	2.53	37.19	0.30
93040.21	7.56	2.31	3.07	5.26	29.65	32.43	17.03	2.67	34.91	0.18
93039.19	10.89	3.04	4.02	4.22	25.82	33.62	15.97	2.41	30.04	0.16
93032.17	8.59	0.00	4.92	8.25	37.33	38.07	0.00	2.84	45.58	0.22
93030.15	15.38	3.71	7.99	9.33	16.22	40.30	7.07	0.00	25.55	0.58
93026.13	13.66	3.17	5.45	8.82	19.90	46.79	0.00	2.21	28.72	0.44
92108.26	14.64	3.39	14.99	3.06	7.43	30.45	24.66	1.38	10.49	0.41
93011.00	9.38	0.00	7.33	4.91	20.75	32.32	23.51	1.79	25.66	0.24